Investigating the Response of *Pseudomonas aeruginosa* PA14 to Acrylic Monomers and Cystic Fibrosis Therapeutics for Industrial and Medical Application

Eilidh Terras

Under the supervision of

Dr Nicholas Tucker and Dr Arnaud Javelle

A thesis submitted in partial fulfilment for the degree of Doctor of Philosophy

Strathclyde Institute of Pharmacy and Biomedical Sciences

2023

This thesis is the result of the author's original research. It has been composed by the author and has not been previously submitted for examination which has led to the award of a degree.

Signed:

Date:

Table of Contents

Table of Abbreviations

Abbreviation	Full Term
ACH	Acetone cyanohydrin
ADP	Adenine di-phosphate
API	Active Pharmaceutical ingredient
ATP	Adenine tri-phosphate
AUC	Area under the growth curve
BMA	*n*-butyl methacrylate
CF	Cystic fibrosis
DDM	Dodecyl-beta-Maltoside
DMSO	Dimethyl sulfoxide
DNA	Deoxyribonucleic acid
HIBAM	alpha-hydroxyisobutyramide
IMAC	Ion metal affinity chromatography
IPTG	Isopropyl β-d-1-thiogalactopyranoside
MEs	Methacrylate esters

MMA	Methyl methacrylate
PCR	Polymerase chain reaction
PDB	Protein database
PDVF	Polyvinylidene difluoride
PMF	Proton motive force
PMMA	Poly-methyl methacrylate
PQS	Pseudomonas quinolone signalling
RNA	Ribonucleic acid
RND	Resistance nodulation division
SDS PAGE	Sodium dodecyl sulfate-polyacrylamide gel electrophoresis
SIBAM	sulfatoisobutyramide
SSME	Solid Supported Membrane Electrophysiology
TM	Transmembrane

Abstract

Increasing global demand for high-clarity and high tensile strength plastic has led to industrial interest in a fermentation process for monomer production from non-petrochemical sources. The main roadblock in a monomer fermentation is the toxicity of the solvent product to the production organism. *Pseudomonas spp.* are promising candidates as production organisms as their intrinsic levels of solvent tolerance is well known. Intrinsic levels of tolerance to many substances allows *Pseudomonas aeruginosa* to persist in infection, particularly demonstrated during infection in patients suffering with cystic fibrosis. PA14 transposon insertion mutants of the genes encoding subunits of the MexAB-OprM multi-drug efflux system show increased sensitivity to industrial solvents compared to the wild type. We have identified a group of membrane bound metalloproteins belonging to the Cbb_3 cytochrome oxidase family and an associated maturation system which also show an increase in solvent sensitivity after transposition. We believe this family of metalloproteins drives RND efflux activity by maintaining a proton gradient within the cell. We demonstrate the purification of subunits of the MexAB-OprM system and Cbb_3 proteins belonging to the maturation system that we believe are essential for solvent tolerance in PA14 for functional characterization using solid supported membrane electrophysiology. The transcriptomic response of *P. aeruginosa* PA14 to the industrial solvents BMA, styrene and ethylbenzene alongside the cystic fibrosis transmembrane conductance regulator modulator drugs Kaftrio and Ivacaftor is described. We provide further evidence of a functional relationship between resistance nodulation division type efflux systems and the Cbb_3 cytochrome oxidases

and suggest its application in bioprocess development. A transcriptional response to Kaftrio and Ivacaftor is also described, providing the basis for further study on the effect of these therapeutics on *P. aeruginosa in vivo.* We therefore demonstrate biochemical, transcriptomic and genetic approaches for the detection of tolerance conferring systems in *P. aeruginosa* PA14 for industrial and medical benefit.

1 Introduction

1.1 The Demand for High Quality Materials Has Resulted in the Popularity of Acrylics

The demand for feedstocks in the aviation, automotive and construction industries is increasing alongside new technologies and the growing world population. Today's industries require sustainable materials which are high in quality and easy to produce. Plastic is easy and cheap to manufacture and is highly versatile, which has seen its popularity soar in recent years. It is estimated that in 2015, 407 million tonnes of plastic were produced to satisfy industry demand (Rhodes 2018).

One type of plastic which has found wide industrial application in recent times is acrylic plastic. Acrylic plastics are a group of polymers produced using a form of acrylic acid, the most common acrylic plastic being polymethyl-methacrylate (PMMA). PMMA is formed using methacrylate esters such as methyl methacrylate (MMA) and *n*-butyl methacrylate (*n*- BMA) (**Table 1**), which can be executed via a variety of pathways. One of the world's biggest producers of PMMA today is Mitsubishi Chemical Corporation UK. The company was the first to invent an industrial process for PMMA polymerization in the 1930s when the company was known as ICI Acrylics, starting production in the 1940s. Today, Mitsubishi Chemical manufactures over a third of all acrylic plastic and is the largest producer of MMA globally, seeing the application of acrylic in a diverse range of roles (International 2020a).

Table 1: Chemical structures of poly-methyl methacrylate and the precursors n-butyl methacrylate and methyl methacrylate.

Chemical	Structure
Methyl methacrylate	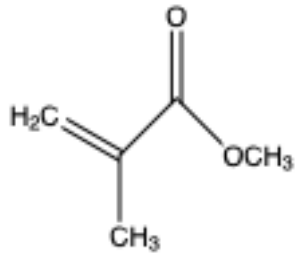
n-butyl methacrylate (BMA)	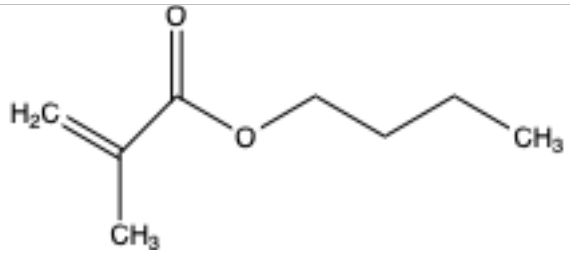
Poly-methyl methacrylate	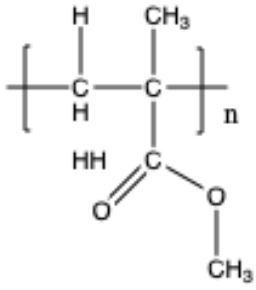

The demand for acrylic comes from its useful properties and its advantages over conventional materials such as glass. PMMA has a high optical clarity, is particularly UV resistant, possesses high tensile strength, is biocompatible and can be easily coloured ((Mitsubishi Chemical Corporation UK 2021). A market analysis report published in 2019 estimated that by 2025 the PMMA market will be worth $8.16 billion (Grand View Research 2019). Construction, transport and sign and display industries are among the main consumers of acrylic plastic. Examples of its use range from replacing glass in aeroplane windows to the manufacture of luxury items such as furniture (**Figure 1**).

Figure 1: The uses of acrylic plastic are diverse. Pictured are some examples of uses of acrylic as an alternative to glass. Acrylic sound barriers are seen lining a busy motorway in Denmark (left). The manufacture of luxury items such as decorative furniture from acrylic is becoming increasingly popular (right). Photographs obtained from Lucite International Case Studies. Available at luciteinternational.com/case studies accessed March 2020.

1.2 Manufacturing the Raw Materials for PMMA Production

As aforementioned, the production of PMMA requires methacrylate ester such as MMA as a starting material. The esterification of MMA can produce alternative methacrylate esters for PMMA production such as BMA, ethyl methacrylate and isobutyl methacrylate (Bauer, 2012). An efficient manufacturing process for MMA generation is therefore at the core of successful acrylic production.

1.2.1 Methyl Methacrylate Production via the Acetone Cyanohydrin Pathway

The first chemical process for methyl methacrylate production on an industrial scale was developed in the 1930s by ICI Acrylics and DuPont and named the acetone cyanohydrin (ACH) process. During this process, sulphuric acid is used to hydrolyse acetone cyanohydrin to alpha-hydroxyisobutyramide (HIBAM) and alpha-sulfatoisobutyramide (SIBAM). Using heat, HIBAM and SIBAM are converted to methacrylic acid (MAA). Treatment with methanol leads to subsequent esterification of MAA to methyl methacrylate (Lemonds n.d.; Spivey et al. 1997). This monomer can be produced via a variety of pathways, but the acetone cyanohydrin (ACH) pathway is unmatched in efficiency, producing yields of 80-90% (William Bauer and Co. 2012).

The ACH pathway was used by Mitsubishi Chemical Corporation (formerly known as Lucite International). However, there are several issues associated with the process. Firstly, the huge volumes of hydrogen cyanide and sulfuric acid required for the

process presents as an environmental and health hazard. Working with large volumes of these chemicals is therefore costly as the handling and disposal of hydrogen cyanide and sulfuric acid must be carried out to comply safety regulations (Patnaik 2010). Secondly, the production of MMA via the acetone cyanohydrin pathway is a complicated process, requiring several sophisticated vessels such as acid stripping columns, dehydration distillation columns and various types of reactors (Willim Bauer and Co. 2012). Maintenance and operation of such a diverse range of vessels required for production is costly. Thus, production of methacrylate esters through this process is highly energy intensive and comes at a high economic and environmental cost.

The escalation of global warming is increasing pressure on companies to decrease their carbon footprint. Mitsubishi Chemical Corporation have an interest in developing a novel process for the production of methacrylate esters that avoids the use of large volumes of toxic materials and requires a simple production process. In line with the United Nations Sustainable Development Goals Mitsubishi Chemical aim to achieve carbon neutrality by the year 2050 (United Nations, 2023). To achieve this, Mitsubishi are funding research to develop a novel biological process to produce this platform chemical in the form of a fermentation. The shift to bioproduction of methacrylate ester promises a dramatic decrease in energy input, could lead to an increase in product yield, and could be a significant step in the Mitsubishi Chemical obtaining carbon neutral status by the year 2050.

1.3 The Bioproduction of Products for Industrial use Has a Successful History

There are many examples of successful bioprocesses which have been developed for the production of various industrially relevant chemicals, pharmaceuticals and fuels (Katz et al. 2018). The first industrial scale production of a chemical by a microorganism was developed in the 1920s by James Currie and Charles Pfizer. Before the 1920s, citric acid was isolated from unripe citrus fruits which had to be imported from overseas at a high cost. Currie and Pfizer developed the first fermentation process in which *Aspergillus niger* utilised sugar to generate large quantities of citric acid (RABER 2008). Pfizer later went on to optimise the fermentation through the development of a deep-tank fermentation, which would later be adapted to drive penicillin production to serve the needs of the US and UK during World War II (Bud 2011). Now, pharmaceutical companies such as Pfizer and GlaxoSmithKline continue to mass produce many of their products such as penicillin G and clavulanic acid through fermentation processes (Paradkar 2013; Patnaik 2000).

1.4 A Novel Bioprocess for Methacrylate Ester Production Will Require the Application of Synthetic Biology

Synthetic biology involves the application of engineering principles to genetic engineering. This principle is applied to the modification or building of biological circuits for the creation of novel pathways and biological processes. When applied to industrial biotechnology, there is great opportunity to create microbial strains with

the ability to produce high yields of products which may be difficult and costly to generate chemically (Boehm and Bock 2019; Hutchison et al. 2016). Methacrylate esters are not naturally occurring chemicals in the environment and are not naturally produced by any living organisms. Therefore, a bioprocess for methacrylate ester production requires a microorganism which has been genetically engineered to contain a biosynthetic gene cluster for the manufacture of these chemicals. The leading biotechnology company Ingenza Ltd have developed a synthetic pathway for methacrylate ester production in several microorganisms including *Pseudomonas putida* KT2440 and *Escherichia coli*.

1.5 A Successful Methacrylate Ester Fermentation Will Require a Highly Tolerant Production Microorganism

The success of a fermentation for methacrylate ester production will rely heavily on the use of a microorganism with a high tolerance for these solvents. Strains of bacteria such as *E. coli* are commonly used in industrial bioprocesses as they are easy to cultivate and genetically engineer (Marisch et al. 2013). However, methacrylate ester production proves problematic for these strains as the product itself has toxic effects on cells (Dahl, Garvik, and Lyberg 1994). These hydrophobic molecules disrupt cell membranes-demonstrated by their toxic effects on liposomes (Fujisawa, Atsumi, and Kadoma 2008). Trial fermentations of MMA and BMA production using *E. coli* and *P. putida* at Ingenza Ltd showed that the toxicity of these products is the most significant bottleneck in the bioprocess currently. Therefore, developing a

fermentation process for methacrylate esters will be challenging for most microorganisms, as the production of small concentrations of the desired product has an inhibitory effect on the process itself. A successful bioprocess will therefore require a tolerant microorganism which can withstand large enough concentrations of these monomers to make a fermentation feasible. There is particular focus on *Pseudomonas* species as candidate organisms for a methacrylate ester fermentation, as their tolerance to many compounds is well established.

1.6 *Pseudomonas* Species are Extremely Adaptable, Tolerant Organisms

Pseudomonas species are known for their intrinsic and acquired resistance and tolerance to a range of substances (Hoffland, Hakulinen, and Van Pelt 1996), and can survive in a spectrum of environments. This is because these microorganisms have evolved a number of mechanisms that allow them to tolerate and thrive in otherwise uninhabitable environments (Grosso-Becerra et al. 2014). These characteristics have allowed several *Pseudomonas* species to establish themselves as successful human pathogens.

1.6.1 *Pseudomonas aeruginosa* in the Clinic

The most important *Pseudomonas* species in the clinic is *Pseudomonas aeruginosa.* This is the causative organism of many nosocomial infections and is a common pathogen in patients suffering from underlying health conditions, frequently cystic

fibrosis and burn wound patients (Bodey et al. 1983). The resistance of *P. aeruginosa* to many harsh chemicals and environments makes it a promising candidate as a production organism for a methacrylate ester bioprocess. Understanding this microorganism's range of mechanisms of tolerance will allow for a better understanding of how it can be genetically manipulated to optimise the production of these platform chemicals.

As *P. aeruginosa* is a significant human pathogen, its use as a production strain is not feasible. This pathogen has become the universal model for biofilm formation and quorum sensing (De Kievit 2009; Mcdougald et al. 2008) in *Pseudomonas* species. Here, we demonstrate the use of *P. aeruginosa* as a model organism for tolerance in *Pseudomonas* species. Another *Pseudomonas* species that we considered a promising candidate as a host for a methacrylate ester bioprocess was *Pseudomonas putida*, this strain is currently undergoing fermentation trials at Ingenza Ltd. Like *P. aeruginosa, P. putida* can colonise a wide range of environments and exhibits a high level of innate tolerance to many substances (Calero et al. 2018), meaning it is commonly used as the species of choice for many bioprocesses, such as the bioproduction of terpenoids (Loeschcke and Thies 2015). Due to its pathogenicity, *P. aeruginosa* is not suitable as a production organism, however, the genetic similarity of *P. aeruginosa* and *P. putida* coupled with the availability of a strain library of *P. aeruginosa* meant that during this study, *P. aeruginosa* PA14 was used as a tool to identify homologue systems of interest for further investigation in *P. putida.*

1.7 *P. aeruginosa* Displays a Variety of Effective Mechanisms of Tolerance to Many Compounds Including Antimicrobials

1.7.1 P. aeruginosa is a Prolific Producer of Biofilms

P. aeruginosa is a prolific producer of biofilms (Thi, Wibowo, and Rehm 2020). It does so in order to protect cells from harsh conditions within the environment, making populations of the pathogen difficult to eradicate from the body or medical equipment using antibiotics or disinfectant products such as hydrogen peroxide (Lineback et al. 2018). Biofilms create a barrier between cells and the extracellular environment by encapsulating the cells within a mucus matrix, rendering them resistant to the effects of antimicrobial agents such as antibiotics and even the immune system (Maurice, Bedi, and Sadikot 2018). The formation of biofilms enables populations of *P. aeruginosa* to colonise environments that would be otherwise challenging for other species, such as fast-moving streams and hot tubs (Lutz and Lee 2011).

1.7.2 Multidrug Resistant Strains of *P. aeruginosa* are a Significant Cause of Persistent Infection

P. aeruginosa is associated with multidrug resistant infections (Oliver et al. 2000). This pathogen has a level of intrinsic resistance to many commonly used antibiotics. For example, encoded on the *P. aeruginosa* genome is a β-lactamase AmpC, allowing for the degradation of β-lactam antibiotics such as penicillins- commonly the first line

of defence against bacterial infections (Hancock and Speert 2000)(Majiduddin, Materon, and Palzkill 2002).

The ability of *P. aeruginosa* to tolerate and adapt in the presence of many antibiotics makes it an effective pathogen and presents a problem in the treatment of infections. Antibiotic resistance has been named one of the top three major threats to human health, and some strains of *P. aeruginosa* infections have been reported as resistant to all known antibiotics (Cabot et al. 2016). This makes this *Pseudomonas* species one of the most lethal of the ESKAPE pathogens (Santajit and Indrawattana 2016). However, the ability of this *Pseudomonas* species to tolerate concentrations of many antimicrobial agents suggests that it may possess tolerance to concentrations of methacrylate esters that other common industrial microorganisms cannot.

1.7.3 The Membrane Permeability of *Pseudomonas* species is Altered to Confer Solvent Tolerance

In the presence of high solvent concentrations, *P.* putida alters its outer membrane composition, increasing the percentage of fatty acids and altering its lipopolysaccharides in order to reduce membrane permeability to increase its tolerance to various solvents (Pinkart et al. 1996). As methacrylate esters are hydrophobic molecules (Azhar et al. 2020), they integrate into the phospholipid membrane of cells and disrupt them. It has been shown that imipenem resistant strains of *P. aeruginosa* have less permeable membranes than susceptible strains

(Studemeister and Quinn 1988). However, the role of the membrane itself in drug resistance has recently been rethought. The protection conferred by the outer membrane can be partly explained by another resistance mechanism- efflux (Livermore 2002).

1.8 Traits Beneficial for Methacrylate Ester Bioproduction in *P. aeruginosa* Contribute to Pathogenicity

The mechanisms of tolerance displayed by *P. aeruginosa* which make it a promising candidate for methacrylate ester bioproduction are the same mechanisms of tolerance which make this strain one of the most significant human pathogens. In patients suffering from cystic fibrosis (CF), the tolerance mechanisms described are often used by *P. aeruginosa* to evade antimicrobials to proliferate and persist within the CF lung (Thomas E. Barton et al. 2022; Lyczak, Cannon, and Pier 2002; Yoon et al. 2002). Therefore, understanding these tolerance mechanisms for exploitation for industrial benefit can also provide insights into how these survival strategies can be targeted for improved treatment outcomes in chronic infection commonly occurring in sufferers of cystic fibrosis.

1.8.1 Efflux is a Major Mechanism of Tolerance in *Pseudomonas* Species

Perhaps the most important tolerance mechanism in *P. aeruginosa* is the export of toxic substances from the cell, mediated by a sophisticated network of multidrug efflux pumps within the cell membrane (Aeschlimann 2003). Although it has been shown that this pathogen is capable of transcribing up to 12 of these systems (Stover et al. 2000), efflux in *P. aeruginosa* is mainly mediated through four major systems, all from the resistance nodulation division family of efflux pumps (**Table 2)**(Masuda et al. 2000).

Table 2: *Pseudomonas aeruginosa* expresses four main efflux systems

Efflux System	Expression
MexAB-OprM	Intrinsically expressed at high levels. Commonly overexpressed in pathogenic strains. Basal levels of expression provide resistance to many chemicals.
MexCD-OprJ	Not expressed during regular growth. Expressed during stress conditions, providing acquired resistance to some chemicals.
MexXY-OprM	Intrinsically expressed at low levels. Commonly overexpressed in pathogenic strains. Basal levels of expression provide some resistance to many chemicals.
MexEF-OprN	Not expressed during regular growth. Expressed during stress conditions, providing acquired resistance to some chemicals.

These systems actively transport harmful substances out from the cell, meaning intrinsic levels of their expression give *P. aeruginosa* an innate level of resistance to concentrations of the substances they extrude (Li, Plésiat, and Nikaido 2015). When subjected to antibiotics, solvents, dyes or other chemicals harmful to cells, an increase in transcription of these systems is observed (Dean et al. 2003; Gotoh et al. 1994; Lorusso et al. 2022) providing resistance in many cases. This makes these systems significant in the clinic, as their overexpression is the cause of many antibiotic resistant *P. aeruginosa* infections (Fabre et al. 2021; Lee et al. 2000). The intrinsic and acquired resistance to many drugs through active efflux is observed over several *Pseudomonas* species (Nikaido and Pagès 2012a).

In the wider context of a methacrylate ester fermentation, the ability of *P. aeruginosa* to actively export substances from the cell reinforces its potential as a promising production microorganism. If methacrylate esters can be transported from the cell before their toxic effects on the cell membrane are seen, then larger concentrations of these chemicals can be produced during a fermentation without compromising productivity. Efflux of methacrylate esters from the cell will be a focus of this study.

1.9 *n*-Butyl Methacrylate is an Attractive Methacrylate Ester for Bioproduction

Currently, methyl methacrylate is the main methacrylate ester produced by Mitsubishi Chemical Corporation. However, there are a few properties of *n*-butyl methacrylate (BMA) which make it an attractive fermentation product. Firstly, BMA is currently derived from MMA, but development of a bioprocess for BMA involves the production of BMA itself, negating the need for an additional production step involving the modification of MMA. Also, while MMA is slightly soluble in water, BMA is completely insoluble in water, meaning that downstream processing of BMA is simpler as the product would float on top of the growth medium. Reduction of downstream processing steps will result in a bioprocess which is more cost effective and less energy consuming. For these reasons, there is focus on BMA as the methacrylate ester of choice for this bioprocess.

A disadvantage of BMA production compared to MMA is that BMA is more hydrophobic than MMA. This means it can integrate into and disrupt cell membranes more easily, so this will be a challenge of the bioprocess which must be addressed. Efflux pumps will play a key role in overcoming this issue.

1.10 Previous Work: a BMA Sensitivity Assay

In 2017 a BMA sensitivity assay was carried out on *Pseudomonas aeruginosa* transposon mutants by Dr Walid El Bestawy at the University of Strathclyde (Bestawy

2017a) by conducting a transposon mutant library screen. These mutants had a mariner transposon insertion in one gene which resulted in the downregulation or complete obstruction of that gene (Liberati et al. 2006). These mutants were subjected to growth with and without BMA, and the difference in growth was recorded as the difference in the area under the plotted growth curve **Table 3**.

Table 3: BMA sensitivity assay results conducted by Walid El Bestawy (University of Strathclyde). Difference in growth of transposon mutants grown with and without BMA as measured by the area under the growth curve were compared. The red boxes highlight the top hits from the assay, showing the two distinct groups of genes which resulted in the biggest difference in growth. * note that *PA14_61980* is not part of the Cbb_3 cytochrome oxidase family of proteins and is an outlier.

	Locus ID	Description	Δ % AUC
More Sensitive*	PA14_05550	OprM	-63.12
	PA14_05540	MexB	-55.70
	PA14_05530	MexA	-55.29
	PA14_44460	cytochrome complex assembly.	-51.03
	PA14_44440	putative cation-transporting P-type ATPase	-49.85
	PA14_61980	chromosome partitioning protein	-45.27
	PA14_44450	putative cytochrome oxidase maturation protein cbb3-type	-45.11
	PA14_07760	SurA	-44.40
	PA14_43950	SucC	-41.62
	PA14_62930	carbamoyl-phosphate synthase small chain subunit	-36.09
	PA14_66310	dihydrolipoamide acetyltransferase aceF	-34.58
	PA14_43940	SucD	-34.18
	PA14_69620	Uncharacterised	-32.67
	PA14_13660	TpbA	-32.47
	PA14_57560	putative cytochrome b	-29.86
	PA14_05620	S-adenosyl-L-homocysteine hydrolase	-27.23
	PA14_19630	folE1 GTP cyclohydrolase	-4.89
More Resistant	PA14_26130	Morphinone reductase	7.37
	PA14_39560	putative chemotaxis transducer	8.97
	PA14_58260	Unknown function	10.55
	PA14_22020	MinD	10.78
	PA14_30290	FtsK	11.48
	PA14_27070	YphA.	11.74
	PA14_23460	TpbB	12.05
	PA14_20080	Similarity HlyD secretion protein	13.16
	PA14_32080	toluate 1,2-dioxygenase alpha subunit. xylX	14.05
	PA14_51430	pqsA	15.98

Strains that displayed the largest Δ%AUC have a transposon insertion in a gene that confers a selective advantage for growth in the presence of BMA. Of the top genes which showed the largest difference in growth in this transposon mutant library screen, 6 of these transposon mutants correspond to genes from two distinct systems as is demonstrated by **Table 3**.

Transposon insertions within genes *PA14_05550*, *PA14_05540* and *PA14_05530* (OprM, MexB and MexA respectively) all correspond to *P. aeruginosa* strains with a downregulation of one component of the MexAB-OprM efflux system. Genes *PA14_44460, PA14_44440* and *PA14_44450* all correspond to mutants with transposon insertions on genes for proteins associated with the assembly of the Cbb_3 cytochrome oxidase complex. As these strains displayed the largest difference in growth during the transposon mutant library screen, these systems must play a crucial role in the tolerance of *P. aeruginosa* to BMA- as reducing their transctiption resulted in decreased growth in the presence of BMA.

Transposon mutants which displayed an increased tolerance to BMA are also shown in **Table 3**. However, the difference in AUC for these strains were significantly lower than in the strains which became more sensitive, and therefore the gene downregulations which resulted in an increase in BMA sensitivity are more attractive as targets for increasing the tolerance of *P. aeruginosa* to *n*-BMA in terms of bioprocess development. Although the significance of these genes cannot be ignored,

this study will focus only on the gene downregulations which produced more sensitive *P. aeruginosa* mutants.

1.11 Two Distinct Systems were Identified by the Transposon Mutant Library Screen

1.11.1 The MexAB-OprM Multidrug efflux System

The three transposon mutants which produced the largest difference in growth in response to BMA had transposon insertions within the genes *MexA, MexB* and *OprM.* These genes are all components of the MexAB-OprM system which is the main efflux machinery utilised by *P. aeruginosa,* spanning the inner and outer membrane (**Figure 2**).

This protein complex belongs to the resistance nodulation division (RND) family of multi-drug exporters, which are ubiquitous to Gram negative bacteria (Nikaido 2010) and are powered by proton motive force (PMF) within the cell. *P. aeruginosa* expresses several RND efflux systems (**Table 2**), but the MexAB-OprM is the major mediator of efflux within this microorganism. This RND pump is expressed at intrinsic levels within the cell and is the main system responsible for the extrusion of a broad range of toxic substrates across the double membrane (Li et al. 2015).

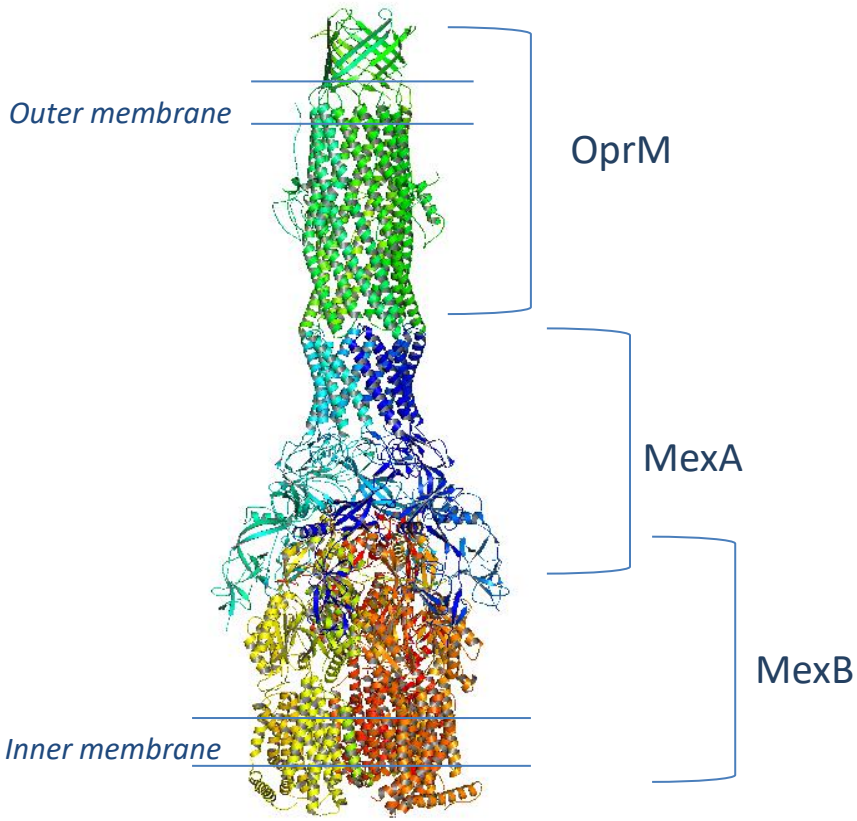

Figure 2: The MexAB-OprM protein complex is formed from three subunits, MexB, MexA and OprM. Protein complex is in the 0-degree state. Protein structure diagram generated using PyMol using the protein database (PDB) structure generated by Tsutsumi et al. 2019, pdb code: 6IOK.

The MexAB-OprM complex is formed from an inner membrane spanning RND protein, a periplasmic membrane fusion protein and an outer membrane factor (OMF) protein (**Figure 2**). Each of these subunits play a role in the function of the pump, each being essential for *in vivo* activity of the system (Du et al. 2018).

The substrate specificity of the MexAB-OprM system is extremely broad (Nikaido and Pagès 2012b). This protein complex supports the extrusion of most categories of antimicrobial agents, dyes, detergents, organic solvents and even quorum sensing molecules from the cell (**Table 4**)- making it a powerful mechanism of broad tolerance in *P. aeruginosa.* Substrates of this pump vary greatly in molecular weight and charge, showing that the mechanism of transport is complex and sophisticated. The versatility of this system continues to place clinical interest upon it as a drug target, as its role in broad antibiotic resistance of *P. aeruginosa* has been demonstrated widely (Goli et al. 2018).

Table 4: the MexAB-OprM multidrug efflux system supports a wide range of substrates. These substrates vary greatly by molecular weight. Biochemical evidence of efflux is listed for each substrate.

MexAB-OprM Substrates				
	Substrate	**Molecular Weight (gM^{-1})**	**Biochemical Evidence**	**Literature**
Organic Solvents	Toluene	92.14	Active energy dependant efflux of toluene in solvent tolerant *P. aeruginosa*	(Isken and De Bont 1996)
	n-butyl methacrylate	142.20	Significant reduction of n-BMA tolerance in *P. aeruginosa* with transposon insertion within genes MexB, MexA and OprM	(Bestawy 2017b)
Detergents	n-dodecylD-maltoside (DDM)	510.60	Binding of maltoside component of DDM observed in MexB crystal structure	(Sennhauser et al. 2009)
Antimicrobial Agents	Chloramphenicol	323.13	Loss of chloramphenicol resistance in MexB *P. aeruginosa* mutants	(Guan and Nakae 2001)
	novobiocin	612.6	Binding of novobiocin to MexB distal drug binding pocket in cryo-EM analysis	(Tsutsumi et al. 2019)

Dyes	Ethidium bromide	394.29	Transport of EtBr by MexAB-OprM through *in vitro* double membrane system	(Verchère et al. 2015)
	2-4-dimethyl-aminostyryl-1-ethylpyridinium (DMP)	380.27	Transport of DMP into MexB proteoliposomes	(Guan and Nakae 2001)
Quorum Sensing Molecules	3-oxo-acyl-homoserine lactone	213.23	Loss of HSL dependant response upon breakdown of MexAB-OprM function by knocking out MexB	(Minagawa et al. 2012)
	HSL inhibitor L-homoserine lactone (OdDHL)	101.1	Increased potency of OdDHL in MexAB-OprM knockouts	(Moore et al. 2014)
Other	Protons (H^+)	1.01	Loss of efflux upon addition of proton uncoupler carbonyl cyanide m-chlorophenylhydrazone (CCCP)	(Nikaido 1996)
	Neopentyl glycol derivative C7NG	1028	Resolved crystal structure of MexB with C7NG inserted within the distal binding pocket	(Sakurai et al. 2019)

The functional subunit of MexAB-OprM is MexB, this subunit forms the RND component of the MexAB-OprM complex (Fernando and Kumar 2013). The crystal structure of MexB has been resolved, revealing its tripartite structure (**Figure 3**). Each monomer spans the inner membrane of *P. aeruginosa* 12 times, and these 12 transmembrane (TM) domains are positioned in a complex configuration leading to the intricate tertiary structure of the inner membrane protein. Elongated curved structures protruding from regions TM1/TM2 and TM7/TM8 form the framework of a periplasmic domain which fold into six subdomains. These subdomains facilitate the binding of substrates to MexB in a pore region and forms an interaction site which allows the membrane fusion protein (MFP) MexA to dock onto MexB (Tsutsumi et al. 2019).

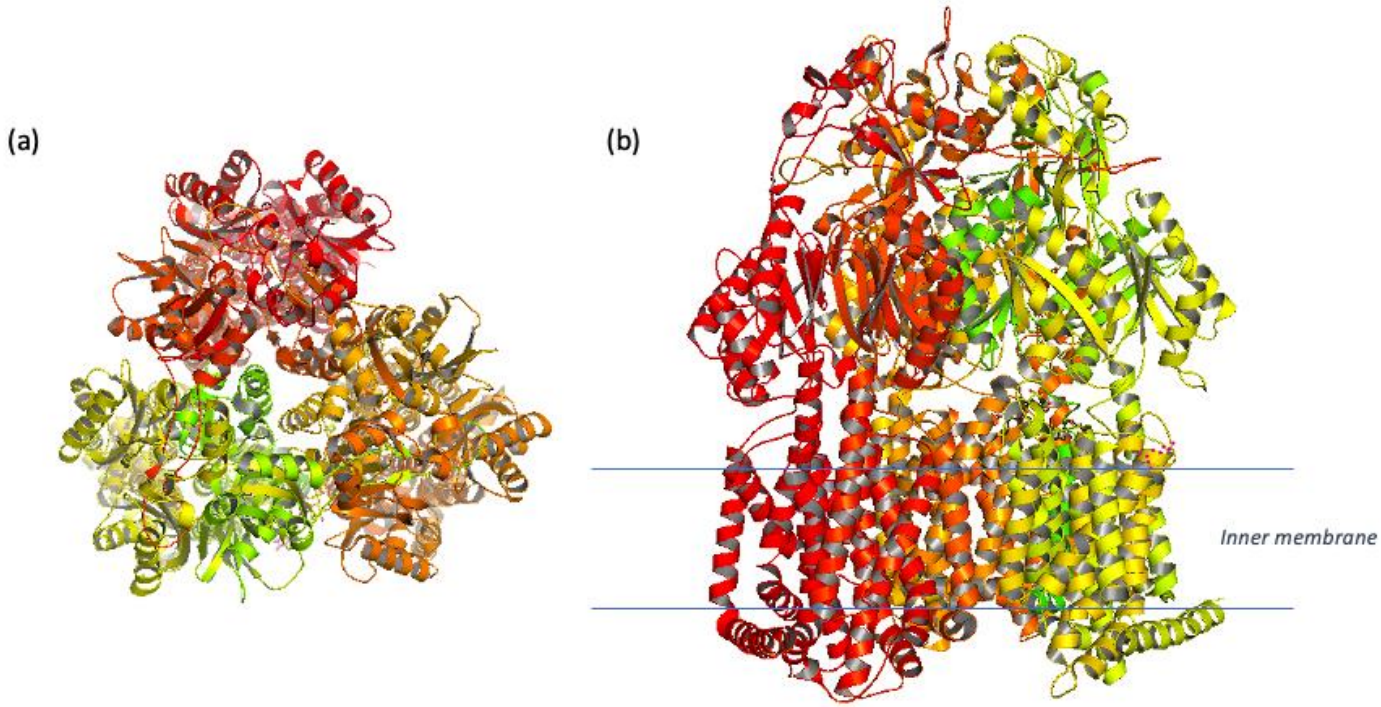

Figure 3: (a) the tripartite structure of MexB (b) the position of MexB within the inner membrane. Protein structure diagram generated using PyMol using the PDB structure generated by Sennhauser et al. 2009, PDB code: 2V50.

It is widely accepted that MexB is the active component of the MexAB-OprM complex. At any one time, each of the three monomers adopts a different conformational state: the access, binding or extrusion state. During the access state, two binding pockets are made accessible for the capture of substrate from either the periplasm or from within the membrane. The binding site is only accessible on the monomer which has taken the access conformation at that time (Seeger et al. 2006).

The binding conformation involves the closing off of the binding site after compounds have bound, preventing the backflow of substrate back through MexB. It has always been accepted that a distal binding pocket allows for the capture of low molecular mass substances, and a proximal binding pocket was responsible for the capture of larger molecular mass compounds. However, it has been shown that the distal binding pocket is capable of capturing substances of both low and high molecular weights (Sakurai et al. 2019). A third biding site has recently been discovered localised within the periplasmic portion of MexB responsible for the efflux of substances from within the membrane and the periplasmic space (Oswald, Tam, and Pos 2016). When the extrusion state is adopted, substrates are pumped through various channels within MexB which open upon adoption of this state and feed to the membrane fusion protein MexA. The three subunits shift between these three states, and in doing so efflux of substrate from MexB to MexA and then through OprM is mediated (Sennhauser et al. 2009).

MexA is the membrane fusion protein component of the MexAB-OprM system. Its structure is complex, comprising of 13 subunits which form a long boomerang shaped structure (**Figure 2**)(Akama, Matsuura, et al. 2004). MexA occupies the periplasmic space, acting as a bridge between the inner membrane protein MexB, and the outer membrane protein (OMP) OprM. MexB and OprM only weakly interact, and so MexA has been described as an adaptor protein which connects the two subunits (Symmons et al. 2009).

The outer membrane component of the MexAB-OprM complex is OprM. Like MexB, this structure is also tripartite, with each protomer assembled to form a pore structure (**Figure 2**), mediating the movement of substrate in one direction only (Akama, Kanemaki, et al. 2004). This protein mediates the extrusion of substrates across the outer membrane of *P.* aeruginosa, and it has been proposed that this process is activated by the interaction of OprM with MexA (López et al. 2017).

1.11.2 MexAB-OprM Requires a Proton Gradient Across the Biological Membrane to Function

Initiation of transport across the biological membrane by MexB requires a proton gradient within the cell (Verchére, Broutin, and Picard 2012). A proton gradient is generated when there is a higher concentration of hydrogen ions (protons, or H^+) in the periplasmic space than there are within the cell. This creates an electrochemical gradient across the inner membrane, which allows certain systems within the

membrane such as MexB to transport substances across the membrane using proton motive force (PMF) instead of hydrolysing adenine triphosphate (ATP)(Alberts B, Johnson A, Lewis J 2002). Without a proton gradient, the MexAB-OprM system is not able to extrude substrate from the cell against its concentration gradient. This was demonstrated in 1994, when Li *et al.* observed a loss of MexAB-OprM mediated drug resistance upon the addition of a proton uncoupler CCCP to the growth medium of *P. aeruginosa* (Li, Livermore, and Nikaido 1994).

In order to mediate substrate extrusion, H^+ ions are captured from the periplasmic space by MexB and transported down their concentration gradient into the cytoplasmic space. The energy generated in this proton transport powers efflux (Du et al. 2018). Charged residues within MexB which are highly conserved across the RND transporters are situated between TM4 and TM10. Among these are Asp407 and Asp408 situated in TM4, and Lys939 on TM10. These residues are thought to form a portion of a channel mediating the translocation of protons through the RND transporter. Substitution of any of these conserved residues for alternative amino acids results in the breakdown of efflux (Guan and Nakae 2001).

1.12 The Cbb_3 Cytochrome Oxidases

Three transposon mutants which produced the largest difference in growth in response to BMA had transposon insertions within the genes *PA14_44460,*

PA14_44440, and *PA14_44450*. These genes are all components of the Cbb_3 cytochrome oxidase assembly system.

These protein complexes were first discovered in *Bradyrhizobium japonicum* within the root nodules of nitrogen fixing plants. These systems played an essential role in the respiratory chain of this microorganism, maintaining the energy demand for the highly energy taxing process of nitrogen fixation from the atmosphere in the root nodules of legumes (Elmerich, Kondorosi, and Newton 1994). Now, these membrane proteins have been identified in a number of microorganisms, including *Pseudomonas aeruginosa.*

When oxygen is not a limiting factor, *P. aeruginosa* transcribes five terminal oxidases (Arai et al. 2014). Two of these are Cbb_3 type cytochrome oxidases: *Cbb_3-1 and Cbb_3-2*, which are under the control of separate promoters. These systems catalyse the reduction of oxygen to water, generating energy. Cytochrome oxidases are the final enzymes involved in the electron transport chain, and use the energy produced from oxygen reduction to transport H^+ ions across the cytoplasmic membrane, generating a proton gradient within the cell (Hill 1991). These systems therefore play an essential role in bacterial energetics.

The *P. aeruginosa* Cbb_3 cytochrome oxidases are structurally complex and are comprised of four distinct subunits (**Figure 4**). The transmembrane catalytic subunit, CcoN contains the active site of the protein complex, a haem-copper metallocentre where the four electron reduction of oxygen occurs (Pitcher and Watmough 2004). CcoN interacts with two other subunits: CcoO and CcoP to mediate the translocation of protons across the inner membrane. Two channels are involved with proton flux. Channel K transports H^+ ions from inside the cell towards the haem-copper metallocentre, and channel D mediates the flux of protons across the inner membrane into the periplasmic space (Comolli and Donohue 2004). A fourth subunit, CcoQ has an unknown function.

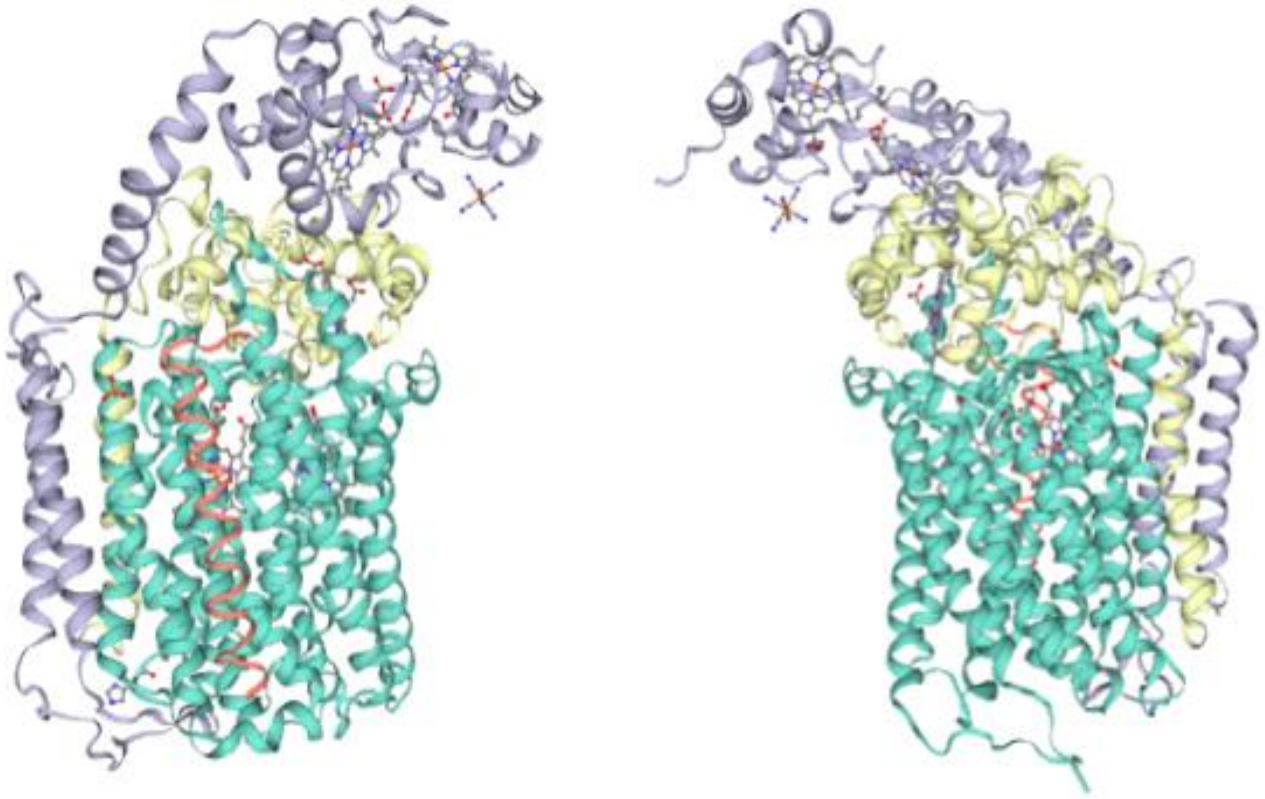

Figure 4: ribbon structure of the Cbb3 cytochrome oxidase from Pseudomonas stutzeri from a front and back view. Protein structure diagram generated using SWISS-MODEL. Subunit CcoN is shown in blue, subunit CcoO is shown in yellow and subunit CcoP is shown in purple. Three Heme C molecules are bound within unit CcoP, and a hexacyanoferrate molecule is observed at the apex of CcoP. Other bound ligands include Copper(II) ions and calcium ions.

This membrane protein is complex in structure, and assembly of a functional Cbb_3 system requires the expression of an operon encoding Cbb_3 maturation proteins (Zufferey et al. 1996). Although there are two copies of the Cbb_3 cytochrome oxidase genes on the *P. aeruginosa* genome, there is only one copy of the genes encoding the machinery for the Cbb_3 assembly system. One of the genes which displayed the highest difference in growth during the transposon mutant library screen was a member of this assembly system- *PA14_44440*, a copper transporting p-type ATPase CopA2 shown in **Figure 5**. This protein is homologous with the protein CopA responsible for copper tolerance in *P. aeruginosa* (Hofmann, Hirsch, and Ruthstein 2021).

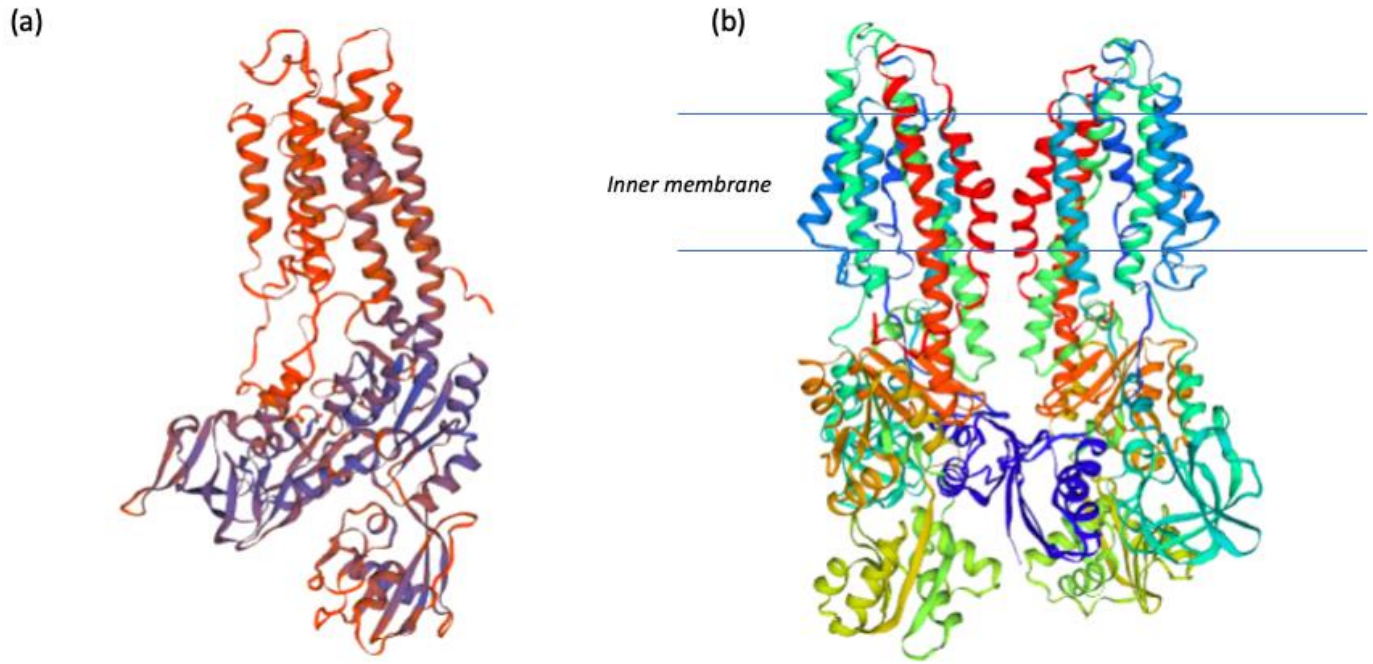

Figure 5: (a) monomeric Cbb3 copper transporting p-type ATPase CopA2. Diagram generated using SWISS-MODEL (b) dimeric CopA2 from *Archaeoglobus fulgidus* within the inner membrane. Diagram generated using SWISS-MODEL SMTL ID: 3j09.1

This p-type ATPase is positioned within the inner membrane of *P. aeruginosa* (**Figure 5**) and is a copper transporting complex also involved in maintaining the proton gradient within the cell. ATPases catalyse the hydrolysis of adenosine triphosphate (ATP) to adenosine diphosphate (ADP), a process which generates energy. ATPases use this energy to transport ions across the cell membrane. In the case of PA14_44440, CopA2, this p-type ATPase transports copper ions across the cytoplasmic membrane into the periplasmic space. These copper ions are accessed by Cbb_3 from the periplasm and used for the formation of the haem copper catalytic centre situated within the CcoN subunit. Therefore, as well as playing a role in the assembly of the Cbb_3 complex, this p-type ATPase also plays an important role in copper tolerance in *P. aeruginosa* by extruding copper ions from the cytoplasmic space (Rademacher and Masepohl 2012).

1.13 A Functional Relationship Between MexAB-OprM and Cbb_3 cytochrome Oxidases is Proposed

A functional relationship between MexAB-OprM and the Cbb_3 cytochrome oxidases has not been reported in the literature. It is expected that the MexAB-OprM system would play an integral role in BMA tolerance, as it plays an essential role in the tolerance of *P. aeruginosa* to many other toxic substances. However, the same cannot be said of the Cbb_3 proteins. It is known that these proteins have a primary role in the respiratory chain, but their role has never been explored in relation to tolerance.

As the MexAB-OprM system requires proton motive force to mediate efflux of substances out of the cell, this study hypothesises that the *P. aeruginosa* Cbb_3 cytochrome oxidases or components of its assembly system provide the proton gradient in order for MexAB-OprM to function **Figure 6**.

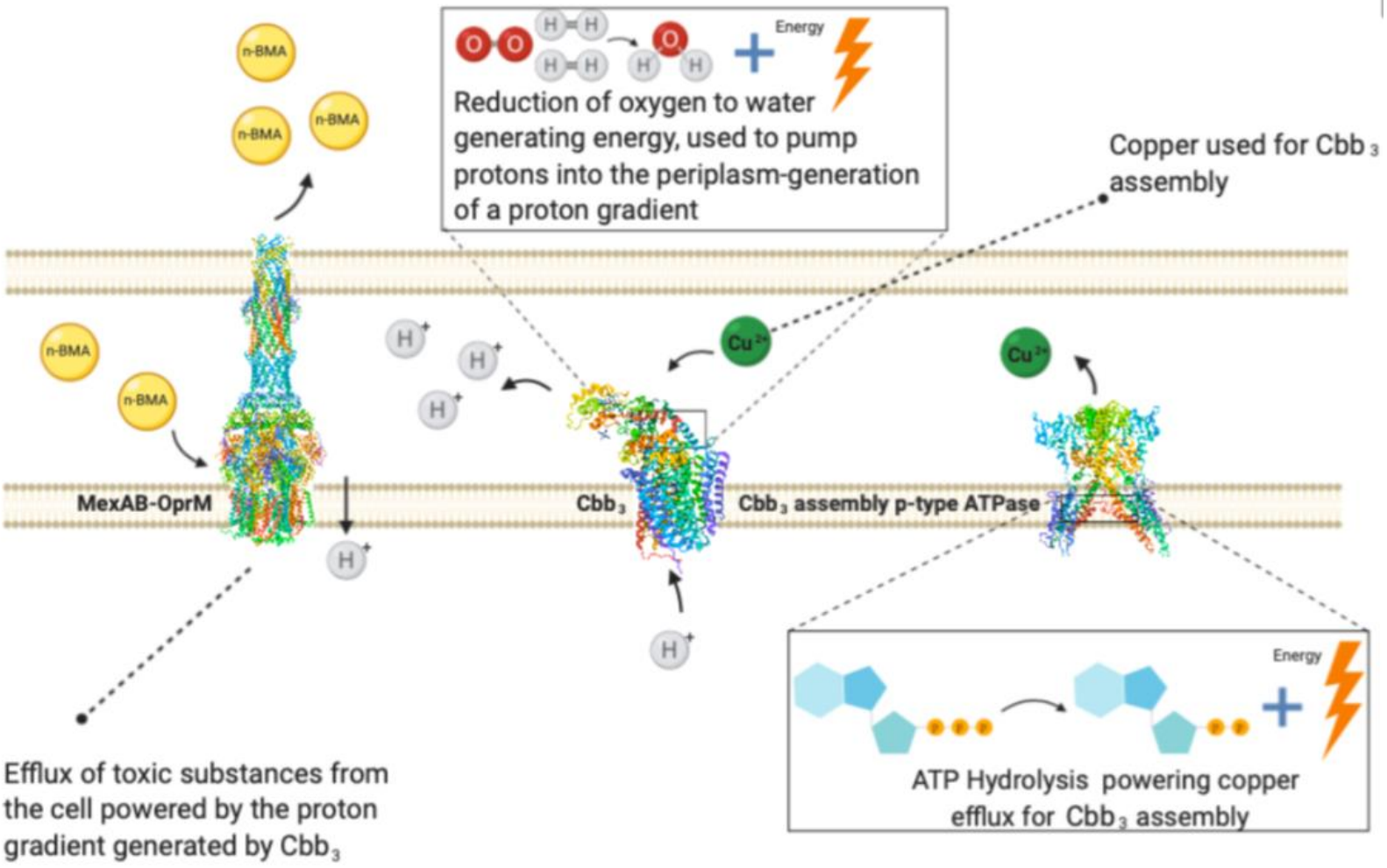
n-BMA
n-BMA
n-BMA
n-BMA
n-BMA
Energy
Reduction of oxygen to water generating energy, used to pump protons into the periplasm-generation of a proton gradient
Copper used for Cbb 3 assembly
Cu 2+
Cu 2+
H
H
H
H
H
MexAB-OprM
Cbb3
Cbb3 assembly p-type ATPase
Energy
ATP Hydrolysis powering copper efflux for Cbb3 assembly
Efflux of toxic substances from the cell powered by the proton gradient generated by Cbb3

Figure 6: proposed model of MexAB-OprM BMA efflux powered by Cbb_3. From the right-hand side of the schematic: PA14_44440- the Cbb_3 assembly copper transporting p-type ATPase catalyses the hydrolysis of ATP to ADP, using the energy generated in doing so to transport copper (II) ions across the inner membrane into the periplasm. These copper (II) ions are accessed in the periplasm by Cbb_3 and are used for the construction of the haem-copper metallocentre on subunit CcoN. Cbb_3 catalyses the four-electron reduction of dioxygen to water and used the energy generated in doing so to transport protons into the periplasm and generation of a proton gradient is obtained within the cell. Note that in the cell there are two copies of Cbb_3 being transcribed: Cbb_3-1 and Cbb_3-2, so the proton gradient generated by Cbb_3 is significant. MexAB-OprM utilises the PMF to extrude BMA from the cell. A proton is transported down its electrochemical gradient, and the energy generated in doing do is used to transport BMA from the cell, which is accessed in the periplasm. Diagram generated using Biorender.

Although *E. coli* and *P. aeruginosa* share a high degree of homology between their main RND efflux pumps, AcrAB-TolC and MexAB-OprM respectively, it is *P. aeruginosa* which exhibits such a high degree of innate resistance and tolerance which has allowed the microorganism to establish itself so successfully within the environment and in the clinic (De Bentzmann and Plésiat 2011). *E. coli* possesses only one Cbb_3 type cytochrome oxidase (Pitcher and Watmough 2004) compared to the two Cbb_3 systems represented by *P. aeruginosa*.

Possessing a second copy of Cbb_3 which has a higher affinity for oxygen (Pitcher and Watmough 2004) and is transcribed under low oxygen conditions may allow *P. aeruginosa* to more easily preserve a proton gradient within the cell where other microorganisms would struggle to do so. This study hypothesises that *P. aeruginosa* is such an established tolerant organism because even though its efflux machinery shares a high degree of similarity to that or other Gram-negative bacteria, it has the tools to power that machinery more effectively-specifically through the Cbb_3 cytochrome oxidase system and the efficient generation and maintenance of proton gradient within the cell.

If this hypothesis is correct, the basis for the exploitation of these systems is proposed for the generation of tolerant strains for industrial benefit. The proposed functional relationship between MexAB-OprM and the Cbb_3 cytochrome oxidases could also be

responsible for the tolerance of *P. aeruginosa* to many antimicrobials allowing the pathogen to persist in infections, particularly in patients suffering with cystic fibrosis.

During this study, we propose a biochemical and transcriptomic approach to elucidating this potential functional relationship while identifying tolerance conferring mechanisms of *P. aeruginosa* PA14 to a number of substances including BMA, styrene, ethylbenzene and the cystic fibrosis transmembrane conductance regulator modulator drugs Kaftrio and Ivacaftor at 1 x and 100 x serum concentrations.

2 Materials and Methods

2.1 Chemicals and Reagents Used Throughout This Study

Table 5: chemicals and reagents used in this study

Reagent	Distributer
1kbp plus ladder	New England Biolabs UK
250kDa protein ladder	New England Biolabs UK
Acrylamide	Scientific Laboratory Supplies Limited
Agar	Sigma-Aldrich
Agarose	Sigma-Aldrich
Ampicillin	Melford Laboratories Ltd
$CaCl_2$	Sigma-Aldrich
Carbenicillin	Melford Laboratories Ltd
Copper(II) Sulphate	Sigma-Aldrich
Dimethyl Sulfoxide (DMSO)	Sigma-Aldrich
DNAse	Sigma-Aldrich
dNTP Mix	New England Biolabs UK
DTAB	Sigma-Aldrich
Ethidium Bromide	Sigma-Aldrich
Gibson Assembly Mastermix	New England Biolabs UK
Glucose	Sigma-Aldrich
Glycerol	Sigma-Aldrich

GoTaq DNA Polymerase	Promega
Green GoTaq Reaction Buffer	Promega
IPTG	Melford Laboratories Ltd
Kanamycin	Melford Laboratories Ltd
KH_2PO_4	Sigma-Aldrich
Loading Dye	New England Biolabs UK
Lysozyme	Sigma-Aldrich
$MgSO_4$	Sigma-Aldrich
n-Dodecyl-B-D-maltoside	Melford Laboratories Ltd
Na_2HPO_4-$7H_2O$	Sigma-Aldrich
NaCl	Sigma-Aldrich
NH_4Cl	Sigma-Aldrich
PDVF membrane	Cytiva Lifesciences
PMSF	Sigma-Aldrich
Primary antibody	ThermoFisher Scientific
Q5 High Fidelity DNA Polymerase	New England Biolabs UK
Q5 High GC Enhancer	New England Biolabs UK
Q5 Reaction Buffer	New England Biolabs UK
RNAlater™ Stabilisation Solution	Invitrogen
RNAseZap™ RNAse Decontamination Solution	Invitrogen
PureLink™ DNase Set	Invitrogen

Secondary antibody	ThermoFisher Scientific
Sodium Citrate	Sigma-Aldrich
T4 DNA Ligase	New England Biolabs UK
TEMED	Sigma-Aldrich
Tetracycline	Melford Laboratories Ltd
Tris Base	Sigma-Aldrich
Tris-CL	Sigma-Aldrich
TRIzol RNA Isolation Reagent	Invitrogen
Tryptone	Sigma-Aldrich
Wattman paper	Cytiva Lifesciences
X-Gal	Promega
Yeast Extract	Sigma-Aldrich

2.2 Preparation of Solutions

All solutions were prepared using deionised water from the Purite HP deionised water dispension system. Solutions were sterilised by autoclaving at 121°C for 20 minutes at 15psi or by filter sterilisation using filters with pore size of 0.22 micron.

2.2.1 Media and Solution Composition

Table 6: Reagent/media composition of solutions used in this study

Reagent/Media	Composition
5x SDS PAGE loading dye (50mL)	30% glycerol, 10% SDS, 5% B-mercaptoethanol, 0.02% bromophenol blue, 250mM Tris-Cl(pH 6.8)
10% APS (50mL)	5g ammonium persulphide was dissolved in 50mL ddH_2O
10x SDS PAGE running buffer (1L)	30g tris base, 144g glycine, 10g SDS
20x NPS	25% glycerol, 2.5% glucose, 10% lactose
50x 5052	0.5M $(NH4)_2SO_4$, 1M KH_2HPO_4
Autoinduction media (200mL)	200uL Amplicillin (100mg/mL), 10mL 20xNPS, 4mL 50x5052, 200uL 1M $MgSO_4$, up to 200mL with ZY broth

Gel destain solution	40% methanol, 10% acetic acid, 50% H2O
Gel stain solution	0.1% Coomassie blue, 50% methanol, 10% acetic acid
IMAC A solution	50mM TrisCl (pH8), 500mM NaCl, 10% glycerol, 0.03% DDM, 10mM imidazole
IMAC B solution	50mM TrisCl (pH8), 500mM NaCl, 10% glycerol, 0.03% DDM
LB agar (250mL)	1.25g yeast extract, 2.5g tryptone, 1.25g NaCl, 2.5g agar
LB broth (250mL)	1.25g yeast extract, 2.5g tryptone, 1.25g NaCl
M9 minimal media (500mL)	100mL M9 salts, 1mL $MgSO_4$ 1M, 10mL sodium citrate 20% w/v, 50µL CaCl 1M
M9 salts (1L)	64g Na_2HPO_4-$7H_2O$, 15g KH_2PO_4, 2.5g NaCl
Membrane protein stabilisation lysis buffer (35mL)	35µL DNase, 700µL PMSF, 150mg lysozyme,0.7g DDM, 3.5mL glycerol

MSA media (1L)	7.89g KH_2PO_4, 2.63mL vishniac trace elements
MSB media (1L)	15g NH_4Cl, 2g $MgSO_4.7H_2O$
MSX minimal media	760mL MSA media, 200mL MSB media, 40mL 12.5% (w/v) glucose
Mueller Hinton broth (1L)	21g Mueller Hinton
PBS (1L)	1.44g Na_2HPO_4, 0.24g H_2PO_4, 0.2g KCl, 8g NaCl
SOC broth (100mL)	2g tryptone, 0.5g yeast extract, 0.06g NaCl, 0.02g KCl, 0.2g $MgCl_26H_2O$, 0.36g glucose
Solution 2	1.5M TrisCl (pH 8.8), 0.3% SDS
Solution 3	0.5M TrisCl (pH6.8), 0.3% SDS
TBS-T (1L)	8.76g NaCl, 6.05g TrisCl, 500µL Tween 20
TBST- 5% Milk	TBS-T supplemented with 5% dried milk

Transfer buffer (1L)	14.4g glycine, 3g Tris base, 1g SDS 20% methanol
ZY broth (1L)	10g tryptone, 5g yeast extract up to 1L with ddH_2O

2.3 Equipment Used Throughout This Study

The equipment used throughout this study is listed in **Table 7.**

Table 7: equipment used throughout this study and their suppliers are shown.

Equipment/Kit	Distributer
2100 Bioanalyzer	Agilent
Benchtop centrifuge	ThermoFisher Scientific
Bio-Rad Mini PROTEAN Tetra Vertical Electrophoresis Kit	Bio-Rad
Gel visualisation camera	Syngene Bioimaging
LI-COR Odyssey Imager	LI-COR
Microbiological Safety Cabinet (MSC)	ThermoFisher Scientific
Microfuge	ThermoFisher Scientific
Monarch® DNA Gel Extraction Kit	New Wngland Biolabs United Kingdom
Nanodrop spectrophotometer	ThermoFisher Scientific
Nonstick, RNAse-free microfuge tubes 2.0mL	Invitrogen
Protein gel doc	Syngene Bioimaging
RNA 6000 Nano Chips	Agilent
RNA 6000 Nano Kit	Agilent
Rotating wheel	ThermoFisher Scientific
Semi dry transfer system	ThermoFisher Scientific
TRIzol™ Plus RNA Purification Kit	Invitrogen
Wizard® Plus Minipreps DNA Purification Systems	Promega United Kingdom

2.4 Bacterial Strains Used During This Study

The bacterial strains used throughout this study and their genotypes are shown in Table *8*.

Table 8: bacterial strains used throughout this study and their genotypes.

Bacterial Strain	Genotype/Comments	Reference
C43(DE3) *Escherichia coli*	DE3 T7 DNA polymerase gene cassette. Optimised for membrane protein overexpression	(S.Wagner et al. 2008)
DH5α *Escherichia coli*	High yield and quantity of DNA due to *endA* mutation	(J. Lin 1992)
P. aeruginosa PA14_WT	PA14 wild type strain	(Liberati et al. 2006)
pETER1	C43(DE3) *Escherichia coli* transformed with CopA2 overexpression plasmid pETER1	This study
pETER2	C43(DE3) *Escherichia coli* transformed with MexB overexpression plasmid pETER2	This study

2.5 Cultivation of Bacteria

Single colonies of *E. coli* and *P. aeruginosa* were obtained by streaking onto LB agar plates and incubating in a static incubator at 37°C for 16 hours. 10mL Overnight cultures were inoculated using a single colony of bacteria in LB broth (supplemented with antibiotics where appropriate) and shaking for 16 hours at 37°C 250RPM.

2.6 Cryostock Preparation

Cryostocks of bacterial strains were prepared for long term storage in the -80 °C freezer. 5 mL of bacterial culture in stationary phase was mixed gently with 400 μL of sterile 60% glycerol and added to a sterile cryogenic tube. Cryostocks were stored at -80 °C.

2.7 DNA Amplification

DNA was amplified throughout this study by polymerase chain reaction (PCR). PCR reactions were set up as detailed in **Table 9.** Negative controls were setup with no DNA template and positive controls with a known DNA template were setup alongside PCR reactions.

Table 9: PCR reaction composition

Reagent	Concentration	Volume
Q5 reaction buffer	5 x	10 µL
Q5 High GC enhancer	5 x	10 µL
Q5 high fidelity DNA polymerase	2000 u/ml	1 µL
Forward primer	10 mM	2.5 µL
Reverse primer	10 mM	2.5 µL
dNTP mixture	10 mM	1 µL
Template DNA		<100 ng
DMSO		2.5 µL
Deionised H_2O		-
	Total volume	50 µL

PCR reactions were carried out following the reaction cycle shown in **Table 10**. Denaturation, annealing, and elongation cycles were repeated 34 times before the final elongation step.

Table 10: PCR reaction cycle conditions.

Stage	Temperature (°C)	Time (minutes:seconds)
Initial denaturation	95	3:00
Denaturation	95	0:30
Annealing	(dependant on primer Tm)	0:30
Elongation	72	1 minute per kbp
Final Elongation	72	5:00
Hold	4	∞

Primers for PCR reactions were synthesised by Integrated DNA Technologies and used at a concentration of 10 mM in the reaction. The primers used throughout this study are listed in **Table 11**.

Table 11: primers used for PCR reactions throughout this study.

Primer	Sequence
PA14_05540Gibfwd	TTTTGTTTAACTTTAAGAAGGAGATATACATATGCA TATGAGCAAGTTCTTTATTGACCG
PA14_05540Gibrev	GAGGCCCCAAGGGGTTATGCTAGTTATTGCTCAGCT TAGTGGTGGTGGTGGTGGT
PA14_44440Gibfwd	GAGGCCCCAAGGGGTTATGCTAGTTATTGCTTAGTG GTGGTGGTGGTGGT
PA14_44440Gibrev	GAGGCCCCAAGGGGTTATGCTAGTTATTGCTTAGTG GTGGTGGTGGTGGT
RNA DNA check intergenic region Fwd	AGCCCGCCTCCGCCAGTGC
RNA DNA check intergenic region Rev	GTTGCCCTCCCATGGGCACCGCG

2.8 Agarose Gel Electrophoresis

DNA samples were analysed using agarose gel electrophoresis. Gels were cast using 100mL of 1x TAE buffer in which 1 g of agarose was added and melted in a microwave. 2μL of ethidium bromide was added per 100 mL of molten gel. Gels were resolved at 90V constant for 60 minutes. Samples were prepared by adding 1 μL of 5 x loading dye per 5 μL of sample.

2.9 Gel Purification of DNA Fragments Resolved Using Agarose Gel Electrophoresis

Fragments were isolated after resolution using agarose gel electrophoresis using the Monarch ® DNA Gel Extraction Kit obtained from New England Biolabs.

Fragments to be purified were removed by excision using a sterile scalpel and transferred to a sterile 1.5 mL Eppendorf tube. Purification of DNA was carried out following the Monarch ® DNA Gel Extraction Kit protocol and DNA concentration was measured using the Nanodrop 2000c spectrophotometer.

2.10 Plasmid DNA Isolation

10mL overnight cultures of *E. coli* transformed with the plasmid of interest in LB were inoculated using a single colony from a transformation. After a 16-hour incubation at 37°C 250 RPM the cells were collected by centrifugation. Plasmid DNA was isolated

from cultures using the Wizard® Plus Minipreps DNA Purification Systems kit and following the appropriate protocol for bacterial cultures. Plasmid DNA was eluted in 50 uL of H_2O and quantified using the Nanodrop 2000c spectrophotometer.

2.11 DNA/RNA Quantification

Quantification of DNA was obtained using the Nanodrop 2000c spectrophotometer.

1 μL of DNA/RNA was loaded onto the nanodrop and the concentration was measured.

Quantification of DNA and RNA was obtained using the Qubit ™ DNA HS Assay Kit and the Qubit ™ RNA HS Assay Kit. Samples were prepared using the appropriate protocols for the kits and measured straight after preparation. Fresh standards were prepared for each new group of samples. Samples were measured on the Qubit™ fluorometer.

2.12 Preparation of Chemically Competent Cells

Chemically competent *Escherichia coli* C43(DE3) and DH5α aliquots were prepared. LB agar plates were streaked for single colonies and incubated overnight at 37 °C in a static incubator. One single colony was used to inoculate a 10 mL overnight culture in LB broth and incubated overnight at 37 °C 250 RPM.

1 mL of overnight culture was used to inoculate 50mL of LB broth in a sterile flask and incubated at 37 °C 250 RPM until the OD_{600} is between 0.4 and 0.6. The culture was decanted into a 50 mL falcon and stored on ice for 10 minutes to halt growth. The cells were pelleted by centrifugation and the supernatant was discarded. Cells were resuspended gently in 10 mL ice cold 0.1 M $CaCl_2$ and incubated on ice for 20 minutes. Cells were pelleted by centrifugation and resuspended in 0.1 M $CaCl_2$ 15% glycerol. The suspension was aliquoted into 50μL aliquots in sterile Eppendorf tubes and snap frozen using liquid nitrogen and stored immediately at -80 °C.

2.12.1 Transformation of Chemically Competent Cells

Heat shock transformations of chemically competent *Escherichia coli* C43(DE3) and DH5α were carried out. 50 μL aliquots of previously prepared chemically competent cells were removed from storage at -80°C and thawed on ice for 10 minutes. Under sterile conditions, 100 ng of plasmid DNA was added to selected aliquots and 1 μL of sterile H_2O was added to an aliquot as a negative control. Cells were incubated on ice for 18 minutes before heat shocking at 42 °C for 30 seconds and returned to ice for a further 2 minutes.

90 μL of sterile LB broth or SOC broth was added to each aliquot and the cells were left to recover for one hour at 37 °C 250 RPM. After recovery 100 μL of cell culture for each plasmid/negative control was spread on an LB plate supplemented with the

appropriate antibiotic using a sterile spreader. In some cases 100 μL of 1:10 and 1:1000 dilutions prepared using LB broth were prepared. Plates were incubated at 37 °C for 16 hours before inspection for single colonies.

2.13 Restriction Digestion of DNA

All enzymes and buffers used for restriction digests were obtained from New England Biolabs. Reaction compositions were as described in **Table 12**. Reactions were incubated at 37 °C for 2 hours before visualisation using agarose gel electrophoresis. Where double digests were carried out, one enzyme was added at the beginning of the reaction for 1 hour before the other was added before leaving the reaction for 1 more hour. Where a high efficiency of digest was required, a further 0.2 μL of enzyme was added after 1 hour of the reaction.

Table 12: restriction digest reaction composition

Component	Quantity
Restriction enzyme	0.1 units
DNA to be digested	1μg
Cutsmart buffer (10x)	5μL
Deionised H_2O	Up to 50μL

2.14 Gibson Assembly of DNA Fragments

Gibson assembly was used to assemble DNA fragments for overexpression construct generation and gene knockout plasmid construction.

Vector and insert preparation was carried out by PCR amplification followed by agarose gel fragment purification and restriction digest where necessary. Gibson Assembly reactions were carried out using the Gibson Assembly® Master Mix obtained from New England Biolabs. Reactions were set up following the kit's protocol to final reaction volumes of 10μL in 100μL tubes. Reactions were incubated at 50 °C for one hour in Bio-Rad T100 Thermal Cycler.

The entire 10 μL reaction volume was used to transform the appropriate strain of *Escherichia coli* (one aliquot was used, prepared as described above) and plated on LB agar plates supplemented with the appropriate antibiotic. 5 single colonies from each transformation were used to inoculate 10 mL overnight cultures and plasmid was purified from each culture and screened using restriction digest and PCR amplification.

2.15 Growth of Cultures for RNA Isolation

2.15.1 Growth of BMA, Styrene and Ethylbenzene Cultures for RNA Isolation

Single colonies of *Pseudomonas aeruginosa* PA14 were obtained by streaking from a cryostock onto an LB agar plate and incubating in the static incubator at 37 °C for 16 hours. Using single colonies obtained from this plate, 10 mL overnight cultures in MSX minimal media were inoculated and incubated for 16 hours overnight at 37 °C 250 RPM.

50mL cultures in the MSX minimal media were inoculated using the overnight cultures to a starting OD_{600} of 0.05 in 250 mL flasks. Cultures were incubated at 37°C 250 RPM and the OD_{600} was measured periodically until the cells reached an OD_{600} between 0.7 and 0.8.

When at the correct OD_{600} was obtained, 4 x 2 mL samples of culture were transferred to a 2 mL tube for the negative control. Cells were pelleted at 4°C using the Thermo Scientific Medifuge Small Benchtop centrifuge at 4,900 RPM for 5 minutes and both pellets were resuspended in one fresh tube containing 500 µL of RNALater. Nonstick, RNAse-free 2.0 mL microfuge tubes obtained from Invitrogen were used for all culture collection for RNA isolation.

BMA, styrene and ethylbenzene were added to the cultures to obtain final overall concentrations of 20 % BMA, 10 mM styrene and 10 mM ethylbenzene and cultures were returned to the incubator for 15 minutes before taking samples as described for the control samples.

2.15.2 Growth of Ivacaftor and Kaftrio Cultures for RNA Isolation

Kalydeco tablets containing 150 mg ivacaftor and Kaftrio tablets containing 75 mg ivacaftor, 50 mg tezacaftor and 100 mg elexacaftor were obtained from Vertex Pharmaceuticals through collaborators at the Queen Elizabeth University Hospital, Glasgow.

Stock solutions were freshly prepared from tablets. Tablets were weighed using the ABS analytical microbalance and ground using a pestle and mortar to obtain a homogenous thin powder before dissolving in DMSO. The mass of ground tablet required to generate stock solutions are shown in **Table 13**. To recreate the reported blood serum concentration of ivacaftor of 0.001 mg/mL a stock solution of 10,000 x (10 mg/mL) concentration was prepared.

Table 13: an overview of the weights and API composition of Kalydeco and Kaftrio used to determine stock solution composition

Tablet Type	Active Pharmaceutical Ingredient (API)	Mass of one Tablet (mg)	Mass of Tablet Required for 10mg Ivacaftor (mg)	Mass of Tablet Required in 10mLs DMSO to obtain 10mg/mL stock solution (mg)
Kalydeco	Ivacaftor	562	37.46	374.6
Kaftrio	Ivacaftor, tezacaftor, elexacaftor	501	66.8	668

50mL cultures of the Mueller Hinton broth were inoculated using the overnight cultures to a starting OD_{600} of 0.05 in 250mL flasks. Cultures were incubated at 37°C 250 RPM and the OD_{600} was measured periodically until the cells reached an OD_{600} between 0.7 and 0.8.

When this OD_{600} was obtained, 500 µL of DMSO was added per 50 mL of culture to the control flasks and incubated for a further 30 minutes before samples were taken. 4 x 2mL samples of culture were transferred to a 2 mL tube and cells were pelleted at 4°C. Both pellets were resuspended in one fresh tube containing 500 µL of RNALater and stored at 4°C until ready for RNA extraction. Nonstick, RNAse-free 2.0 mL microfuge tubes obtained from Invitrogen were used for all culture collection for RNA isolation.

When the correct OD_{600} of 0.7-0.8 was obtained, stock solution was added to cultures as previously described for the negative control. 5µL of stock solution per 50 mL of culture was added to the 1 x ivacaftor and 1 x Kaftio cultures supplemented with 495 µL of DMSO per 50 mLs of culture to normalise the volume of DMSO across all cultures. 500 µL of stock solution was added to the 100x ivacaftor and Kaftrio cultures per 50 mL of culture. 4 x 2 mL samples of culture were transferred to a 2 mL tube and cells were pelleted at 4°C. Both pellets were resuspended in one fresh tube

containing 500 µL of RNALater and stored at 4°C until ready for RNA extraction. All cultures were performed in quadruplicate.

2.16 RNA Extraction and DNase Treatment

All RNA work was carried out in a microbiological safety cabinet (MSC) cleaned thoroughly with 70 % ethanol solution followed by RNAseZap™ RNAse Decontamination Solution using blue roll. The Sigma 1-14K microfuge required for column purification steps was moved into the MSC and decontaminated with the rest of the cabinet as previously described. Starlab filter tips were used for all RNA work and only fresh bags of unopened 1.5 mL Eppendorf tubes and 2mL RNase free tubes (Thermo Fisher Scientific) were used. Reagents and equipment were thoroughly cleaned with RNAseZap™ RNAse Decontamination Solution before entering the MSC.

4 mL culture samples pelleted and resuspended in 500 µL of RNAlater were removed from 4 °C storage and spun down in the Sigma 1-14K microfuge at maximum speed for 3 minutes at 4 °C. Samples were resuspended in 700 µL TRIzol™ RNA Isolation Reagent and RNA was isolated using the TRIzol™ Plus RNA Purification Kit following the user guide. During purification, RNA was DNase treated using the PureLink™ DNase Set as described in the TRIzol™ Plus RNA Purification Kit following the user guide. RNA was checked for DNA contamination by PCR using primers designed to amplify a region of intergenic *Pseudomonas aeruginosa* DNA and products were

visualised using agarose gel electrophoresis as compared to a positive control using PA14 gDNA as a PCR template. RNA was eluted in 20 µL of RNase free H_20 and stored at -80 °C. The integrity of RNA after isolation was evaluated using the Agilent 2100 Bioanalyzer. 1 µL of each sample was loaded into each sample well of an RNA 6000 Nano Chip. Chips were prepared using the RNA 6000 Nano Kit. RNA integrity numbers (RINs) were obtained and RNA electropherograms and gels were inspected before proceeding to rRNA depletion.

2.17 Analysis of Illumina Sequencing Data using Galaxy Europe

To analyse the reads from Illumina sequencing, a variety of programmes were used through Galaxy Europe (Afgan et al. 2018). All reads were trimmed using TrimGalore! (Kreuger, 2021) and aligned to the *Pseudomonas aeruginosa* PA14 genome using HISAT2 (Kim, Langmead, and Salzberg 2015). The number of aligned reads mapping to features on the chromosome were counted using Htseq-count (Anders, Pyl, and Huber 2015) and the differential expression of genes in each solvent treated condition was calculated based on the control samples using DESeq2 (Love, Huber, and Anders 2014).

2.18 Overexpression of Membrane proteins using *E. coli* C43(DE3)

An overnight culture was used to inoculate overexpression cultures to obtain a starting optical density of OD_{600} 0.05. Overexpression cultures were incubated in sterile conical flasks of various sizes depending on culture volume.

Overexpression cultures of various volumes, media compositions, IPTG concentrations (IPTG was prepared fresh for each overexpression by dissolving in deionised H_2O and filter sterilising using a filter with a pore size of 22 microns), incubation times and incubation temperatures were carried out. Cultures always had a final concentration of 100 µg/mL carbenicillin. Where protein overexpression was being induced by the addition of IPTG, the cultures were grown to an OD_{600} of 0.6 when sterile IPTG stocks were added to achieve the appropriate IPTG final concentration.

2.19 Overexpression Culture Cell Lysis

After overexpression, cell cultures were aliquoted into 200mL samples and pelleted at 4000 RPM. The supernatant was discarded and each pellet was resuspended in 5mL membrane protein stabilisation lysis buffer. The solution was incubated at room temperature on the rotating wheel for 2 hours to lyse the cells. Cell debris was pelleted at 4000 RPM for 20 minutes and the supernatant was analysed either by SDS PAGE gel or western blot.

2.20 SDS PAGE Analysis

In this study protein size was determined by resolving proteins using sodium dodecyl sulphate-polyacrylamide gel electrophoresis (SDS PAGE). All SDS PAGE gels used in this study were hand cast. SDS PAGE gel composition for 4 gels 10% acrylamide is detailed in **Table 14**.

Table 14: SDS PAGE gel composition

Separating Gel			**Stacking Gel**	
Component	Volume (mL)		Component	Volume (mL)
Acrylamide	6.5		Acrylamide	1.5
Solution 2	5		Solution 3	2.5
H_2O	8.5		H_2O	6
10% APS	200µL		10% APS	100µL
TEMED	20µL		TEMED	10µL

Glass moulds were set up using the Bio-Rad hand cast gel system and filled with water prior to casting to check the system for leaks. Once the systems were confirmed as watertight, the water was drained from the systems and the moulds were filled to ¾ volumes with separating solution using a stripette gun. 500 µL of isopropanol was pipetted over the separating solution to straighten the top of the gel and the gels were left at room temperature to set. Once set, the isopropanol was removed, and the mould washed with water before filling with stacking solution to the top with a stripette gun and the well mould added and left to set. Once set, gels were wrapped in damp tissue and sealed using foil wrap to prevent drying and stored at 4 ºC until used.

SDS PAGE gels were used to visualise protein samples. 7 µL of New England Biolabs protein ladder was always loaded in the first well of all gels. 20 µL of sample was mixed with 5 µL of 5x SDS loading dye supplemented with fresh B-mercaptoethanol before loading onto the gel. Gels were run using the Bio-Rad Mini PROTEAN Tetra Vertical Electrophoresis system for 1 hour at 150V.

After running, gels were added to gel stain buffer and left to stain overnight. The next day, destain was added to gels for 20 minutes and the gels washed with water and added to fresh water for a day to rehydrate before visualising using the protein gel doc.

2.21 Sonication

Sonication was carried out using the Bioruptor Plus Sonicator. Cells were kept on ice at all times in 50 mL falcon tubes. Using 50 % amplitude, cells were pulsed for 3 minutes pulsing for 10 seconds on and 10 seconds off continuously. The tip was never allowed to touch the side of the falcon tube. After pulsing, the cell debris was pelleted and the lysate visualised using SDS PAGE.

2.22 Western Blotting

Western blotting was used to confirm the existence of histidine tagged membrane proteins from overexpression cultures.

Two identical SDS PAGE gels were resolved of the samples to be visualised. One was stained as normal and protein was transferred from the other SDS GEL to PDVF membrane using the semi dry transfer system.

To prepare for protein transfer, 6 pieces of Wattman paper were cut with dimensions 8.5 x 6.5 cm. One piece of PDVF membrane was also prepared at the same size, care was taken to only handle the membrane by tweezers at the very edge at all times. The PDVF membrane was activated by soaking in ethanol for one minute before moving to transfer buffer for equilibration for 10 minutes. Whatman paper was also equilibrated in transfer buffer for 1 minute. Three pieces of Whatman paper were removed from transfer buffer and stacked on the semidry transfer system, followed by the PDVF membrane, SDS PAGE Gel, and finally the 3 remaining pieces of

Whatman paper on top. The sandwich was pressed to remove any air bubbles and the lid was placed on top. A heavy bottle was always placed on top of the lid to keep the sandwich compressed inside the system. The semi dry transfer system was run for 30 minutes 221 mA constant.

The PDVF membrane was removed from the semi dry transfer system and placed in TBS-T 5% milk to block for one hour, before adding 2.5 µL and leaving overnight to incubate at 4 ºC on a shaking platform. After the overnight incubation the membrane was washed thoroughly with TBS-T to remove all primary antibody by rinsing and shaking with TBS-T for 15 minutes 3 times. Fresh TBS-T 5 % milk was then added and 2.5 µL of secondary antibody was added and incubated at room temperature for 2 hours. The container was wrapped with metal foil to protect the membrane from light as the secondary antibodies are light sensitive. The membrane was then thoroughly washed as before and visualised using the LICOR system.

3 Results Chapter 1: The Biochemical Characterisation of CopA2 and MexB from *Pseudomonas aeruginosa*

3.1 Introduction

3.1.1 Identifying Methacrylate Ester Tolerance Conferring Systems in *Pseudomonas aeruginosa* PA14

One of the problematic bottlenecks in methacrylate ester bioproduction is the toxicity of these compounds to production strains such as *E. coli* (Ingenza Ltd, personal communication). Identification of systems within the host strain which confer tolerance to these products and their subsequent exploitation could prove as a useful strategy in production strain development (Dai and Nielsen 2015; Nanda, Kumar, and Sharma 2019). In 2017, Dr Walid El Bestawy carried out a BMA sensitivity transposon mutant library screen in the Tucker lab at the University of Strathclyde to identify possible tolerance conferring systems within *Pseudomonas aeruginosa* PA14 at the University of Strathclyde.

3.1.2 A Transposon Mutagenesis Methacrylate Ester Sensitivity Assay Has Identified Systems Which Confer *n*-Butyl Methacrylate Tolerance

The transposon mutagenesis sensitivity assay carried out by Walid El Bestawy has provided evidence that specific systems play a role in methacrylate ester tolerance in *P. aeruginosa* PA14 (Bestawy 2017a; Liberati et al. 2006). During this experiment, over 6000 strains of *P. aeruginosa* PA14 were subjected to growth in the presence and absence of the methacrylate ester *n*-butyl methacrylate (BMA). Each PA14 strain had a transposon insertion within one gene resulting in the downregulation or complete silencing of that gene. Growth of strains with and without BMA was

measured by the difference in the area under the growth curve (AUC) and the difference in AUC between conditions was measured (**Table 3**).

Several transposon mutant strains of PA14 showed a reduction in AUC when BMA was present. This decrease in growth was suggestive of a reduction in BMA tolerance which could be attributed to the disrupted gene containing the transposon insertion within that *P. aeruginosa* strain.

3.1.3 The MexAB-OprM and Cbb_3 Cytochrome Oxidase Systems Play a Role in BMA Tolerance

Δ% AUC in the presence and absence of BMA for each transposon insertion mutant was calculated and is described in **Table 3**. This data shows that from the strains with the highest Δ% AUC, 6 of the top 7 strains correspond to transposon insertions within genes which all belong to the MexAB-OprM multidrug efflux pump or the Cbb_3 cytochrome oxidase assembly system. The large decrease in growth of these transposon mutant strains in the presence of BMA is suggestive that the MexAB-OprM and Cbb_3 cytochrome oxidase systems provide a level of tolerance to BMA in *P. aeruginosa* PA14.

3.1.4 The Transposon Mutagenesis Results May Suggest a Functional Relationship Between MexAB-OprM and the Cbb_3 Cytochrome Oxidase Systems

In this study, we hypothesise that when BMA is present within *P. aeruginosa* cell culture the MexAB-OprM multi-drug efflux pump extrudes BMA from the periplasmic space and the cell membrane. We hypothesise that the Cbb_3 cytochrome oxidase system is responsible for the maintenance of the PMF required to power the efflux of BMA from the cell through the highly energy intensive process of extrusion through MexAB-OprM.

Investigating the functional relationship between these systems and how this plays a role in methacrylate ester tolerance will provide valuable targets for production strain improvement. This will also aid in the understanding of the response of *P. aeruginosa* PA14 to other toxic substances such as antimicrobials or therapeutics which could be useful from a clinical perspective and provide possible new drug targets. Gaining an insight into *P. aeruginosa* bacterial energetics under stressful conditions could provide answers to why this microorganism is such a successful pathogen.

3.1.5 The Biochemical Characterization of These Systems Will Provide an Insight into the Bacterial Energetics of *P. aeruginosa*

The biochemical characterisation of these systems will be determined throughout this study, and the implications this has for *Pseudomonas aeruginosa* PA14 BMA tolerance will be investigated. The aim of this study is to express and purify *P. aeruginosa* MexB and CopA2 from *Escherichia coli* C43(DE3) and measure the translocation of proxy substrates through these systems using SSME technology.

In order to develop an assay to measure transport of substances through these systems quantitatively, a technique called solid supported membrane electrophysiology (SSME) will be used (Bazzone et al. 2013). This technology can detect minute charge translocation across biological membranes using proteoliposome systems, providing precise quantitative transport kinetics of membrane proteins (Bazzone, Barthmes, and Fendler 2017). This will allow for the development of an *in vitro* assay for transport measurement, where variables such as substrate, substrate concentration and pH can be easily altered to gather valuable transport kinetics data for each transport protein under a range of conditions (**Figure 7**).

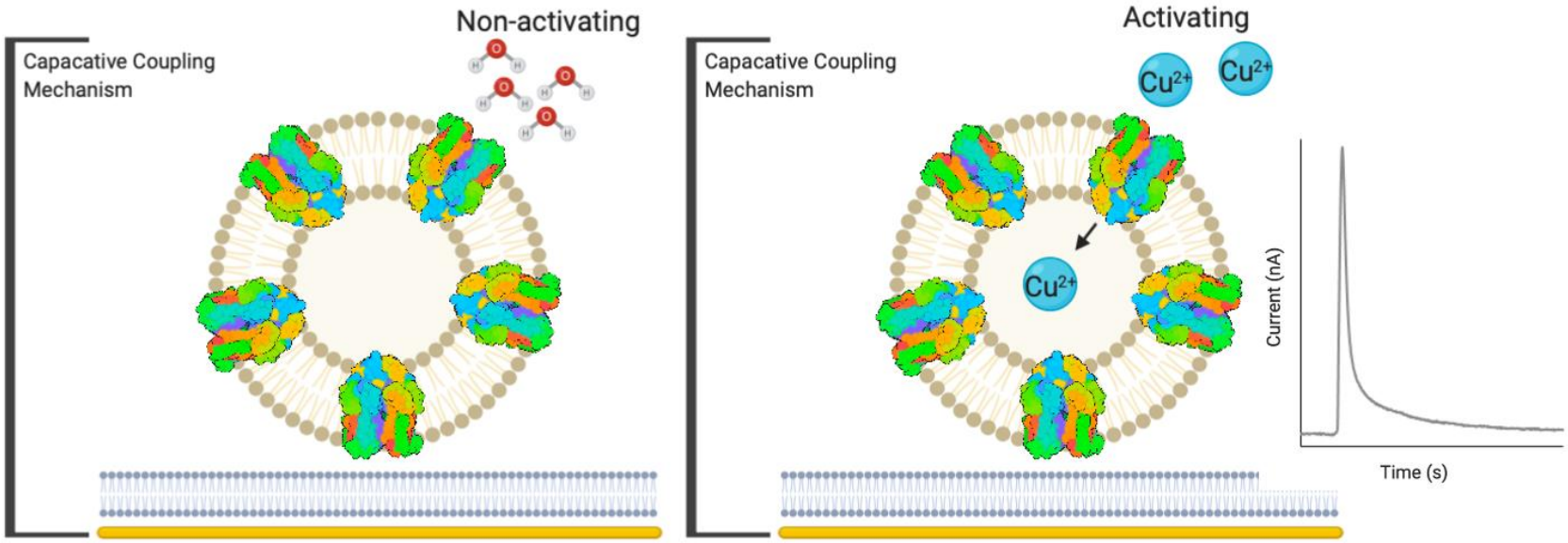

Figure 7: **Representation of charge transport measurement using SSME technology.** Proteoliposomes are shown with MexB reconstituted. Proteoliposomes are loaded onto a gold sensor chip, creating a double capacitance system. Non activating (left) and activating (right) solution are passed over the proteoliposomes. The non-activating solution is a neutral solution, and the activating solution contains substrate. Transport of charged substances into the proteoliposome is measured through the double capacitance system and shown as a trace. Using several traces, valuable enzyme kinetics can be calculated for the protein systems used.

BMA is not a charged substance, and therefore SSME cannot be used to directly measure the transport of the monomer through these protein systems. However, analysis of transport of similarly sized and shaped molecules may provide an insight into how the MexAB-OprM complex actively transports this substance out from the cell. The effect of different ranges of proton gradients across the membrane on MexAB-OprM transport will be measured by altering the pH inside the proteoliposomes. In the case of the Cbb_3 proteins, important quantitative analysis of the proton gradient generated by ATP hydrolysis can be obtained, which may give insights into the relationship between Cbb_3 and MexAB-OprM in relation to proton motive force.

SSME analysis has not been carried out on either of these systems before, and so the quantitative insights into the transport and enzyme kinetics of MexAB-OprM and Cbb_3 will be significant. In the wider context of methacrylate ester tolerance, an understanding of how these systems interact to provide a level of tolerance in *Pseudomonas aeruginosa* will be valuable for the development of a production strain. As MexAB-OprM is also an important protein in the clinic, this information could provide important insights into how multidrug resistant infections are treated and how novel therapeutics can be developed.

3.2 Results

3.2.1 Cloning of Overexpression Plasmids for Expression of MexB and CopA2 in *Escherichia coli* C43(DE3)

To biochemically characterise MexB and CopA2, constructs for their overexpression were generated using the overexpression vector pET21a+ by Gibson assembly (**Figure 8**).

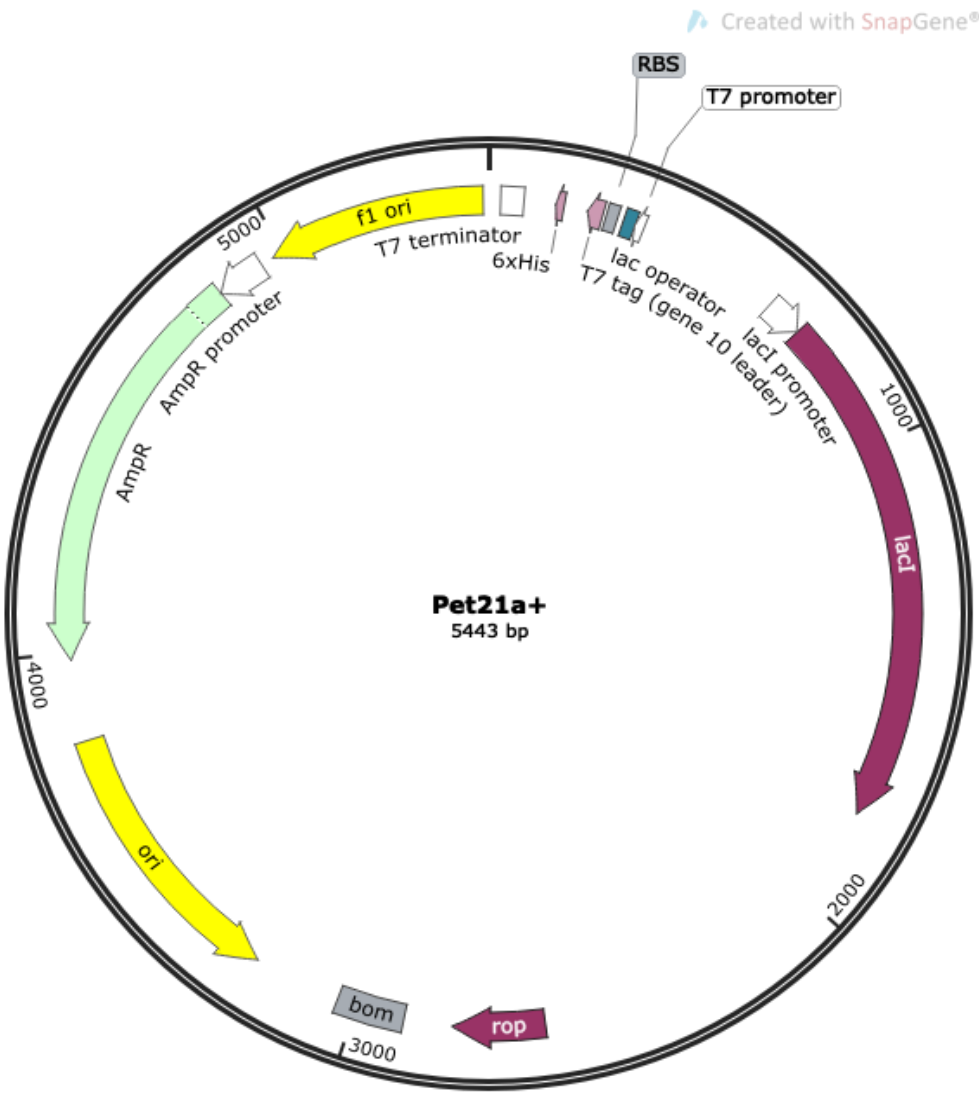

Figure 8: Plasmid map of the overexpression vector pET21a+. pET21a+ was used in this study for the expression of MexB and CopA2 in *Escherichia coli* C43(DE3). This vector utilises the T7 viral overexpression system controlled by the *lac* operator system to allow for inducible expression of proteins in the presence of lactose or IPTG. The vector contains an ampicillin resistance cassette to ensure the plasmid is maintained in the presence of ampicillin.

Plasmids containing sequences for the genes MexB and CopA2 which were codon optimised for *Escherichia coli* were obtained from Ingenza Ltd. Primers PA14_MexBGibFwd, PA14_MexBGibRev, PA14_CopAGibFwd and PA14_CopAGibRev were used to amplify both genes via polymerase chain reaction (PCR) using Q5 high fidelity polymerase. During DNA amplification histidine tags and tobacco etch virus (TEV) protease cleavage sites were incorporated onto the C terminus of each protein. Blunt overhangs complimentary to the pET21a+ vector were also incorporated and the resulting PCR products were visualised using agarose gel electrophoresis (**Figure 9**).

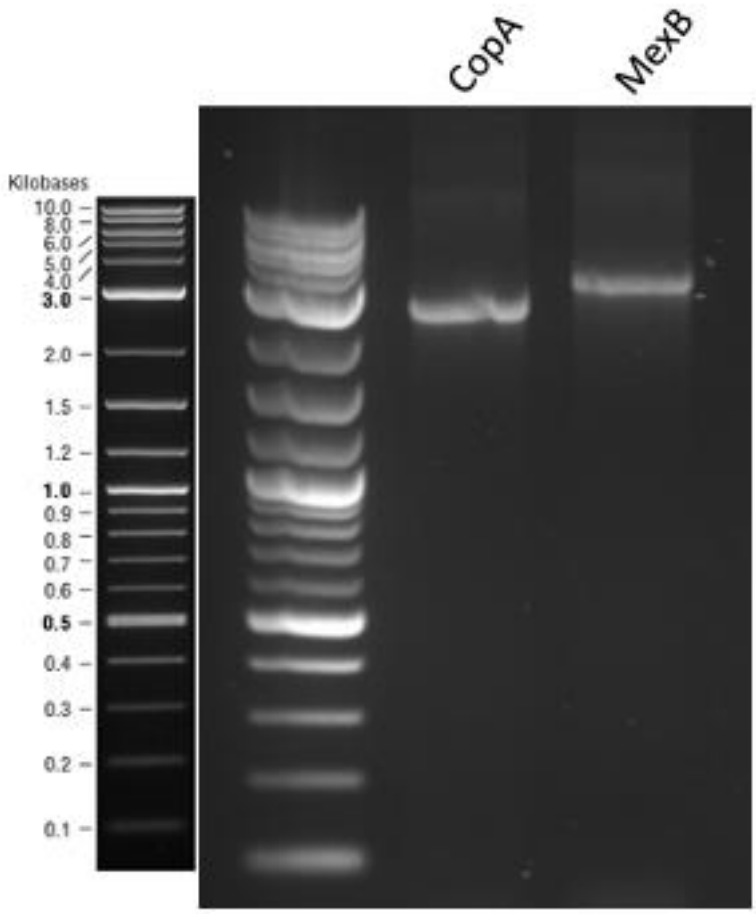

Figure 9: PCR extension of CopA and MexB for Gibson Assembly. Fragments of 2.3Kbp for CopA2 and 3.2Kbp for MexB genes are observed, confirming the genes were fully amplified.

Linearised pET21a+ was obtained via PCR and restriction digested using the enzymes BlpI and NdeI. *MexB* and *copA2* genes amplified using PCR were cleaned up and Gibson assembly reactions for each gene were setup (**Figure 10**). The resulting plasmids were named pETER1 and pETER2 for CopA2 and MexB respectively (**Figure 11**). Overexpression constructs were created for each gene and the resulting plasmids were used to transform *Escherichia coli* DH5α chemically competent cells.

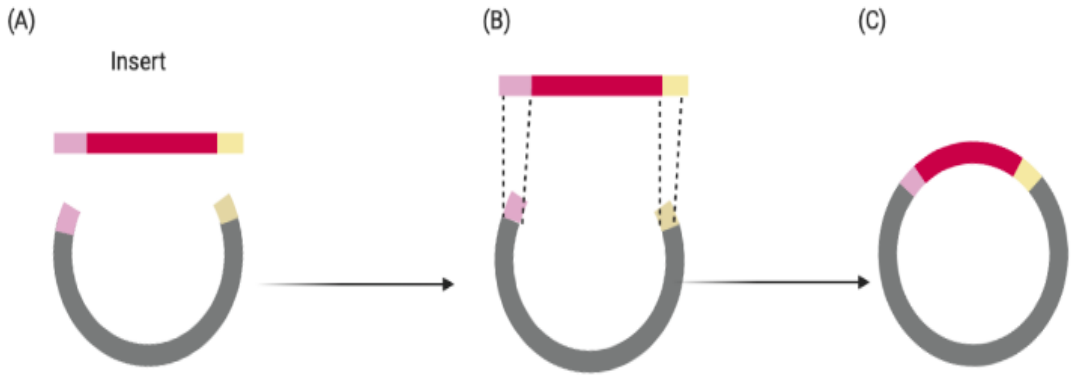

Figure 10: Schematic of the principle of a Gibson assembly reaction. (A) Insert DNA is amplified using PCR to obtain ends which are complimentary to the ends of the linearized vector backbone. (B) Insert and vector DNA are added to Gibson assembly mastermix containing T5 exonuclease to chew back blunt ends and generate cohesive overhangs, Q5 DNA polymerase to fill any gaps in the DNA, and T4 DNA ligase to anneal DNA fragments together.

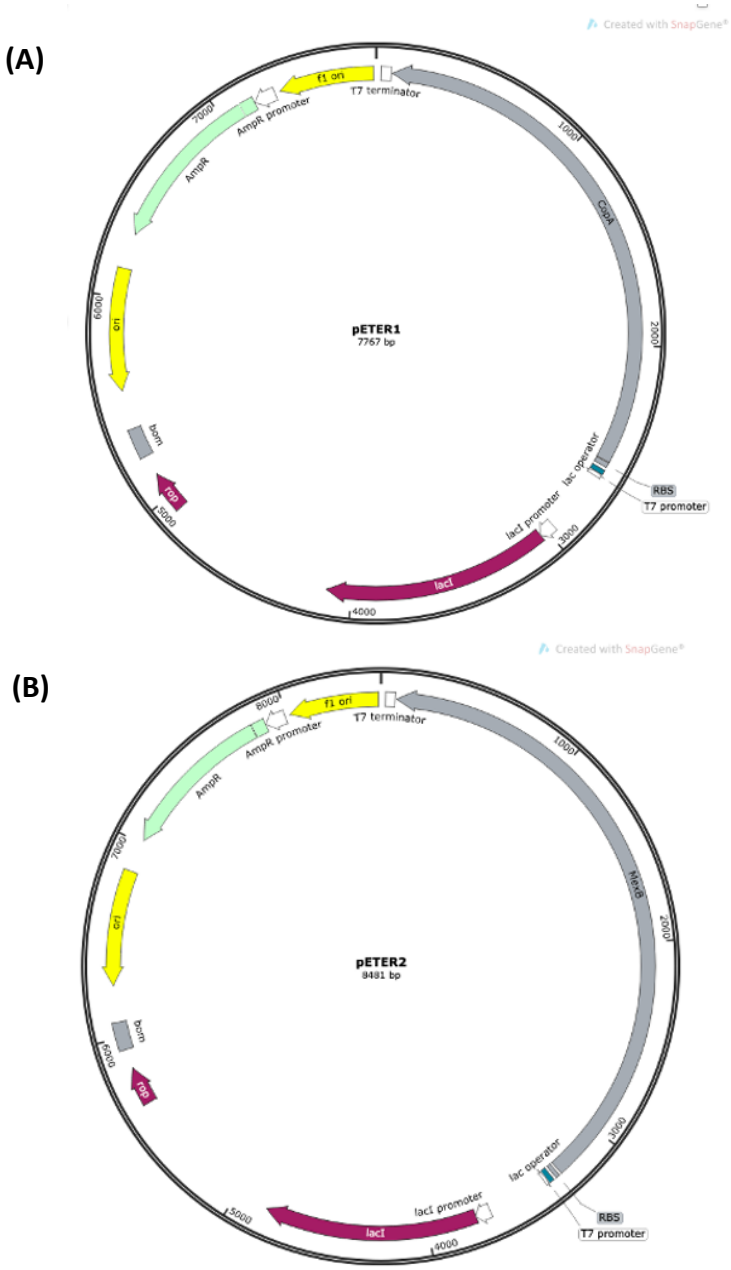

Figure 11:Overexpression Constructs (A) pETER1 (CopA) and (B) pETER2 (MexB). The pET21a+ overexpression vector utilises the T7 viral expression system which results in a high level of protein expression. the T7 system is under the control of the Lac operator meaning protein overexpression can be induced by either lactose or IPTG. Genes *copA2* and *mexB* are annotated in grey.

Single colonies of transformed *E. coli* DH5α were used to inoculate 10 mL overnight cultures of LB broth supplemented with ampicillin and incubated at 37°C 220RPM overnight. Plasmid DNA was purified from overnight cultures and restriction digested to confirm the Gibson assembly was successful (**Figure 12**). Purified plasmid was sanger sequenced by Eurofins Genomics to confirm successful Gibson assembly and maintenance of the correct gene sequences for Copa and MexB on the pET21a+ vectors.

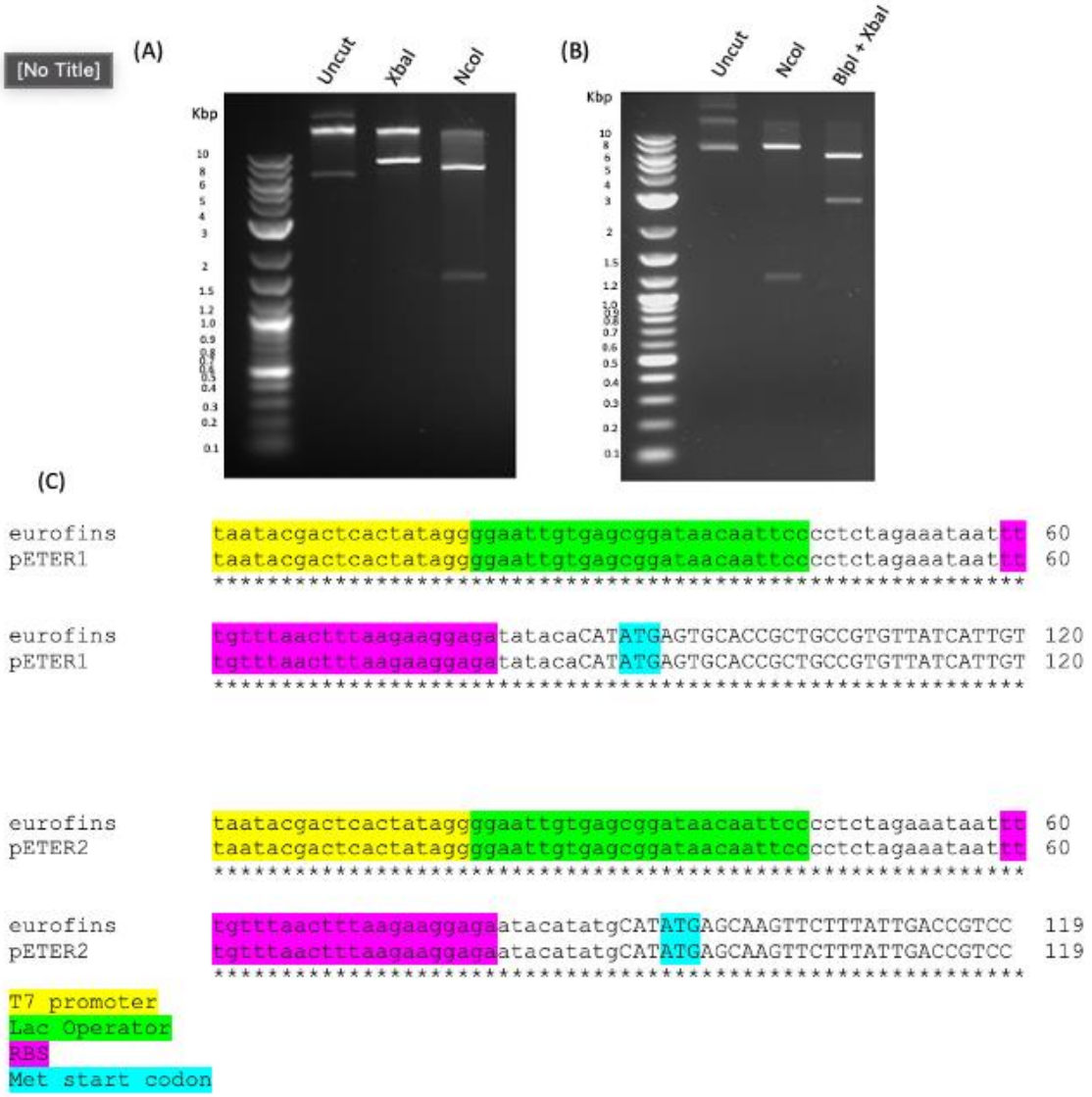

Figure 12: Restriction digest map of the (A) CopA2 overexpression plasmid pETER1 (B) the MexB overexpression plasmid pETER2 (A) Uncut pERTER1 plasmid, pETER1 plasmid cut with XbaI to linearise, and pETER1 plasmid cut with NcoI which has liberated a fragment of 1.5Kbp (B) Uncut pETER2 plasmid, pETER2 plasmid cut with NcoI to liberate a fragment of 1.2 kbp, and pETER2 plasmid cut with BlpI and XbaI to liberate a fragment of 2.7 kbp (C) eurofins sequencing results of pETER1 and pETER2 aligned with the reference sequence over the T7 promoter showing the sequence is correct and in frame with the T7 promoter

3.2.2 Optimisation of Overexpression of Membrane Proteins in C43(DE3) *Escherichia coli*

To biochemically characterise the proteins MexB and CopA2, plasmids pETER1 and pETER2 were used to express these proteins in *E. coli* C43(DE3). This strain of *E. coli* has been engineered for overexpression of membrane proteins at non-toxic levels and was used for all membrane protein expression throughout this study. *E. coli* C43(DE3) possesses the T7 polymerase gene cassette (DE3) compatible with the T7 promoter present on the pET21a+ overexpression constructs pETER1 and pETER2 (Dumon-Seignovert, Cariot, and Vuillard 2004). To determine whether expression of membrane proteins MexB and CopA2 were induced using the plasmids pETER1 and pETER2, overexpression cultures were run testing a range of conditions and the protein content of these cultures was analysed by SDS PAGE.

3.2.2.1 Lysis of Overexpression Cultures Using a Boiling Method

To determine whether expression of CopA2 and MexB could be induced in *E. coli* C43(DE3) using the pETER1 and pETER2 plasmids, 100 mL cultures were inoculated with *E. coli* C43(DE3) transformed with pETER1 and pETER2 plasmids to generate the strains *pETER1* and *pETER2* respectively. When the cultures reached an OD_{600} of 0.6 they were induced with IPTG at varying final concentrations. IPTG cannot be metabolised by *E. coli* and therefore should activate continuous induction of the T7 overexpression system. Cultures were incubated with IPTG for 6 hours before

samples were taken and lysed using the boiling technique described in the methods and the protein content of the cultures was analysed using SDS PAGE (**Figure 13**).

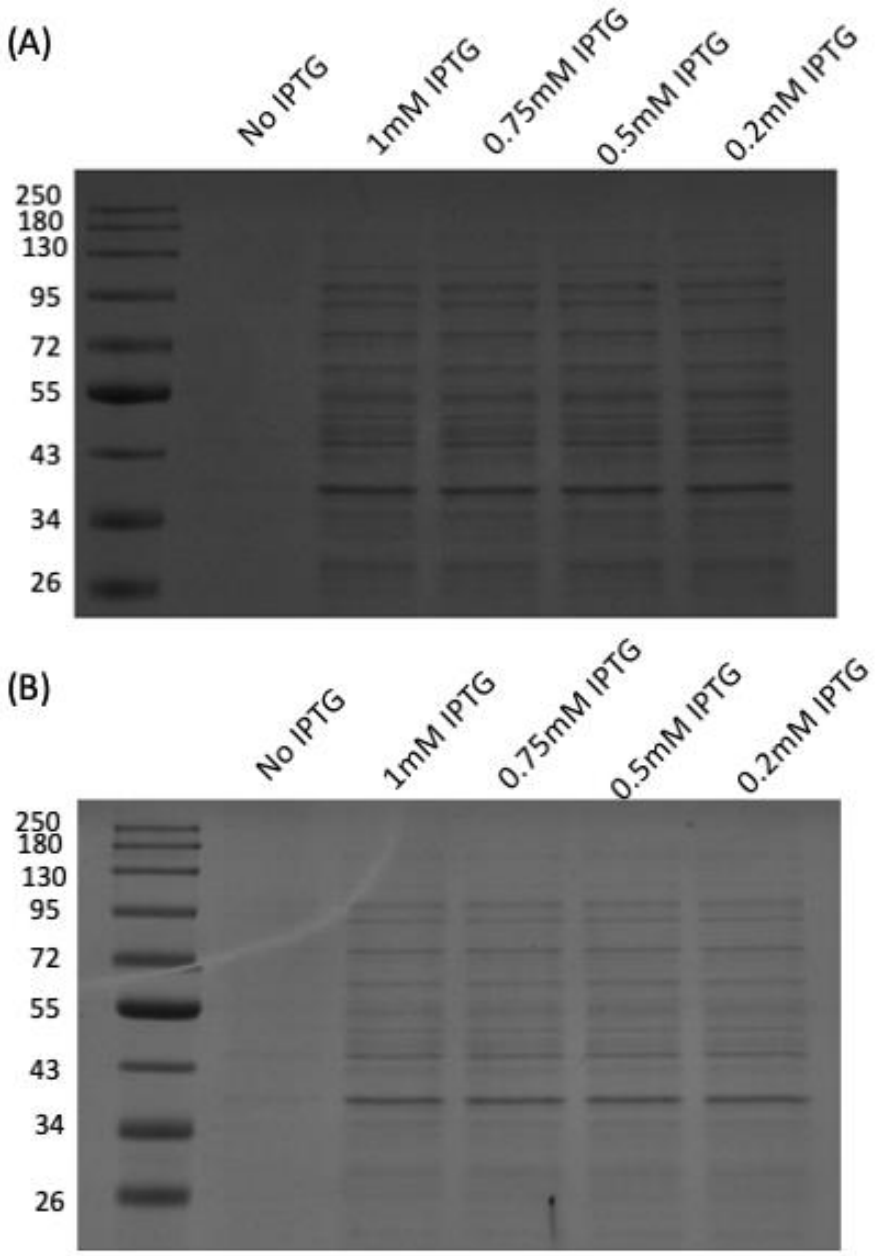

Figure 13: SDS PAGE analysis of lysed cell cultures (A) *pETER1*, the CopA2 expression strain and (B) *pETER2*, the MexB expression strain after a 6-hour incubation. Cultures were grown to an OD_{600} of 0.6 before the addition of IPTG at final concentrations of 1 mM, 0.75 mM, 0.5 mM and 0.2 mM.

Using SDS PAGE, CopA2 should resolve at a size of 90 KDa and MexB should resolve at 95 KDa. If protein overexpression was achieved, it would be expected that a large band corresponding to the correct sized for each protein would be present in the IPTG induced cultures which would be faint or absent in the uninduced control. As **Figure 13** shows, protein bands in the uninduced control sample appear very faint. However, as the bands present in the induced samples can be seen in the control samples, and they are present in both *pETER1* and *pETER2* cultures it is assumed they are naturally occurring. Therefore, no protein overexpression is observed.

To determine whether a longer incubation time after IPTG addition would result in protein overexpression, cultures were set up as previously described and incubation after IPTG addition was extended from 6 hours to 16 (**Figure 14**).

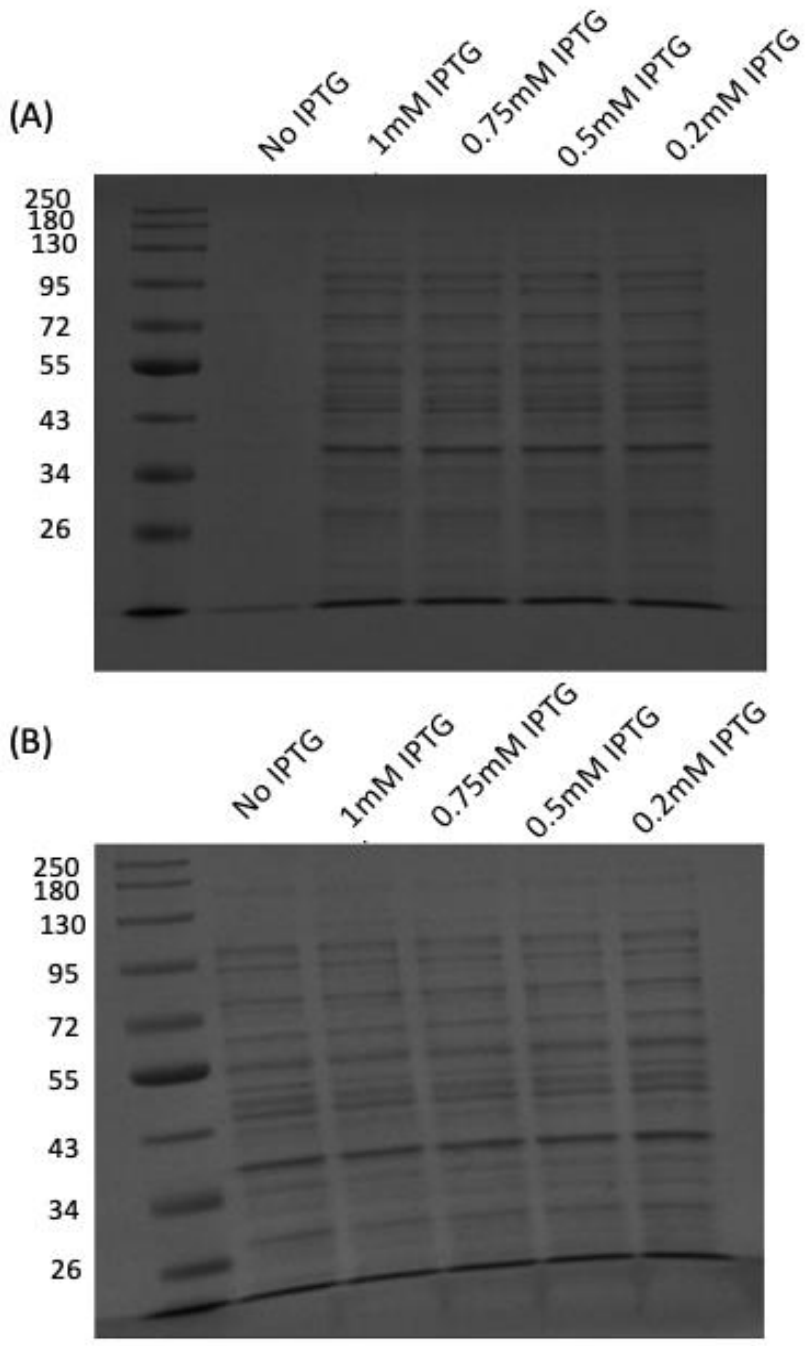

Figure 14: **SDS PAGE analysis of lysed cell cultures (A) *pETER1*, the CopA2 expression strain and (B) *pETER2*, the MexB expression strain after a 16-hour incubation.** Cultures were grown to an OD_{600} of 0.6 before the addition of IPTG at final concentrations of 1 mM, 0.75 mM, 0.5 mM and 0.2 mM.

As before, **Figure 14** shows that the uninduced controls for both *pETER1*and *pETER2* overexpression cultures show only faint bands of protein and there are no significant bands present at the corresponding sizes expected for CopA2 and MexB proteins and so no overexpression was observed.

3.2.3 Lysis of Overexpression Cultures Using Sonication

To determine whether protein overexpression was in fact occurring, but the method of cell lysis by boiling in SDS loading dye was not efficient, a different method was trialled. Overexpression cultures were setup as previously described, but instead of boiling the cultures in SDS loading dye cells were subjected to sonication before SDS PAGE analysis (**Figure 15**). A positive control was used which has been visualised using the same overexpression culturing method, EcAmtB. EcAmtB should resolve using SDS PAGE at the same size expected for CopA- ~ 95 kDa.

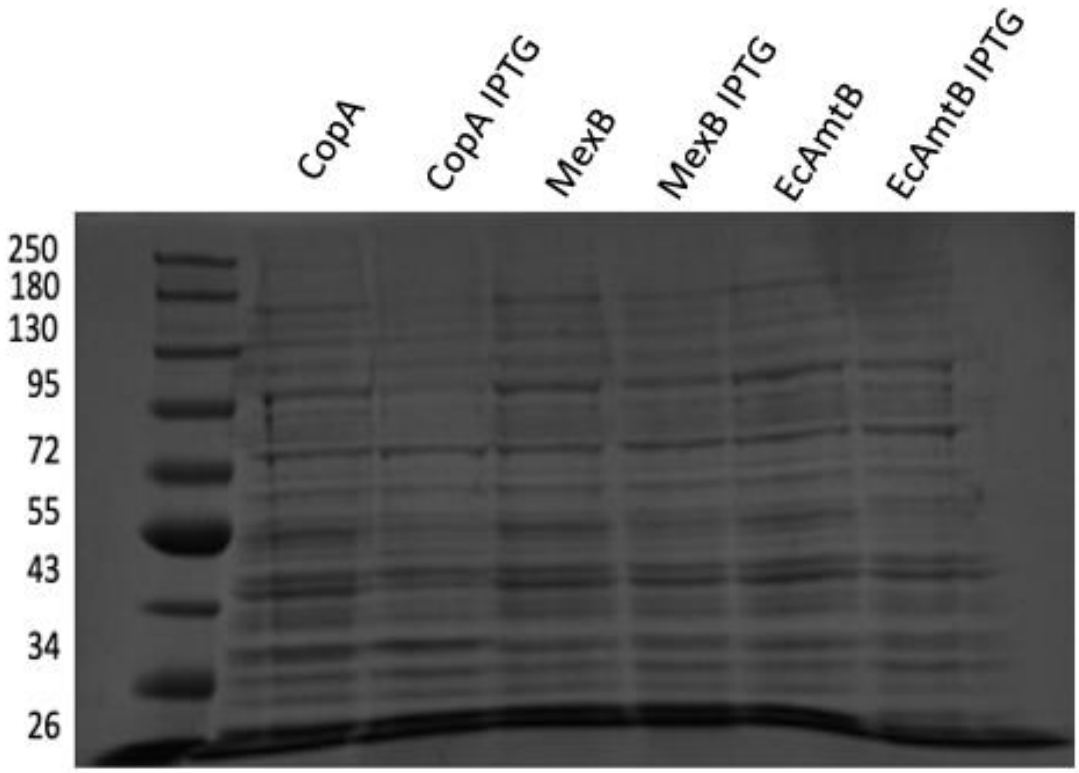

Figure 15: **SDS PAGE analysis of cell cultures lysed by sonication of *E. coli* C43(DE3) transformed with pETER1, the CopA2 expression plasmid pETER2, the MexB expression plasmid and an overexpression plasmid for the bacterial ammonium transporter EcAmtB.** Cultures were setup as previously described with a 16-hour incubation with IPTG at a final concentration of 1 mM.

No overexpression of CopA, MexB or EcAmtB is observed using SDS PAGE when the cultures are lysed by sonication, even in the positive control protein EcAmtB (**Figure 15**). Sonication was therefore disregarded as a lysis tool for analysis of overexpression cultures.

3.2.4 Using an Alternative Method of Induction for the Overexpression of CopA and MexB

To try and generate overexpression of CopA2 and MexB from *E. coli* C43(DE3) an alternative method of induction was trialled. Autoinduction media negates the need for IPTG addition into the cell culture media once a high cell density has been obtained within the culture. The media contains glucose which is the preferred carbon source for *E. coli* and lactose which is an inducer of the T7 overexpression system. Using autoinduction media the cells use glucose as the preferred carbon source- allowing the culture to reach a high cell density before the glucose content of the media is exhausted. Once the cells have used up the glucose content of the media, lactose is taken up by the cells and the T7 overexpression system is activated and should result in protein overexpression.

To determine whether protein overexpression detectable by SDS PAGE analysis could be induced using autoinduction media, 100 mL cultures were setup using autoinduction media and inoculated using a fresh overnight culture to obtain a starting OD_{600} of 0.05 and incubated at 37 °C for 19 hours. Cultures were lysed using

the boiling method previously described and the protein content of the cultures analysed using SDS PAGE (**Figure 16**). As before, EcAmtB was used as a positive control.

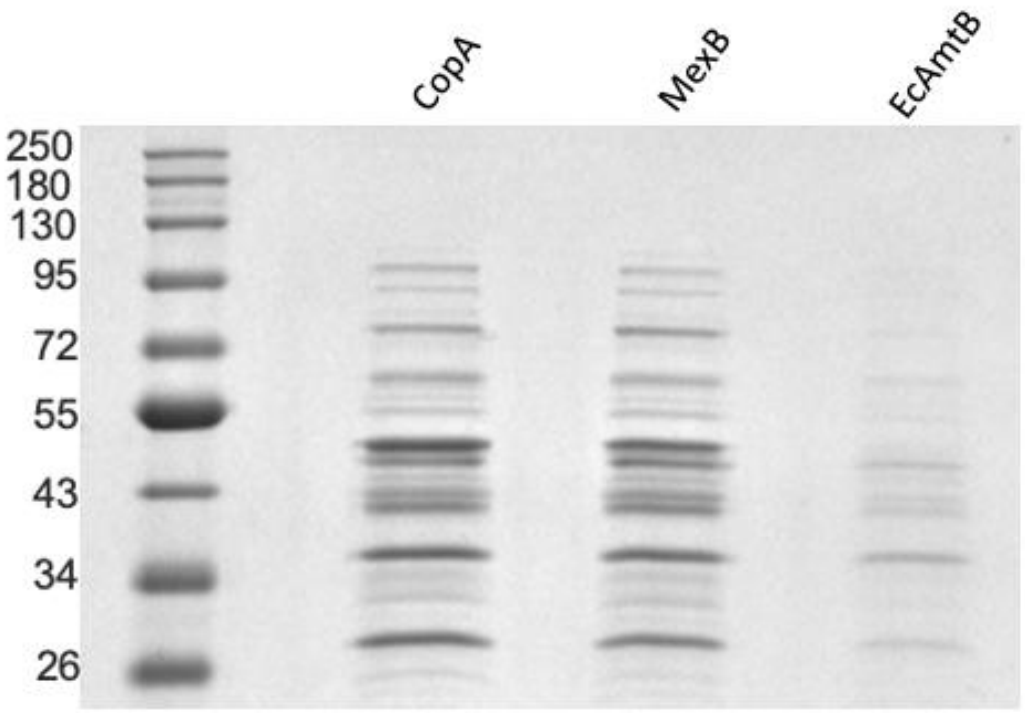

Figure 16: SDS PAGE analysis of the protein content of CopA2, MexB and EcAmtB *E. coli* C43(DE3) overexpression cultures induced using autoinduction media. 100 mL cultures were setup using autoinduction media as described in the methods and incubated at 37°C for 19 hours before lysing culture samples using the boiling method.

No large band was visualised at the expected size for CopA2, MexB or EcAmtB overexpression cultures using autoinduction media (**Figure 16**). It was unclear whether there was no protein being overexpressed in the *pETER1, pETER2* or EcAmtB cultures or if the visualisation method was preventing the detection of these proteins by SDS PAGE, as the positive control did not show that the visualisation technique was performing as expected.

3.2.5 An Alternative Method of Cell Lysis Allows for the Detection of Proteins by SDS PAGE and Western Blot

3.2.5.1 Increasing Membrane Protein Stability using a Lysis Buffer Supplemented With Dodecyl-beta-Maltoside (DDM)

As boiling culture samples in loading dye and sonication both proved unsuccessful as tools for the preparation of overexpression cultures for SDS PAGE analysis, an alternative method of cell culture lysis was trialled. To determine whether membrane protein stability after overexpression was too poor for visualisation using SDS PAGE, the use of a chemical lysis buffer with a membrane protein stabilisation detergent was used to lyse cells after overexpression. Lysis buffer was used containing 2 % n-dodecyl-beta-maltoside (DDM) detergent which is known to increase the stability of membrane proteins (Privé 2007). Overexpression cultures were setup and induced using IPTG for 3 hours as previously described. After incubation, cells were harvested and lysed using the DDM cell culture lysis method described in the methods. The

protein content of the soluble fractions of lysed cell cultures was analysed using SDS PAGE (**Figure 17**).

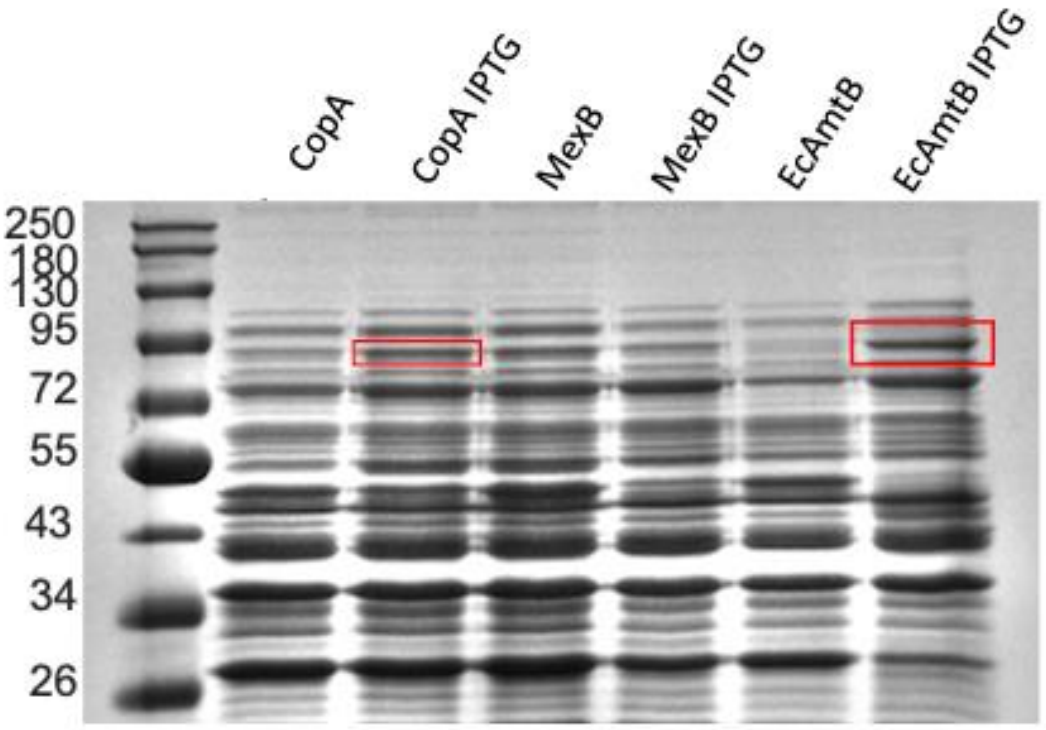

Figure 17: **SDS PAGE analysis of the protein content of CopA2, MexB and EcAmtB *E. coli* C43(DE3) overexpression cultures induced using IPTG and lysed using a lysis buffer supplemented with DDM to increase membrane protein stability.** 100 mL cultures were induced with IPTG at an OD_{600} of 0.6, incubated for 3 hours and lysed using the DDM lysis buffer as described in the methods. After lysis, samples were pelleted, and the protein content of the soluble fraction was analysed using SDS PAGE.

An increase in band intensity for CopA at ~90 kDa and for EcAmtB at ~95 kDa was observed compared to their no IPTG controls (**Figure 17**). This is indicative of an increase in solubilised protein in the IPTG cultures. The use of a lysis buffer containing DDM led to stabilisation of both CopA2 and EcAmtB at a level that they could be visualised using SDS PAGE. This method of cell lysis was adopted from this point forward.

3.2.5.2 Western Blot Analysis of Overexpression Cultures Lysed Using a Lysis Buffer Supplemented With DDM

An increase in expression of CopA2 and EcAmtB was visualised using SDS PAGE after cell culture lysis using lysis buffer supplemented with DDM. An increase in expression of MexB was not observed using SDS PAGE analysis. To determine whether there was any expression of MexB by *E. coli* C43(DE3), western blot analysis was carried out on the content of overexpression cultures.

Western blotting detects histidine tagged proteins using fluorescently tagged antibodies which bind the histidine tag that has been artificially added to the membrane proteins being overexpressed. Overexpression cultures were setup as previously described using autoinduction media and cell cultures were lysed using the lysis buffer supplemented with DDM to improve membrane protein stabilisation. Western blot analysis as described in the methods was carried out on the soluble fraction of lysed CopA2, MexB and EcAmtB *E. coli* C43(DE3) cultures (**Figure 18**).

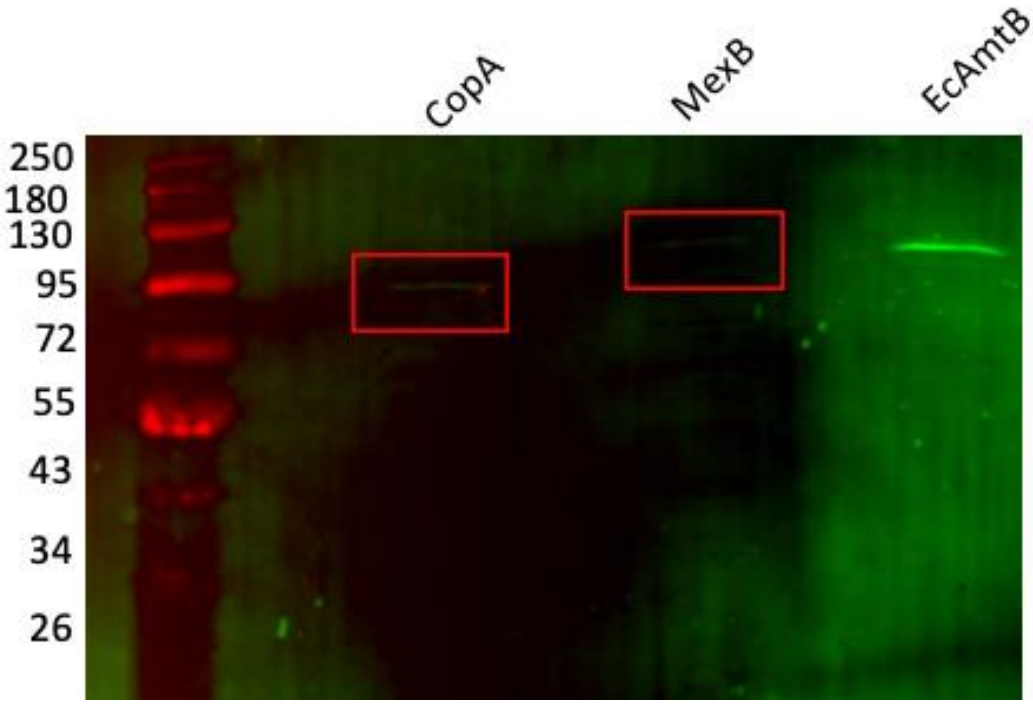

Figure 18: Western blot analysis of soluble fractions of DDM lysed *E. coli* C43(DE3) cultures expressing CopA2, MexB and EcAmtB. Using a semi-dry transfer system, proteins were transferred along with the ladder from the SDS PAGE gel onto a PDVF membrane. This membrane was incubated with mouse primary antibody which binds specifically to the histidine tag on the membrane proteins. This antibody was washed from the PDVF membrane and incubated with a secondary fluorescent antibody specific for the mouse primary antibodies. Using fluorescent imaging, the detection of histidine tagged proteins is observed.

Western blot analysis of the soluble fractions of DDM lysed CopA2, MexB and EcAmtB *E. coli* C43(DE3) overexpression cultures revealed the presence of each protein at the expected size. Detection of these proteins via their histidine tags confirms that their expression is induced by the T7 expression system in pETER1 and pETER2. **Figure 18** therefore confirms that expression of CopA2 and MexB was occurring in in cultures of *pETER1* and *pETER2.*

To show that the detection of these proteins via western blot was not due to empty pET21a+, overexpression cultures of *E. coli* C43(DE3) transformed with pET21a+, pETER1 and pETER2 were setup using autoinduction media and lysed using lysis buffer supplemented with DDM and the soluble and insoluble fractions were analysed using western blot (**Figure 19**).

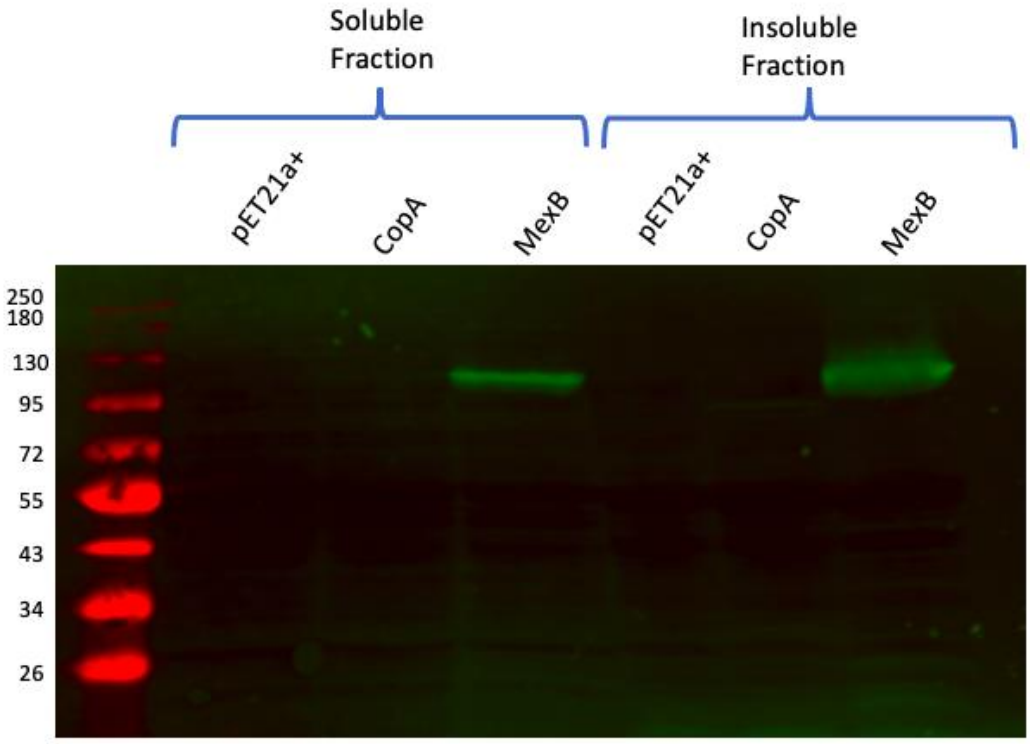

Figure 19: Western blot analysis of soluble and insoluble fractions of DDM lysed *E. coli* C43(DE3) cultures expressing pET21a+ plasmid, pETER1 the CopA2 expression plasmid and pETER2 the MexB plasmid. No histidine tagged protein is observed in the empty pET21a+ plasmid control. A very faint band is observed at ~90KDa in the soluble fraction of the CopA culture and a band for MexB is observed in both the soluble and insoluble fractions.

When *E. coli* C43(DE3) is transformed with pET21a+ vector no histidine tagged protein is detected by western blot analysis as is shown in **Figure 19**. CopA2 is observed in the soluble fraction of DDM lysed cells and MexB is detected in both the soluble and insoluble fractions.

3.2.6 Membrane Proteins Could not be Visualised Using Sepharose Bead Micropurification

In order to concentrate the low levels of CopA2 and MexB expression in *E. coli* C43(DE3) overexpression cultures, sepharose bead micropurification was carried out and the fractions were analysed using SDS PAGE.

Micropurification works on the basis that proteins can be captured by their histidine tag by passing them through sepharose beads fixed on a filter which are loaded with metals with a high affinity for the histidine tag. Proteins can then be eluted using imidazole which outcompetes with the metal for the histidine tag. Overexpression cultures were setup as before in autoinduction media and lysed using lysis buffer supplemented with DDM. The soluble fraction was passed through a micropurification filter plate loaded with sepharose beads charged with cobalt. Load, wash, and 2 elution fractions were collected and the protein content was analysed by SDS PAGE (**Figure 20**).

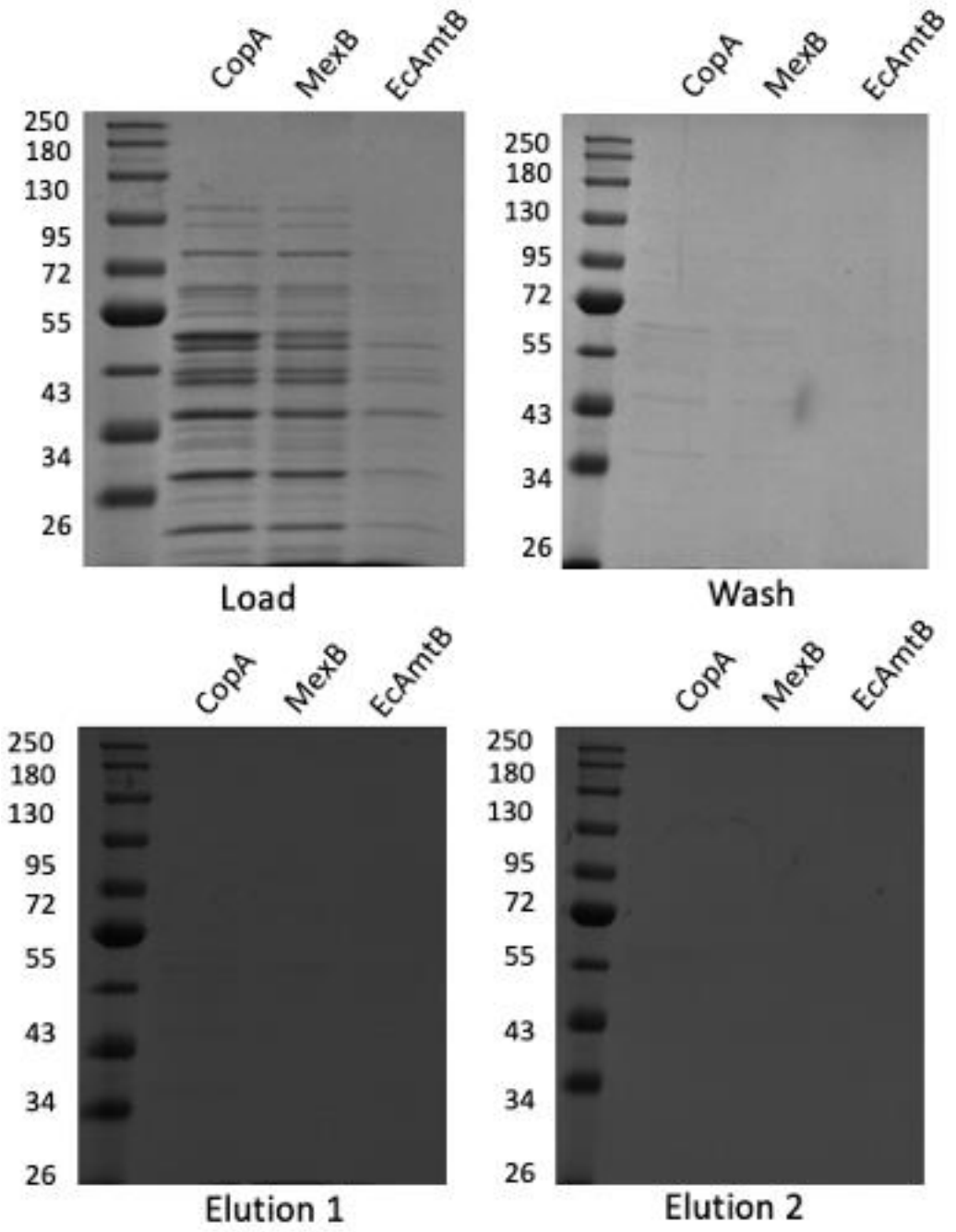

Figure 20: SDS PAGE analysis of DDM lysed *E. coli* C43(DE3) cultures expressing CopA2, MexB and EcAmtB subjected to cobalt sepharose bead micropurification. Load, wash and 2 elution fractions were analysed for the soluble fraction of each overexpression culture.

In the load fraction for all cultures a range of proteins can be seen none of which correspond to CopA MexB or EcAmtB. In the wash and both elution fractions, no CopA, MexB or EcAmtB is observed.

To determine whether loading the sepharose beads with a metal with a stronger affinity for the histidine tag would result in the capture of enough protein to visualise using SDS PAGE, micropurification was carried out again this time loading the sepharose beads with nickel (**Figure 21**). The micropurification was carried out as before and this time EcAmtB proteoliposomes were used as a positive control for the micropurification process.

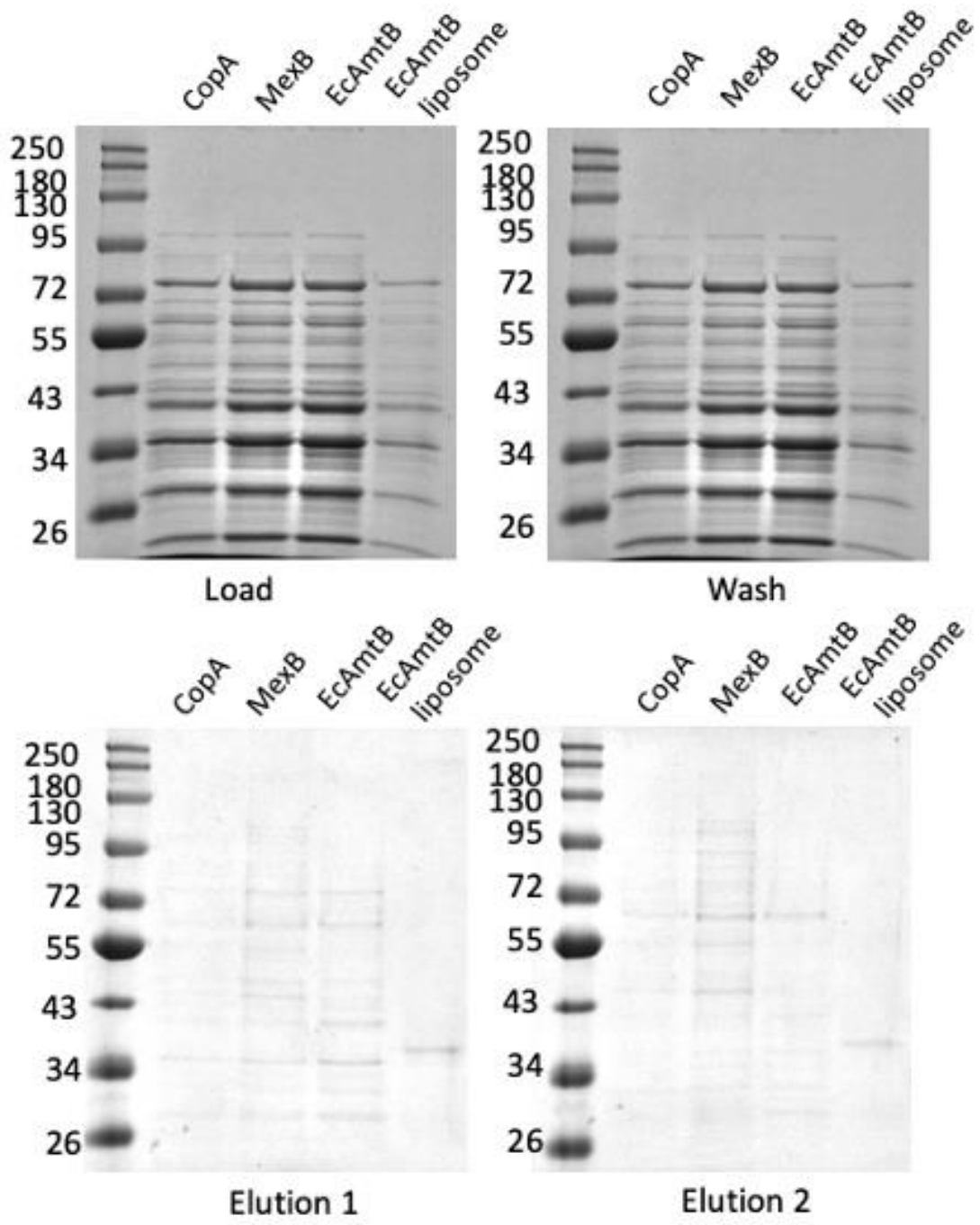

Figure 21: SDS PAGE analysis of DDM lysed *E. coli* C43(DE3) cultures expressing CopA2, MexB and EcAmtB subjected to nickel sepharose bead micropurification. Load, wash and 2 elution fractions were analysed for the soluble fraction of each overexpression culture.

h

As before, no protein was observed in any of the fractions at the expected sizes for any of the proteins (**Figure 21**). As the EcAmtB proteoliposome sample contains EcAmtB only, yet other proteins are observed in all fractions it seems that sample from the other wells in the micropurification plate are leaking into each other. No EcAmtB was observed for the proteoliposome sample in any fractions meaning that the micropurification process itself was not working and no protein is being retained on the sepharose beads.

3.2.7 IMAC Column Manual Purification of Membrane Proteins Analysed Using SDS PAGE and Western Blot

In order to determine whether CopA2 and MexB membrane proteins could be expressed and purified to high enough levels to detect using SDS PAGE analysis, purification of membrane proteins was carried out manually using an ion metal affinity column (IMAC) column loaded with nickel.

500 mL autoinduction overexpression cultures were grown of *E. coli* C43(DE3) transformed with overexpression plasmids for CopA2, MexB and EcAmtB. Cells were broken as before using lysis buffer supplemented with DDM. Cell lysis supernatant was manually passed through a 1 mL His-Trap column loaded with nickel before washing with IMAC buffer A containing a low concentration of imidazole and then eluted using IMAC buffer B containing a high concentration of imidazole to elute all

bound protein from the column. SDS PAGE and western blot analysis was carried out for all fractions for each protein (**Figure 22**).

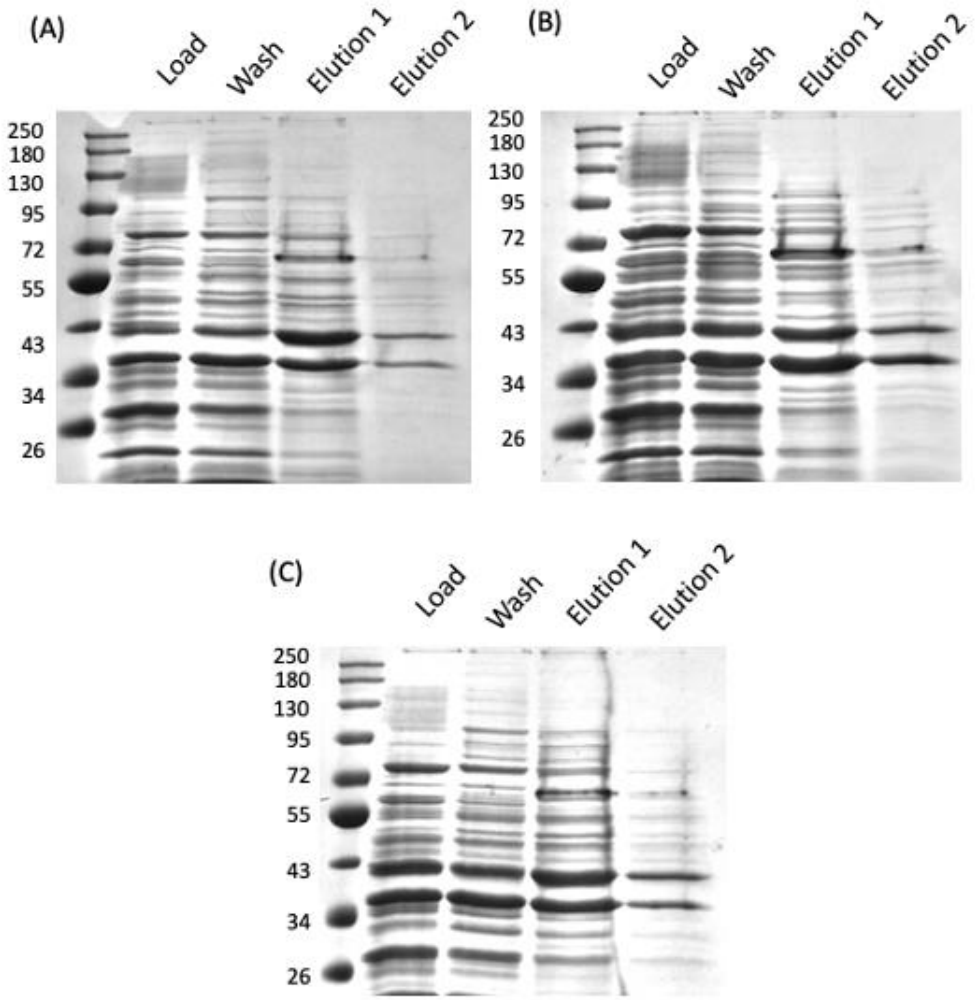

Figure 22: SDS PAGE analysis of IMAC column purification of the soluble fraction of lysed *E. coli* C43(DE3) expressing (A) CopA2 (B) MexB and (C) EcAmtB. Loading, wash and 2 elution fractions for each culture are shown.

Proteins were not successfully purified using the manual IMAC column method as no visible bands corresponding to any of the three purified proteins were visible using SDS PAGE analysis shown in **Figure 22**. To determine whether any membrane proteins were present in the IMAC collection fractions, the same samples were subjected to Western Blot analysis (**Figure 23**).

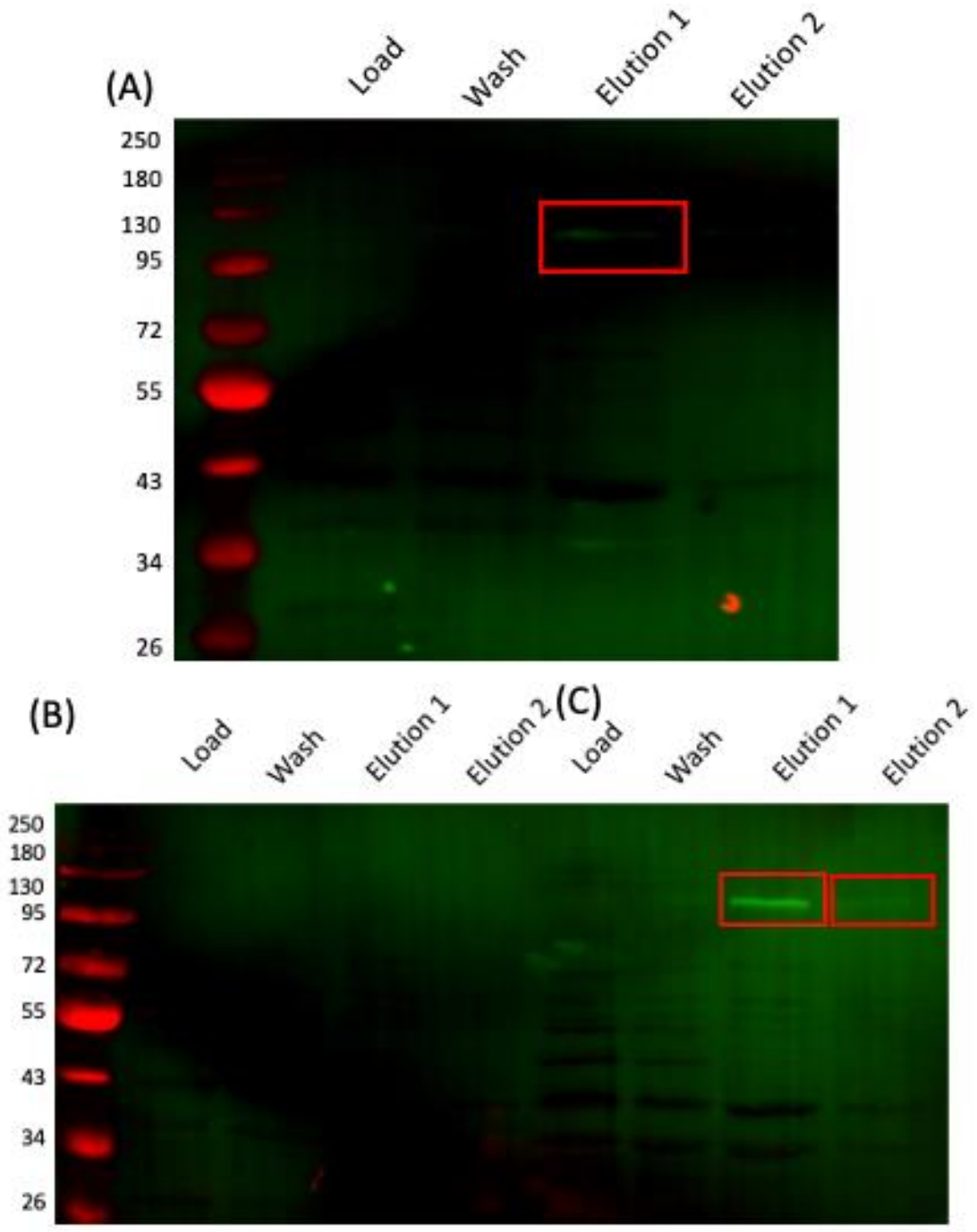

Figure 23: Western blot analysis of IMAC column purification of the soluble fraction of lysed *E. coli* C43(DE3) expressing (A) EcAmtB (B) CopA2 and (C) MexB. Loading, wash and 2 elution fractions for each culture are shown.

Western blot analysis of the manual IMAC column purification detected both EcAmtB and MexB in the elution fractions (**Figure 23**). However, CopA2 was not detected. Although these proteins are detected by western blot and are therefore present in the soluble fraction of the cell lysate, they were not present in large enough quantities to be detectable via SDS PAGE analysis.

3.2.8 Analysis of the Insoluble Fraction of Cultures Lysed Using DDM Lysis Buffer Leads to the Detection of Membrane Protein

After chemical lysis with buffer supplemented with DDM, the insoluble pellet fraction of CopA2 and MexB overexpression cultures was analysed using SDS PAGE and western blot to determine whether the CopA2 and MexB proteins were present in this fraction (**Figure 24**, **Figure 25**).

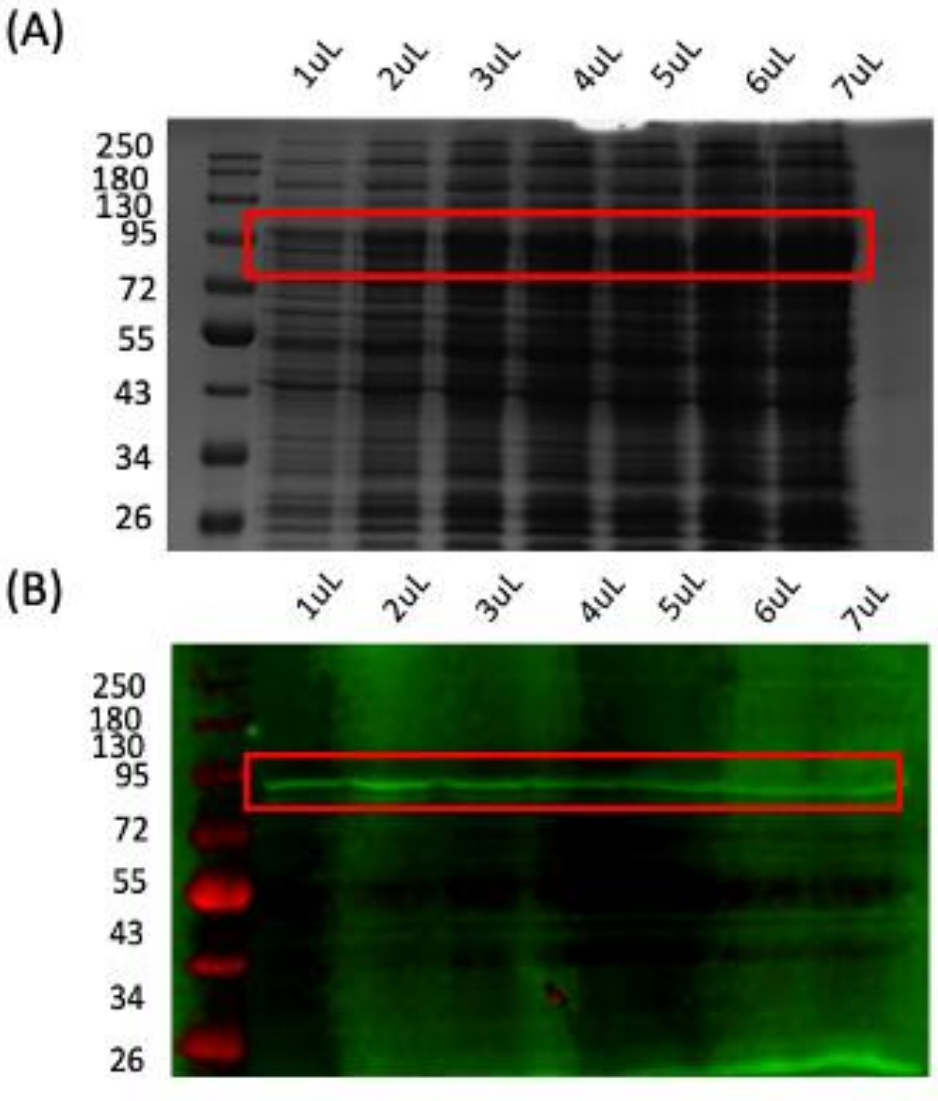

Figure 24: Analysis of the insoluble fraction of *E. coli* C43(DE3) CopA2 overexpression culture lysed using lysis buffer supplemented with DDM by (A) SDS PAGE and (B) western blot analysis. Various volumes of resuspended pellet were run in each lane of the gels to obtain optimal resolution of the resolved proteins. CopA2 is detected in the insoluble fraction by both SDS PAGE and Western blot analysis.

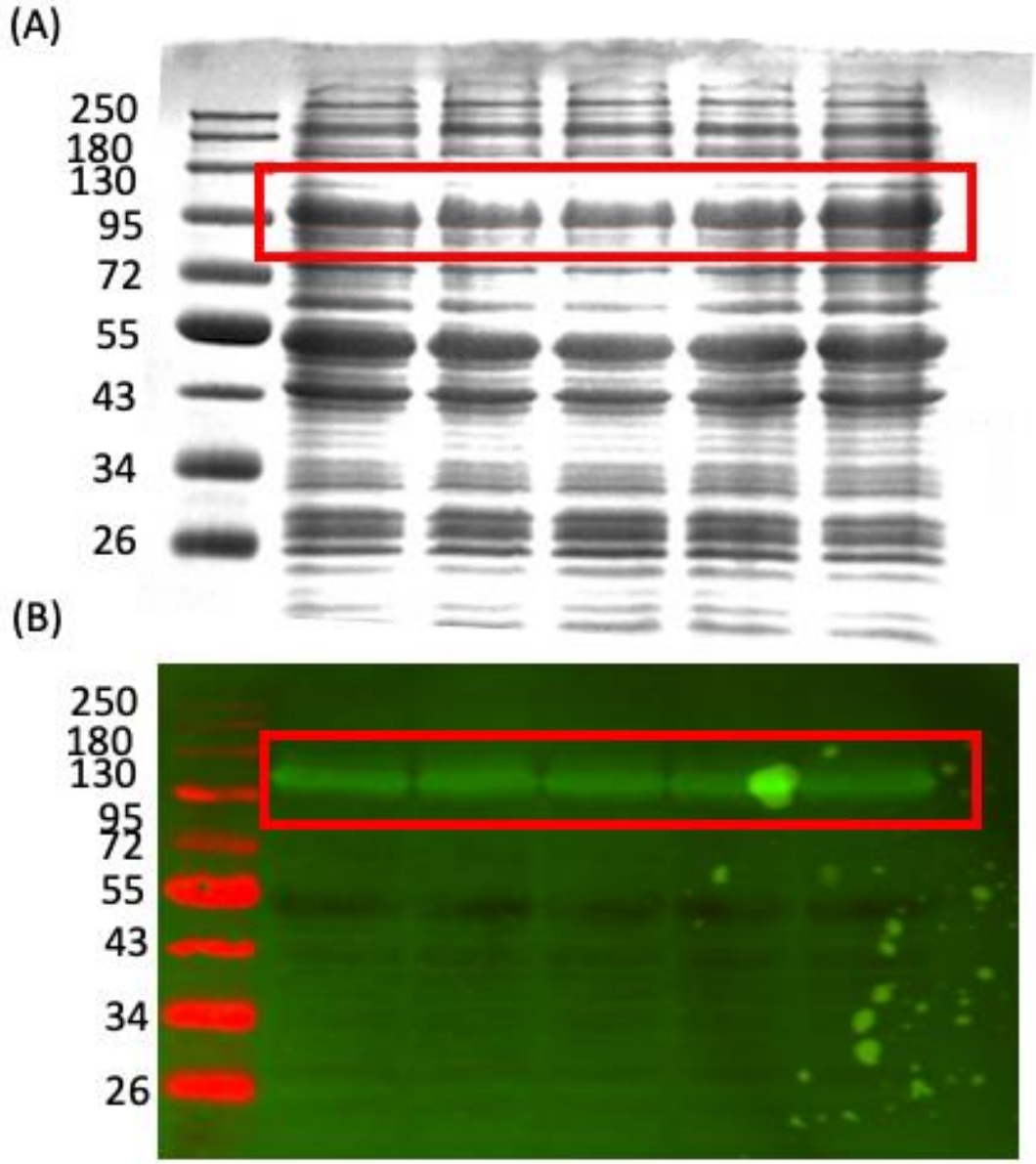

Figure 25: Analysis of the insoluble fraction of *E. coli* C43(DE3) MexB overexpression culture lysed using lysis buffer supplemented with DDM by (A) SDS PAGE and (B) western blot analysis. 2uL of resuspended pellet were run in each lane of the gels to obtain optimal resolution of the resolved proteins. MexB is detected in the insoluble fraction by both SDS PAGE and western blot analysis.

Western blot analysis showed that a large quantity of both CopA2 and MexB were present within the insoluble pellet fraction of cultures after lysis with buffer supplemented with DDM. These proteins are observed using both SDS PAGE and western blot analysis. Various volumes of *E. coli* C43(DE3) resuspended pellet were run on the SDS PAGE gel and the volume of 2 μL gave optimal resolution of the protein content of the sample. Therefore, this volume was loaded into every well of the MexB SDS PAGE gel/western blot. To determine whether solubilised protein could be obtained from overexpression cultures, the French press method of breaking cells was trialled once this equipment became available.

3.2.9 Using the French Pressure Cell to Break Cells Allowed for the Detection of CopA and MexB using SDS PAGE and Western Blot

At the end of this study, access to working French pressure cell was obtained. To determine whether the French pressure cell method of breaking cells would lead to detection of larger quantities of the membrane proteins CopA2 and MexB, 200 mL overexpression cultures were grown using autoinduction media as previously described. The cells were harvested after 19 hours and resuspended in the breaking buffers described in the methods and subjected to a pressure of 1100 Psi 3 times through a French pressure cell. Broken cell cultures were subjected to 2 rounds of centrifugation at 20,000 RPM followed by 100,000 RPM to obtain cell membrane. Cell fractions were collected from each step and analysed using SDS PAGE and western

blot (**Figure 26, Figure 27**). For both cultures ~25 mg of membrane was obtained which was resuspended in solubilisation buffer for analysis.

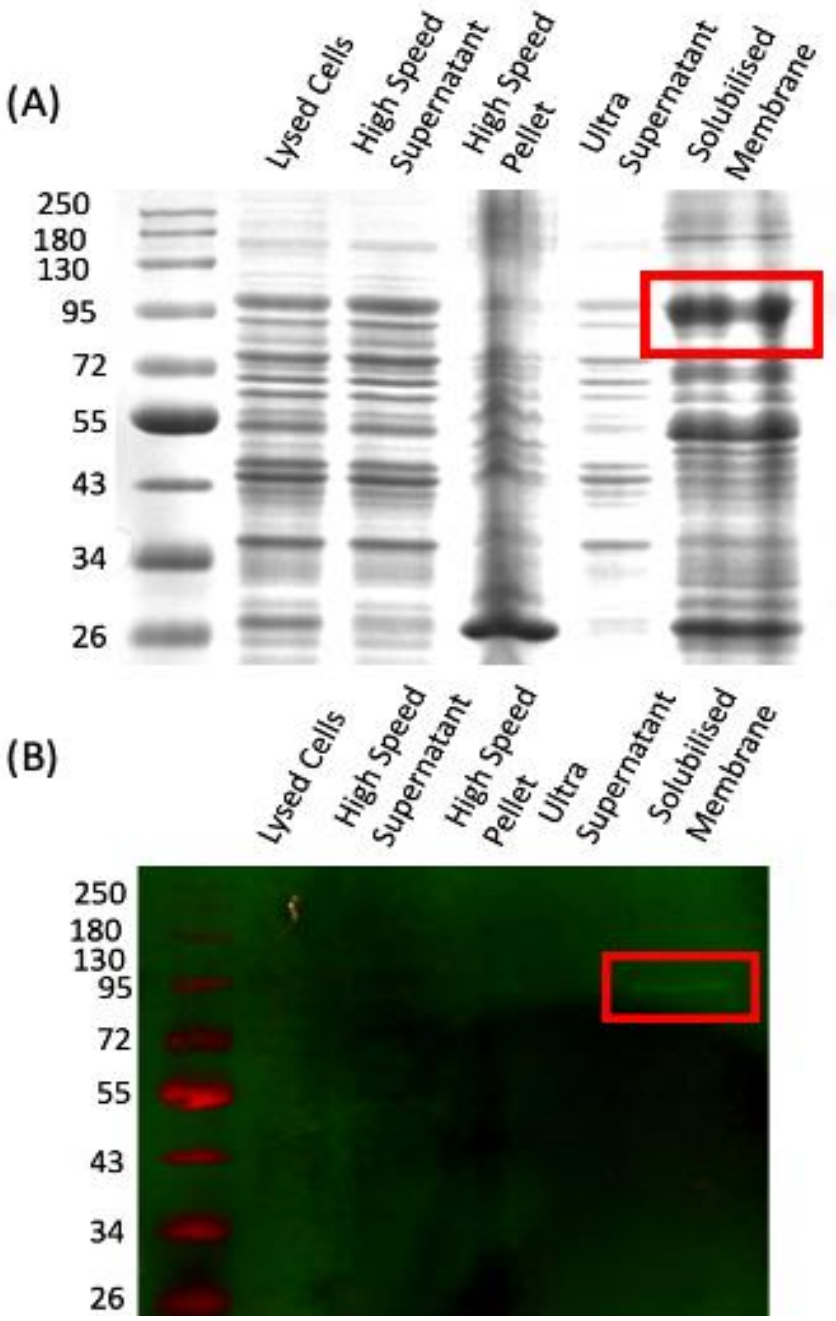

Figure 26: Analysis of *E. coli* C43(DE3) CopA2 overexpression culture broken using a French pressure cell and processed by various centrifugation steps. Using (A) SDS PAGE and (B) western blot. Pellets and supernatant from high-speed centrifugation and ultracentrifugation are shown. CopA2 protein is visualised at ~90KDa using both SDS PAGE and western blot.

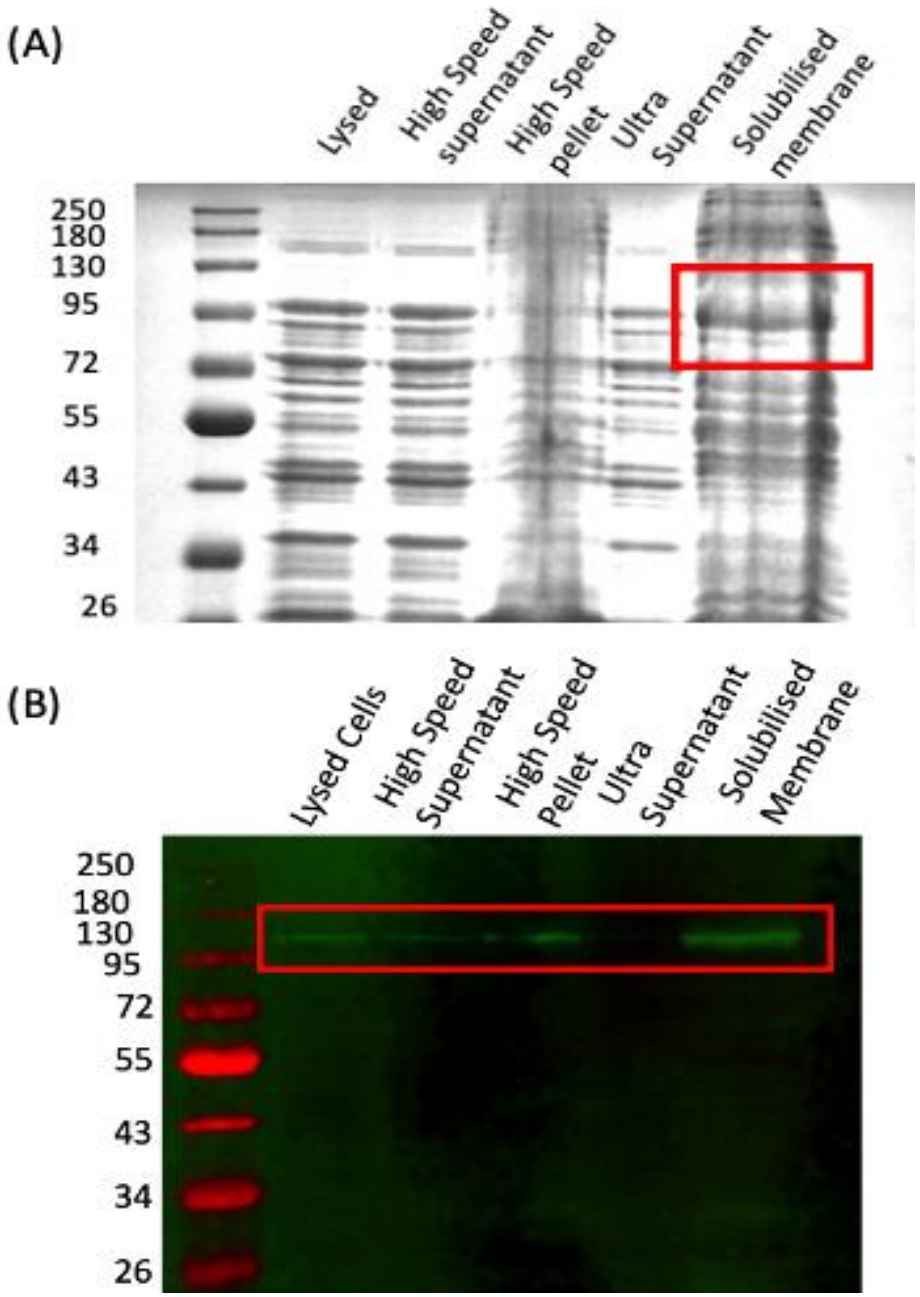

Figure 27: Analysis of *E. coli* C43(DE3) MexB overexpression culture broken using a French pressure cell and processed by various centrifugation steps. Using (A) SDS PAGE and (B) western blot. Pellets and supernatant from high-speed centrifugation and ultracentrifugation are shown. MexB protein is visualised at ~115KDa using both SDS PAGE and western blot.

Using the French press method to break cells after overexpression allowed for the detection of both CopA2 and MexB using SDS PAGE and western blot analysis. Collecting pure membrane from 200 mL of overexpression culture provided membrane proteins in enough quantity to visualise a thick band using SDS PAGE which was not possible using the other methods trialled throughout this study such as boiling in SDS loading dye, sonication, and chemical lysis using buffer supplemented with DDM. Membrane proteins were also present in the soluble fraction of lysed cell cultures in large quantities which was only observed in the insoluble fraction of lysed cell cultures previously.

3.3 Discussion

3.3.1 Biochemical Characterization of Membrane Proteins of Interest

A BMA sensitivity transposon mutant library screen carried out by Dr Walid El Bestawy provided evidence that the MexAB-OprM and Cbb_3 type cytochrome oxidase maturation proteins play a role in methacrylate ester tolerance in *P. aeruginosa* PA14. To determine whether these systems have a functional relationship, this study set out to biochemically characterise these systems and measure the transport of proxy substrates through these proteins using SSME technology. This study focused on the proteins CopA2 and MexB. To biochemically characterise these proteins, large quantities of these proteins must be isolated. Constructs for their overexpression in *Escherichia coli* C43(DE3) were generated and various methods of expression were trialled.

3.3.2 *P. aeruginosa* Proteins CopA2 and MexB were Successfully expressed using Escherichia *coli* C43(DE3)

We describe the expression of the *P. aeruginosa* proteins CopA2 and MexB in *E. coli* C43(DE3) using overexpression constructs pETER1 and pETER2 generated using Gibson assembly. *E. coli* C43(DE3) has been widely demonstrated in the literature as an expression system optimised for membrane protein overexpression (Wagner et al. 2008)(Miroux and Walker 1996). Mutations present within several genes including the *lac* repressor *lacI* in this bacterial strain result in overexpression of membrane proteins at levels which are non-toxic to the bacteria, compared to the lineal strain

Escherichia coli BL21(DE3) (Kwon et al. 2015). MexB expression has been achieved in *E. coli* C43(DE3) previously (Mokhonov et al. 2005), therefore this expression system was chosen during this study. CopA2 of *P. aeruginosa* has not been characterised previously (González-Guerrero et al. 2010), so we demonstrate the first purification of this protein using *E. coli* C43(DE3).

Using western blot analysis, the presence of both proteins CopA2 and MexB were detected in overexpression cultures, confirming overexpression constructs pETER1 and pETER2 facilitate the expression of these *P. aeruginosa* proteins in *E. coli* C43(DE3). We therefore demonstrate the heterologous expression of these *P. aeruginosa* proteins using *E. coli* C43(DE3) as the precursor to the biochemical characterisation of these systems using SSME analysis.

3.3.3 Breaking Cells using the French Pressure Cell System and Supplementation of Buffer with the Detergent DDM Results in the Generation of Solubilised Membrane Protein

During the period of this study the use of various cell lysis methods were trialled to obtain soluble protein detectible by SDS PAGE and western blot. The success of cell lysis using a French pressure cell system and preservation of membrane protein integrity has been demonstrated previously (Molloy 2008; Moore, Hess, and Jorgenson 2016), and so this was the preferred method of cell lysis during this study. However, the lack of availability of this system at the beginning of this study meant

that other lysis methods including sonication, chemical and a boiling method were used. Using these lysis techniques poor solubilisation of membrane protein was observed by SDS PAGE and western blot analysis. When the French press system became available it proved as a superior method of cell lysis.

Using the French pressure cell in combination with the supplementation of resuspension buffer with the detergent DDM allowed for the isolation of membrane from *E. coli* C43(DE3) CopA2 and MexB expression cultures and subsequent visualisation of these membrane proteins within the soluble fractions using SDS PAGE and western blot. DDM is a known protectant and stabiliser of membrane proteins including MexB (Mokhonov et al. 2005; Seddon, Curnow, and Booth 2004). Maintaining the stability of membrane proteins once they are isolated from bacterial membranes has long been a challenge in the purification of membrane protein systems (Kotov et al. 2019). We show an improvement in solubility of MexB and CopA2 when resuspended using buffer supplemented with DDM and provide the basis for further study regarding the solubility of these proteins using solubility trials to test a range of detergents.

3.3.4 Optimisation of CopA2 and MexB Expression Conditions During this Study

During this study, various cell culture conditions were trialled to induce expression of CopA2 and MexB in *E. coli* C43(DE3) transformed with the plasmids pETER1 and

pETER2. Induction of the T7 overexpression system using IPTG at various concentrations for different lengths of incubation time were trialled as well as the use of autoinduction media containing lactose. These methods are widely reported in the literature as effective for protein overexpression in *E. coli* (Angius et al. 2018)(Du et al. 2021). Using autoinduction media, a high density of cells in culture is achieved before protein overexpression is induced by lactose uptake (Fox and Blommel 2009), negating the need to measure the OD_{600} during cell culture which risks contamination and reduces culture yield. This method of induction was determined as the most efficient induction system for growth of expression cultures during this study.

During this study, we demonstrate the heterologous expression of the *P. aeruginosa* membrane proteins CopA2 and MexB in *E. coli* C43(DE3) that were identified as tolerance conferring systems to methacrylate esters in *P. aeruginosa* PA14 previously (Bestawy 2017a). Using autoinduction media for growth and French pressure cell lysis to obtain purified membrane subsequently resuspended with DDM supplemented buffer allowed for the visualisation of soluble CopA2 and MexB proteins using SDS PAGE and western blot. To biochemically characterize these systems using SSME technology, large amounts of these solubilised proteins must be produced to construct proteoliposomes (Bazzone et al. 2017). We present the basis for an expression system which can be developed into an efficient overexpression system to allow for the purification of these proteins required to conduct this biochemical

characterisation. Unfortunately, due to time restrictions because of the Covid-19 pandemic, this was not possible during the period of this study.

3.4 Future Work

3.4.1 Purification of Solubilised MexB and CopA2 in the Future will allow for the Biochemical Characterization of these Membrane Proteins Using Solid Supported Membrane Electrophysiology

The aim of this study was to biochemically characterize the membrane proteins MexB and CopA2 using solid supported membrane electrophysiology (SSME). To enable characterization using this technology, purified membrane proteins must be reconstituted into liposomes which required large quantities of pure solubilised protein. Due to time restrictions imposed on this study by the Covid-19 pandemic, the purification of the membrane proteins MexB and CopA2 was not achieved. However, we during this study we demonstrated that these membrane proteins can be overexpressed in *E. coli* C43(DE3) and the presence of solubilised protein was demonstrated from liquid culture. Therefore, we present the basis for future work to be carried out to purify these membrane proteins in the quantities needed required for liposome reconstitution to allow for SSME study of these system.

3.4.2 The Biochemical Characterisation of MexB and CopA2 Could be Conducted Using SSME Technology

If purified soluble MexB and CopA2 protein is generated in the future, this can be used to reconstitute into liposomes (generating proteoliposomes) which can be used to conduct SSME studies on these membrane protein systems. The measurement of translocation of proxy substrates through these proteins can be measured with high

sensitivity using this technology through the displacement of charge across a double capacitance system (Bazzone et al. 2013, 2017). This technology allows for high throughput screening of transport under a wide range of conditions allowing for the biochemical characterization of these systems *in vitro.*

3.4.3 Site Directed Mutagenesis of Membrane Proteins and Biochemical Characterization using SSME Could Lead to the Generation of Bacterial Strains with Increased Tolerance to BMA

Random or site directed mutagenesis of MexB or CopA2 could be carried out and used to complement knockout strains of *P. aeruginosa* which could be fed back through the transposon mutant library screen described earlier in this chapter. Strains with an increased tolerance to BMA due to mutated complemented protein could be further analysed by purified protein characterization using SSME technology. If increased transport is observed using SSME due to mutation of these proteins then these proteins could be used instead of the WT to generate production strains with an increased tolerance to BMA for fermentation. This process is described in **Figure 28**

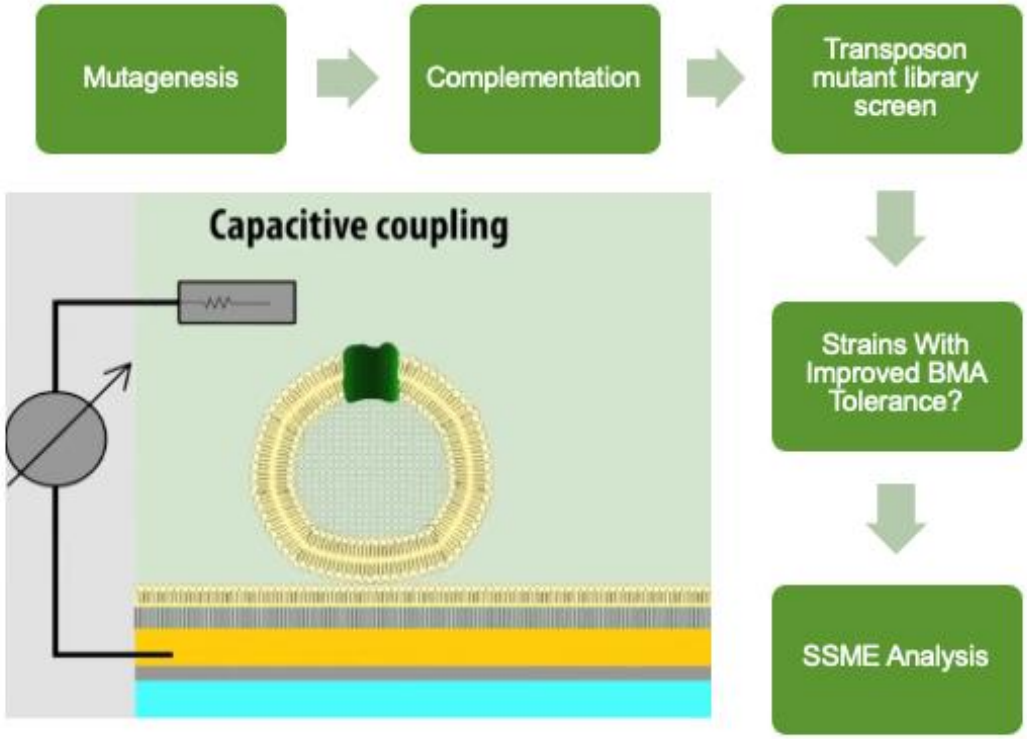

Figure 28: The process for BMA tolerant strain development using mutagenesis and SSME is shown

Tolerant strain production generation following the process detailed in **Figure 28** was the original aim of this study. However, due to time constraints caused by the Covid-19 pandemic it was not possible to carry out this work.

4 Results Chapter 2: Transcriptomic Characterisation of BMA Tolerance in *P. aeruginosa* PA14

4.1 Introduction

4.1.1 The Identification of Tolerance Conferring Systems Using a Transposon Mutant Library Screen

P. putida is a promising candidate as a production strain for Mitsubishi Chemical Corporation's methacrylate ester fermentation as it displays an intrinsic level of tolerance to BMA and can produce promising yields of the compound. However, BMA toxicity still presents as a bottleneck in test fermentations carried out by Ingenza Ltd (Mitsubishi Chemical, Personal Communication). The identification of BMA tolerance conferring systems in *P. putida* could generate targets for exploitation to generate even more successful candidates for fermentation. During this study, the availability of an ordered, nonredundant *P. aeruginosa* PA14 transposon insertion mutant library meant that this strain was used as a model organism for tolerance in *Pseudomonas* species (Liberati et al. 2006). As this microorganism is a human pathogen it would not be suitable as a production strain, however, this strain was used as a tool to identify homologue systems of interest for further investigation in *P. putida.*

A transposon mutant library screen identified systems within *Pseudomonas aeruginosa* PA14 which resulted in decreased tolerance to the methacrylate ester BMA when disrupted by a transposon insertion (**Table 3**),(Bestawy and Tucker, Personal Communication). Using this approach, the MexAB-OprM and Cbb_3 cytochrome oxidase assembly systems were identified as possible BMA tolerance

conferring systems in *P. aeruginosa* PA14 and were therefore subjected to further study through biochemical characterisation.

4.1.2 The Limitations of a Transposon Mutant Library Screen

Although a useful tool for high throughput phenotypic analysis of PA14 mutants, transposon mutant library screening has limitations. Transposon mutagenesis can lead to polar effects of gene expression downstream from the transposon insertion site. This means that some genes may be categorised as crucial during the experimental conditions when in fact what is being observed is the polar effect of transposition (Calos and Miller 1980; van Opijnen, Bodi, and Camilli 2009). The position of the transposon within a gene or operon may also lead to partial expression of some systems meaning that functional genes of interest are not identified by %Δ AUC (Liberati et al. 2006). Transposon mutant library screening was also only carried out using the methacrylate ester BMA and therefore the effect of other solvents such as styrene and ethylbenzene was not investigated.

4.1.3 Using a Transcriptomic Approach to Identify Solvent Tolerance Conferring Systems in *P. aeruginosa* PA14

The availability and accuracy of next generation sequencing technologies means that the characterisation of the bacterial transcriptome is now accessible and precise (Denoeud et al. 2008; Holt and Jones 2008; Mutz et al. 2013). RNA sequencing has been demonstrated previously as a useful tool in the characterisation of the

transcriptomic response of Pseudomonads to solvents such as toluene (Molina-Santiago et al. 2017).

Here, the transcriptomic response of *P. aeruginosa* PA14 to the solvents BMA, styrene and ethylbenzene was investigated by whole transcriptome analysis using RNA sequencing. The solvents styrene and ethylbenzene are also platform chemicals of the plastics industry and were chosen alongside BMA to provide further understanding of the transcriptomic response of *P. aeruginosa* PA14 to other solvents as well as BMA. Ethylbenzene is used in the production of the monomer styrene, which is polymerised to form polystyrene (Bethany Halford 2021). These chemicals display similar octanol/water partition coefficients (log Kow) which is a measure of hydrophobicity (**Figure 29**).

	N-butyl methacrylate	Styrene	Ethylbenzene
	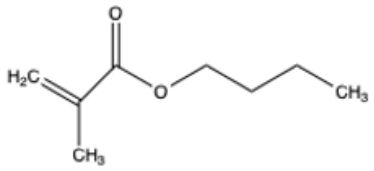	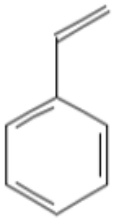	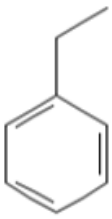
Log Kow	2.88	2.95	3.15

Figure 29: The structures and log Kow values for BMA, styrene and ethylbenzene are shown.

Using this approach, the differential expression of genes when *P. aeruginosa* PA14 is challenged with various solvents was determined, providing a valuable insight into which systems within the cell play an important role in solvent tolerance. The identification of such systems will be valuable in the generation of a suitable production strain for a BMA fermentation process. Investigating the transcriptomic response of *P. aeruginosa* PA14 to other platform chemicals of the plastics industry such as styrene and ethylbenzene will aid in the understanding of the general stress response of this pathogen. Here, it is demonstrated that whole transcriptome analysis by RNA sequencing in conjunction with a transposon mutant library screen is a powerful tool for understanding the mechanism of intrinsic solvent tolerance in *P. aeruginosa* PA14.

4.2 Results

To characterise the transcriptomic response of *P. aeruginosa* PA14 to the solvents BMA, styrene and ethylbenzene, *P. aeruginosa* PA14 cultures were grown in the presence and absence of these solvents. RNA was isolated from cultures and analysed using Illumina Miniseq sequencing.

4.2.1 Isolation of RNA from *P. aeruginosa* PA14 Cultures Treated with Solvent

Cultures of *P. aeruginosa* PA14 were grown in MSX minimal media to be consistent with similar experiments carried out at Ingenza Ltd and by Charles Begley (Begley and Tucker, Personal Communication). When the OD_{600} of the cultures reached 0.6, the cultures were supplemented with either 20% BMA, 10 mM styrene or 10 mM ethylbenzene. No solvent controls were left untreated. Cultures were incubated for 15 minutes with solvent before cells were harvested and RNA was isolated from each sample using the Trizol™ RNA Plus Purification Kit. To determine if the quality of isolated RNA from cultures was sufficient for ribosomal RNA (rRNA) depletion, RNA samples were subjected to chip electrophoresis using the Agilent Bioanalyzer (**Figure 30**).

(A)

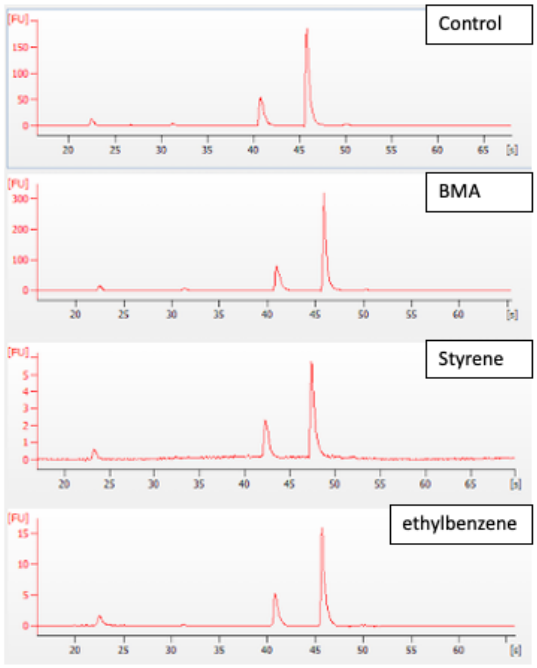

(B)

Sample Name	Result Label
control 1	RIN: 8.70
control 2	RIN: 8.80
control 3	RIN: 8.60
bma 1	RIN: 8.30
bma 2	RIN: 8.60
bma 3	RIN:9
styrene 1	RIN: 8.20
styrene 2	RIN: 8.20
styrene 3	RIN: 8.40
ethylbenzeze 1	RIN: 8.90
ethylbenzene 2	RIN: 8.20
ethylbenzene 3	RIN:9

Figure 30: (A) Chip electrophoresis electropherograms of example RNA extractions for each solvent treated sample generated using the Agilent Bioanalyzer. Cultures and RNA extractions were performed in triplicate, however, one of each is shown here as an example. Two ribosomal RNA peaks are observed in each sample, showing each sample has not degraded **(B) RNA integrity numbers (RINs) of each RNA extraction in triplicate are shown.** A RIN above 8 for all samples is observed, indicating that the quality of each RNA extraction was high.

The results show two peaks in each RNA sample electropherogram which represent the 16S and 23S ribosomal RNA subunits which is characteristic of intact RNA (**Figure 30**). The RNA integrity number (RIN) for each sample was above 8 which showed the samples were of a high quality.

To determine whether any of the samples were contaminated by DNA, samples were used as templates for PCR using primers to amplify a region of intergenic DNA (**Figure 31**). Primers for the amplification of a 500 bp region of intergenic DNA was designed as this region of DNA would not be transcribed into mRNAs and therefore would provide as a reliable target for DNA detection (**Table 11**).

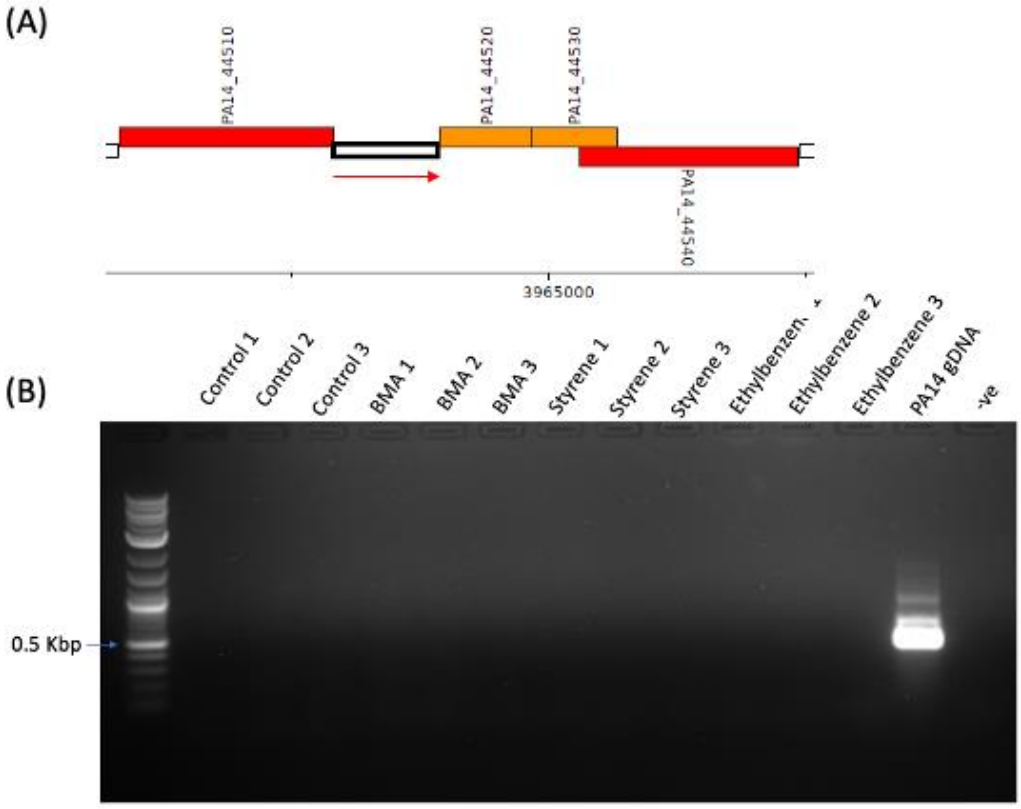

Figure 31: Contamination analysis of RNA extractions (A) Schematic diagram of the 500 bp region of intergenic DNA used for PCR amplification. PCR primers were designed to amplify the 500 bp region between the genes *PA14_44510* and *PA14_44520.* Cytoplasmic genes are represented in red and inner membrane proteins are shown in orange. Figure generated using Pseudomonas.com **(B) PCR and agarose gel electrophoresis analysis of extracted RNA.** Each RNA extraction sample was used as template. *P. aeruginosa* PA14 genomic DNA was used as a positive control reaction template and a no template reaction was run as a control.

DNA products were not amplified from any of the RNA extraction samples (**Figure 31**). The samples were therefore considered free of DNA contamination and were taken forward for further analysis.

4.2.1.1 Ribosomal RNA Depletion of RNA Extractions

Total RNA extracted from cell cultures contains ~80 % ribosomal RNA (rRNA). Therefore, to obtain a high read depth of mRNA from each sample using sequencing by synthesis technology, the rRNA content must be removed from total RNA samples. rRNA was depleted from each RNA sample as described in the methods, and to determine whether any rRNA remained in the samples, RNA samples were subjected to chip electrophoresis using the Agilent Bioanalyzer (**Figure 32**).

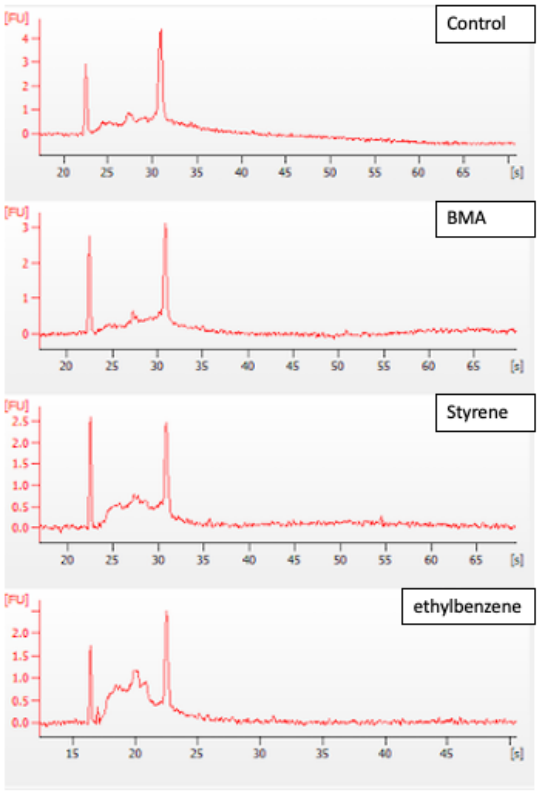

Figure 32: Chip electrophoresis electropherograms of example ribosomal RNA depleted RNA extractions for each solvent treated condition generated using the Agilent Bioanalyzer. Only one rRNA depletion for each solvent treatment group is shown as an example although this was performed in triplicate. No ribosomal RNA is observed in the electropherograms of any samples. After the removal of the rRNA from each sample, an mRNA peak is observed between 25-35 seconds for every sample.

Once the ribosomal RNA was removed from RNA samples it was possible to identify mRNA peaks between 25-35 seconds on the sample electropherograms (**Figure 32**). Peaks resolving at this retention time range are characteristic of high-quality mRNA. No 16S or 23S ribosomal RNA was observed in the electropherograms, showing that rRNA had successfully been depleted from all samples.

4.2.1.2 Preparation of Complimentary DNA Sequencing Libraries of RNA Extractions

To sequence the purified mRNA from each sample, complimentary DNA (cDNA) libraries were generated for Illumina sequencing. Adaptor ligated and indexed double stranded paired end libraries were generated with an average length of ~300 bp using a New England Biolabs library preparation kit. After library preparation, to ensure the libraries were free from adapter and primer contamination and were the correct size, the libraries were subjected to chip electrophoresis using the Agilent Bioanalyzer (**Figure 33**).

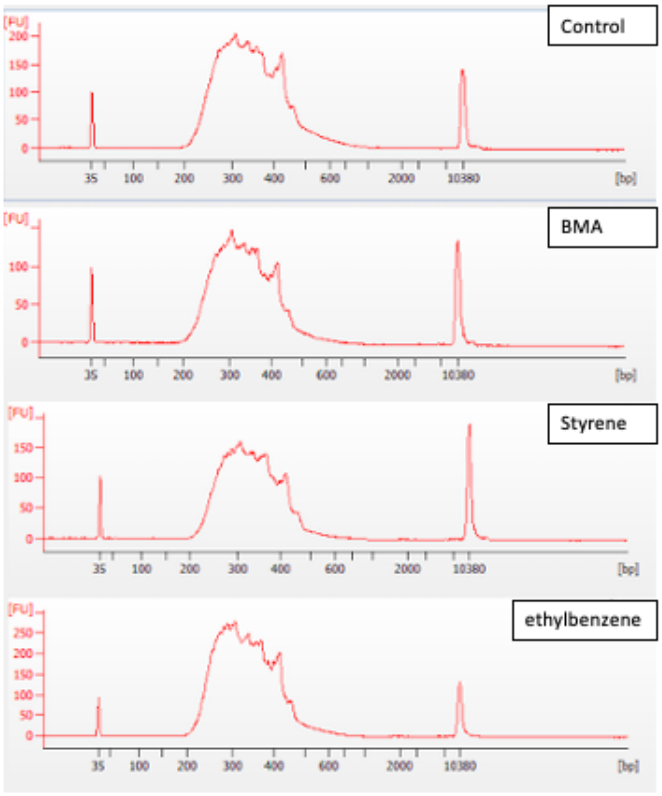

Figure 33: Chip electrophoresis electropherograms of example cDNA library preparations for each solvent treatment sample generated using the Agilent Bioanalyzer. One library preparation for each sample is shown although this was performed in triplicate. The size distribution of each library ranges from ~200 bp to ~400 bp, peaking at ~300 bp.

The chip electrophoresis electropherograms generated on the Agilent Bioanalyzer demonstrate that the average size of each cDNA library was ~300bp (**Figure 33**). Libraries were quantified using a Qubit fluorometer and diluted to a final pooled loading concentration of 5 pM. cDNA libraries were sequenced using an Illumina Miniseq sequencer loaded with a high throughput cartridge and flow cell. The sequencing run had a cluster density of 344 K/mm2 of which 80% passed the quality filter. Between 3 and 5 million reads were obtained for each indexed sample, totalling an output of ~40 million reads. The quality of the reads was determined using FastQC (Wingett and Andrews 2018).

4.2.2 Principal Component Analysis Confirms the Absence of Outliers in the Data

To determine whether any of the replicates were technical outliers, principal component analysis (PCA) was carried out on all RNA sequencing data through the DESeq2 Galaxy Europe package (**Figure 34**). The PCA software finds patterns in high dimensional data, PCA establishes groups of variables within datasets allowing for the identification of data which deviates within replicates with high sensitivity. PCA plots show the differences within datasets calculated by the algorithms as represented by distance on the plot. This means that datasets which are deemed highly similar will reside close together on the plot. Therefore, triplicates of datasets with no technical outliers are expected to reside close to one another on a PCA plot,

and datasets which deviate from the other triplicates are represented as far from the other datasets on the plot.

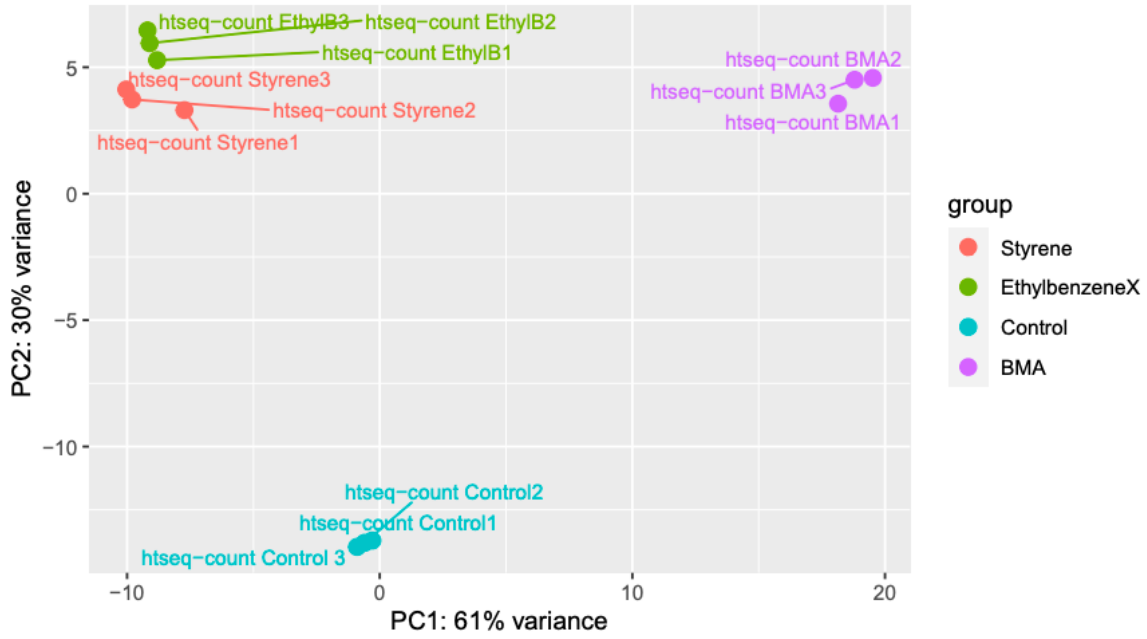

Figure 34: Principal component analysis of differential gene expression between control, BMA treated, styrene treated and ethylbenzene treated samples in triplicate. The PCA plot shows grouping of samples in triplicate. This figure was generated using DESeq2 in Galaxy Europe.

All triplicates within the BMA, styrene, ethylbenzene and control samples were clustered together on the PCA plot, providing evidence that there were no outliers within the datasets (**Figure 34**).

4.2.3 Analysis of Differential Gene Expression in Solvent Treated Samples Reveals Significantly Different Expression Profiles Between Control and Solvent Treated Samples

To determine changes in the transcriptome of solvent treated *P. aeruginosa* PA14 cultures, analysis of differential gene expression was carried out using DEseq2 in Galaxy Europe. DESeq2 uses the number of reads from the sequencing data mapped to each feature on the chromosome by Htseq-count and calculates the differential expression of genes within high dimensional data based on negative binomial distribution. Differential gene expression is calculated as the logarithm to the basis 2 of the fold change (LFC) of the number of reads in the treated sample compared to the untreated control. The p was is calculated for each LFC and corrected for false discovery rate using the Benjamini-Hochberg procedure. Results were outputted as a tabular file containing the LFC of every gene within the dataset listed in order of significance. Using this kind of analysis allowed for the identification of the significantly upregulated and downregulated genes in *P. aeruginosa* PA14 in response to BMA, styrene and ethylbenzene. Tabular output files from DESeq2 were used to generate volcano plots using Volcano Plot in Galaxy Europe (**Figure 35**, **Figure 41**, **Figure 42**).

4.2.4 Analysis of Differential Gene Expression in *P. aeruginosa* PA14 Treated with the Methacrylate Ester BMA

To interpret the DESeq2 analysis carried out on BMA treated PA14 cultures, a volcano plot was generated showing all genes with a significant logarithmic fold change in expression compared to the control samples (**Figure 35**).

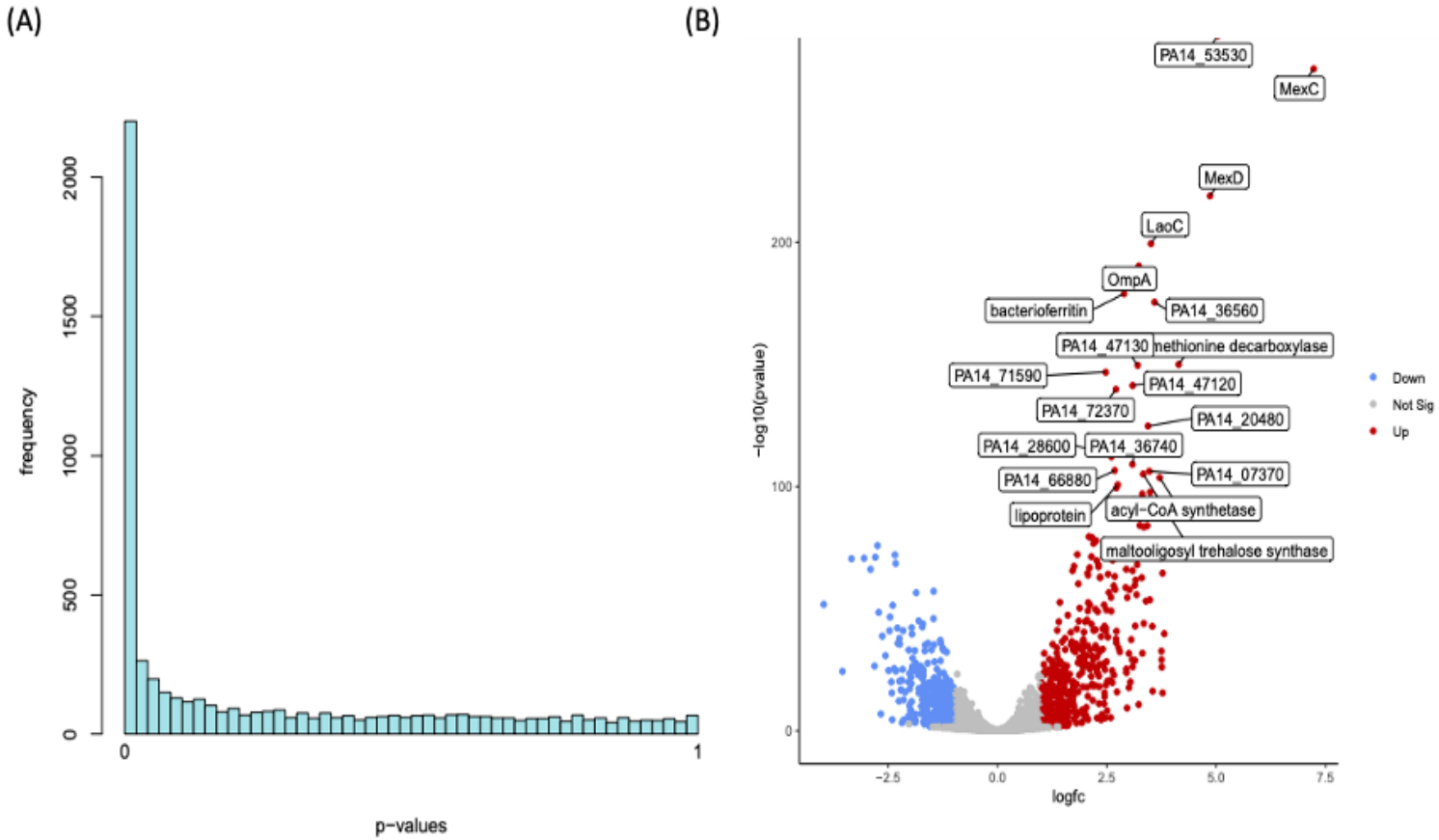

Figure 35: (A) Histogram of p-values of log fold change in expression of upregulated and downregulated genes in *P. aeruginosa* PA14 when exposed to the methacrylate ester BMA (B) Volcano plot of differentially expressed genes in *P. aeruginosa* PA14 when exposed to the methacrylate ester BMA. Genes which showed no significant differential expression are shown in grey, genes which showed a significant increase in expression are shown in red and genes which showed a significant decrease in expression are shown in blue. The top 20 most significantly differentially expressed genes are labelled. Unannotated genes are labelled with locus tag and the gene name is given where possible.

The frequency of differentially expressed genes within the dataset with a p value close to zero was significant, providing evidence that the dataset is reliable (**Figure 35**). The volcano plot representation of this data shows the top twenty differentially expressed genes with the most significant p values in *P. aeruginosa* PA14 when treated with BMA. The genes identified can be categorised into groups based on their function, which is carried out throughout this chapter.

4.2.5 Comparison of Transposon Mutant Library Screen and Transcriptomic Analysis of BMA Cultures

To determine whether the same systems shown in the transposon mutant library screen were significantly upregulated in the RNA sequencing data, the data was compared in **Table 15**.

Table 15: Comparison of the Δ% AUC and LFC of the top 10 genes of interest identified during the transposon mutant library screen. The mean number of reads mapped to each gene, change in expression, LFC, and p value significance from the RNA sequencing data are shown.

Transposon Mutant Library Screen			Transcriptomic Analysis			
Gene ID	**Description**	**Δ%AUC**	**Mean Number of Reads Across All Samples Mapped to Gene**	**Change in Expression**	**Log Fold Change in Expression**	**P Value < 0.05?**
PA14_05550	OprM	-63.12	1032	Increase	+1.36	Yes
PA14_05540	MexB	-55.70	2700	Increase	+1.41	Yes
PA14_05530	MexA	-55.29	1658	Increase	+1.59	Yes
PA14_44460	Cbb_3 Cytochrome Oxidase Assembly	-51.03	39	No Change	+0.46	No
PA14_44440	Cbb_3 Cytochrome Oxidase Assembly CopA2	-49.85	193	Increase	+1.10	Yes
PA14_61980	Chromosome Partitioning Protein	-45.27	13	No Change	-0.39	No
PA14_44450	Cbb_3 Cytochrome Oxidase Assembly	-45.11	6	No Change	+0.27	No
PA14_07760	SurA	-44.40	588	Decrease	-0.43	Yes
PA14_43950	SucC	-41.62	3508	Increase	+0.32	Yes
PA14_62930	Carbomyl-phosphate synthase small chain subunit	-36.09	439	Increase	+0.16	No

The RNA sequencing data corresponding to the top 10 systems of interest identified during the transposon mutant library screen is shown in **Table 15** . All components of the MexAB-OprM system were significantly upregulated in the RNA sequencing dataset, and one component of the Cbb_3 cytochrome oxidase maturation system was significantly upregulated, as indicated by green font.

4.2.5.1 RNA Sequencing Data Reinforces the Importance of the MexAB-OprM in BMA Tolerance

There is an increase in transcription of *oprM, mexB* and *mexA* in *P. aeruginosa* PA14 in response to treatment with the methacrylate ester BMA (**Table 15**). These 3 genes also showed the most significant Δ%AUC in response to BMA during the transposon mutant library screen. The RNA sequencing data shows that these 3 genes all show an increase in the average number of reads across all samples, and an increase in the LFC which is statistically significant. The significant increase in gene expression of every subunit of the MexAB-OprM when BMA is added to culture provides further evidence of its importance in the role of tolerance to this methacrylate ester.

4.2.5.2 The MexAB-OprM is not the only Efflux System Upregulated in Response to BMA

An increase in gene expression was observed for several efflux systems in *P. aeruginosa* when BMA was added to the culture. These systems are listed in **Table 16**.

Table 16: Significantly upregulated efflux systems are shown from the top 300 upregulated genes from *Pseudomonas aeruginosa* PA14 in response to BMA. These genes showed a significantly increased LFC in expression compared to the control samples. The LFC is shown for each gene within the systems which are upregulated

System	Genes Significantly Upregulated	logarithm to the Basis 2 of the Fold Change
MexAB-OprM	*MexA, MexB, OprM*	+1.59, +1.41, +1.36
MexCD-OprJ	*MexC, MexD, OprJ*	*+7.23, +5.04, +3.74*
MexPQ-OpmE	*MexQ, OpmE*	*+2.5, +3.0*
MexGHI-OpmD	*MexG, MexH*	*+2.07, +0.94*
TriABC	*TriA, TriC*	*+1.48, +1.12*

The range of efflux systems upregulated *P. aeruginosa* PA14 in response to BMA are shown in **Table 16**. Components of these 5 systems each displayed an LFC > +1, all of them being RND type multi-drug exporters. The increase in gene expression of so many RND type exporters in *P. aeruginosa* PA14 provides evidence that these multi-drug efflux pumps play a key role in BMA tolerance.

The efflux system which showed the highest increase in expression was MexCD-OprJ. *MexC, mexD* and *oprJ* were placed amongst the top 11 genes with the highest increase in gene expression levels in response to BMA. Despite the disruption of the MexAB-OprM system generating the largest Δ% AUC during the transposon mutant library screen, the level of gene expression of components of this system were only shown to slightly increase in comparison to other pumps such as MexCD-OprJ using RNA sequencing. To further understand the gene expression levels of the MexAB-OprM in comparison to other upregulated RND systems such as MexCD-OprJ, the raw number of reads associated with components of these systems from RNA sequencing data were analysed (**Figure 36**).

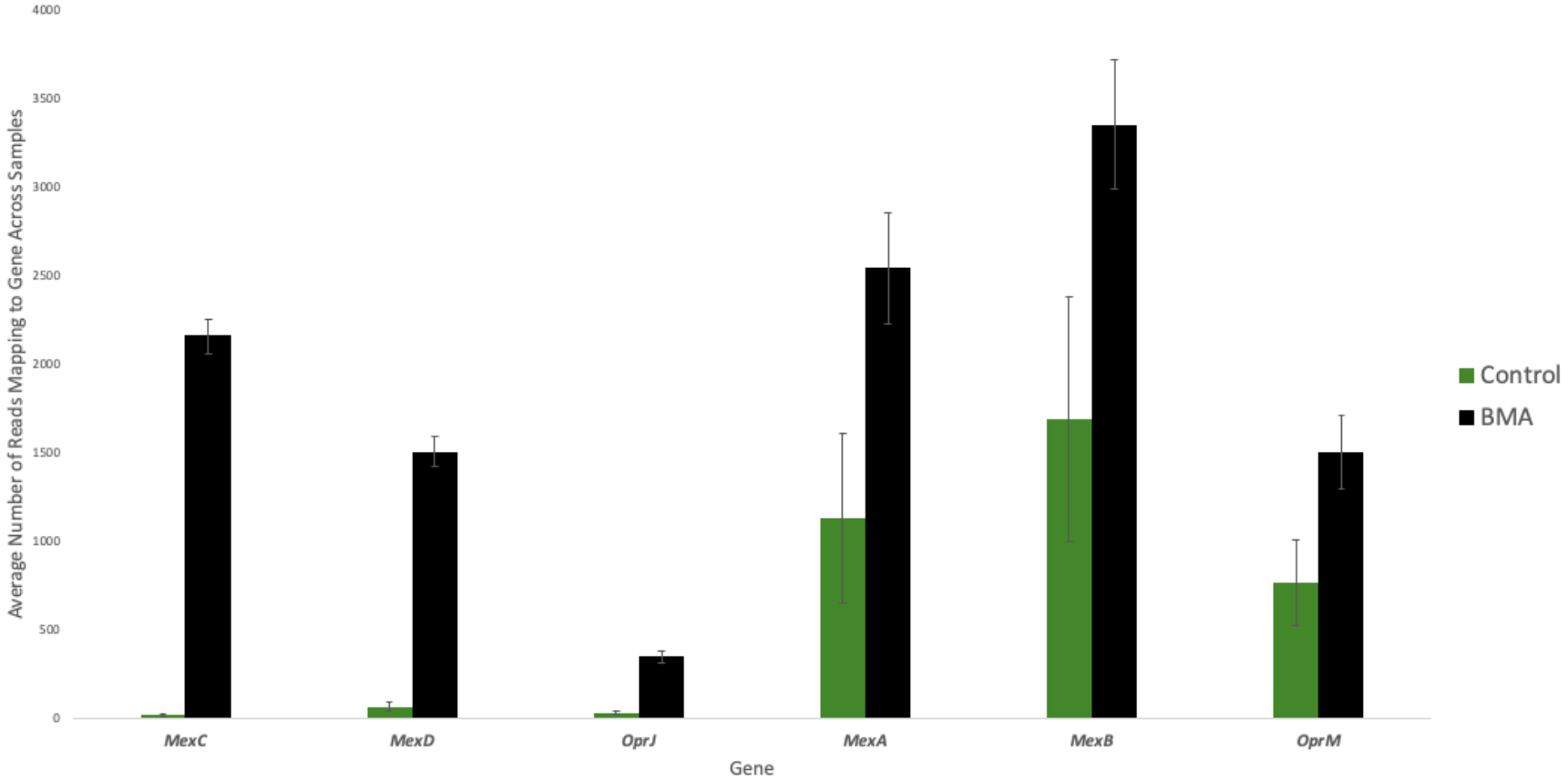

Figure 36: The average number of raw sequencing reads mapped to MexAB-OprM and MexCD-OprJ genes using htseq-count for both control and BMA cultures is shown. Standard deviation from the mean is shown for the number of reads mapping to each gene.

The log fold changes in expression of *mexA, mexB and oprM* were low in comparison to *mexC, mexD and oprJ* as is demonstrated in **Figure 36**. However, analysis of the raw number of reads obtained for each of these genes during RNA sequencing shows that *mexA, mexB* and *oprM* were expressed at high levels when BMA is both present and absent.

The number of transcripts sequenced corresponding to the MexCD-OprJ genes show that the efflux pump was expressed at relatively low levels in the absence of BMA (average reads mapped to *MexC* = 16, *MexD* = 64, *OprJ* = 30). In comparison, MexAB-OprM genes are expressed at high levels even in the absence of BMA (average reads mapped to *MexA* = 912, *MexB* = 1281*, OprM* = 602*)*. Therefore, the increase in expression of the MexCD-OprJ pump led to a large significant increase in log fold change in expression in comparison to the MexAB-OprM genes despite this pump is being highly expressed in both conditions. Taking raw reads into account as well as log fold change in expression is therefore important as systems which are functional at their background levels during the experimental conditions will not be reflected in the data using this kind of analysis alone.

The levels of expression of the MexCD-OprJ genes in the presence of BMA are not much higher than that of the MexAB-OprM in the control samples (average number of reads mapped to *MexC* = 2156, *MexD* = 1504, *OprJ* = 347 in the BMA samples vs *MexA* = 1126, *MexB* = 1687and *OprM* = 1500 in the control samples as is

demonstrated in **Figure 36**).Even though the expression of the MexAB-OprM pump is increased and shows a significant log fold increase in expression, this value is lower than that of the MexCD-OprJ because the pump is already intrinsically expressed at high levels. This data is suggestive that levels of expression of *mexA, mexB* and *oprM* are at levels high enough to provide some BMA tolerance in even the control sample, and a small increase in MexAB-OprM expression therefore provides sufficient tolerance for survival under the experimental conditions.

4.2.6 There is Significant Upregulation in *P. aeruginosa* PA14 in Components of the Cbb_3 Cytochrome Oxidase Maturation System in Response to BMA

A transposon mutagenesis library screen showed that disruption of genes involved in the maturation and assembly of the Cbb_3 cytochrome oxidase system resulted in significant Δ% AUC in the presence and absence of BMA, suggesting these genes could play a role in tolerance to BMA. The Cbb_3 cytochrome oxidases play a role in bacterial energetics in *P. aeruginosa*- their role is to maintain the proton gradient within the cell. The Cbb_3 maturation genes ensure that fully functional Cbb_3-1 and Cbb_3-2 proteins are formed within the cell (Pitcher and Watmough 2004). To further investigate the role of these proteins in BMA tolerance, whole transcriptome analysis was carried out and the differential expression of these systems using the RNA sequencing data was analysed **Figure 39**.

(A)

Gene_ID	Annotation	Mean Number of Reads Across All Samples	Logarithm to the Basis 2 of the Fold Change	P Value < 0.05?
PA14_44420	Ferrodoxin	574	+0.55	yes
PA14_44430	Hypothetical	156	+1.23	yes
PA14_44440	CopA2	193	+1.10	yes
PA14_44450	Hypothetical	6	+0.27	no
PA14_44460	Hypothetical	39	+0.46	no

(B)

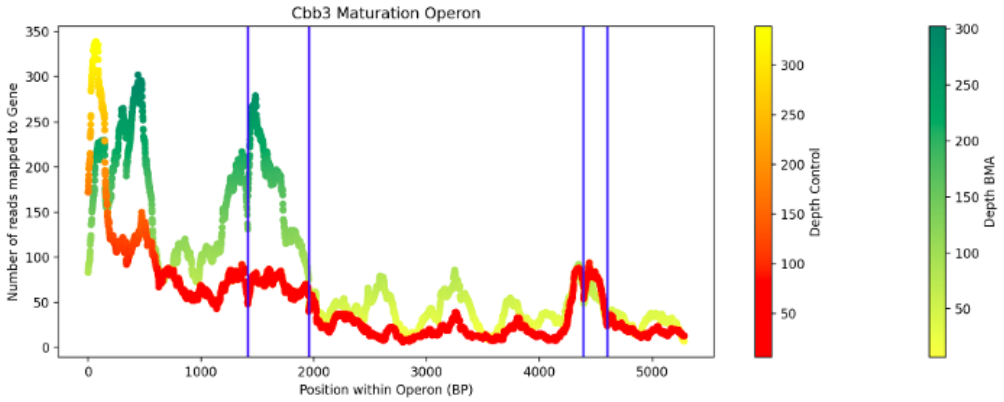

Figure 37: (A) the Cbb_3 maturation operon genes and their differential expression in response to BMA treatment is shown (B) the number of reads mapped to each of the genes in the Cbb_3 maturation operon on the chromosome is represented as read depth. Control reads are shown in red and BMA treated reads are shown in green. Separation of genes in the operon is represented by blue vertical lines. The depth scale is shown for each condition. Figure generated from the first BAM file of the samples in triplicate.

Whole transcriptome analysis shows that the levels of expression of all components of the Cbb_3 cytochrome oxidase assembly system were upregulated when BMA was present (**Figure 39**). *PA14_44420, PA14_44430* and *CopA2* displayed significant increases in expression when cultures were treated with BMA.

The ferrodoxin gene *PA14_44420* displayed a small increase in log fold change in expression and a large number of average sequencing reads were mapped to this gene in the BMA treated samples (LFC = 0.55 and average number of sequencing reads mapped to *PA14_44420* = 574). The unannotated gene *PA14_44430* also showed positive log fold change in expression (LFC = 1.23 and average number of sequencing reads mapped to *PA14_44430* = 156). The highest log fold change in expression from this group of genes was seen for the copper transporting p-type ATPase *copA2* (LFC = 1.09 and average number of sequencing reads mapped to *copA2* = 193). The 3 Cbb_3 type maturation proteins which were identified during the transposon mutant library screen were *copA2, PA14_44450* and *PA14_44460.* Although the RNA sequencing data showed that all these genes increased in expression during the experimental conditions, this change was only statistically significant for *copA2* and *PA14_44430.*

The disruption of the Cbb_3 maturation protein gene *copA2* led to the highest Δ% AUC during the transposon mutagenesis library screen. This gene also showed one of the highest log fold changes in expression when treated with BMA from the whole

transcriptome analysis discussed throughout this chapter. This provides further evidence that CopA2 could play a crucial role in the tolerance of *P. aeruginosa* to BMA.

4.2.7 Investigation of the General Cell Envelope Stress Response of *P. aeruginosa* PA14 to BMA

Personal communication with Ingenza Ltd and Mitsubishi Chemical Corporation UK revealed that during trial fermentations with *Pseudomonas putida* KT2440, carbon was not directed efficiently towards BMA production and large amounts of carbon could not be accounted for during the fermentation trials. The hydrophobicity of BMA places stress on the cell envelope and so a general cell envelope stress response to BMA in culture is expected. The production of trehalose as an osmoprotectant is a common osmotic stress response in Gram negative bacteria (Larsen et al. 1987; Woodcock et al. 2021). Here, we hypothesised that the redirection of carbon away from BMA production and towards trehalose production may be responsible for the loss of carbon observed in trial fermentations. Genes upregulated in the whole transcriptome analysis were investigated to further understand the general cell envelope stress response of *P. aeruginosa* PA14 to BMA and whether this was the cause of unaccounted carbon during trial fermentation runs at Ingenza Ltd.

4.2.7.1 Genes Associated with Osmotic Stress are Upregulated in P. aeruginosa PA14 in Response to BMA

The RNA sequencing data was analysed using the functional analysis and gene enrichment tool Funage-Pro. Genes associated with the general cell envelope stress response and osmotic stress were identified amongst the upregulated genes (**Table 17**).

Table 17: Upregulated genes associated with osmotic stress within the RNA sequencing data using Funage Pro are listed. Genes associated with osmotic stress which were within the top 300 significantly differentially expressed genes are shown

Osmotic Stress Response Genes Identified by Funage Pro			
Gene_ID	**Gene Name**	**Product**	**Logarithm to the Basis 2 of the Fold Change**
PA14_36630	*GlgX*	Glycogen operon protein	+3.4
PA14_36840	*GlgP*	Glycogen phosphorylase	+2.72
PA14_36570	*GlgA*	Glycogen synthase	+2.74
PA14_36710	*GlgB*	1,4-alpha-glucan branching enzyme	+3.19
PA14_33450	*TreA*	Trehalase	+1.53
PA14_36605	-	Maltooligosyl trehalose synthase	+3.33
PA14_36730	*TreS*	Trehalose synthase	+3.13
PA14_38350	*GalU*	UTP- glucose-1-phosphate uridylyltransferase	+2.34
PA14_13580	*OsmV*	Osmoprotectant import ATP-binding protein	+2.11
PA14_13610	*OsmY*	Osmoprotectant import permease protein	+2.03

Genes associated with osmotic stress are significantly upregulated in response to BMA, as shown in **Table 17**. Significant upregulation of the osmoprotectant genes *osmV* and *osmY* are indicative of cell envelope stress(Frossard et al. 2012). The other upregulated genes which were identified play a role in the biosynthesis of trehalose and glycogen within the cell. The role of these genes in the trehalose biosynthetic pathway are displayed in **Figure 40**.

.

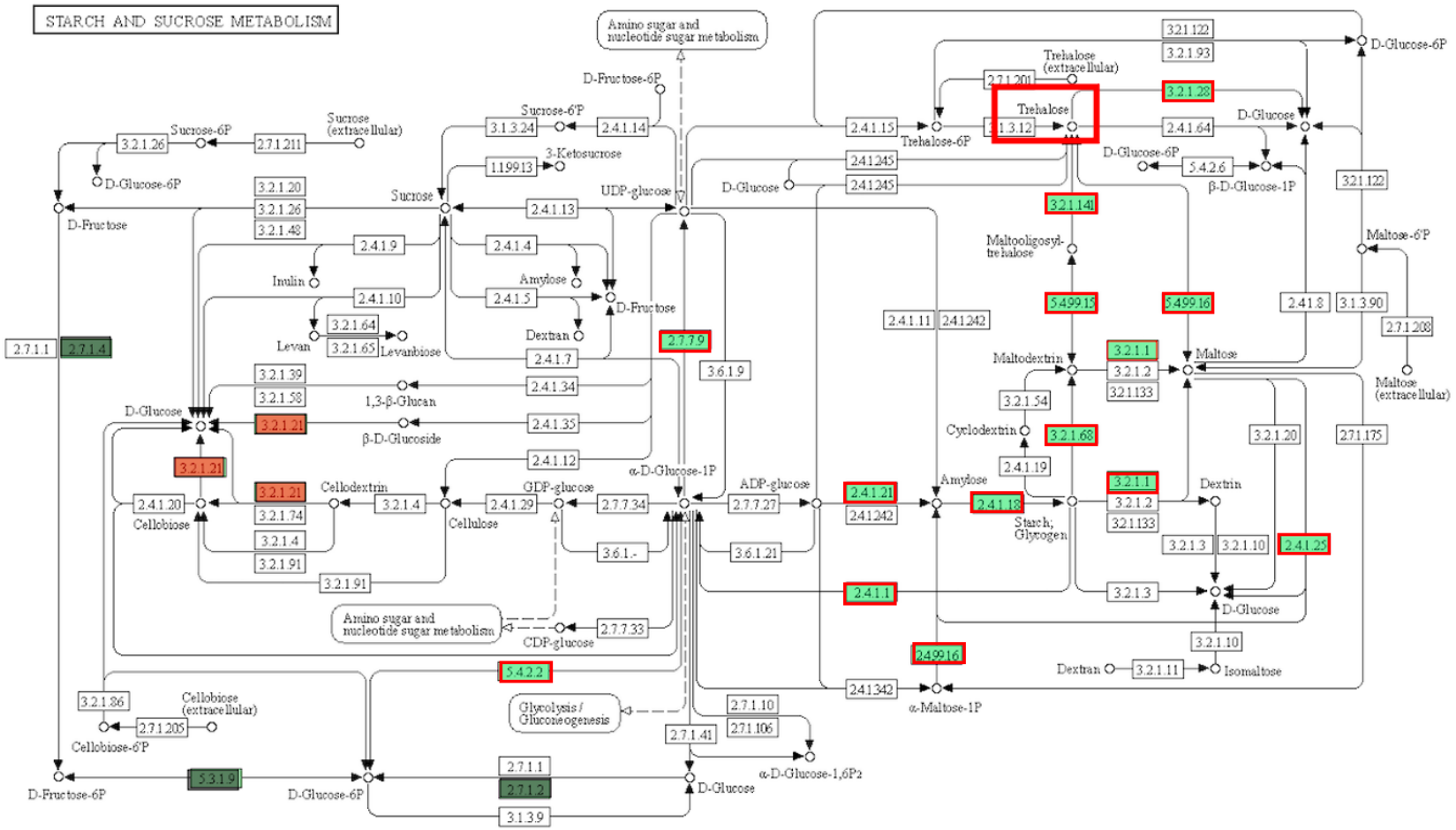

Figure 38: The *P. aeruginosa* PA14 starch and sucrose metabolism KEGG pathway map is shown. Trehalose is highlighted and the genes absent in *P. aeruginosa* PA14 are displayed in white. Genes which are upregulated in response to BMA are shown with a red border, genes which display no change are shown in grey and genes which were downregulated in response to BMA are shown in red.

The *P. aeruginosa* PA14 starch and sucrose metabolism pathway is shown in **Figure 40**. Genes associated with the conversion of glycogen to trehalose are upregulated as indicated by boxes with a red border. The data represented by the KEGG map shows clearly that *P. aeruginosa* PA14 displays a specific response associated with trehalose production in response to treatment with BMA. This is evidence of a generalised cell envelope stress response to BMA and the production of trehalose as an osmoprotectant could be responsible for the redirection of carbon away from BMA production observed in trial fermentations at Ingenza Ltd.

4.2.8 There is Significant Downregulation of some Genes in Response to BMA

The top 5 genes with the highest significant downregulation in response to BMA are shown in **Table 18**.

Table 18: The top 5 genes with the highest significant downregulation in *P. aeruginosa* PA14 in response to BMA are shown. The LFC is displayed for each gene.

Gene ID	Annotation	Logarithm to the Basis 2 of the Fold Change
PA14_19680	Putative peptidoglycan hydrolase	-3.97
PA14_68470	Carbon storage regulator *RsmN*	-3.34
PA14_22990	Sugar transporter *GltF*	-3.05
PA14_23000	Sugar transporter *GltG*	-2.90
PA14_23010	Sugar transporter *GltK*	-2.80

The top 5 downregulated genes in *P. aeruginosa* PA14 in response to BMA include a peptidoglycan hydrolase, the carbon storage regulator *rsmN* and three sugar transporters.

4.2.9 Analysis of Differential Gene Expression in *P. aeruginosa* PA14 Treated with the Solvents Styrene and Ethylbenzene

To determine whether *P. aeruginosa* PA14 exhibited a similar transcriptomic response to BMA when treated with the platform chemicals styrene and ethylbenzene, the RNA sequencing data was analysed using DeSeq2.

To interpret the DESeq2 analysis carried out on styrene and ethylbenzene treated PA14 cultures, volcano plots were generated showing genes with a significant LFC in response to these solvents. The top 20 most significantly upregulated genes are labelled. Also shown are histograms of the p values of differentially expressed genes within each dataset (**Figure 41**, and **Figure 42**).

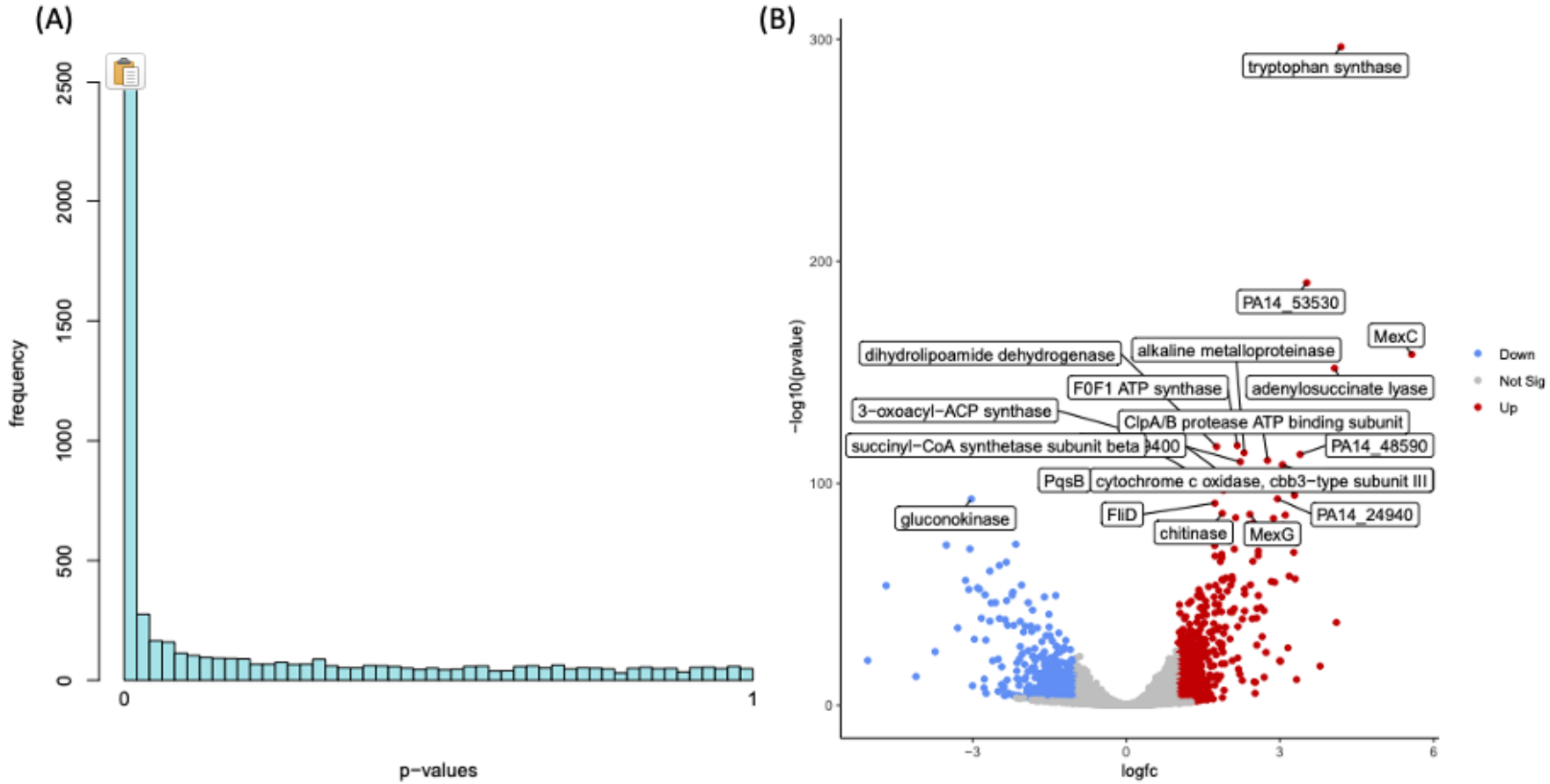

Figure 39: Histogram of p-values of log fold change in expression of upregulated and downregulated genes in *P. aeruginosa* PA14 when exposed to the solvent styrene (B) Volcano plot of differentially expressed genes in *P. aeruginosa* PA14 when exposed to the solvent styrene. Genes which showed no significant differential expression are shown in grey, genes which showed a significant increase in expression are shown in red and genes which showed a significant decrease in expression are shown in blue. The top 20 most significantly differentially expressed genes are labelled. Unannotated genes are labelled with locus tag and the gene name is given where possible.

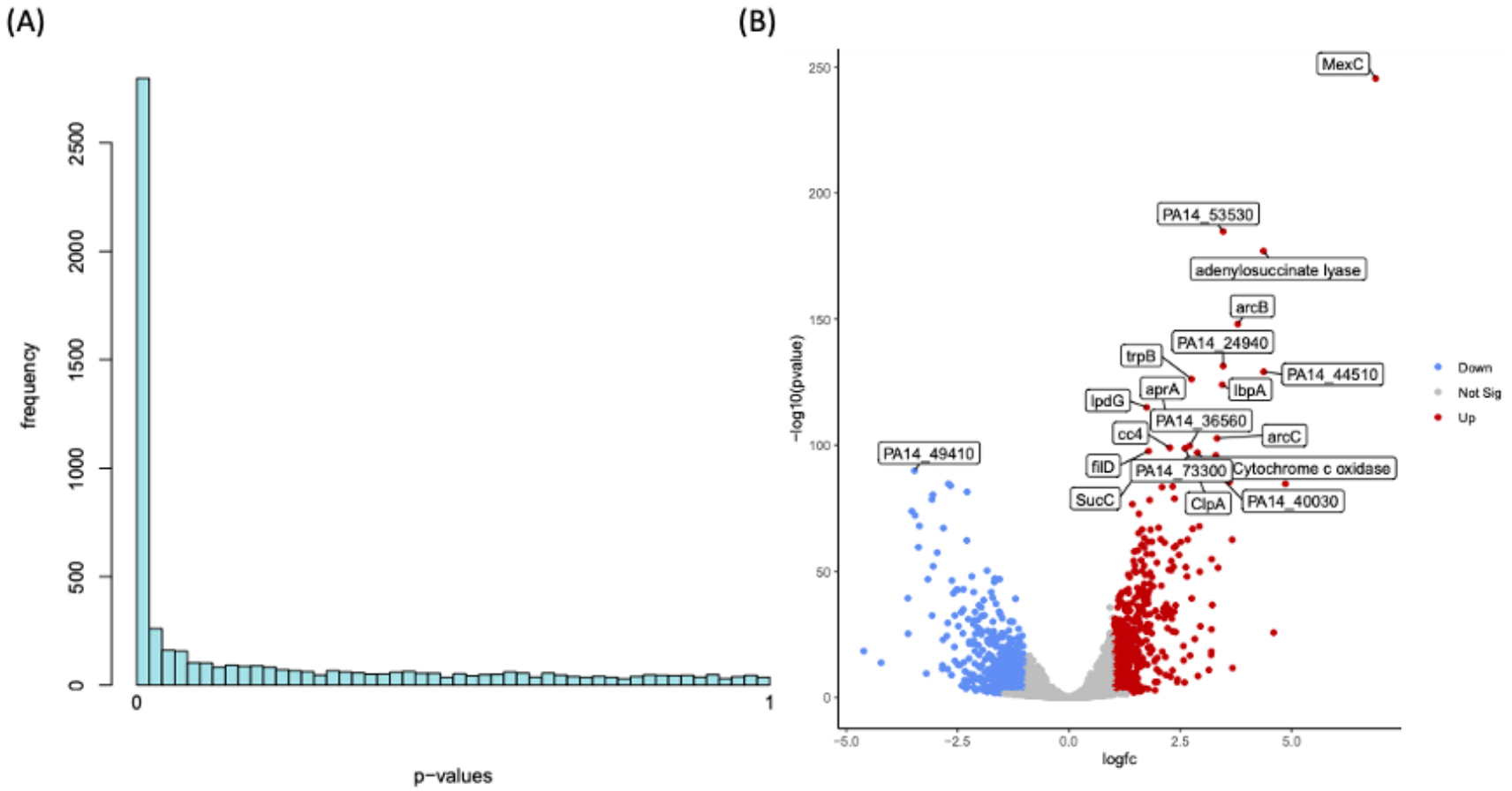

Figure 40: Histogram of p-values of log fold change in expression of upregulated and downregulated genes in *P. aeruginosa* PA14 when exposed to the solvent ethylbenzene (B) Volcano plot of differentially expressed genes in *P. aeruginosa* PA14 when exposed to the solvent ethylbenzene. Genes which showed no significant differential expression are shown in grey, genes which showed a significant increase in expression are shown in red and genes which showed a significant decrease in expression are shown in blue. The top 20 most significantly differentially expressed genes are labelled. Unannotated genes are labelled with locus tag and the genename is given where possible.

The frequency of differentially expressed genes within both the styrene and ethylbenzene datasets with a p value close to zero was significant, as shown in **Figure 41** and **Figure 42**. This provides evidence that the dataset is reliable. The volcano plot representation of these datasets shows the labelled top 20 significantly differentially expressed genes in *P. aeruginosa* PA14 when treated with the solvents styrene and ethylbenzene. The genes identified can be categorised into groups based on their function.

4.2.10 Comparison of BMA Transposon Mutant Library Screen and Transcriptomic Analysis of Styrene and Ethylbenzene Treated Cultures

To determine whether the same systems shown in the BMA transposon mutant library screen were significantly upregulated in the styrene and ethylbenzene RNA sequencing data, the data was compared (**Table 19**).

Table 19: The Δ% AUC and log fold change in expression of the top 10 systems of interest identified during the BMA transposon mutant library screen are shown alongside the differential expression analysis of the same systems from the BMA, styrene and ethylbenzene RNA sequencing data.

BMA Transposon Mutant Library Screen			Transcriptomic Analysis by RNA Sequencing					
			Styrene		Ethylbenzene		BMA	
Gene ID	Description	Δ%AUC	LFC	P Value < 0.05?	LFC	P Value < 0.05?	LFC	P Value < 0.05?
PA14_05550	OprM	-63.12	+0.79	yes	+1.07	Yes	+1.36	Yes
PA14_05540	MexB	-55.70	+1.05	Yes	+1.68	Yes	+1.41	Yes
PA14_05530	MexA	-55.29	+0.70	Yes	+1.37	Yes	+1.59	Yes
PA14_44460	Cbb_3 Cytochrome Oxidase Assembly	-51.03	-0.15	No	+0.44	No	+0.46	No
PA14_44440	Cbb_3 Cytochrome Oxidase Assembly CopA2	-49.85	+1.01	Yes	+1.46	Yes	+1.1	Yes
PA14_61980	Chromosome partitioning protein	-45.27	+0.35	No	+0.56	No	-0.39	No
PA14_44450	Cbb_3 Cytochrome Oxidase Assembly	-45.11	-1.83	Yes	-0.75	No	+0.27	No
PA14_07760	SurA	-44.40	+0.24	Yes	+0.1	No	-0.43	Yes
PA14_43950	SucC	-41.62	+1.75	Yes	+1.69	Yes	+0.32	Yes
PA14_62930	Carbomyl-phosphate synthase	-36.09	+0.04	No	+0.44	Yes	+0.16	No

The differential expression of the top 10 systems of interest identified during the BMA transposon mutant library screen was analysed in response to treatment BMA, styrene and ethylbenzene (**Table 19**). Genes which displayed significant upregulation across all solvent-treated samples are indicated by green text. The genes *oprM, mexB, mexA, copA2,* and *sucC* were all upregulated by *P. aeruginosa* PA14 in response to BMA, styrene and ethylbenzene.

4.2.10.1 RNA Sequencing Data Reinforces the Importance of the MexAB-OprM in Solvent Tolerance

There is an increase in transcripts detected of the genes *oprM, mexB* and *mexA* genes in *P. aeruginosa* PA14 in response to treatment with the solvents BMA, styrene and ethylbenzene (**Table 19**). These 3 genes also showed the most significant Δ% AUC in response to BMA during the transposon mutant library screen. The RNA sequencing data shows that these three genes all show an LFC in expression which is statistically significant. The significant increase in expression of every subunit of MexAB-OprM when BMA, styrene and ethylbenzene are added to cultures provides further evidence of its importance in the role of tolerance to these solvents.

4.2.10.2 The MexAB-OprM is one of Several Efflux System Upregulated in Response to Styrene and Ethylbenzene

Several efflux systems in *P. aeruginosa* showed an increase in expression when styrene and ethylbenzene were added to the cultures. The efflux systems significantly upregulated in the RNA sequencing datasets for these solvents are shown in **Table 20**.

Table 20: Significantly upregulated efflux systems are shown from the top 300 upregulated genes from *Pseudomonas aeruginosa* PA14 in response to the solvents styrene and ethylbenzene. All genes listed showed a significantly increased LFC in expression compared to the control samples.

	Styrene		Ethylbenzene	
System	Genes Significantly Upregulated	Log Fold Change in Gene Expression	Genes Significantly Upregulated	Log Fold Change in Gene Expression
MexAB-OprM	*MexA, MexB, OprM*	+0.70, +1.05, +0.79	*MexA, MexB, OprM*	+1.37, +1.68, +1.07
MexCD-OprJ	*MexC*	+5.6,	*MexC, MexD*	+6.90, +1.63
PA14_46580, RND type membrane fusion protein	*PA14_46580*	+4.1	PA14_46580	+1.5
MexEF-OprN	*MexE, MexF, OprN*	+1.58, +3.78, +1.62	*MexE, MexF, OprN*	+1.63, +4.60, +4.86
PA14_48630, MSF type transporter	*PA14_48630*	+2.63	PA14_48630	+2.39
MexGHI-OpmD	*MexG, MexH, OpmD*	*+2.41, +1.09, +0.50*	*MexG, MexH*	*+2.06, +0.33*
PA14_16800, RND type MFP	*PA14_16800*	+2.07	*PA14_16800*	+1.52
PA14_20900, MSF type transporter	*PA14_20900*	+1.81	*PA14_20900*	+1.69
MexPQ-OpmE	*MexP, MexQ, OpmE*	+1.58, +3.78, +1.62	*MexP, MexQ, OpmE*	+1.63, +4.60, +4.86

The range of efflux systems with an increase in expression in *P. aeruginosa* PA14 in response to styrene and ethylbenzene are shown in **Table 20**. Components of these systems appeared within the top 300 most highly upregulated genes within the datasets, all of them being RND type multi-drug exporters with the exception of two MFS-type exporters. The increase in expression of so many RND-type exporters in *P. aeruginosa* PA14 provides further evidence that these multi-drug efflux pumps play a key role in solvent tolerance. Most efflux systems upregulated in response to styrene and ethylbenzene are upregulated in both datasets. Therefore, according to the differential expression analysis carried out on the RNA sequencing data, the profile of exporting systems upregulated in *P. aeruginosa* PA14 in response to these systems is highly similar.

4.2.10.3 Components of the Cbb_3 Cytochrome Oxidase Assembly System are Upregulated in Response to Styrene and Ethylbenzene

Some components of the Cbb_3 maturation system showed an increase in expression when treated with styrene and ethylbenzene. The p-type ATPase*copA2* which showed the highest Δ% AUC during the BMA transposon mutant library screen when disrupted showed a significant increase in expression when treated with BMA. The same result is observed when *P. aeruginosa* PA14 is treated with styrene and ethylbenzene, this gene showing the highest upregulation of Cbb_3 maturation genes across all solvent treated samples as is shown in **Table 19**. These results provide further evidence of the importance of this membrane protein in tolerance to all three solvents tested during this study.

There was no significant change in expression of the Cbb_3 assembly gene *PA14_44460* across any of the solvent treated samples, despite the disruption of this gene exhibiting one of the highest Δ% AUC during the BMA transposon mutant library screen. The gene *PA14_44450* showed a significant decrease in expression when treated with styrene. However, this result is not replicated in the ethylbenzene and BMA treated samples which do not show a statistically significant change. The transposon mutant library screen demonstrated that some Cbb_3 maturation genes could play a role in BMA tolerance, however, whole transcriptome analysis for BMA, styrene and ethylbenzene treated *P. aeruginosa* PA14 cultures reinforces this for the p-type ATPase gene *copA2.*

4.2.11 Components of the Cbb_3 Cytochrome Oxidase System are Upregulated in Response to Styrene and Ethylbenzene

The BMA transposon mutant library screen demonstrated that components of the Cbb_3 maturation system could play a role in BMA tolerance in *P. aeruginosa* PA14. The differential gene expression analysis of components of the Cbb_3 assembly system from the RNA sequencing data generated from BMA, styrene and ethylbenzene treated samples are shown in **Table 21**. This data shows the increase in expression of *copA2* but a significant increase in expression of other Cbb_3 type assembly genes is not observed. As there is only one set of genes encoding the maturation system of Cbb_3 cytochrome oxidases, but 2 sets of genes encoding the cytochrome oxidases themselves, this study set out to investigate the role of these systems in solvent tolerance in *P. aeruginosa* PA14. To investigate the role of these systems further, differential gene expression analysis was carried out on components of the Cbb_3 cytochrome oxidase genes in response to BMA, styrene and ethylbenzene (**Table 21**).

Table 21: Comparison of the log fold change in expression of Cbb_3 cytochrome oxidase genes between BMA, styrene and ethylbenzene treated samples. Shown is the LFC for each gene and the significance is indicated by a p value is less than 0.05.

	BMA		Styrene		Ethylbenzene	
Cbb_3 -1 Genes	Log Fold Change in Expression	P Value < 0.05?	Log Fold Change in Expression	P Value < 0.05?	Log Fold Change in Expression	P Value < 0.05?
PA14_44340	-0.19	no	+1.86	yes	+1.51	yes
PA14_44350	+1.0	yes	+3.18	yes	+2.94	yes
PA14_44360	+1.38	yes	+3.28	yes	+3.30	yes
Cbb_3-2 Genes						
PA14_44370	+0.46	yes	+1.08	yes	+1.45	yes
PA14_44380	-0.43	yes	+0.33	yes	+0.26	no
PA14_44390	-0.77	no	-0.53	no	-0.34	no
PA14_44400	-0.27	yes	+0.62	Yes	+0.31	yes

Shown in **Table 21** is the differential gene expression analysis carried out on all Cbb_3-1 and Cbb_3-2 genes in *P. aeruginosa* PA14 in response to BMA, styrene and ethylbenzene.

Wole transcriptome analysis of BMA treated samples did not indicate the potential for a large increase in expression of any Cbb_3 cytochrome oxidase genes. The genes *PA14_44350* and *PA14_44360* from Cbb_3-1 and *PA14_44370* from Cbb_3-2 showed a small significant increase (LFC= 1.0, 1.38, and 0.43 respectively), while the rest of the genes showed slight decreases in expression, however, these were not all statistically significant.

4.2.11.1 An Increase in Expression of Cbb_3-1 Cytochrome Oxidase is Associated with Exposure to Styrene and Ethylbenzene

In response to exposure to styrene and ethylbenzene, a large significant increase in RNA transcripts was observed in the Cbb_3-1 genes *PA14_44340, PA14_44350* and *PA14_44360.* The gene *PA14_44360* was within the top twenty significantly upregulated genes in both the styrene and ethylbenzene datasets. Although some significant upregulation is observed for Cbb_3-2 genes under these conditions, the differential expression of genes associated with Cbb_3-1 is significantly higher as is indicated by green text in **Table 21**. This provides further evidence that the Cbb_3 cytochrome oxidase system plays a key role in solvent tolerance in *P. aeruginosa* PA14. Additionally, this data suggests that the Cbb_3 cytochrome oxidase which is

facilitating styrene and ethylbenzene tolerance is Cbb_3-1 due to the large significant increase of RNA transcripts mapping to the Cbb_3-1 associated genes under these conditions.

4.2.12 The *P. aeruginosa* PA14 Transcriptomic Response to the Solvents Styrene and Ethylbenzene

Using RNA sequencing analysis of *P. aeruginosa* PA14 cultures treated with BMA, styrene and ethylbenzene the differential expression of genes was analysed in response to each solvent. To compare the similarity of the transcriptomic response of *P. aeruginosa* PA14 to each of these solvents, the frequency of significantly upregulated genes within each dataset was compared. The top twenty and top 300 significantly upregulated genes were compared from each solvent condition (**Figure 43**).

(A)

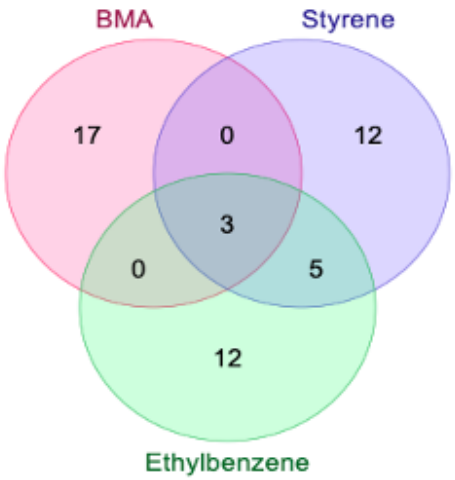

(B)

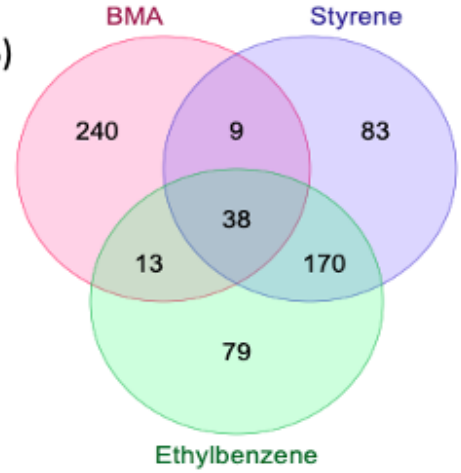

(C)

All Solvent Groups		Styrene and Ethylbenzene	
Gene ID	Function	Gene ID	Function
PA14_60850, *MexC*	RND type exporter	PA14_18780, *MexF*	RND type exporter
PA14_53530	Possible metal dependant hydrolase	PA14_18830	adenylosuccinate lyase
PA14_36920	Possible histidine kinase	PA14_24940	Putative oxidase
		PA14_44360	Cbb_3 type cytochrome oxidase subunit
		PA14_44510	Possible metal dependant hydrolase

Figure 41: Summary of common upregulated genes among solvent treated cultures (A) Venn diagram representation of upregulated genes (top twenty) (B) Venn diagram representation of the number of upregulated genes within the top 300 genes shared between different solvent treatment groups is shown (C) Table describing the upregulated genes shared between solvent groups from within the top twenty upregulated genes, listed with their functions. Where genes aren't fully functionally annotated, their predicted function using gene ontology functional annotation using InterPro2GO Mapping is shown and indicated by 'possible'.

The number of significantly upregulated genes shared between the top 20 and 300 upregulated genes within the different solvent-treated RNA sequencing datasets are displayed in **Figure 43**.

From the top twenty upregulated genes from each treatment group three genes are shared by all groups, five genes are shared between styrene and ethylbenzene and three are shared between all groups. The RND type exporter *MexC* is shared by all solvent treatment groups as one of the most highly upregulated genes within the dataset, exhibiting the highest significant LFC in expression of all genes within the dataset for all groups (LFC = 7.23, 5.57 and 6.89 for BMA, styrene and ethylbenzene respectively). This indicates the importance of the function of the MexCD-OprJ in solvent tolerance and provides evidence for the multi-drug efflux pumps broad specificity for the range of solvents tested during this study.

Also shared between the top 20 significantly upregulated genes by all solvent treatment groups are the genes *PA14_53530,* a possible metal dependant hydrolase and *PA14_36920,* a possible histidine kinase. These genes are not fully functionally annotated and so their functions were assigned using gene ontology functional annotation through InterPro2GO Mapping. The significant increase in RNA transcripts mapping to these genes throughout all three datasets suggests they play a crucial role in solvent tolerance in *P. aeruginosa* PA14. The three shared genes between all

solvent treatment groups indicates a small but universal response occurs to BMA, styrene and ethylbenzene.

The five genes shared between the top twenty upregulated genes within the styrene and ethylbenzene datasets are shown in **Figure 43** . Among these genes is the RND type exporter *mexF.* This RND exporter is differentially expressed only in the styrene and ethylbenzene datasets and is absent from the top 300 upregulated genes in the BMA treatment group. This suggests a substrate-specific response of efflux pump upregulation between the treatment groups. **Table 16** and **Table 20** show there are many shared efflux pumps upregulated between the datasets, however, the number of RNA transcripts mapping to *mexF* was unchanged between the control and BMA treatment group. The increase in RNA transcripts mapping to *mexF* is specific to styrene and ethylbenzene.

Among the five upregulated genes shared exclusively between styrene and ethylbenzene from the top twenty upregulated genes within the dataset are *PA14_24940,* a possible putative oxidase (functional annotation analysis carried out using InterPro2GO Mapping) and *PA14_44360*, a subunit of the Cbb_3-1 cytochrome oxidase. This result supports the hypothesis that these cytochrome oxidase systems play a key role in solvent tolerance and suggests this response is more prominent when cultures are treated with styrene and ethylbenzene in comparison to BMA.

The genes *PA14_ 18830,* an adenylosuccinate lyase and *PA14_44510,* a possible metal dependant hydrolase (functional annotation analysis carried out using InterPro2GO Mapping) are also upregulated in the top 20 upregulated genes within the styrene and ethylbenzene datasets.

4.2.12.1 A Significant Number of Upregulated Genes are Shared Between the Styrene and Ethylbenzene Treated Cultures

Of the top three hundred significantly upregulated genes in *P. aeruginosa* PA14 to styrene and ethylbenzene, 170 of these genes are shared between the two groups, compared to 38 genes shared between all three groups **Figure 43**. This data suggests that the transcriptomic responses of *P. aeruginosa* PA14 to the solvents styrene and ethylbenzene share a relatively high degree of similarity in comparison to the response of these solvents compared to the methacrylate ester BMA. The high degree of structural similarity between styrene and ethylbenzene could explain this result.

4.3 Discussion

The need for industrially capable microorganisms for fermentation processes has put an emphasis on the discovery of tolerance conferring mechanisms within these microorganisms to the platform chemicals they produce (Mohedano, Konzock, and Chen 2022). Advances within synthetic biology have meant that the generation of production strains to overcome bioprocess bottlenecks such as tolerance has been demonstrated (Katz et al. 2018; Nicolaou, Gaida, and Papoutsakis 2010). During this study, the identification of tolerance conferring systems within *P. aeruginosa* PA14 to various platform chemicals of the plastics industry is demonstrated through whole transcriptome analysis using RNA sequencing and in-depth differential gene expression analysis, in addition to a complimentary transposon mutant library screen previously carried out by Walid El Bestawy.

4.3.1 High Quality RNA was Extracted from Cultures Using a Trizol™ Column Based Method of Isolation

RNA was extracted from *P. aeruginosa* PA14 cultures using Trizol™ in combination with the Trizol™ Plus RNA Purification Kit. This method was chosen over other common methods such as bead-bashing or sonication as it has been widely reported in the literature as a successful technique for the generation of high-quality RNA isolation from *P. aeruginosa* cultures (Pust et al. 2022; Waite et al. 2005; Whiteley et al. 2001). Using the Trizol method of RNA extraction ensured that there was no solvent carryover from cultures, as solvent is efficiently separated from the RNA

during phase separation stage of the protocol (Rio et al. 2010). This was demonstrated by the high quality of RNA extracted using this method as indicated by the RIN numbers of samples (**Figure 30** and **Figure 32**).

4.3.2 Transcriptomic Analysis in Combination with a Transposon Mutant Library Screen is an Efficient Method for Demonstrating the Importance of Efflux in Tolerance to BMA, Styrene and Ethylbenzene in *P. aeruginosa* PA14

A transposon mutant library screen showed the importance of the RND MexAB-OprM multi-drug efflux pump in BMA tolerance in *P. aeruginosa* PA14. This was demonstrated by the largest Δ% AUC in response to BMA when the genes *mexA, mexB* and *oprM* were disrupted by transposition. Although transcriptomic analysis reinforced the importance of this system, the data has showed that many other efflux systems are significantly upregulated in response to BMA, styrene and ethylbenzene. Here, our data shows that efflux of solvents from the cell is a major component of tolerance, and that both intrinsic levels of expression and upregulation of RND systems are important for tolerance to these solvents.

The solvents used in this study are toxic as they partition themselves within the cell membrane and the periplasmic space, causing the disruption of cell membranes because of their hydrophobicity (Fujisawa et al. 2008; Stancu 2018). RND systems are widely reported in the literature to be a crucial tolerance mechanism in *P. aeruginosa*

and their role is most important in exponential growth phase when the membrane is most unstable (J. Blair, personal communication). During this study, solvents were added to cultures in exponential phase when cell membranes are already reported to be weakened, increasing the need for efflux of these solvents from the cell.

During the transposon mutant library screen the impact on growth of *P. aeruginosa* when the efflux genes *mexA, mexB* and *oprM* was demonstrated by the largest Δ% AUC reported during the experiment. During this study, whole transcriptome analysis demonstrated that the number of RNA transcripts mapping to various efflux systems in the presence of BMA, styrene and ethylbenzene showed a significant increase compared to no solvent control samples. These results compliment what is already known about the relationship between efflux and solvent tolerance (Fernandes, Sommer Ferreira, and Sampaio Cabral 2003; Li, Zhang, and Poole 1998a; Ramos et al. 2003), and further demonstrate the importance of RND type efflux pumps in solvent tolerance in *P. aeruginosa* PA14.

4.3.3 RND Efflux Systems Play a Significant Role in *P. aeruginosa* PA14 Solvent Tolerance

4.3.3.1 MexAB-OprM and MexCD-OprJ are Upregulated in Response to BMA

Analysis of the RNA sequencing data using DESeq2 revealed that all the *MexAB-OprM* genes identified during the transposon mutant library screen were upregulated in *P. aeruginosa* PA14 response to BMA. However, despite the genes encoding this system

showing the largest Δ% AUC during the transposon mutant library screen, the increase in RNA transcripts mapping to these genes in response to BMA exposure was less than other efflux pumps as is demonstrated in **Figure 36**. The efflux pump with the largest increase in RNA transcripts mapping to itself in response to BMA is MexCD-OprJ.

Analysis of the raw number of sequencing reads aligned to the *mexA, mexB* and *oprM* genes showed that the MexAB-OprM system is highly expressed in both the BMA and control samples. Although the pump is upregulated in response to BMA, its expression in the control samples is at a high level in comparison to other efflux pumps such as MexCD-OprJ as is demonstrated in **Figure 36**. This is consistent with that demonstrated previously in the literature- intrinsic levels of constitutive *MexAB-OprM* expression conferred tolerance to many antimicrobial agents (Li, Poole, and Nikaido 2003; López-Causapé et al. 2018; Nakae et al. 1999). This data shows that the basal levels of expression of MexAB-OprM are sufficient to provide a level of BMA tolerance such that the upregulation required for the pump's expression is small in the BMA cultures.

The number of sequencing reads mapped to *mexC, mexD* and *oprJ* in the control sample are low in comparison to the MexAB-OprM genes within the same sample- the average number of RNA transcripts mapped to *mexA, mexB* and *oprM* were 1126, 1687 and 765 respectively compared to 16, 64 and 30 for *mexC, mexD* and *oprJ*.

Despite the large change in expression associated with the MexCD-OprJ efflux pump in response to BMA, the raw number of reads of the *mexC, mexD* and *oprJ* genes is comparable to that of the MexAB-OprM genes in the BMA sample- the average number of RNA transcripts mapped to *mexC, mexD* and *oprJ* were 2156, 1504 and 347 respectively compared to 2540, 3348 and 1500 for *mexA, mexB* and *oprM*.

Overexpression of MexCD-OprJ in the clinic is associated with increased pathogenicity and resistance to a range of compounds including chloramphenicol and ciprofloxacin (Jeannot et al. 2008). The results demonstrated during this study are consistent with previously reported results in the literature showing that the upregulation of MexCD-OprJ is associated with tolerance to many compounds as opposed to its intrinsic levels of expression (Llanes et al. 2004; Poole et al. 1996). MexCD-OprJ provides acquired tolerance rather than intrinsic to several antibiotics (Masuda et al. 2000). Both MexAB-OprM and MexCD-OprJ are implicated in the solvent tolerance of *P. aeruginosa* to organic compounds such as hexane and xylene (Li et al. 1998a). These results suggest that in contrast to MexAB-OprM, the basal levels of MexCD-OprJ expression is not sufficient to provide BMA tolerance since its upregulation to BMA is one of the largest in the dataset.

Using differential gene expression analysis on its own can have limitations (Uygun et al. 2016). Here it is shown that using differential gene expression analysis alone shows that the most highly upregulated efflux pump within the BMA dataset is the

MexCD-OprJ. However, when the number of raw sequencing reads is considered, it is clear the MexAB-OprM efflux pump also plays a key role in tolerance. The results of this study demonstrate that analysing the differential expression of genes in combination with the raw number of sequencing reads means that systems with important intrinsic function are not overlooked. Having transposon mutant library screening data to compliment the whole transcriptome analysis carried out during this study also accounts for these limitations of using differential gene expression analysis alone.

4.3.4 Systems Involved With Cell Wall Degradation and Sugar Transporters are Downregulated in Response to BMA

The gene which showed the highest significant decrease in number of RNA transcripts mapping to the gene in the BMA dataset was a putative peptidoglycan hydrolase. The role of peptidoglycan hydrolases in *P. aeruginosa* and other Gram-negative bacteria is to hydrolyse portions of peptidoglycan within the cell wall to enable the insertion of newly synthesised peptidoglycan for cell wall strengthening (Vollmer et al. 2008). During this study, the addition of BMA placed stress on the cell membrane and a decrease in the number of RNA transcripts sequenced of this peptidoglycan hydrolase was observed in comparison to the no BMA control. The downregulation of this enzyme may be caused by the compromised cell envelope due to high concentrations of BMA in the cell culture, as hydrolysing peptidoglycan within the

cell wall has short-term weakening effects which cannot be afforded when the cell envelope is already compromised.

The second gene within the BMA dataset exhibiting the largest significant decrease in RNA transcripts sequenced in comparison to the control sample is the regulator *rsmN.* This regulator has been shown to repress exopolysaccharide synthesis genes, and so its downregulation is suggestive that genes involved with cell wall synthesis are being derepressed (Irie et al. 2010; Romero et al. 2018). This in addition with the downregulation of the peptidoglycan hydrolase provides evidence that *P. aeruginosa* PA14 is protecting and regenerating its cell wall in response to BMA.

The number of RNA transcripts mapping to the genes *gltF, gltG* and *gltK* significantly decreases in response to BMA. These genes involved in glucose transport within the cell, as glucose was the main carbon source during this experiment and so this result is surprising. However, the downregulation of these genes in *P. aeruginosa* in the literature has been implicated in the general cell envelope stress response which may explain this effect (Chevalier et al. 2017). Downregulation of these transporters may aid in membrane stabilisation by making room for the large number of RND pumps upregulated in these conditions, as overexpression of membrane proteins at high levels has been demonstrated in the literature to destabilise the cell membrane (Bernaudat et al. 2011; Errasti-Murugarren, Bartoccioni, and Palacín 2021).

4.3.5 RNA Sequencing Data Shows the Importance of Efflux in *P. aeruginosa* PA14 to BMA, Styrene and Ethylbenzene

The fundamental role of efflux systems in the tolerance of gram-negative bacteria to various organic solvents has been widely described (Rojas et al. 2001)(Ikehata and Doukyu 2022)(Vasylkivska and Patakova 2020)(Ramos et al. 2003). In this study we describe the potential significant upregulation of a wide range of RND efflux pumps in *P. aeruginosa* PA14 in response to BMA, styrene and ethylbenzene.

4.3.5.1 The Profile of Upregulated of Efflux Pumps Between Different Solvent Groups Varies

The wide range of RND efflux pumps in *Pseudomonas aeruginosa* display broad specificities covering many substrates of varying sizes, charges and toxicities (Nikaido and Pagès 2012a). The substrate overlap between some RND efflux pumps means the expression of several pumps at one time gives *P. aeruginosa* the ability to efflux an enormous number of substrates from the cell at any one time (Murata et al. 2002)(Mao et al. 2002)(Nikaido and Pagès 2012a). Although there is a degree of substrate overlap between some RND pumps, these systems do display their own specificities (Puzari and Chetia 2017). Here, we describe the profile of significantly upregulated RND efflux pumps in *P. aeruginosa* PA14 in response to BMA, styrene and ethylbenzene.

4.3.5.2 Efflux Systems are Upregulated in Response to all Three Solvents

Differential gene expression analysis of the RNA sequencing data revealed that four RND type efflux pumps are significantly upregulated in response to BMA, styrene and ethylbenzene. A significant increase in the number of RNA transcripts mapped to MexCD-OprJ, MexAB-OprM, MexGHI-OpmD and MexPQ-OpmE are observed in all three datasets. This provides evidence that these RND systems can export BMA, styrene and ethylbenzene. It has been reported previously that *P. aeruginosa* is able to tolerate a larger range of compounds at higher concentrations by expressing various RND type pumps simultaneously (Lee et al. 2000; Llanes et al. 2004). We report the increase in RNA transcripts transcribed for a wide range of efflux pumps in response to BMA, styrene and ethylbenzene in *P. aeruginosa* PA14. This simultaneous expression of various RND pumps at once could be responsible for the high levels of solvent tolerance exhibited by this microorganism during this study.

4.3.5.3 Efflux Systems Within the Datasets Display Specificity to Solvents

Although there is overlap of RND efflux pumps between the various solvent treated cultures, some significantly upregulated efflux pumps show specificity within the data.

The number of RNA transcripts sequenced corresponding to the triclosan efflux pump TriABC is significantly upregulated in the BMA data only, providing evidence that it exports BMA from the cell but not styrene and ethylbenzene. TriABC is unusual in its

structure in that it has two membrane fusion components, it is hypothesised that this could explain its narrow substrate specificity in comparison to other RND efflux pumps (Mima et al. 2007). This pump has a small repertoire of only three known substrates (Fabre et al. 2021). Here, we report the fourth substrate of TriABC - BMA. Gene knockout and recomplimentation studies could be carried out to confirm this.

Differential gene expression analysis shows the efflux profile of *P. aeruginosa* PA14 to styrene and ethylbenzene are similar. Although there is slight variation between the genes within RND systems which have an increase in transcription, the RND systems exhibiting an increase in RNA transcripts for both solvents are the same. This could be explained by the highly similar structures of styrene and ethylbenzene. Here it is shown that the RNA transcripts mapping to nine efflux systems are significantly increased in response to styrene and ethylbenzene whereas only five are increased in response to BMA. The similar response of *Pseudomonas* species to styrene and ethylbenzene has been demonstrated previously (Mosqueda, Ramos-González, and Ramos 1999; Stancu 2018). Styrene and Ethylbenzene display higher log Kow values which pertain to hydrophobicity than BMA, meaning their membrane disruption mediated toxicity is higher. This could explain the more defined efflux response in the styrene and ethylbenzene treated cultures. Although some efflux pumps were upregulated in response to all solvents in this study, here it is shown that the efflux mediated response of *P. aeruginosa* PA14 to styrene and ethylbenzene is distinct.

4.3.6 *P. aeruginosa* PA14 Exhibits a General Cell Envelope Stress Response to BMA

We report the general cell envelope stress response of *P. aeruginosa* PA14 to BMA characterised by the increase in RNA transcripts mapped to a range of trehalose biosynthesis genes. Trehalose production by Gram negative bacteria has been demonstrated previously as an osmotic stress response (Larsen et al. 1987; Reina-Bueno et al. 2012; Woodcock et al. 2021). During this study, the treatment of bacterial culture with the toxic hydrophobic methacrylate ester leads to upregulation of genes involved with trehalose biosynthesis as an osmoprotectant strategy. During trial BMA fermentations using *P. putida* at Ingenza Ltd, carbon was not being efficiently directed towards BMA production and carbon could not be accounted for after fermentations. Here, we propose that the upregulation of trehalose biosynthesis genes in response to BMA accumulation within the fermenter could be responsible for this inefficient direction of carbon towards BMA production. Based on this data, the deletion of trehalose biosynthesis genes could be a useful strategy to redirect carbon towards BMA production in trial fermentations.

4.3.7 Some Genes are Implicated in the *P. aeruginosa* PA14 Response to all Solvents in the Study

4.3.7.1 Three Genes are Significantly Upregulated in Response to BMA, Styrene and Ethylbenzene

As previously discussed, the RND exporter MexC is the most highly upregulated system within all datasets. The genes *PA14_53530* and *PA14_36920* encoding a

possible metal dependant hydrolase and possible histidine kinase respectively are also upregulated within all 3 datasets.

Mitsubishi Chemical Corporation are in the process of developing a fermentation process for BMA production where BMA is sequestered away from the production microorganism within the fermenter by sequestration by the solvent hexadecane. Here, we present the increase in transcription of a possible metal dependant hydrolase gene in response to all solvents; *PA14_53530.* This gene is important in the survival of *P. aeruginosa* in fluid interfaces caused by solvents such as hexadecane (Niepa et al. 2017). The upregulation of this gene in response to BMA could be advantageous in a fermentation vessel where hexadecane is present in large quantities to sequester BMA as its role in tolerance of both BMA and hexadecane has been reported. This protein has also been implicated in *P. aeruginosa* transcriptomic response to fuel and has been shown to play a role in the hydrocarbon degrading capabilities of *Pseudomonas* and *Alkanivorax* species previously (Gunasekera et al. 2017; Martins et al. 2021). This gene has further been characterised as part of the *P. aeruginosa* general stress protection transcriptional response (Rodríguez-Rojas and Blázquez 2009). The possible histidine kinase upregulated within all datasets in this study has an involvement in virulence in *P. aeruginosa* strains in the clinic (Francis, Stevenson, and Porter 2017; Kaihami et al. 2017).

4.3.7.2 Genes are Upregulated in Response to Styrene and Ethylbenzene

The RND type exporter *mexF* was significantly upregulated in the styrene and ethylbenzene datasets only, suggesting its export substrate specificity is inclusive of styrene and ethylbenzene but not BMA. Deletion of the *MexEF-OprN* operon has been demonstrated to result in increased susceptibility to chloramphenicol and ciprofloxacin (Köhler et al. 1997). Here, we report this genes involvement in *P. aeruginosa* styrene and ethylbenzene tolerance.

PA14_24940, a putative oxidase has also been implicated in fluid interface tolerance in the presence of hexadecane (Niepa et al. 2017). Further promising evidence that *P. aeruginosa* will exhibit tolerance to hexadecane in a fermentation vessel. *PA14_44510,* another possible metal dependant metal dependant hydrolase has also been shown in the literature to play a role in hexadecane fluid interface tolerance as well as hydrocarbon degradation in niches such as fuel tanks (Gunasekera et al. 2017).

4.3.8 The Cbb_3 Maturation Protein CopA2 is Upregulated in Response to BMA, Styrene and Ethylbenzene

The transposon mutant library screen identified three Cbb_3 maturation genes (*PA14_44460, PA14_44440* and *PA14_44450*) to be important in BMA tolerance in *P. aeruginosa* PA14. The whole transcriptome analysis carried out during this study found no change in the level of transcription of *PA14_44460* and *PA14_44450* when

the cultures are treated with BMA, however, a significant increase in reads mapping to *CopA2* and *PA14_44430* was observed. The expression of *copA2* is also significantly upregulated in response to styrene and ethylbenzene, however, the number of RNA transcripts mapping to *PA14_44450* and *PA14_44460* decreases.

The Cbb_3 maturation gene *PA14_44430* which showed a significant increase in transcription in response to BMA is unannotated. However, the literature shows that upregulation of expression of this gene is implicated in increased virulence and multidrug resistance (Beaume et al. 2017; Montemari et al. 2022; Morgan et al. 2019). CopA2 is essential for the maturation and assembly of fully functional Cbb_3 cytochrome oxidases in the cell, its role being to transport copper into the periplasm where it accessed to form the catalytic core of the Cbb_3 cytochrome oxidases (Zufferey et al. 1996). Deletion mutants of CopA2 display a large reduction of Cbb_3 cytochrome oxidase activity (Hassani et al. 2010), showing the essential indirect role this protein plays in bacterial energetics. The upregulation of CopA2 in response to all solvents supports the hypothesis that the Cbb_3 cytochrome oxidases play a principal role in bacterial energetics associated with tolerance to BMA. We hypothesise that expression of Cbb_3 in *P. aeruginosa* drives the generation of a proton gradient essential for the function of many RND efflux pumps in the presence of toxins such as BMA, styrene and ethylbenzene. Overexpression of the Cbb_3 cytochrome oxidases in bacteria has been shown to aid pathogenesis in the literature (Pitcher and Watmough 2004), supporting this hypothesis.

4.3.9 *P. aeruginosa* PA14 Upregulates Expression of *Cbb$_3$-1* in Response to Styrene and Ethylbenzene

In *P. aeruginosa,* there are two copies of the Cbb_3 cytochrome oxidase genes but only one copy of the genes associated with their maturation (Buschmann et al. 2010). The transposon mutant library screen did not provide evidence whether Cbb_3-1, Cbb_3-2 or both proteins were responsible for BMA tolerance, as only Cbb_3 maturation and assembly proteins were identified during this experiment. Here, whole transcriptome analysis shows an increase in RNA transcripts associated with all Cbb_3-1 genes are increased in *P. aeruginosa* in response to styrene and ethylbenzene, and an increase in transcription of some *Cbb$_3$-1* genes are observed in response to BMA.

Cbb_3-1 is responsible for proton gradient generation in high oxygen conditions (Comolli and Donohue 2004). During the experimental conditions in this study, oxygen was not a limiting factor in bacterial cultures and so it is unsurprising that an increase in transcription of Cbb_3-1 but not Cbb_3-2 is observed. This increase in RNA transcripts mapping to *Cbb$_3$-1* was more prominent in the styrene and ethylbenzene cultures as described in **Table 21**.

4.3.10 Whole Transcriptome Analysis Provides Evidence that Cbb3-1 Could be Powering RND Efflux Systems in *P. aeruginosa* PA14 to Mediate Tolerance

The increase in transcription of efflux systems is pronounced in all three solvent conditions during this study. However, more efflux systems were upregulated in *P. aeruginosa* PA14 in response to styrene and ethylbenzene. It is in these cultures that the increase in transcription of *Cbb_3-1* is more evident. We therefore present the increase in transcription of *Cbb_3-1* alongside RND efflux systems to mediate tolerance to solvents by their extrusion from the cell. In this study we hypothesise that the role of the Cbb_3 cytochrome oxidases in tolerance is to generate the proton gradient required to power the energy intensive process of efflux of solvents from the cell. We also suggest that *P. aeruginosa* PA14 and other *Pseudomonas* species have such a high level of intrinsic tolerance to many substances because they possess many RND efflux systems as well as the ability to power their use under a range of oxygen conditions using the Cbb_3 cytochrome oxidases. Here, our data supports this hypothesis and we present the increase in transcription of many RND systems as well as the Cbb_3-1 cytochrome oxidase in response to BMA, styrene and ethylbenzene in *P. aeruginosa* PA14.

4.3.11 Exploitation of RND Efflux Pumps Alongside Cbb_3 Cytochrome Oxidases for Solvent Tolerant Strain Generation

These findings present possible application to the generation of a tolerant production strain for methacrylate ester production. Previously, managed expression of the

efflux pump TtgABC in *P. putida* has been used to optimise tolerance to several biofuels in culture (Basler et al. 2018). The importance of these efflux pumps in *P. aeruginosa* solvent tolerance has been previously demonstrated (Nicolaou et al. 2010)(Li, Zhang, and Poole 1998b) and so these findings suggest that the homologues of these systems present as potential targets for strain engineering using synthetic biology in *P. putida.* Upregulation of the homologues of the RND systems identified during this study in *P. putida* could increase tolerance to BMA and therefore yield in a fermenter. We propose that the findings of this study suggest that overexpression of RND efflux pumps in *P. putida* alongside the Cbb_3 cytochrome oxidase assembly system and Cbb_3-1 could generate a highly BMA tolerant strain fit for fermentations generating high quantities of product without the limitations of a tolerance bottleneck.

4.4 Future Work

4.4.1 Complementation Studies Could Build Upon the Transcriptomic Data Gathered During this Study

The generation of complete gene knockouts of genes identified as tolerance conferring systems by the transcriptomic data generated during this study and subsequent complementation of these genes could be carried out in the future. Loss and restoration of the tolerance phenotype in *P. aeruginosa* PA14 by these genes would provide substantial evidence that these systems are responsible for tolerance to the industrial solvents BMA, styrene and ethylbenene. This strategy could also be used to further investigate the hypothesised functional relationship between RND type efflux systems and the Cbb_3 type cytochrome oxidases. Using Cbb_3 type cytochrome oxidase gene knockouts, the expression of RND type efflux pumps could be monitored to confirm if the loss of these systems to 'power' efflux has an effect on the transcription of these systems to facilitate efflux.

4.4.2 Targeted Engineering of *P. putida* to Generate Efficient Bioproduction Strains is an Attractive Strategy in Bioprocess Development

The transcriptomic data we report in this study provides the basis for targeted engineering of solvent tolerant strains to overcome the bottleneck of BMA toxicity during fermentation. We report data suggesting there is a functional relationship between RND type efflux systems and the Cbb_3 type efflux systems. The development of strains overexpressing these systems simultaneously in *P. putida* could generate

production strains with enhanced efflux capabilities as well as the ability to power the use of these energetically demanding efflux systems. Trial fermentations utilising such strains could be carried out at Ingenza Ltd to demonstrate the potential tolerance capabilities of such strains in a real fermentation.

4.4.3 Comparison of the Results Demonstrated During this Study with a *P. putida* Study Would Provide Insights into the Effectiveness of *P. aeruginosa* as a Model Organism for Tolerance in *Pseudomonas* Species

Since the completion of this study, a similar experiment has been reported investigating the transcriptomic response of *P. putida* KT2440 to BMA, styrene and ethylbenzene (Tucker and Begley 2021). The comparison of the results of this study against the findings we report would provide as a useful tool to gauge the effectiveness of the use of *P. aeruginosa* as a model organism for tolerance in *Pseudomonas* species. A comparison of these data could also provide insights into the difference in tolerance conferring mechanisms to these industrial solvents between these two *Pseudomonas* species.

5 Results Chapter 3: Transcriptomic Characterisation of the Response of *Pseudomonas aeruginosa* PA14 to Kaftrio and Ivacaftor

5.1 Introduction

5.1.1 Cystic Fibrosis

Cystic fibrosis is the most prevalent autosomal recessive disorder in Caucasians today, caused by the inheritance of a mutation in the cystic fibrosis transmembrane conductance regulator (CFTR) gene from both parents (Goldstein and Prystowsky 2017). First identified as a disease of the pancreas in 1938, this genetic disorder now affects over 70,000 people across the globe and results in mortality before the age of 40 in half of patients affected (McColley et al. 2022).

The *CFTR* gene encodes the cystic fibrosis transmembrane conductance regulator protein which facilitates the export of chloride ions across epithelial tissues, most notably within the respiratory and digestive organs.

5.1.2 Pathogenic Mutation within the *CFTR* Gene is Diverse

Over 1500 mutations in the *CFTR* gene have been recorded, some of which lead to defective or absent CFTR protein causing disease (Castellani et al. 2008). Mutations in the *CFTR* gene are traditionally divided into 6 major categories described in **Table 22**. Although this classification system is widely used, some mutations cannot be defined by one category. In two thirds of CF cases the disease-causing mutation is F508del. F508del results in the deletion of a phenylalanine residue which leads to the generation of misfolded and non-functional proteins which are degraded in the proteosome (Wang and Li 2014). This mutation is categorised as a class 2 mutation,

however, F508del mutants also display features of both class 3 and 7 mutants (Veit et al. 2016).

Table 22: The 6 classes of CFTR protein mutations which cause cystic fibrosis are described.

Class of CFTR Mutation	Category	Description	Consequence for CFTR Protein
Class 1	Protein production	Nonsense/frameshift mutation results in truncated mRNA	No functional CFTR protein translated
Class 2	Protein processing	Missense mutations or amino acid deletions result in misfolded CFTR protein	Misfolded CFTR is degraded in the proteosome (e.g. F508del)
Class 3	Gating	Missense mutations or amino acid changes result in CFTR proteins with closed channels	CFTR chloride channels are closed and non-functional. Protein is present in sufficient quantities in the membrane but can't transport substrate
Class 4	Conduction	Missense mutations and amino acid changed lead to reduced chloride conduction	CFTR protein is present in sufficient quantities at the membrane but exhibits reduced chloride permeability
Class 5	Low CFTR levels	Splicing defects and missense mutations lead to reduction in CFTR synthesis	Only small amounts of CFTR proteins are synthesised and are present within the membrane
Class 6	Low CFTR stability	Missense mutations and amino acid changes lead to misfolded CFTR protein	Misfolded CFTR protein in the membrane is destroyed by endoplasmic reticulum associated degradation (ERAD)

Pathogenic *CFTR* mutation ultimately results in the accumulation of chloride and sodium ions within epithelial tissues causing the disruption of water movement across these tissues. This leads to the formation of thick and sticky mucus which cannot be swept to the larynx for mucociliary clearance by ciliated cells (Elborn 2016).

Bacteria which are cleared to the larynx by the cilial epithelia in healthy individuals are able to proliferate and reside within the lung mucous in CF patients. CF patients, therefore, experience infections commonly throughout their lifetime (Yoon et al. 2002). Infection in CF patients subsequently leads to the onset of inflammation and the infiltration of the lungs by immune cells which deliver a damaging immune response causing lung atrophy and disease progression (Gibson, Burns, and Ramsey 2012).

The most common pathogens of people with CF are *Staphylococcus aureus* and *Pseudomonas aeruginosa.* In early childhood, *S. aureus* is the most common cause of infection in CF patients, infecting more than 50% of CF children under the age of two (Rumpf et al. 2021). The Annual Data Report curated by the Cystic Fibrosis Foundation in 2022 reported that in individuals over the age of 35, *P. aeruginosa* becomes the leading cause of airway infection (Cystic Fibrosis Foundation, 2022).

Lung colonisation by this pathogen in individuals with CF is associated with increased morbidity and is a major cause of death (Emerson et al. 2002).

5.1.3 The Availability of the Triple Combination Therapy Kaftrio has Revolutionised CF Therapy

There is no cure for cystic fibrosis, and until recent years the availability of treatment for the symptoms has been limited. For patients carrying less common CFTR mutations, lung transplant is still the only main treatment for the chronic symptoms of the disease (Edmondson and Davies 2016). Where treatment has been available, it has largely been aimed to treat the downstream symptoms such as mucous viscosity rather than the underlying cause of disease (Ratjen 2009).

The triple combination therapy Kaftrio (known as Trikafta in the United States) developed by Vertex Pharmaceuticals was approved for use in the UK in July 2020. This therapy is a combination of the three drugs elexacaftor, tezacaftor and ivacaftor and has been approved for use for individuals carrying the most common mutation type F508del and has revolutionised CF therapy for thousands of patients.

Table 23: The chemical structures of elexacaftor, ivacaftor and tezacaftor are shown.

Chemical structures obtained from the CHEMBL database

Drug	Chemical Structure
Elexacaftor	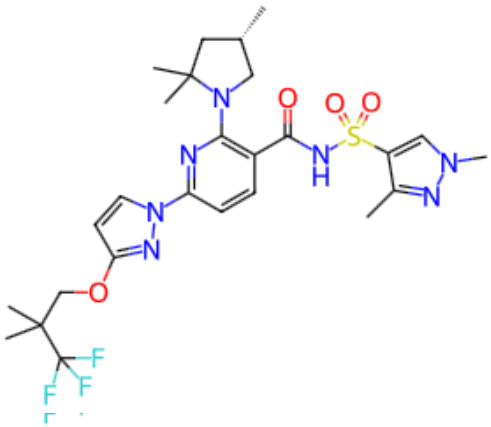
Ivacaftor	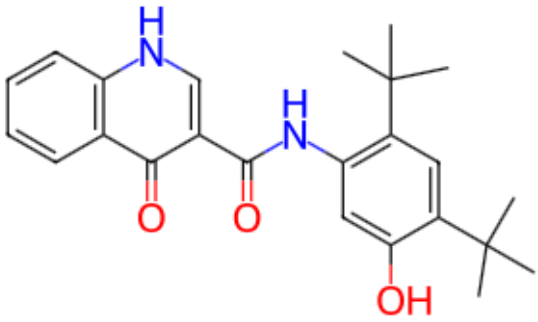
Tezacaftor	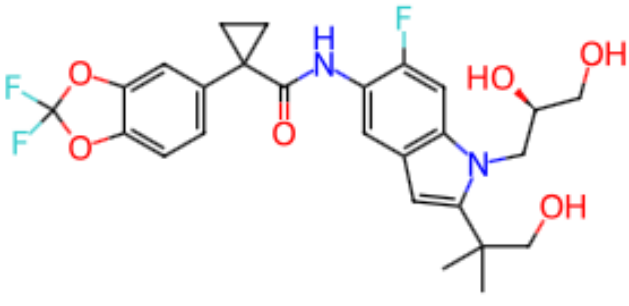

Kaftrio is one of the few available drugs which targets the underlying cause of CF symptoms; lack of or defective CFTR protein at the cell surface. Ivacaftor falls within a category of drugs called modulators, which improve the function of defective CFTR proteins which are at the cell surface (Veit et al. 2020). Ivacaftor is further classed as a CFTR gating potentiator, targeting the gating defects observed in class two, three and six CF mutations. Ivacaftor interacts with CFTR through an unknown mechanism and facilitates channel opening and therefore partially restores chloride transport (Tomati et al. 2022).

Tezacaftor and elexacaftor are categorised as CFTR correctors, targeting folding defects of the protein. Reducing misfolding of CFTR results in less degradation of proteins and therefore more protein being successfully trafficked to the cell surface (Donaldson et al. 2018). The triple combination therapy of the correcting and potentiating properties of these drugs has been proven as an effective treatment for sufferers of CF, resulting in the partial restoration of CFTR function to levels which allow for thinning of mucous and therefore a reduction of typical symptoms (Aspinall et al. 2022; Keyte et al. 2022; Zhang et al. 2022).

5.1.4 There is a Lack of Knowledge of the Response of CF Pathogens to Kaftrio

Thinning of the mucous and the alleviation of some CF symptoms upon the prolonged use of Kaftrio has allowed patients to clear persistent lung infections of pathogens

such as *Aspergillus* (Chesnay et al. 2022). However, in many patients, even with prolonged use of Kaftrio is unable to clear *P. aeruginosa* infection (Gordon MacGregor, personal communication). There has been little study carried out on the effects of this drug on CF lung pathogens. One study showed a positive effect on the lung microbiome as a result of Kaftrio treatment, but the results show an increase in the number of patients with *P. aeruginosa* residing within the lungs (Sosinski et al. 2022).

Throughout this study, the stress response of *P. aeruginosa* to various solvents has been investigated. During this chapter the response of this pathogen to the CF drug Kaftrio was investigated to further characterise the general stress response of this pathogen. To gain an understanding of the general stress response profile of *P. aeruginosa* to various substances, full transcriptome analysis was carried out in the presence and absence of Kaftrio in liquid culture. As the Ivacaftor component of the Kaftrio triple combination therapy is often taken alone, we also set out to investigate the transcriptomic response of *P. aeruginosa* to Ivacaftor alone compared to Ivacaftor in combination with elexacaftor and tezacaftor as Kaftrio. Here, we present the first study of this kind and we describe the possible effect of Kaftrio and Ivacaftor on pathogenesis during CF infection with *P. aeruginosa.*

5.2 Results

To characterise the transcriptomic response of *P. aeruginosa* PA14 to the triple combination CF therapy Kaftrio and Ivacaftor, *P. aeruginosa* cultures were grown in the presence and absence of 1x and 100x serum concentrations of Kaftrio and Ivacaftor. RNA was isolated from cultures and analysed using Illumina Miniseq sequencing.

5.2.1 Isolation of RNA from *P. aeruginosa* PA14 Cultures Treated with Kaftiro and Ivacaftor

Cultures of *P. aeruginosa* PA14 were grown in Mueller Hinton broth which was selected as it is commonly used for antibiotic susceptibility testing. When the OD_{600} of the cultures reached 0.6, cultures were supplemented with either 1 x or 100 x serum concentration of Kaftrio, 1 x or 100 x serum concentration of Ivacaftor (as described in the materials and methods). As Kaftrio and Ivacaftor were solubilised in DMSO, control samples were supplemented with DMSO alone. The concentration of DMSO across all cultures was consistent at 1%. Cultures were incubated for 15 minutes with solvent before cells were harvested and RNA was isolated from each sample using the Trizol™ RNA Plus Purification Kit. To determine if the quality of isolated RNA from cultures was sufficient for ribosomal RNA (rRNA) depletion, RNA samples were subjected to chip electrophoresis using the Agilent Bioanalyzer (**Figure 44**).

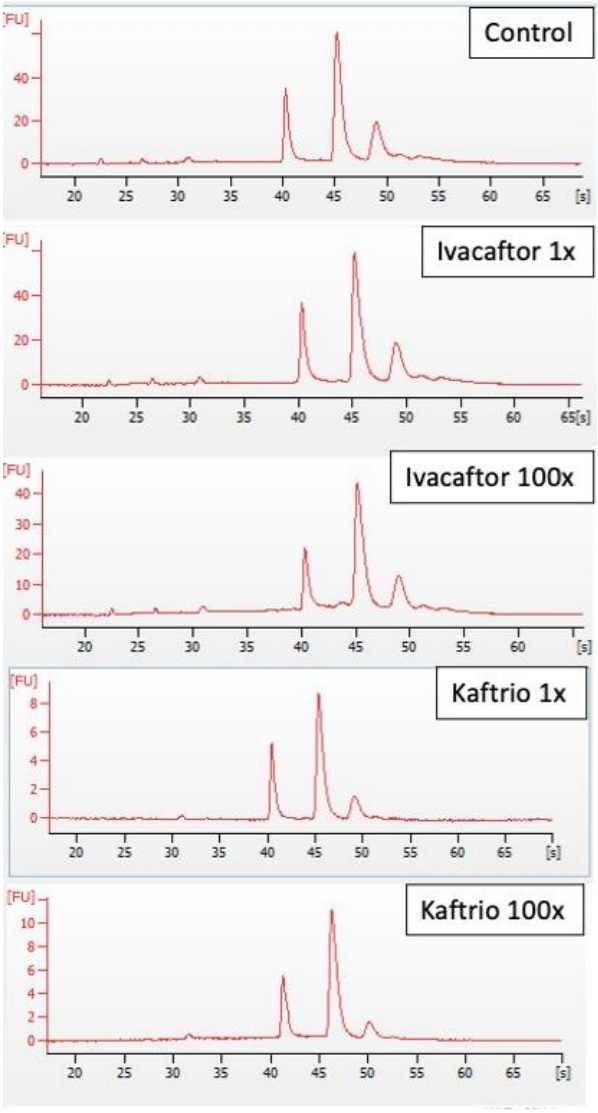

Figure 42: Chip electrophoresis electropherograms of example RNA extractions for each drug treated and control sample generated using the Agilent Bioanalyzer. Cultures and RNA extractions were performed in quadruplicate, however, one of each is shown here as an example. Two ribosomal RNA peaks are observed in each sample, showing each sample has not degraded. A third peak is observed in the ribosomal RNA region which could represent ribosomal RNA.

The results show two peaks in each RNA sample electropherogram which represent the 16S and 23S ribosomal RNA subunits which is characteristic of intact RNA. The RNA integrity number (RIN) for each sample was above 8 which showed the samples were of a high quality. A third peak is observed in the large ribosomal RNA region of the electropherogram of each sample.

To determine whether any of the samples were contaminated by DNA, samples were used as templates for PCR using primers to amplify a region of intergenic DNA (Figure x). Primers for the amplification of a 500 bp region of intergenic DNA was designed as this region of DNA would not be transcribed into mRNAs and therefore would provide as a reliable target for DNA detection.

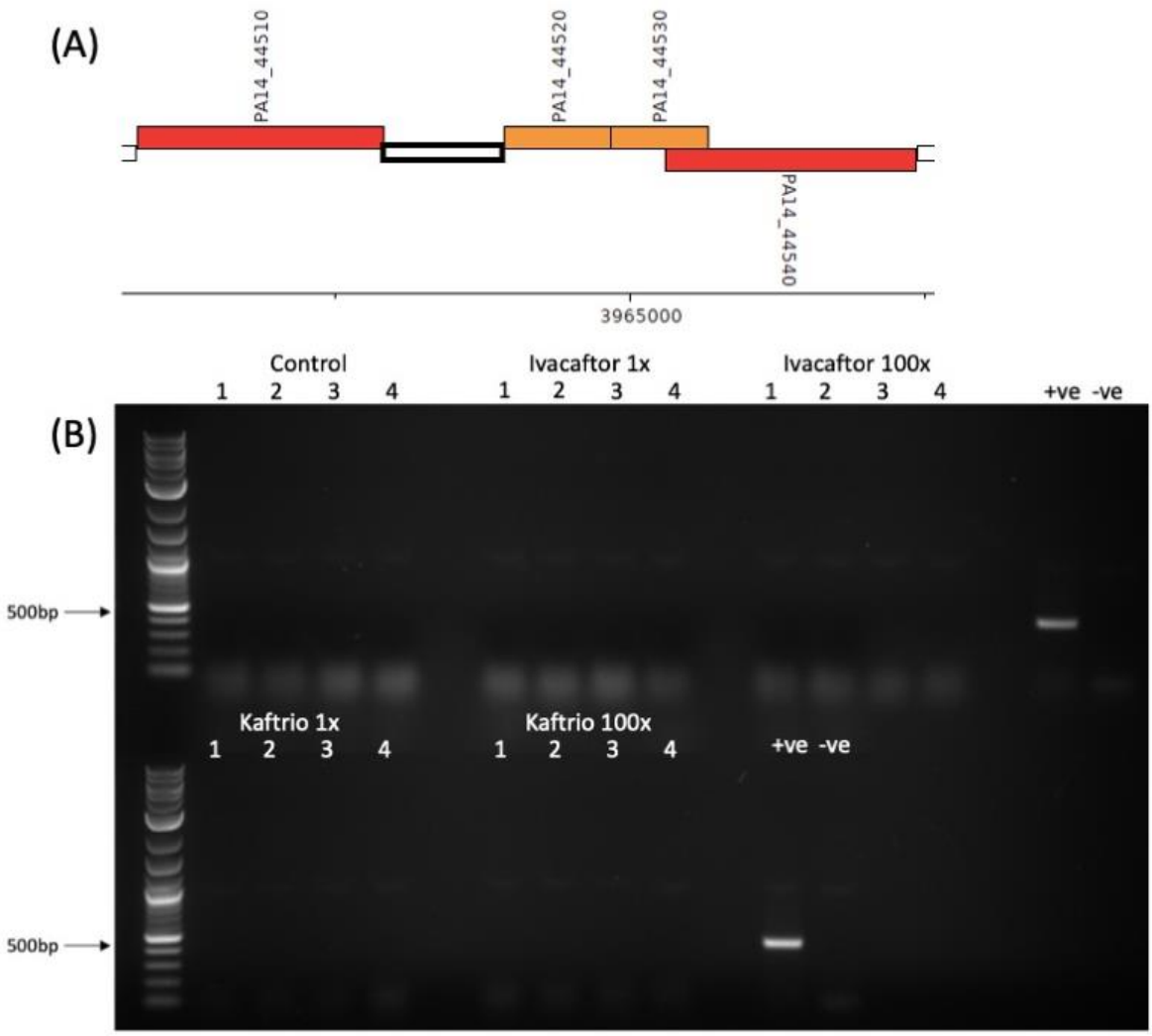

Figure 43: Contamination analysis of RNA extractions (A) Schematic diagram of the 500 bp region of intergenic DNA used for PCR amplification. PCR primers were designed to amplify the 500 bp region between the genes *PA14_44510* and *PA14_44520.* Cytoplasmic genes are represented in red and inner membrane proteins are shown in orange. Figure generated using Pseudomonas.com **(B) PCR and agarose gel electrophoresis analysis of extracted RNA.** Each RNA extraction sample was used as template. *P. aeruginosa* PA14 genomic DNA was used as a positive control reaction template and a no template reaction was run as a control.

DNA products were not amplified from any of the RNA extraction samples (**Figure 45**). The samples were therefore considered free of DNA contamination and were taken forward for further analysis. DNA contamination was ruled out as the cause of the third peak observed in the electropherograms for each RNA extraction.

To remove rRNA from RNA extractions to obtain high sequencing read depth of mRNAs, RNA extractions were subjected to rRNA depletion. To determine whether any rRNA remained in the samples, RNA samples were subjected to chip electrophoresis using the Agilent Bioanalyzer (**Figure 46**).

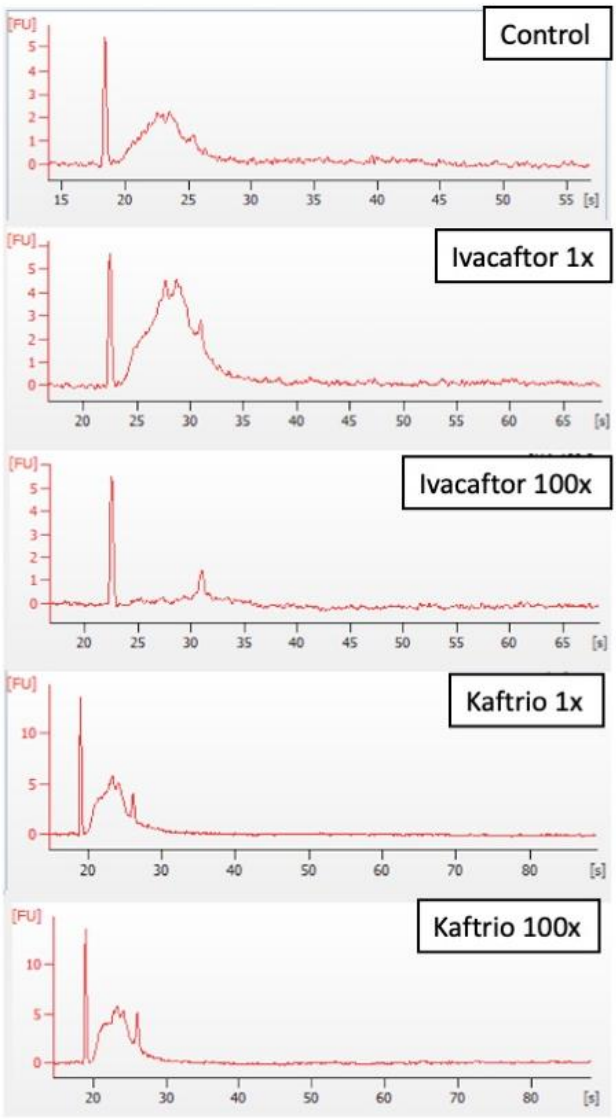

Figure 44: Chip electrophoresis electropherograms of example ribosomal RNA depleted RNA extractions for each drug treated condition generated using the Agilent Bioanalyzer. Only one rRNA depletion for each solvent treatment group is shown as an example although this was performed in triplicate. No ribosomal RNA is observed in the electropherograms of any samples. After the removal of the rRNA from each sample, an mRNA peak is observed between 25-35 seconds for every sample.

Once the ribosomal RNA was removed from RNA samples it was possible to identify mRNA peaks between 25-35 seconds on the sample electropherograms (**Figure 46**). Peaks resolving at this retention time range are characteristic of high-quality mRNA. No 16S or 23S ribosomal RNA was observed in the electropherograms, showing that rRNA had successfully been depleted from all samples.

5.2.1.1 Preparation of Complimentary DNA Sequencing Libraries of RNA Extractions

To sequence the purified mRNA from each sample, complimentary DNA (cDNA) libraries were generated for Illumina sequencing. After library preparation, to ensure the libraries were free from adapter and primer contamination and were the correct size, the libraries were subjected to chip electrophoresis using the Agilent Bioanalyzer (**Figure 47**).

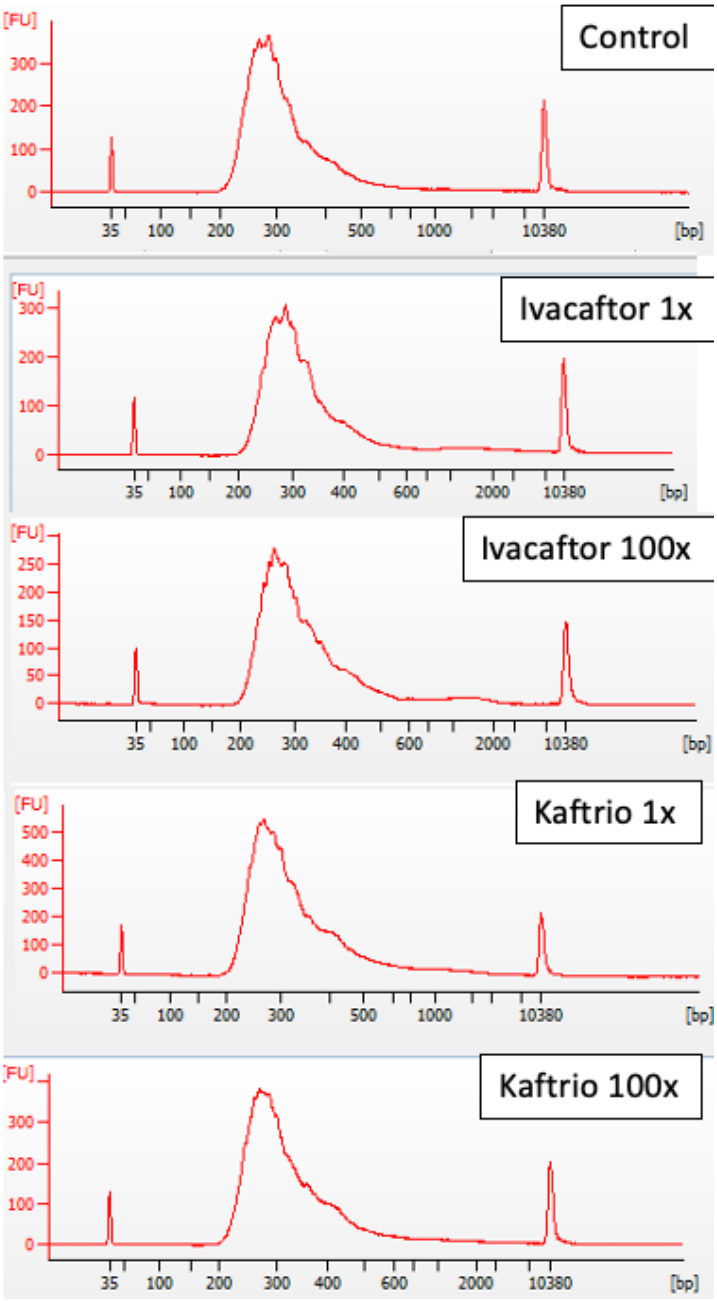

Figure 45: Chip electrophoresis electropherograms of example cDNA library preparations for each solvent treatment sample generated using the Agilent Bioanalyzer. One library preparation for each sample is shown although this was performed in triplicate. The size distribution of each library ranges from ~200 bp to ~400 bp, peaking at ~300 bp.

The chip electrophoresis electropherograms generated on the Agilent Bioanalyzer demonstrate that the average size of each cDNA library was ~300bp (**Figure 47**). Libraries were quantified using a Qubit fluorometer and diluted to a final pooled loading concentration of 5 pM. cDNA libraries were sequenced using an Illumina Miniseq sequencer across two high throughput cartridges and flow cells. Control and ivacaftor 1x/100x were run on one sequencing run which had a cluster density of 316 K/mm2 of which 80.9% passed the quality filter. Kaftrio 1x/100x samples were run on another sequencing run which had a cluster density of 296 K/mm2 of which 80.5% passed the quality filter. Between 3 and 5 million reads were obtained for each indexed sample. The quality of the reads was determined using FastQC (Wingett and Andrews 2018).

To analyse the reads a variety of programmes were used through Galaxy Europe (Afgan et al. 2018). All reads were trimmed using TrimGalore! (Kreuger, 2021) and aligned to the *Pseudomonas aeruginosa* PA14 genome using HISAT2 (Kim et al. 2015). The number of aligned reads mapping to features on the chromosome were counted using Htseq-count (Anders et al. 2015) and the differential expression of genes in each solvent treated condition was calculated based on the control samples using DESeq2 (Love et al. 2014).

5.2.2 Principal Component Analysis Confirms the Absence of Outliers in the Data

To determine whether any of the replicates were technical outliers, principal component analysis (PCA) was carried out on all RNA sequencing data through the DESeq2 Galaxy Europe package (**Figure 48, Figure 49**). As described in the previous chapter, using various algorithms to find patterns in high dimensional data, PCA analysis establishes groups of variables within datasets allowing for the identification of data which deviates within replicates with high sensitivity. PCA plots show the differences within datasets calculated by the algorithms as represented by distance on the plot. This means that datasets which are deemed highly similar will reside close together on the plot. Therefore, triplicates of datasets with no technical outliers are expected to reside close to one another on a PCA plot, and datasets which deviate from the other triplicates are represented as far from the other datasets on the plot.

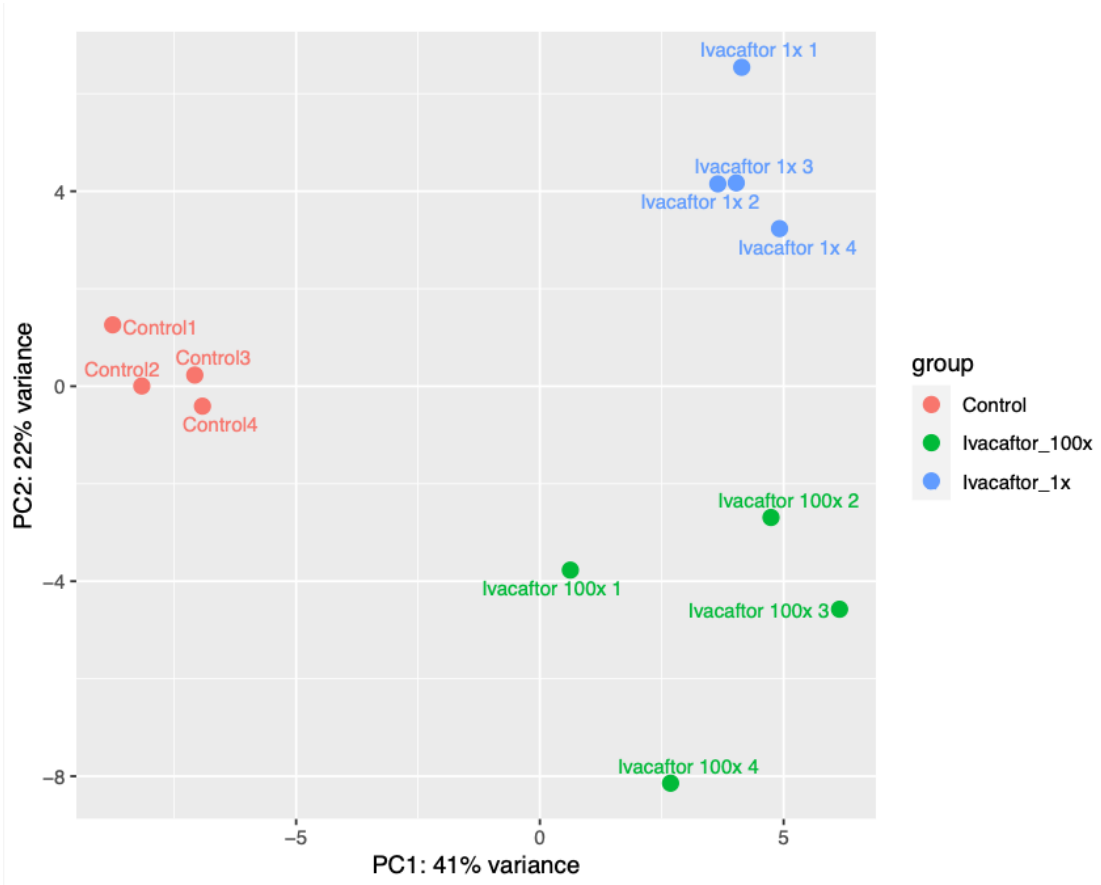

Figure 46: Principal component analysis of differential gene expression between control (DMSO only), ivacaftor 100x and ivacaftor 1x treated samples in quadruplicate. The PCA plot shows grouping of samples in quadruplicate. This figure was generated using DESeq2 in Galaxy Europe.

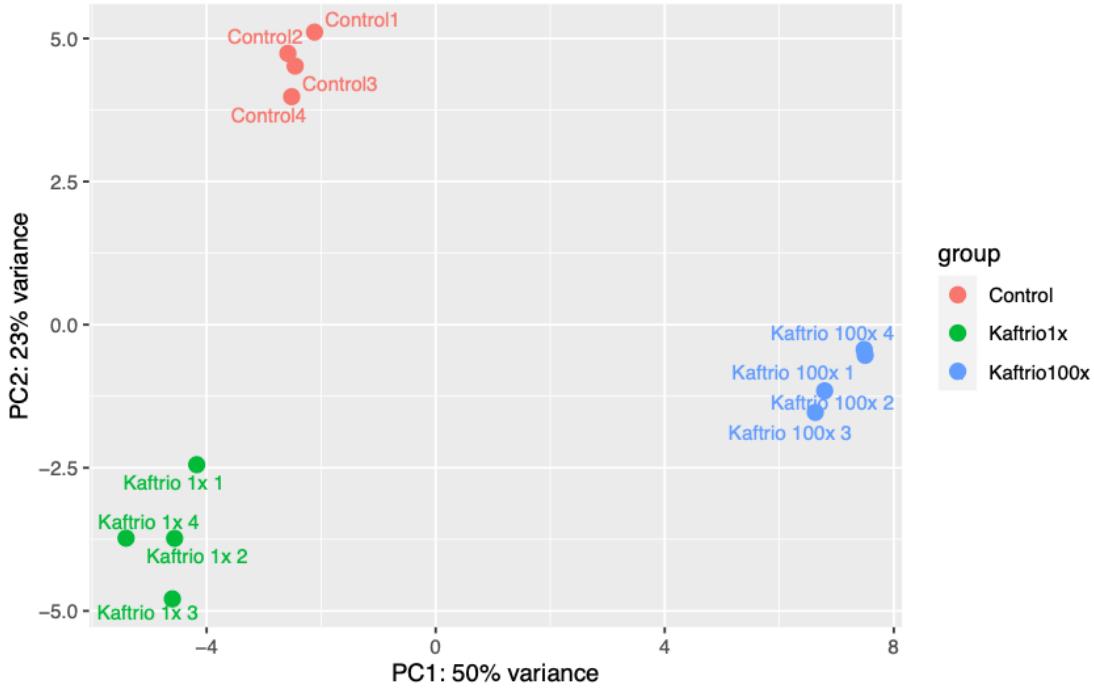

Figure 47: Principal component analysis of differential gene expression between control (DMSO only), kaftrio 100x and kaftrio 1x treated samples in quadruplicate. The PCA plot shows grouping of samples in quadruplicate. This figure was generated using DESeq2 in Galaxy Europe.

All quadruplicates were clustered together on the PCA plot, providing evidence that there were no outliers within the datasets (**Figure 48, Figure 49**).

5.2.3 Analysis of Differential Gene Expression in Ivacaftor and Kaftrio Treated Samples Reveals Significantly Different Expression Profiles Between Treatment Groups

In order to determine if there were changes in the transcriptome of *P. aeruginosa* PA14 when subjected to exposure to Ivacaftor and Kaftrio at 1 x and 100 x serum concentrations, analysis of differential gene expression was carried out using DEseq2 in Galaxy Europe. DESeq2 uses the number of reads from the sequencing data mapped to each feature on the chromosome by Htseq-count and calculates the differential expression of genes within high dimensional data based on negative binomial distribution. Differential gene expression is calculated as the logarithm to the base 2 of the fold change (LFC) of the number of reads in the treated sample compared to the untreated control. The p value is calculated for each LFC and corrected for false discovery rate using the Benjamini-Hochberg procedure. Results are output as a tabular file containing the LFC of every gene within the dataset listed in order of significance. Using this kind of analysis allowed for the identification of the significantly upregulated and downregulated genes in *P. aeruginosa* PA14 in response to ivacaftor and Kaftrio and 1 x and 100 x serum concentrations.

To visualise the differential gene expression between control and drug treated samples, tabular output files from DESeq2 were used to generate volcano plots using Volcano Plot in Galaxy Europe (**Figure 50, Figure 51, Figure 52 and Figure 53**).

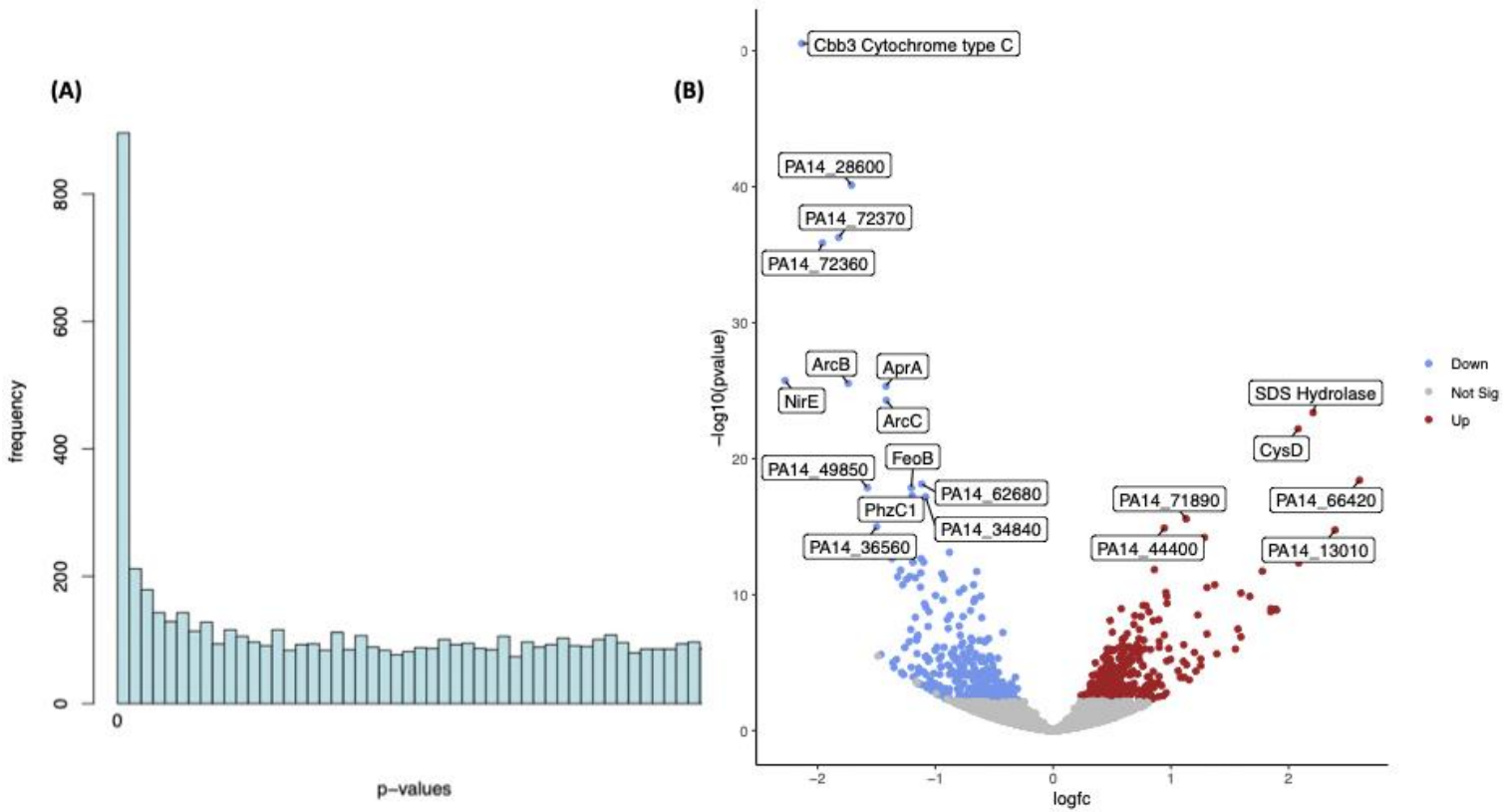

Figure 48: **(A) Histogram of p-values of log fold change in expression of upregulated and downregulated genes in *P. aeruginosa* PA14 when exposed to Ivacaftor at 1 x serum concentration (B) Volcano plot of differentially expressed genes in *P. aeruginosa* PA14 when exposed to Ivacaftor at 1x serum concentration.** Genes which showed no significant differential expression are shown in grey, genes which showed a significant increase in expression are shown in red and genes which showed a significant decrease in expression are shown in blue. The top 20 most significantly differentially expressed genes are labelled. Unannotated genes are labelled with locus tag and the gene name is given where possible.

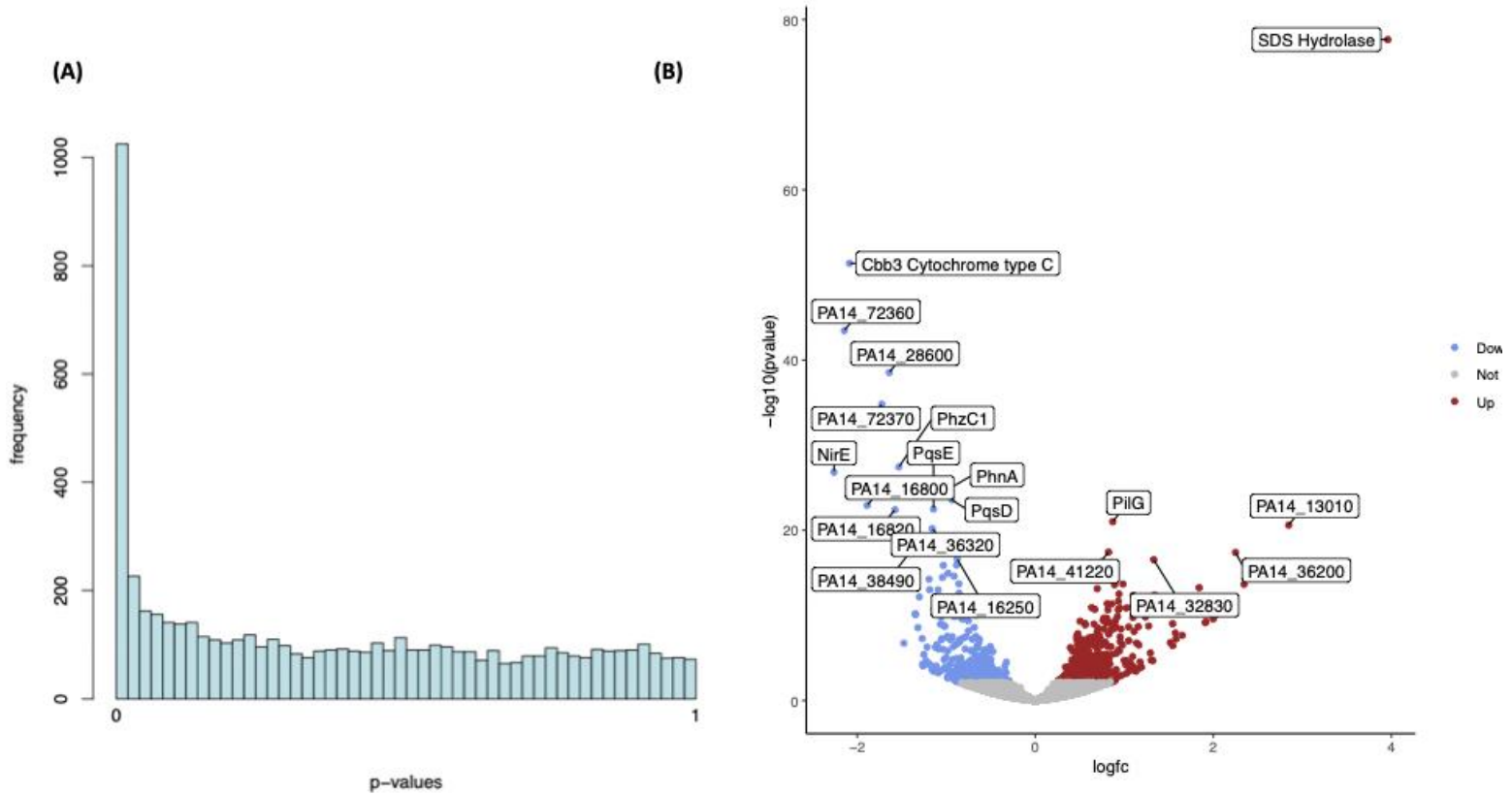

Figure 49: **(A) Histogram of p-values of log fold change in expression of upregulated and downregulated genes in P. aeruginosa PA14 when exposed to Ivacaftor at 100 x serum concentration (B) Volcano plot of differentially expressed genes in P. aeruginosa PA14 when exposed to Ivacaftor at 100 x serum concentration.** Genes which showed no significant differential expression are shown in grey, genes which showed a significant increase in expression are shown in red and genes which showed a significant decrease in expression are shown in blue. The top 20 most significantly differentially expressed genes are labelled. Unannotated genes are labelled with locus tag and the gene name is given where possible.

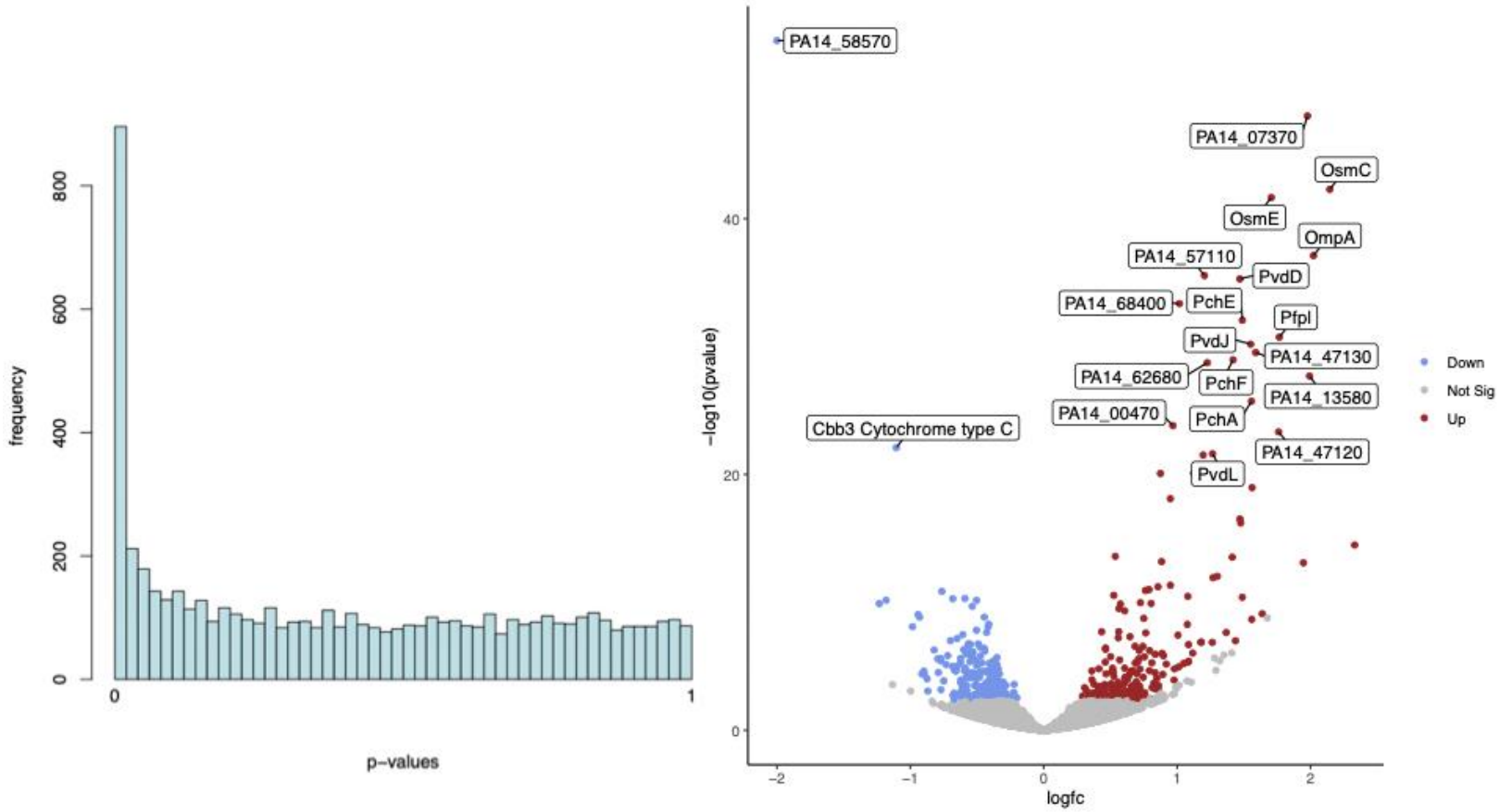

Figure 50: **(A) Histogram of p-values of log fold change in expression of upregulated and downregulated genes in *P. aeruginosa* PA14 when exposed to Kaftrio at 1 x serum concentration (B) Volcano plot of differentially expressed genes in *P. aeruginosa* PA14 when exposed to Kaftrio at 1x serum concentration.** Genes which showed no significant differential expression are shown in grey, genes which showed a significant increase in expression are shown in red and genes which showed a significant decrease in expression are shown in blue. The top 20 most significantly differentially expressed genes are labelled. Unannotated genes are labelled with locus tag and the gene name is given where possible.

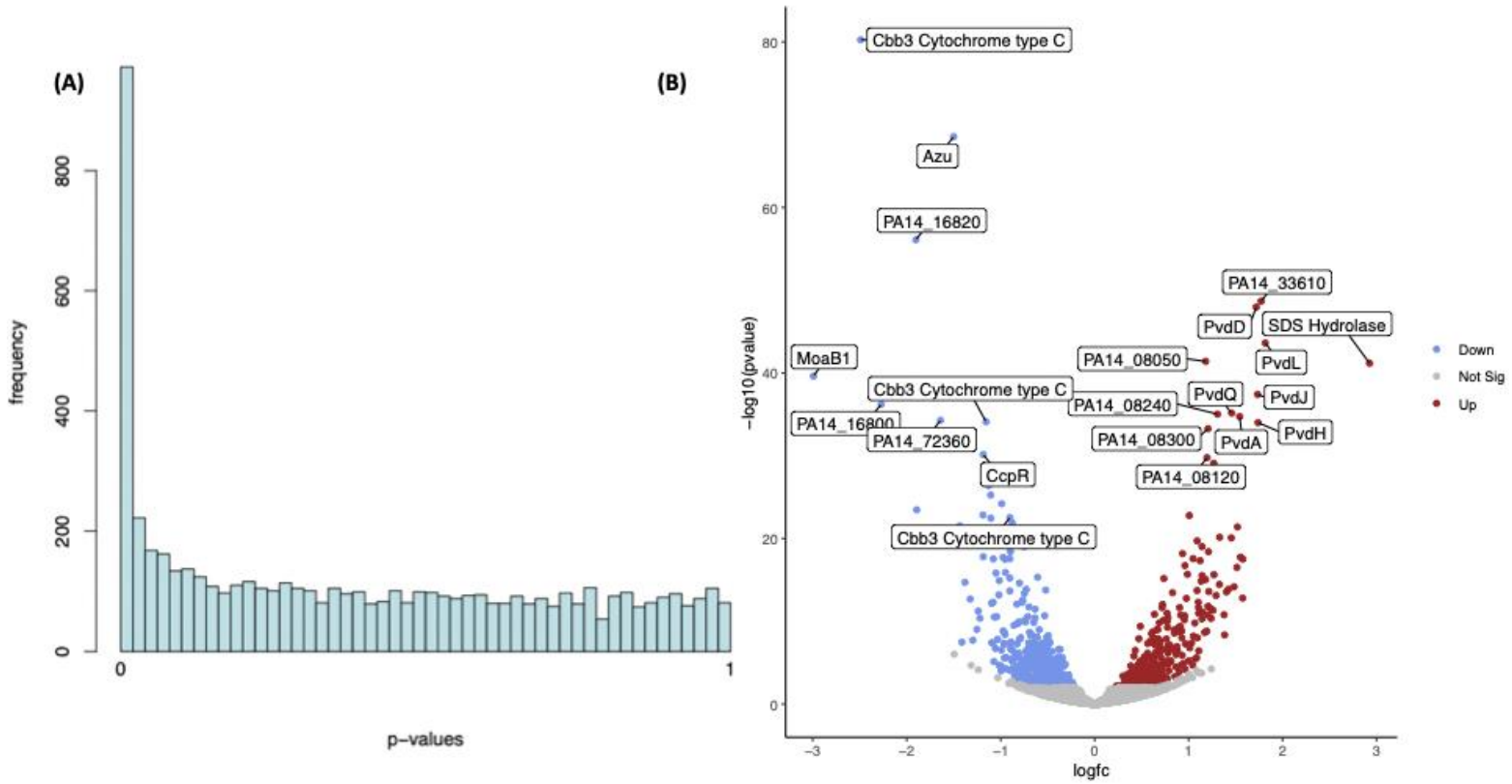

Figure 51: **(A) Histogram of p-values of log fold change in expression of upregulated and downregulated genes in *P. aeruginosa* PA14 when exposed to Kaftrio at 100 x serum concentration (B) Volcano plot of differentially expressed genes in *P. aeruginosa* PA14 when exposed to Kaftrio at 100 x serum concentration.** Genes which showed no significant differential expression are shown in grey, genes which showed a significant increase in expression are shown in red and genes which showed a significant decrease in expression are shown in blue. The top 20 most significantly differentially expressed genes are labelled. Unannotated genes are labelled with locus tag and the gene name is given where possible.

The frequency of differentially expressed genes within the dataset with a p value close to zero was more abundant than p values with larger values equalling insignificant results, as shown in (**Figure 50 (A), Figure 51 (A), Figure 52 (A) and Figure 53 (A)**.

There is significant differential gene expression in response to the drugs ivacaftor and Kaftrio at 1 x and 100x serum concentrations in *P. aeruginosa* PA14, This is clearly demonstrated in **Figure 50 (B), Figure 51 (B), Figure 52 (B) and Figure 53 (B).** The volcano plot representation of this data shows the top twenty differentially expressed genes with the most significant p values in *P. aeruginosa* PA14 when treated with the drugs at both serum concentrations. The genes identified can be categorised into groups based on their function, which is carried out throughout this chapter.

5.2.4 Analysis of the Transcriptome of *P. aeruginosa* PA14 in response to Treatment with Ivacaftor at 1 x Serum Concentration

When treated with ivacaftor at 1 x serum concentration for thirty minutes, significant differential expression of genes is observed in *P. aeruginosa* PA14 as shown in **Figure 50**. To determine whether genes with associated functions were differentially expressed in response to Ivacaftor at 1x serum concentration, the RNA sequencing data was analysed using the functional analysis and gene enrichment tool Funage-

Pro. Using this tool, differentially expressed genes were grouped by function (**Table 24**).

Table 24: Differentially expressed genes in response to Ivacaftor at 1 x serum concentration are displayed as groups based on function. This data generated using the gene enrichment analysis tool Funage Pro.

Downregulated Genes		Upregulated Genes	
Class Description	**Gene Name/Function**	**Class Description**	**Gene Name/Function**
Arginine Deaminase Pathway	*ArcA* – arginine deiminase *ArcB* – orthinine carbamoyltransferase, catabolic *ArcC* – carbamate kinase	2FE-2S cluster assembly	*IscS* – cysteine desulfurase IscS *IscS* – cysteine desulfurase IscS (locus tags: *PA14_14730, PA14_37830*)
Glycine dehydrogenase (cyanide forming) activity	*HcnA* – hydrogen cyanide synthase subunit *HcnB* - hydrogen cyanide synthase subunit *HcnC* - hydrogen cyanide synthase subunit	Lipopolysaccharide transport	*LptD* – LPS assembly protein *MsbA* – ATP dependant flippase
Iron Transport system FecR	*PA14_06170, PA14_13450, PA14_32720, PA14_39810, PA14_47390*	Structural constituent of ribosome	*RplM, RplU, RplY, RplI, RpmG, RplV, RplP, RplN, RplX, RplE, RplH, RplF, RplO, RplT, RplU, RpmB*– 50S ribosomal subunit protein *RpsT, RpsR, RpsF, RpsL, RpsG, RpsS, RpsE, RpsD, RpsB, RpsQ, RpsK,* – 30S ribosomal subunit protein *InfA* – translation initiation factor *RimM* – ribosome maturation factor
2FE-2S cluster binding	*FeoB* - ferrous iron transport proteinB *Sir2* - sulfite reductase (ferrodoxin) 2	Translation elongation factor	*Tuf2, FusA, Tsf, Efp, LepA* – elongation factor
Heme binding	*Sir2* - sulfite reductase (ferrodoxin) 2 *CcoN1* – Cbb3 type cytochrome oxidase (*PA14_10500, PA14_44340)* *CcoP2* – Cbb3 type cytochrome oxidase *CcmF* – Cytochrome c type biogenesis protein	Sulfate starvation response	*PA14_03700, PA14_45110* – sulfate binding protein *CysA* – sulfate binding protein *CysNC* – sulfate starvation protein *CysD* – sulfate anenylyltransferase *TauA* – taurine binding protein

Using Funage Pro, functional group of genes which exhibited significant differential expression in *P. aeruginosa* PA14 in response to Ivacaftor at 1 x serum concentration were identified as shown in **Table 24**.

5.2.5 Genes Associated with Translation were Significantly Upregulated in *P. aeruginosa* PA14 in Response to Ivacaftor at 1 x Serum Concentration

There is significant upregulation of genes associated with translation in response to Ivacaftor at 1 x serum concentration (**Table 24**). 16 50 subunit (50S) and 11 30 subunit (30S) genes encoding ribosomal subunit proteins were upregulated, as well as *infA* – a translation initiation factor and *rimM* – a ribosome maturation protein. Five translation elongation factor proteins were also significantly upregulated.

The ribosome is composed of two subunits- the small 30S and large 50S subunits, these are the structural components of the bacterial ribosome which make up the functional 70S ribosomal complex (Sykes and Williamson 2009) The translation initiation factor *infA* plays a role in the association of the 70S ribosomal complex, this process is essential for protein synthesis (Sette et al. 1997). The ribosomal maturation factor *rimM* has a functional role in the maturation of a functional 30S ribosomal subunit (Suzuki et al. 2007). Significant upregulation of five translation elongation factors is shown, these proteins chaperone transfer RNAs (tRNAs) to the ribosome during the elongation phase of translation (Hughes 2013).

The significant upregulation of so many genes associated with translation is indicative that *P. aeruginosa* PA14 is increasing protein synthesis in response to Ivacaftor at 1 x serum concentration. During this study, potential differential gene expression in response to various stimuli is measured by the characterization of the transcriptome using RNA sequencing. However, regulation of gene expression can also occur at the level of translation (Tollerson and Ibba 2020a). These results indicate that there is not only a clear transcriptomic response to treatment with this drug at this concentration, but the upregulation of so many genes associated with translation clearly shows there is also a significant response at the level of protein synthesis.

5.2.6 Genes Associated with Lipopolysaccharide Transport are Upregulated in Response to Ivacaftor at 1 x Serum Concentration

lptD, a lipopolysaccharide (LPS) assembly protein and *msbA,* an ATP dependant flippase were significantly upregulated in response to Ivacaftor at 1 x serum concentration (**Table 24**). LptD is involved in the delivery of LPS to the outer membrane, and MsbA is an ABC transporter responsible for transport of LPS across the inner membrane (Ghanei, Abeyrathne, and Lam 2007; Sciuto et al. 2018). Lipopolysaccharide is a core component of the outer membrane of most Gram-negative bacteria (Bertani and Ruiz 2018). This molecule is a major stimulant of the human immune system and plays a significant role in the pathogenesis of *P. aeruginosa* (Huszczynski, Lam, and Khursigara 2020). Distinct changes in LPS

structure have been linked to chronic infection in cystic fibrosis patients, and upregulation of these genes is associated with disease persistence (Maldonado, Sá-Correia, and Valvano 2016; Moskowitz and Ernst 2010). A lipopolysaccharide mediated response to the cystic fibrosis drug Ivacaftor at serum concentration could have negative implications for patients.

5.2.7 A Sulphate Starvation Response is Observed in *P. aeruginosa* PA14 in Response to Ivacaftor at 1 x Serum Concentration

Five genes associated with sulphate starvation displayed significant upregulation in response to Ivacaftor at 1 x serum concentration. It is unclear why this response as induced by the CF drug. However, it has been reported in the literature that a known response of *P. aeruginosa* to sulphur limitation is the utilisation of human mucin as a source of both sulphur and carbon (Quadroni et al. 1999). Upregulation of sulphate starvation genes has been shown to have an association with virulence in the *P. aeruginosa* strain PA01 (Tralau et al. 2007).

5.2.8 *P. aeruginosa* PA14 Displays a Clear Response Associated with Iron Acquisition in Response to Ivacaftor at 1 x Serum Concentration

A range of genes with functions associated with iron acquisition were differentially expressed in response to Ivacaftor at 1 x serum concentration (**Table 24**). *IscS* (locus tags *PA14_14730, PA14_37830)* showed significant upregulation. These genes are associated with iron-sulphur cluster assembly. Iron sulphur clusters are essential

components of the catalytic sites of various enzymes, and therefore play a vital role in many biochemical pathways in the cell (Wofford et al. 2019). Formation of these clusters can also be a stress response to protect the cell from the toxic properties of free iron and sulphide molecules within the cell (Ayala-Castro, Saini, and Outten 2008). Upregulation of these genes is therefore indicative of an abundance of iron in the environment.

In contrast to *iscS,* significant downregulation of many iron acquisition genes is observed. Five genes associated with the iron transport system FecR and the iron transporter FeoB were significantly downregulated in response to Ivacaftor at 1 x serum concentration.

It is reported in the literature that upregulation of the *FecR* system occurs when iron is in abundance in the environment (Ochs et al. 1995). Downregulation of this system is therefore indicative of low amounts of iron in the environment during the experimental conditions in this study, it has been reported in the literature that lack of iron leads to inactivation of *FecR* (Van Delden, Page, and Köhler 2013). *FeoB* has been widely reported in the literature as another transporter responsible for the import of ferrous iron in *P. aeruginosa.* When grown in iron starved conditions, upregulation of *FeoB* is observed. The FeoB system has been shown in the literature as an important iron uptake system during infection in the CF lung (Konings et al. 2013). Here, *P. aeruginosa* PA14 exhibits significant downregulation of the ferrous

ion transporter *FeoB* in response to Ivacaftor at 1 x serum concentration. The downregulation of both of these iron uptake systems suggests that iron uptake is being switched from these uptake systems to alternative systems during the experimental conditions, or that an abundance of iron during the experimental conditions limited the need for iron acquisition in the first place. The iron content of the Mueller Hinton broth used during this study is not known, however, there is no iron present in the Ivacaftor tablets used during this study.

Significant downregulation of several iron binding proteins is observed in response to Ivacaftor at 1 x serum concentration, including four proteins associated with the Cbb_3 type cytochrome oxidase system. The Cbb_3 cytochrome oxidases possess an iron and copper catalytic centre, and their downregulation could be associated with the clear response to iron acquisition observed in this RNA sequencing data.

Genes associated with the formation of hydrogen cyanide are also significantly downregulated in this dataset. Formation of this compound in *P. aeruginosa* has been shown in the literature as a consequence of iron abundance and concentrations of hydrogen cyanide produced have been shown to be proportional to levels of iron in the environment, although the reason for this link is not well understood (Blumer and Haas 2000). Production of hydrogen cyanide has been shown to inhibit the function of iron containing enzymes such as cytochrome c oxidases (Manoj et al. 2020). This is

further evidence of a response associated with iron as a consequence of treatment with Ivacaftor at 1 x serum concentration.

It has been reported in the literature that *P. aeruginosa* species have been shown to produce hydrogen cyanide when at high cell densities in order to compete for resources with *S. aureus* species (Létoffé et al. 2022). This has been shown to occur within the lungs of CF patients and is associated with increased pathogenicity of the strain (Ryall et al. n.d.; Tuon et al. 2022). This differential gene expression associated with and downregulation in hydrogen cyanide production is also observed in *P. aeruginosa* PA14 treated with Kaftrio at 100 x serum concentration.

5.2.9 Genes Associated with the Arginine Deaminase Pathway are Significantly Downregulated in Response to Ivacaftor at 1 x Serum Concentration

ArcA, arcB and *arcC* all displayed significant downregulation in response to treatment with Ivacaftor at 1 x serum concentration. These genes all play functional roles in the arginine deaminase pathway, the pathway converting arginine to ammonia, ATP and carbon dioxide (Xiong et al. 2016). The reason for the downregulation of this system in response to the CF drug is not clear.

5.2.10 Analysis of the Transcriptome of *P. aeruginosa* PA14 in response to Treatment with Ivacaftor at 100 x Serum Concentration

When treated with ivacaftor at 100 x serum concentration for thirty minutes, significant differential expression of genes is observed in *P. aeruginosa* PA14 as shown in **Figure 51**. To determine whether genes with associated functions were differentially expressed in response to Ivacaftor at 100 x serum concentration, the RNA sequencing data was analysed using the functional analysis and gene enrichment tool Funage-Pro. Using this tool, differentially expressed genes were grouped by function **Table 25**.

Table 25: **Differentially expressed genes in response to Ivacaftor at 100 x serum concentration are displayed as groups based on function.** This data generated using the gene enrichment analysis tool Funage Pro.

Downregulated Genes		Upregulated Genes	
Class Description	**Gene Name/Function**	**Class Description**	**Gene Name/Function**
Phenazine biosynthesis	PhzB, PhzC ,*PhzD, PhzD1, PhzB1, PhzA1, PhzA2* – phenazine biosynthesis protein	Sulfate starvation response	*PA14_03700, PA14_45110* – sulfate binding protein *CysA* – sulfate binding protein *CysW* – sulfate binding protein *CysU* – sulfate binding protein
Arginine Deaminase Pathway	*ArcB* – orthinine carbamoyltransferase, catabolic *ArcC* – carbamate kinase	Structural constituent of ribosome/translation	*RplV, RplP, RplN, RplX, RplE, RplU, RpmI, RpmE, RpmG,* – 50S ribosomal subunit protein RpsL, RpsS, RpsC, RpsQ, RpsM, RpsK, RpsD, RpsB- 30S ribosomal subunit protein *RimM* – ribosome maturation factor *Def* – peptide deformylase
Heme Binding	*Sir2* - sulfite reductase (ferrodoxin) 2 *CcoN1* – Cbb3 type cytochrome oxidase *CcoP* – Cbb3 type cytochrome oxidase *CcmF* – cytochrome c type biogenesis protein *CcmB* – heme exporter protein *CcmC* – heme exporter protein *Cyp107B1* – cytochrome 107B1 *NirM* – cytochrome C	Bacteriocidin production	*Pys2 – pyocin S2 type (PA14_13940, PA14_49520, PA14_59220)* *(Associated with iron starvation)*
Pseudomonas Quinolone Signalling	*PqsA, PqsB, PqsC, PqsD, PqsE* – secondary metabolite biosynthetic process quinolone signalling process		

Using Funage Pro, functional groups of genes which exhibited significant differential expression in *P. aeruginosa* PA14 in response to Ivacaftor at 100 x serum concentration were identified as shown in **Table 25.**

5.2.11 Phezanine Biosynthesis Genes are Significantly Downregulated in *P. aeruginosa* PA14 in Response to Ivacaftor at 100 x Serum Concentration

Seven genes associated with the biosynthesis of phezanine compounds were significantly downregulated in response to Ivacaftor at 100 x serum concentration. These proteins were categorised as phenazine biosynthesis proteins by the functional analysis and gene enrichment tool Funage Pro. A diverse range of phenazines are expressed by pseudomonads in comparison to other bacteria, and their roles within the cell range from electron acceptors to antibiotics (Pierson and Pierson 2010). It is unclear why these genes are downregulated in response to Ivacaftor at 100 x serum concentration.

5.2.12 Quinolone Signalling Proteins are Differentially Expressed in *P. aeruginosa* PA14 in Response to Ivacaftor at 100 x Serum Concentration

P. aeruginosa is well known for its ability to communicate in a cell density dependant manner by quorum sensing (Rutherford and Bassler 2012). There are three main quorum sensing systems in *P. aeruginosa.* The *Pseudomonas* quinolone signal (PQS)

system has been shown to regulate the gene expression of over 10% of *P. aeruginosa* genes and is associated with significantly increased virulence of the pathogen (Schuster et al. 2003). A significant decrease in transcription of the PQ system genes *pqsQ, pqsB, pqsC, pqsD* and *pqsE* was observed in response to treatment with Ivacaftor at 100 x serum concentration, suggesting there was a decrease in the expression of PQ genes and therefore PQ signalling. The upregulation of this system is associated with the induction of many virulence factors such as biofilm formation and persistent infection of the cystic fibrosis lung (Winstanley and Fothergill 2009), making it an attractive therapeutic target for chronic infection (Jiang et al. 2019). A reduction in PQS signalling due to Ivacaftor could lead to good outcomes for patients, however, further research is required to confirm this effect. Differential expression of these genes was not observed due to treatment with Ivacaftor at 1 x serum concentration, therefore, this effect may only be due to the significant concentrations of the drug present under these experimental conditions which is not representative of the CF lung.

5.2.13 Pyocins are Differentially Expressed in Response to Ivacaftor at 100 x Serum Concentration

An increase in the transcription of three genes associated with pyocin production in *P. aeruginosa* PA14 was observed during this study. These bacteriocins are produced by bacteria as a weapon against other bacteria in the fight for resources by puncturing the cell membrane (Michel-Briand and Baysse 2002). The importance of

pyocyins in *P. aeruginosa* cystic fibrosis infection is disputed in the literature; some studies suggesting it is a mechanism used by strains to dominate and persist in infections and others suggesting the role of pyocins in the CF lung is not significant (Ghoul et al. 2015; Oluyombo, Penfold, and Diggle 2019). Here, the significant increase in transcription of three pyocin production genes is observed in response to Ivacaftor at 100 x serum concentration. However, this effect is not observed when *P. aeruginosa* PA14 is treated with Ivacaftor at 1 x serum concentration suggesting this effect is dose dependant.

5.2.14 Similarities in Differential Expression of Genes is Observed Between 1 x and 100 x Serum concentration Treated Cultures of *P. aeruginosa* PA14

The differential expression of genes associated with the arginine deaminase pathway, iron acquisition, sulphate starvation and translation are observed in *P. aeruginosa* PA14 is observed in response to both concentrations of Ivacaftor treatment carried out during this study. The results of this study show the differences in differential expression of genes observed between 1 x and 100 x Ivacaftor serum concentration treated samples are concentration dependant. These results show the differences between the transcriptome of *P. aeruginosa* PA14 when treated with this drug at serum concentration and 100 x serum concentration. As the 100 x serum concentration of Ivacaftor is significantly higher than serum concentration, the differences in transcription observed in these cultures may be indicative of a stress

response of the pathogen to the drug. As 100 x serum concentration is not indicative of concentrations of Ivacaftor found in the cystic fibrosis lung, the changes in transcription observed in these conditions are unlikely to be reflective of *P. aeruginosa* strains in the clinic.

5.2.15 Analysis of the Transcriptome of *P. aeruginosa* PA14 in response to Treatment with Kaftrio at 1 x Serum Concentration

When treated with Kaftrio at 1 x serum concentration for thirty minutes, significant differential expression of genes was observed in *P. aeruginosa* PA14 as shown in **Figure 52.** To determine whether genes with associated functions were differentially expressed in response to Kaftrio at 1 x serum concentration, the RNA sequencing data was analysed using the functional analysis and gene enrichment tool Funage-Pro. Using this tool, differentially expressed genes were grouped by function **Table 26**.

Table 26: Differentially expressed genes in response to Kaftrio at 1 x serum concentration are displayed as groups based on function. This data generated using the gene enrichment analysis tool Funage Pro

Downregulated Genes		Upregulated Genes	
Class Description	**Gene Name/Function**	**Class Description**	**Gene Name/Function**
Arginine Deaminase Pathway	*ArcA – arginine diaminase* *ArcB* – orthinine carbamoyltransferase, catabolic	Pyoverdine iron acquisition system	PvdL, PvdO, PvdJ , PvdD, PvdY, PvdP, PvdG, PvdN, PvdF– pyoverdine peptide sythetase
Heme Binding	*CcoP* – Cbb3 type cytochrome oxidase *PetA* – Cytochrome c iron sulphur subunit CycC – Cytochrome oxidase c type	Pyochelin iron acquisition system	*PchE* – pyochelin synthase PchG, PchD, PchC – pyochelin biosynthetic protein PchF – Pyochelin synthase PchB - salicylate biosynthesis protein PchA – Isochorismate synthase FptA – pyochelin outer membrane receptor
Iron Transport systems	FecA – Fe(3+) dicitrate transport protein *FpvA* – Ferripyoverdine receptor *HmuS* – Heme transport protein *HmuR* – Heme receptor	Osmotic Stress	*OsmC, OsmE* - osmotic stress protein TreA – periplasmic trehalase
Pseudomonas Quinolone Signalling	*PqsA, PqsB, PqsC, PqsD, PqsE* – secondary metabolite biosynthetic process quinolone signalling process	Iron storage/acquisition	HasAp- heme acquisition protein PA14_64520 – bacterioferritin
		Lipopotein	OsmE – osmotically inducible lipoprotein PA14_16640, PA14_43900 – lipoprotein
		Efflux systems RND type	MexH – membrane fusion protein AprE – membrane fusion protein OmpA – outer membrane protein PA14_ 31890, PA14_31900 – putative RND type exporter

Using Funage Pro, functional groups of genes which exhibited significant differential expression in *P. aeruginosa* PA14 in response to Kaftrio at 1 x serum concentration were identified as shown in **Table 26**.

5.2.16 Treatment with Kaftrio at 1 x Serum Concentration Induces Differential Expression of RND type Efflux Pumps

Kaftrio at 1 x serum concentration was the only treatment group to induce differential expression of RND type efflux pumps in this study. An increase in transcription is shown for the membrane fusion protein MexH. This effect was also observed when *P. aeruginosa* PA14 was treated with the acrylic solvents BMA, styrene and ethylbenzene in the previous chapter. MexH is the membrane fusion component of the RND pump MexGHI-OpmD which has been shown in the literature to contribute towards PQS signalling and pathogenicity (Aedekerk et al. 2005). In contrast to the increase in transcription of *MexH,* the PQS genes *PqsA, PqsB, PqsC, PqsD,* and *PqsE* all exhibited a decrease in transcription under the experimental conditions. This suggests that the potential upregulation of MexH observed during this study is not associated with the PQS system. The other RND systems which showed an increase in transcription in Kaftrio 1 x serum concentration cultures were not differentially expressed in the solvent treated cultures and so their increase in transcription is Kaftrio dependant.

5.2.17 Iron Acquisition Systems are Differentially Expressed in *P. aeruginosa* PA14 in Response to Treatment with Kaftrio at 1 x Serum Concentration

A Significant increase in transcription in 8 genes associated with the pyochelin siderophore system was observed after treatment with Kaftrio at 1 x serum concentration, and no other treatment group. This response in conjunction with the increase in transcription of genes associated with pyoverdine synthesis as well as iron acquisition and storage genes show that *P. aeruginosa* PA14 displays a clear response to Kaftrio at 1 x serum concentration associated with iron starvation. However, a decrease in transcription in other iron transport systems is also observed such as *FecA, HmuS* and *HmuR.* The genes *HasAP* and *PA14_64520* a bacterioferritin associated with iron storage also showed an increase in transcription.

5.2.18 Treatment with Kaftrio at 1 x Serum concentration Results in an Increase in Transcription in Osmotic Stress Genes

The genes *OsmC* and *OsmE* displayed an increase in transcription as a result of treatment with Kaftrio at 1 x serum concentration. Expression of these proteins is characteristic of the *P. aeruginosa* osmotic stress response (Atichartpongkul et al. 2001). A similar osmotic stress response was described in the previous chapter in response to treatment with the methacrylate ester BMA. Upregulation of the *OsmE* gene encoding lipoprotein has an association with increased pathogenicity in people with CF and is related to the virulent mucoid phenotype (Firoved and Deretic 2003; Firoved, Ornatowski, and Deretic 2004).

5.2.19 Analysis of the Transcriptome of *P. aeruginosa* PA14 in response to Treatment with Kaftrio at 100 x Serum Concentration

When treated with Kaftrio at 100 x serum concentration for thirty minutes, significant differential expression of genes was observed in *P. aeruginosa* PA14 as shown in **Figure 53.** To determine whether genes with associated functions were differentially expressed in response to Kaftrio at 1 x serum concentration, the RNA sequencing data was analysed using the functional analysis and gene enrichment tool Funage-Pro. Using this tool, differentially expressed genes were grouped by function **Table 27**.

Table 27: Differentially expressed genes in response to Kaftrio at 100 x serum concentration are displayed as groups based on function. This data generated using the gene enrichment analysis tool Funage Pro

Downregulated Genes		Upregulated Genes	
Class Description	**Gene Name/Function**	**Class Description**	**Gene Name/Function**
Arginine Deaminase Pathway	*ArcA* – arginine diaminase *ArcB, ArcC* – orthinine carbamoyltransferase, catabolic	Bacteriocidin production	*Pys2 – pyocin S2 type (PA14_13940, PA14_49520, PA14_59220)* *(Associated with iron starvation)*
Phenazine biosynthesis	PhzB, PhzC ,*PhzD, PhzD1, PhzB1, PhzA1, PhzA2, PhzF, PhzS, PhnB, PhnA,* – phenazine biosynthesis protein	Pyoverdine iron acquisition system	*FpvA* – Ferripyoverdine receptor *PvdA, PvdQ, PvdO, PvdP* - pyoverdine peptide sythetase
Glycine dehydrogenase (cyanide forming) activity	*HcnA* – hydrogen cyanide synthase subunit *HcnB* - hydrogen cyanide synthase subunit *HcnC* - hydrogen cyanide synthase subunit	Iron storage/acquisition	*Fur* – Iron uptake regulation protein
Pseudomonas Quinolone Signalling	*PqsB, PqsC, PqsD* - secondary metabolite biosynthetic process quinolone signalling process	Structural constituent of ribosome	*RpsI, RpsL, RpsT* - 30S ribosomal subunit protein *RpmE, RpmF, RpmG* – 50S ribosomal subunit *InfA* – translation initiation factor
Heme Binding	CycC – Cytochrome oxidase c type *CcoP* – Cbb3 type cytochrome oxidase CcoN1 – Cbb3 type oxidase c type *NirM* – Cytochrome oxidase c type		

Using Funage Pro, functional groups of genes which exhibited significant differential expression in *P. aeruginosa* PA14 in response to Kaftrio at 100 x serum concentration were identified as shown in **Table 27**.

5.2.20 Correlation of Differential Gene Expression Between *P. aeruginosa* PA14 Cultures Treated with Kaftrio at 1 x and 100 x Serum Concentrations

Both Kaftrio treatment groups displayed an increase in transcription of genes associated with the siderophore system pyoverdine. However, while Kaftrio at 1 x serum concentration causes upregulation of both pyoverdine and polychelin genes, only the former iron acquisition system is upregulated in response to Kaftrio at 100 x serum concentration. A decrease in the transcription of genes associated with the PQS system is observed in Kaftrio at 1 x and 100 x serum concentrations as well as Ivacaftor at 100 x serum concentration. Arginine deaminase pathway genes are also downregulated in response to treatment with Kaftrio at 100 x serum concentration. This is another response which is displayed by all treatment groups during this study.

5.2.21 The Iron Acquisition Response of *P. aeruginosa* PA14 when Treated with Kaftrio at 1 x and 100 x Serum Concentrations shows Similarities

Heme binding enzymes show a decrease in transcription across all testing conditions in this study. Most notably, Cbb3 type cytochrome oxidases are amongst these genes.

This is in contrast to the response of *P. aeruginosa* PA14 in the previous chapter where these genes were upregulated in response to treatment with the acrylic solvents BMA, styrene and ethylbenzene.

Both Kaftrio treatment groups of *P. aeruginosa* PA14 show an increase in the transcription of genes associated with iron acquisition. At 100 x serum concentration of Kaftrio, a significant upregulation of the *Fur* ferric uptake regulatory protein gene is shown. Fur is upregulated when iron is scarce within the environment and regulates the expression of a large network of genes linked to iron scavenging (Reinhart and Oglesby-Sherrouse 2016). The induction of many virulence factors is controlled by the activation of *Fur* when iron is scarce, as the host environment is usually lacking in free iron (Cornelis and Dingemans 2013a). The significant increase in the transcription of *Fur* is indicative of the activation of iron scavenging mechanisms as well as virulence factors. This is consistent with the data in this study which shows that when treated with Kaftrio at 100 x serum concentration, pyoverdine and pyocin associated genes are upregulated. This is mirrored in the Kaftrio 1 x serum concentration treatment group, where iron storage genes are upregulated alongside pyoverdine and pyochelin siderophore genes.

5.2.22 Correlation of Differential Gene Expression Between Kaftrio 100 x and Ivacaftor 100 x Treated Groups

A decrease in transcription of genes associated with phenazine biosynthesis is displayed in both Kaftrio 100 x and Ivacaftor 100 x serum concentration treatment groups. The same similarity is observed between these groups with the upregulation of genes associated with the production of bacteriocidins. As these changes in gene expression were not observed in the cultures treated with drugs at 1 x serum concentration, this response appears to be dose specific to the higher concentrations of drug tested.

5.3 Discussion

The availability of the drugs Kaftrio and Ivacaftor to cystic fibrosis patients to treat the underlying cause of disease has been a breakthrough in the treatment of those suffering from the disease (Hussey et al. 2023; Mathews and Kirby 2022; Purkayastha et al. 2023). Although CFTR modulator therapy in the form of Kaftrio and Ivacaftor results in a clear improvement in patient outcomes for CF patients, communication with the CF respiratory consultant Gordon MacGregor revealed that patients undergoing treatment within his clinic struggle to clear *P. aeruginosa* infections despite prolonged use of Kaftrio and Ivacaftor (Gordon MacGregor, personal communication). During this study, the transcriptomic response of *P. aeruginosa* PA14 to the CF modulator drugs Kaftrio and Ivacaftor is demonstrated using RNA sequencing and in-depth differential gene expression analysis.

Research on the effect of CFTR modulator drugs on patient outcomes has been extensive and clearly shows the benefits these drugs offer to patients suffering from the symptoms of CF (Bear 2020; Graeber et al. 2021; Ridley and Condren 2020). The bacterial population within the CF lung has been studied pre and post-Kaftrio treatment and has been shown to be responsible for a substantial change in the biochemistry of the lung resulting in a population change in the lung microbiome (Sosinski et al. 2022). Although the population change observed during this study is a positive one showing a decrease in the number of pathogenic bacteria residing within the lungs of CF patients, an increase in the number of patients with *P. aeruginosa*

within the lungs showed an increase. This data is consistent with the observation made by Gordon MacGregor described earlier in this chapter. As *P. aeruginosa* is the most significant CF lung pathogen (Graeber et al. 2021), the transcriptomic effect of CFTR modulators on *P. aeruginosa* could aid in understanding why it's hard to shift this pathogen despite the hugely positive effect these drugs have on patients.

Research has been conducted to study the effect of Kaftrio on sputum composition (Lepissier et al. 2023), biofilm formation (Jones et al. 2023) and inflammatory response (Gabillard-Lefort et al. 2022). There are currently no published studies documenting the transcriptomic response of *P. aeruginosa* to the CFTR modulators Kaftiro and Ivacaftor. Here, we report the first study of this kind using *P. aeruginosa* PA14. The transcriptomic response of *P. aeruginosa* PA14 to these drugs was measured at 1 x and 100 x serum concentration. It must be noted that 100 x serum concentration is not comparable to conditions in the CF lung.

5.3.1 The Difference in the Growth Conditions used Throughout this Study and the Conditions Within the Cystic Fibrosis Lung are Substantial

During this study, cultures of *P. aeruginosa* PA14 were grown in laboratory conditions using Mueller Hinton broth. The differences between these conditions and the conditions within the CF lung must be noted. The development of antimicrobials against *P. aeruginosa* infections for CF patients often face the challenge of successfully mimicking the conditions found within the CF lung to ensure the benefits

observed *in vitro* translate to *in vivo* (Thomas E Barton et al. 2022). It must be noted that the growth conditions used throughout this study lack the complexity of the CF lung niche and this could be explored in future work. Acidic pH, availability of extracellular DNA and unique microbial population within the CF lung are some of the many conditions which must be recreated to ensure the CF lung environment is successfully recreated *in vitro* (Losada et al. 2016; Marcos et al. 2015; Tate et al. 2002). The results described throughout this study provide evidence that *P. aeruginosa* PA14 shows a significant transcriptomic response to Kaftrio and Ivacaftor under the experimental conditions tested, which can be explored further in the future using conditions more representative of the CF lung as described in the future work section of this chapter.

5.3.2 *P. aeruginosa* PA14 Shows a Transcriptomic Response to the Cystic Fibrosis Modulator Drugs Kaftrio and Ivacaftor at 1 x and 100 x Serum Concentrations under the Growth Conditions used Throughout this Study

During this study, cultures of *P. aeruginosa* PA14 were subjected to treatment with the CF modulator drugs at 1 x and 100 x serum concentrations. RNA was extracted and sequenced using the Illumina Miniseq and the transcriptome was sequenced against a DMSO only control culture. Differential gene expression analysis carried out using DESeq2 shows that significant differential gene expression was observed in response to both drugs at both serum concentrations tested.

5.3.3 *P. aeruginosa* PA14 Exhibits an Increase in Transcription of Genes Associated with Translation in Response to Ivacaftor at 1x and 100 x serum concentration and Kaftrio at 100 x serum Concentration

Translation is an essential part of cell growth and is a common target of antibiotics against various pathogens (Wüllner et al. 2022). We report an increase in the transcription of genes in *P. aeruginosa* PA14 associated with translation initiation and ribosome structure in response to treatment with Ivacaftor at 1 x and 100 x serum concentration and Kaftrio at 100 x serum concentration. Early research found that during exponential phase the synthesis of ribosomal RNAs is at the cells highest in *E. coli* (Bodilis et al. 2012). However this can't be responsible for the increase in transcription observed during this study as differential gene expression was measured against a DMSO only control at the same stage of growth as the drug treated cultures.

Bacteria have differing numbers of operons responsible for the synthesis of rRNA, allowing for the rapid synthesis of rRNAs when required by the cell (Tollerson and Ibba 2020b). These operons have been named *rrns* and seven have been reported in *P. aeruginosa* (Bodilis et al. 2012). When environmental changes or stressful conditions for the cell are encountered, these operons are activated allowing for the synthesis of the translational machinery required to synthesise complex proteins required to overcome the change in environmental condition (Condon et al. 1995;

Gyorfy et al. 2015). The increase in transcription of structural constituents of the ribosome as well as translation initiation factors in this study could be indicative of the activation of multiple *rrns* associated with the *P. aeruginosa* stress response, however, further work is required to confirm this. This response was Ivacaftor specific at 1 x serum concentration, which is interesting as the concentration of ivacaftor was consistent across both drug treated cultures. This effect was observed in both treatment groups with 100 x serum concentration of drug present. 100 x serum concentration of these drugs present is far higher than would be found in the CF lung and so is not indicative of what might happen during infection, therefore this response to 100 x serum concentration both drugs present may indicate the stress response of *P. aeruginosa* PA14 in these conditions.

However, this response at 1 x Ivacaftor serum concentration could mimic infection within the CF lung as this concentration of drug is consistent with the conditions during infection. The translational stress response of pathogenic bacteria has been linked with virulence (Starosta et al. 2014), and so could explain bad patient outcomes associated with *P. aeruginosa* infections despite prolonged use of Ivacaftor.

5.3.4 A Clear Iron Associated Transcriptional Response is Observed in *P. aeruginosa* to all Drugs at both Serum Concentrations During this Study

The link between iron acquisition and virulence in *P. aeruginosa* is widely reported in the literature (Lamont et al. 2002). The iron acquisition machinery of *P. aeruginosa* is highly sophisticated and allows the pathogen to proliferate within a wide range of niches with various levels of iron availability (Balasubramanian et al. 2013). As such, iron uptake systems are a popular target for antimicrobials (Tyrrell and Callaghan 2016). As an important virulence factor, the transcriptional response we report of *P. aeruginosa* PA14 to the CFTR modulators Kaftrio and Ivacaftor towards iron acquisition is significant and could provide insights into the response of this pathogen to these drugs *in vivo.*

5.3.4.1 The Response of P. aeruginosa PA14 to all Drug Conditions is Indicative of Low Iron Availability

We report that across all conditions tested during this study, there is a transcriptional response observed in *P. aeruginosa* PA14 which is indicative of low iron availability within the surrounding environment. Iron is taken up by this pathogen in two main forms from the surrounding environment – Fe^{2+} and Fe^{3+} (Andrews, Robinson, and Rodríguez-Quiñones 2003). The availability of each of these forms of iron is dependent on the environment and the uptake of these forms of iron differs and involves different iron uptake systems (Xiong et al. 2000). The results of this study show a cellular response to low levels or iron across all treatment conditions,

however, the response between different conditions varies. We cannot rule out that the drugs Ivacaftor, Elexacaftor and Tezacaftor sequester iron and create an iron limited environment which elicits this response in *P. aeruginosa* PA14. Further experimentation is required to explore this hypothesis further.

5.3.4.2 An Increase in Transcription in Siderophores is observed in P. aeruginosa PA14 in Response to treatment with Kaftrio and Ivacaftor

There is an increase in transcription in *P. aeruginosa* PA14 of genes associated with the siderophore pyoverdine in response to treatment with Kaftrio at 1 x and 100 x serum concentrations. *P. aeruginosa* pyoverdines are synthesized and released to scavenge extracellular Fe^{3+} from the environment (Kang et al. 2018). The release of pyoverdines has been described in the literature as essential for virulence in *P. aeruginosa* infections and the use of pyoverdines as opposed to other siderophores has a link with acute infection in the CF lung (De Vos et al. 2001). Pyoverdines are found to accumulate in the sputum of CF patients and a positive correlation between pyoverdine concentrations within the CF lung and severity of disease outcome has been reported in mouse models (Kang et al. 2019; De Vos et al. 2001). The release of pyoverdines by *P. aeruginosa* is associated with the production of other virulence factors and plays a role in the formation of biofilms (Cornelis and Dingemans 2013b). Here, we report the increase in transcription of genes associated with the pyoverdine iron acquisition system *in vitro* in response to Kaftrio at 1 x and 100 x serum concentrations. If this effect is representative of the effect of Kaftrio on *P. aeruginosa*

within the CF lung this could be indicative of negative patient outcomes because of this pathogenic response.

We also report an increase in transcription of the siderophore polychelin in response to treatment with Kaftrio at 1 x serum concentration. Like pyoverdine, this siderophore is used to scavenge extracellular Fe^{3+} from the environment but has a lower affinity for Fe^{3+} than pyoverdine (Britigan, Rasmussen, and Cox 1994). In the CF lung, the release of polychelin is associated with inflammation, tissue damage and prolonged infection (Lyczak et al. 2002).

As described, the release of the siderophores pyoverdine and pyochelin by *P. aeruginosa* in the CF lung is widely reported in the literature to have a detrimental effect on patient outcomes. In this study we describe the induction of this response by treatment of *P. aeruginosa* PA14 to Kaftrio at 1 x and 100 x serum concentrations. The induction of this response within the CF lung would typically lead to infection progression, our results show that the presence of Kaftrio at 1 x and 100 x serum concentrations within the environment may play a role in initiating this Fe^{3+} iron acquisition response associated with virulence in *P. aeruginosa* PA14.

Uptake of soluble Fe^{2+} by *P. aeruginosa* is controlled by the FecR system (Tyrrell and Callaghan 2016). Here, we describe the decrease in transcription of genes associated

with the FecR Fe^{2+} uptake system in response to treatment with Ivacaftor and Kaftrio at 1 x serum concentrations. Phenazines are released into the extracellular environment by *P. aeruginosa* to catalyse the reduction of Fe^{3+} to Fe^{2+} so iron can be taken up as Fe^{2+} through systems such as FecR (Cornelis and Dingemans 2013b). We report that phenazine biosynthesis is decreased at the transcriptional level in response to Kaftrio and Ivacaftor at 100 x serum concentrations. This shows a switch in iron uptake from soluble Fe^{2+} from the environment to Fe^{3+} using siderophores in the Kaftrio 1 x serum concentration treated geoup. As previously discussed, this is indicative of a pathogenic response to low amounts of iron in the environment.

5.3.4.3 There is a decrease in Transcription of Iron Binding Protein Genes Observed in all Treatment Groups

In all treatment groups described in this study, there is a decrease in transcription of heme binding protein genes including components of Cbb_3 type cytochrome oxidases described in the previous chapter. This conflicts with the decrease in transcription of HCN production genes observed in Ivacaftor 1 x serum concentration and Kaftrio 100 x serum concentration groups. HCN production has been shown in the literature to limit the activity of iron binding proteins (Blumer and Haas 2000). HCN production has also been reported as a mechanism used by *P. aeruginosa* to dominate infection in the CF lung and is associated with mature biofilm formation (Létoffé et al. 2022; Manoj et al. 2020; Ryall et al. n.d.). As HCN production genes are downregulated it is surprising that there is also a decrease in transcription of iron binding protein genes.

This data suggests that the downregulation of heme binding proteins observed during this study is HCN independent. The decrease in transcription of heme binding genes is consistent with the low iron availability response of *P. aeruginosa*, this response may be due to lack of available iron to form these proteins.

The transcriptomic response of *P. aeruginosa* PA14 to the CFTR modulator drugs associated with iron acquisition that we report is significant. As iron acquisition is tightly linked to virulence and plays a clear role in infection progression within the CF lung (Reinhart and Oglesby-Sherrouse 2016), gaining an in depth understanding of the effect of Kaftrio and Ivacaftor on this pathogen within the CF lung could provide insights into why this pathogen is able to reside within the lung even after prolonged treatment with these drugs. Further study *in vivo* to complement the data recorded during this study could aid to further understand the iron acquisition response observed here.

It is unclear why *P. aeruginosa* PA14 exhibited such a clear response associated with iron starvation when exposed to Kaftrio and Ivacaftor at 1 x and 100 x serum concentrations during this study. However, the implications for infection within the CF lung are distinct. The induction of iron scavenging using the siderophores pyoverdine and pyochelin is clearly described in the literature to have negative consequences for CF patients suffering from *P. aeruginosa* infection (Darling et al. 1998; Martin et al. 2011; Mossialos and Amoutzias 2009). The data we present

suggests a decrease in iron uptake in the Fe^{2+} form towards Fe^{3+} uptake using siderophores. Further study is needed to confirm that these effects are mirrored *in vivo* during infection within the CF lung.

5.4 Future Work

5.4.1 The use of Active Pharmaceutical Ingredients Instead of Tablets Could Strengthen the Reliability of the Data Generated During this Study

During this study, whole tablets of Ivacaftor and Kaftrio were used to investigate the transcriptomic response of the pathogen *P. aeruginosa* to these drugs *in vitro.* As these tablet drugs are formulated using a variety of compounds the transcriptomic effects of these drugs on the *P. aeruginosa* PA14 could be in part due to the presence of any of these compounds. To mitigate this in the future, the use of the active pharmaceutical ingredients instead of drug tablets within the *P. aeruginosa* cultures could be used to gain more accurate data about the transcriptomic response of this pathogen to the CFTR modulators. Discussions were underway with Vertex Pharmaceuticals before this study was carried out to provide the APIs required for this study, but time constraints due to the Covid-19 pandemic meant that it was not possible to obtain these APIs and therefore, the tablet form of these drugs was provided by Gordon MacGregor as previously described.

5.4.2 Further investigation of the Translational Response of *P. aeruginosa* to Kaftrio and Ivacaftor Could Provide Valuable Insights into Infection in the CF Lung

During this study, a defined translational response of *P. aeruginosa* PA14 to Kaftrio and Ivacaftor was observed as an increase in transcription of structural components of the ribosome as well as translation initiation factors. Proteomic studies in the

future could provide insights into whether the transcriptional responses observed during this study are carried through to expression at the protein synthesis level of expression.

5.4.3 The Use of A Cystic Fibrosis Lung Model Could Strengthen the Reliability of the Data Produced during this Study

Cultures during this study were grown in Mueller Hinton broth as this culture media is commonly used for antibiotic susceptibility trials in *P. aeruginosa* and other pathogens. To improve the similarity of the experiment to the CF lung, artificial cystic fibrosis sputum media could be used to grow cultures of *P. aeruginosa* in the future. As this media better mimics the conditions found within the CF lung, a transcriptomics study carried out using this as a growth media would provide a more reliable simulation of *P. aeruginosa* infection within the CF lung.

5.4.4 A Clinical Trial is Currently Underway which Provides a Reliable *in vivo* Model of the Transcriptomic Study we Report Here

Currently, the clinical trial 'Trikafta/Kaftrio and *Pseudomonas aeruginosa'* (Clinical Trial.gov identifier: NCT05675592) is in the recruiting stage. This study will take samples of *P. aeruginosa* from infected cystic fibrosis patients before and after taking Kaftrio at timepoints of 12 and 18 months and sequence these strains to look for genetic differences before and after treatment. This approach will solve the issues associated with our experiment model by measuring the changes induced by the

active pharmaceutical ingredients within a real CF lung model. Although this study will not look at the transcriptome of these *P. aeruginosa* isolates, the genetic changes that these strains undergo after treatment with Kaftrio which will be measured will provide invaluable insights into the response of the pathogen to this drug and could lead to the identification of new drug targets to be used in conjunction with Kaftrio therapy. The timepoints measured during this study were also small (30 minutes exposure with Kaftrio or Ivacaftor), however, this clinical trial will measure the long-term effects of usage of Kaftrio which is representative of real-life treatment as this therapy is used long term.

6 Discussion

The bioproduction of industrially relevant products using bacteria and fungi is becoming an increasingly popular energy efficient alternative to traditional chemical methods of platform chemical production (Gavrilescu and Chisti 2005; Murphy 2011; Willke and Vorlop 2004). A common bottleneck in industrial bioprocesses is the toxicity of the final products to the production strain (Akinosho et al. 2015; Borden and Papoutsakis 2007). Gaining insights into the mechanisms of tolerance of historically successful production strains can provide targets for exploitation and subsequent bioprocess improvement. The improvement in the tolerance of yeasts to bioethanol to enhance yields in fermentation is an example of successful exploitation of tolerance conferring systems for bioprocess improvement (Kim et al. 2011; Teixeira et al. 2009; Yazawa, Iwahashi, and Uemura 2007). Understanding the response of bacteria to relevant stimuli can similarly identify tolerance conferring systems which may provide as drug targets to improve the treatment of infection (Goossens, Sampson, and Van Rie 2021; Kim et al. 2013). Here, we present the investigation of the response of *P. aeruginosa* PA14 to platform chemicals of the plastics industry and the CFTR modulators Kaftrio and Ivacaftor for bioprocess and patient outcome optimisation.

During this study, we use *P. aeruginosa* PA14 as a model organism for tolerance in *Pseudomonas* species. As a human pathogen *P. aeruginosa* PA14 is not a suitable candidate as a bioproduction strain, however, this strain was used as a tool to identify

homologue systems of interest for further investigation in *P. putida.* This pathogen has become the universal model for biofilm formation and quorum sensing (De Kievit 2009; Mcdougald et al. 2008). Here, we demonstrate *P. aeruginosa* as a model organism for tolerance. This strain is, however, relevant for the investigation of the response to the CFTR modulators Kaftrio and Ivacaftor as *P. aeruginosa* is the leading pathogen of interest in those suffering from cystic fibrosis (Malhotra, Hayes, and Wozniak 2019).

6.1 A Multidisciplinary Approach for Identifying Tolerance Conferring Systems was Utilised Throughout this Study

Throughout this study, we describe the identification of solvent tolerance conferring systems in *P. aeruginosa* PA14 using a combination of genetic, biochemical and transcriptomic approaches. Previous work carried out using a transposon mutant library screen provided the basis for the biochemical characterization of the proteins CopA2 and MexB (Bestawy 2017a). Disruption of expression of Cbb_3 type cytochrome oxidase assembly system or MexAB-OprM genes during this study resulted in a significant decrease in growth in growth conditions when the methacrylate ester BMA was present. A functional relationship between these systems wherein the Cbb_3 cytochrome oxidase system powers the sophisticated network of efflux systems of *P. aeruginosa* by providing the proton gradient necessary for their function is hypothesised in this study. The exploitation of this functional relationship has

significant industrial application in the development of bacterial strains with high levels of tolerance to this methacrylate ester.

6.1.1 The Biochemical Characterization of CopA2 and MexB Could Provide Insights into a Functional Relationship

The overexpression, purification and subsequent characterization of the membrane proteins Cbb_3 and MexB was aimed to be carried out during this study. Because of the time constraints placed on this study due to the Covid-19 pandemic, purification and biochemical characterization using SSME was not carried out, however, the expression of both CopA2 and MexB was achieved in *E. coli* C43(DE3). Here, we demonstrate the first study aiming to understand the potential functional relationship between Cbb_3 and MexB using biochemical characterization in conjunction with transcriptomic studies.

The measurement of proxy substances through CopA2 and MexB using SSME technology in the future could provide insights into the hypothesised functional relationship between these membrane proteins. Understanding this potential relationship holds incredible industrial and medical value. The intrinsic tolerance of *Pseudomonas* species to a wide range of compounds is well described in the literature (Ciofu and Tolker-Nielsen 2019; Cox and Markham 2007). Understanding the mechanisms of these tolerance conferring systems will not only provide as targets for exploitation for subsequent industrial strain development but could also provide as

drug targets for drug resistant strains (Sanya et al. 2023). The effectiveness of SSME to biochemically characterize proteins has been demonstrated previously by the identification of substrates and transport mechanisms of the bacterial ammonium transporter AmtB (Tamburrino 2018; Wacker et al. 2014; Williamson et al. 2020). Here, we aimed to apply this approach to MexB and CopA2, however, this will have to be carried out in future work. We demonstrate that soluble protein can be expressed in *E. coli* C43(DE3) which is the first step in this biochemical characterization approach.

6.2 Investigating the Transcriptomic Response of *P. aeruginosa* PA14 to Industrially relevant Solvents has Identified Targets for the Optimisation of a BMA Fermentation for Mitsubishi Chemical Corporation UK

Mitsubishi Chemical Corporation UK in collaboration with Ingenza Ltd are developing a fermentation process using *P. putida* for the bioproduction of the methacrylate ester BMA. This process will replace their energy intensive chemical process currently in use. The toxicity of BMA to *P. putida* is the biggest bottleneck currently within the process (Ingenza Ltd n.d.), therefore, the identification of tolerance conferring systems within *Pseudomonas* species will provide as targets for exploitation and subsequent bioprocess optimisation. Analysis of the transcriptional response of bacteria to platform chemicals such as isobutanol and styrene has previously identified mechanisms of tolerance with industrial application (Gupta et al. 2020;

Machas et al. 2021). Here, we describe the transcriptomic characterization of the response of *P. aeruginosa* PA14 to BMA to identify tolerance mechanisms for potential exploitation. The transcriptomic response of this pathogen to the platform chemicals of the plastics industry styrene and ethylbenzene was also investigated.

6.2.1 The Importance of RND type Efflux in Solvent Tolerance is Reinforced by this Transcriptomic Data

The increase in transcription of RND type multidrug efflux pumps was ubiquitous across all solvent conditions tested throughout this study. This data clearly presents evidence that these efflux systems are integral to the tolerance of *P. aeruginosa* PA14 to BMA, styrene and ethylbenzene. This data reinforces what is already heavily reported on in the literature about the tolerance of *P. aeruginosa* tolerance to many substances including solvents (Carrara et al. 2022; Li, Zhang, and Poole 1998c; Poole and Srikumar 2005). This data even reports BMA as the fourth known substrate of the triclosan efflux pump TriABC.

Improved tolerance in bacteria to toxic products of fermentation through overexpression or genetic engineering of RND type efflux pumps has been demonstrated as a successful tool in improving product yields in bioprocesses previously (Dunlop et al. 2011; Fisher et al. 2014; Jones, Hernández Lozada, and Pfleger 2015). The data in this study shows that this approach could provide benefit in the context of a BMA fermentation using *P. putida.* Optimisation of efflux of BMA

from the cell would not only improve tolerance and yield, but efficient excretion of BMA from the cell using RND efflux systems after production within the cell could also expedite costly and time-consuming downstream processing steps to recover BMA sequestered within cells. Active efflux of styrene and ethylbenzene from the cell as a mechanism of tolerance has been reported previously in *P. putida* (Kieboom et al. 1998; Tucker and Begley 2021). Here, we report similar findings using *P. aeruginosa* PA14.

6.2.2 An Increase in Transcription of Cbb_3 Cytochrome Oxidase Assembly Genes was Demonstrated Across all Solvent Treatment Groups

Here, we report an increase in transcription of Cbb_3 cytochrome oxidase assembly genes including *copA2* in response to BMA, styrene and ethylbenzene. The data presented here supports the functional relationship between the Cbb_3 cytochrome oxidases and RND efflux systems hypothesised throughout this study, as both groups are upregulated in response to solvent treatment in *P. aeruginosa* PA14. The evidence supporting this functional relationship is demonstrated across all three solvents tested. The role of CopA2 and the Cbb_3 cytochrome oxidases in bacterial energetics, virulence and drug tolerance has been reported (Buschmann et al. 2010; Hamada et al. 2014; Pitcher and Watmough 2004). The clear upregulation of CopA2 and the Cbb_3 cytochrome oxidases in response to BMA, styrene and ethylbenzene alongside RND efflux systems supports the hypothesis that the Cbb_3 cytochrome

oxidases play a principal role in bacterial energetics associated with solvent tolerance.

Here, we provide further evidence that expression of the Cbb_3 cytochrome oxidases in *P. aeruginosa* drives the generation of a proton gradient essential for the function of many RND efflux pumps which aids in bacterial tolerance to various solvents. This data is consistent with the findings of the transposon mutant library screen which highlighted the MexAB-OprM and Cbb_3 cytochrome oxidase assembly systems as important for *P. aeruginosa* PA14 tolerance to the methacrylate ester BMA. Our findings build upon the observations taken from this experiment and reinforce the hypothesis that these systems have a functional role related to tolerance within the cell. The industrial application of this functional relationship could allow for the engineering of bacterial strains not only with the biochemical machinery to mediate efficient efflux of BMA from the cell, but with a sophisticated energetics system providing the necessary conditions to allow for the function of the energetically expensive efflux through RND pumps. Understanding this functional relationship could also provide advancements in the identification of potential drug targets for multi drug resistant strains of *P. aeruginosa.* Efflux of antimicrobials through RND systems is a widely used virulence tactic employed by *P. aeruginosa* in the clinic (Hirakata et al. 2002; Lorusso et al. 2022). If the Cbb_3 cytochrome oxidase system aids in powering efflux of antimicrobials from the cell through RND efflux systems then

this presents as an attractive therapeutic target. Here, we report the first study proposing this functional relationship.

We demonstrate the benefit of combining a transposon mutant library screen plus transcriptomic analysis as a tool for the identification of tolerance conferring systems in *P. aeruginosa* PA14. The data we present in favour of the functional relationship between RND systems and Cbb_3 cytochrome oxidase systems is strengthened the combinatorial approach through which the data was accumulated. Developing a transposon mutant library screen to identify tolerance conferring systems to Kaftrio and Ivacaftor could strengthen the reliability of the transcriptomic dataset described throughout this study.

6.2.3 The Cell Envelope Stress Response of *P. aeruginosa* PA14 to BMA could Explain Anomalous Results Observed During Fermentation at Ingenza Ltd

Trial BMA fermentations carried out at Ingenza Ltd using *P. putida* as a production strain encountered issues directing carbon flux towards BMA production efficiently. At the end of fermentation runs carbon could not be accounted for. Here, we report the upregulation of trehalose biosynthesis genes as a result of treatment with BMA consistent with the inefficient direction of carbon towards BMA production observed during fermentation trials. Inefficient direction of carbon towards products of fermentation is reported as a common bioprocess bottleneck (Tilloy, Ortiz-Julien, and

Dequin 2014; Varela, Baez, and Agosin 2004). Our findings suggest that efficient bioproduction of BMA *Pseudomonas* species could be optimised by deletion of osmoprotectant genes involved in trehalose biosynthesis- the effects of this on cellular susceptibility to BMA must be investigated.

6.3 We Report the First Study Investigating the Transcriptional Response of *P. aeruginosa* PA14 to the CFTR Modulators Kaftrio and Ivacaftor

We report the transcriptional response of *P. aeruginosa* PA14 to the CFTR modulators used for CF therapy Kaftrio and Ivacaftor at 1 x and 100 x serum concentrations *in vitro. P. aeruginosa* infection is a significant cause of death in patients suffering from CF (Hasan et al. 2022). Although treatment using Kaftrio and Ivacaftor has significantly improved the outcomes of disease for many patients, *P. aeruginosa* is often able to persist within the CF lung (Sosinski et al. 2022). The mechanisms behind the persistence of *P. aeruginosa* within the CF lung must be elucidated to improve the outcome of chronic infection, here, we provide data suggesting that further study built upon the work conducted here could be beneficial in understanding infection.

6.3.1 We Report a Transcriptional Response *P. aeruginosa* PA14 to Kaftrio and Ivacaftor at 1 x and 100x Serum Concentrations

Under the conditions tested throughout this study, we describe the distinct increase in transcription in *P. aeruginosa* PA14 of genes associated with translation of proteins

and iron acquisition. This transcriptional response is distinct from the response described to BMA, styrene and ethylbenzene. Upregulation of translation and iron acquisition systems have both been linked to virulence in the literature (Reinhart and Oglesby-Sherrouse 2016; Starosta et al. 2014; Xiong et al. 2000). If these results are mirrored *in vivo* this would implicate the response of *P. aeruginosa* to these drugs in pathogenicity. Upregulation of RND efflux systems in conjunction with Cbb_3 type cytochrome oxidases was not observed in response to Kaftrio and Ivacaftor at 1 x or 100 x concentrations.

The lack of complexity of the growth conditions used throughout this study in comparison to the CF lung must be noted. Typical lab growth conditions such as are described throughout this study have been shown in the literature to lack the complexity required to recreate bacterial behaviours *in vivo* (Thomas E. Barton et al. 2022; Ruhluel et al. 2022). The data we report here provides the basis for further study using more sophisticated culturing methods *in vitro.*

6.4 The Benefits of a Multidisciplinary Approach for the Identification of Tolerance Conferring Systems in *P. aeruginosa* PA14 is Described Throughout this Study

Here, we describe a multidisciplinary approach to understanding the mechanisms of tolerance and resistance in *P. aeruginosa* PA14 in an industrial and medical context. We clearly demonstrate the benefit of acquiring transcriptomic data to compliment

a transposon mutant library screen for identifying solvent tolerance conferring mechanisms in *P. aeruginosa* PA14, particularly in the context of strain development for BMA fermentation development. The importance of this data to Mitsubishi Chemical Corporation UK in the development of an industrially relevant strain cannot be undermined. This study reports the identification of BMA tolerance conferring systems as well as evidence to suggest a functional relationship between RND type efflux systems and the Cbb_3 cytochrome oxidases which could be exploited for industrial benefit. The redirection of carbon towards BMA production by knocking out trehalose biosynthesis genes in *P. aeruginosa* PA14 has been identified as a solution to carbon flux issues described during trial fermentations at Ingenza Ltd. The basis for further study including a transposon mutant library screen of *P. aeruginosa* PA14 against Kaftrio and Ivacaftor and the use of a CF lung model is also demonstrated.

7 Bibliography

Adewoye, Lateef, Ainsley Sutherland, Ramakrishnan Srikumar, and Keith Poole. 2002. "The MexR Repressor of the MexAB-OprM Multidrug Efflux Operon in Pseudomonas Aeruginosa: Characterization of Mutations Compromising Activity." *Journal of Bacteriology* 184(15):4308. doi: 10.1128/JB.184.15.4308-4312.2002.

Aedekerk, Séverine, Stephen P. Diggle, Zhijun Song, Niels Høiby, Pierre Cornelis, Paul Williams, and Miguel Cámara. 2005. "The MexGHI-OpmD Multidrug Efflux Pump Controls Growth, Antibiotic Susceptibility and Virulence in Pseudomonas Aeruginosa via 4-Quinolone-Dependent Cell-to-Cell Communication." *Microbiology (Reading, England)* 151(Pt 4):1113–25. doi: 10.1099/MIC.0.27631-0.

Aeschlimann, Jeffrey R. 2003. "The Role of Multidrug Efflux Pumps in the Antibiotic Resistance of Pseudomonas Aeruginosa and Other Gram-Negative Bacteria Insights from the Society of Infectious Diseases Pharmacists." *Pharmacotherapy*.

Afgan, Enis, Dannon Baker, Bérénice Batut, Marius Van Den Beek, Dave Bouvier, Martin Ech, John Chilton, Dave Clements, Nate Coraor, Björn A. Grüning, Aysam Guerler, Jennifer Hillman-Jackson, Saskia Hiltemann, Vahid Jalili, Helena Rasche, Nicola Soranzo, Jeremy Goecks, James Taylor, Anton Nekrutenko, and Daniel Blankenberg. 2018. "The Galaxy Platform for Accessible, Reproducible and Collaborative Biomedical Analyses: 2018 Update." *Nucleic Acids Research* 46(W1):W537–44. doi: 10.1093/NAR/GKY379.

Akama, Hiroyuki, Misa Kanemaki, Masato Yoshimura, Tomitake Tsukihara, Tomoe Kashiwagi, Hiroshi Yoneyama, Shin Ichiro Narita, Atsushi Nakagawa, and Taiji Nakae. 2004. “Crystal Structure of the Drug Discharge Outer Membrane Protein, OprM, of Pseudomonas Aeruginosa: Dual Modes of Membrane Anchoring and Occluded Cavity End.” *Journal of Biological Chemistry*. doi: 10.1074/jbc.C400445200.

Akama, Hiroyuki, Takanori Matsuura, Sachiko Kashiwagi, Hiroshi Yoneyama, Shin Ichiro Narita, Tomitake Tsukihara, Atsushi Nakagawa, and Taiji Nakae. 2004. “Crystal Structure of the Membrane Fusion Protein, MexA, of the Multidrug Transporter in Pseudomonas Aeruginosa.” *Journal of Biological Chemistry*. doi: 10.1074/jbc.C400164200.

Akinosho, Hannah, Thomas Rydzak, Abhijeet Borole, Arthur Ragauskas, and Dan Close. 2015. “Toxicological Challenges to Microbial Bioethanol Production and Strategies for Improved Tolerance.” *Ecotoxicology 2015 24:10* 24(10):2156–74. doi: 10.1007/S10646-015-1543-4.

Alberts B, Johnson A, Lewis J, et al. 2002. “Electron Transport Chains and Their Proton Pumps.” *Molecular Biology of the Cell 4th Edition*.

Anders, Simon, Paul Theodor Pyl, and Wolfgang Huber. 2015. “HTSeq—a Python Framework to Work with High-Throughput Sequencing Data.” *Bioinformatics* 31(2):166–69. doi: 10.1093/BIOINFORMATICS/BTU638.

Andrews, Simon C., Andrea K. Robinson, and Francisco Rodríguez-Quiñones. 2003. "Bacterial Iron Homeostasis." *FEMS Microbiology Reviews* 27(2–3):215–37. doi: 10.1016/S0168-6445(03)00055-X.

Angius, Federica, Oana Ilioaia, Amira Amrani, Annabelle Suisse, Lindsay Rosset, Amélie Legrand, Abbas Abou-Hamdan, Marc Uzan, Francesca Zito, and Bruno Miroux. 2018. "A Novel Regulation Mechanism of the T7 RNA Polymerase Based Expression System Improves Overproduction and Folding of Membrane Proteins." *Scientific Reports 2018 8:1* 8(1):1–11. doi: 10.1038/s41598-018-26668-y.

Anon. n.d.-a. "Babraham Bioinformatics - Trim Galore!" Retrieved November 28, 2022 (https://www.bioinformatics.babraham.ac.uk/projects/trim_galore/).

Anon. n.d.-b. "THE 17 GOALS | Sustainable Development." Retrieved September 23, 2023 (https://sdgs.un.org/goals).

Arai, Hiroyuki, Takuro Kawakami, Tatsuya Osamura, Takehiro Hirai, Yoshiaki Sakai, and Masaharu Ishii. 2014. "Enzymatic Characterization and in Vivo Function of Five Terminal Oxidases in Pseudomonas Aeruginosa." *Journal of Bacteriology*. doi: 10.1128/JB.02176-14.

Aspinall, Sean A., Kelly A. Mackintosh, Denise M. Hill, Bethany Cope, and Melitta A. McNarry. 2022. "Evaluating the Effect of Kaftrio on Perspectives of Health and Wellbeing in Individuals with Cystic Fibrosis." *International Journal of*

Environmental Research and Public Health 19(10). doi: 10.3390/IJERPH19106114.

Atichartpongkul, S., S. Loprasert, P. Vattanaviboon, W. Whangsuk, J. D. Helmann, and S. Mongkolsuk. 2001. "Bacterial Ohr and OsmC Paralogues Define Two Protein Families with Distinct Functions and Patterns of Expression." *Microbiology* 147(7):1775–82. doi: 10.1099/00221287-147-7-1775.

Ayala-Castro, Carla, Avneesh Saini, and F. Wayne Outten. 2008. "Fe-S Cluster Assembly Pathways in Bacteria." *Microbiology and Molecular Biology Reviews : MMBR* 72(1):110. doi: 10.1128/MMBR.00034-07.

Azhar, Umair, Rimsha Yaqub, Huateng Li, Ghulam Abbas, Yongkang Wang, Jian Chen, Chuanyong Zong, Anhou Xu, Zhang Yabin, Shuxiang Zhang, and Bing Geng. 2020. "Di-Block Copolymer Stabilized Methyl Methacrylate Based PolyHIPEs: Influence of Hydrophilic and Hydrophobic Co-Monomers on Morphology, Wettability and Thermal Properties." *Arabian Journal of Chemistry*. doi: 10.1016/j.arabjc.2019.01.005.

Balasubramanian, Deepak, Lisa Schneper, Hansi Kumari, and Kalai Mathee. 2013. "A Dynamic and Intricate Regulatory Network Determines Pseudomonas Aeruginosa Virulence." *Nucleic Acids Research* 41(1):1. doi: 10.1093/NAR/GKS1039.

Barton, Thomas E., Frederick Frost, Joanne L. Fothergill, and Daniel R. Neill. 2022. "Challenges and Opportunities in the Development of Novel Antimicrobial

Therapeutics for Cystic Fibrosis." *Journal of Medical Microbiology* 71(12). doi: 10.1099/JMM.0.001643.

Barton, Thomas E, Frederick Frost, Joanne L. Fothergill, Daniel R. Neill, and T. E. Barton@. 2022. "Challenges and Opportunities in the Development of Novel Antimicrobial Therapeutics for Cystic Fibrosis." *Journal of Medical Microbiology* 71:1643. doi: 10.1099/jmm.0.001643.

Basler, Georg, Mitchell Thompson, Danielle Tullman-Ercek, and Jay Keasling. 2018. "A Pseudomonas Putida Efflux Pump Acts on Short-Chain Alcohols." *Biotechnology for Biofuels* 11(1):1–10. doi: 10.1186/S13068-018-1133-9/FIGURES/4.

Bazzone, Andre, Maria Barthmes, and Klaus Fendler. 2017. "SSM-Based Electrophysiology for Transporter Research." Pp. 31–83 in *Methods in Enzymology*. Vol. 594.

Bazzone, Andre, Wagner Steuer Costa, Markus Braner, Octavian Călinescu, Lina Hatahet, and Klaus Fendler. 2013. "Introduction to Solid Supported Membrane Based Electrophysiology." *Journal of Visualized Experiments* (75). doi: 10.3791/50230.

Bear, Christine E. 2020. "A Therapy for Most with Cystic Fibrosis." *Cell* 180(2):211. doi: 10.1016/J.CELL.2019.12.032.

Beaume, M., T. Köhler, G. Greub, O. Manuel, J. D. Aubert, L. Baerlocher, L. Farinelli, A. Buckling, and C. van Delden. 2017. "Rapid Adaptation Drives Invasion of

Airway Donor Microbiota by Pseudomonas after Lung Transplantation." *Scientific Reports* 7. doi: 10.1038/SREP40309.

De Bentzmann, Sophie, and Patrick Plésiat. 2011. "The Pseudomonas Aeruginosa Opportunistic Pathogen and Human Infections." *Environmental Microbiology*. doi: 10.1111/j.1462-2920.2011.02469.x.

Bernaudat, Florent, Annie Frelet-Barrand, Nathalie Pochon, Sébastien Dementin, Patrick Hivin, Sylvain Boutigny, Jean Baptiste Rioux, Daniel Salvi, Daphné Seigneurin-Berny, Pierre Richaud, Jacques Joyard, David Pignol, Monique Sabaty, Thierry Desnos, Eva Pebay-Peyroula, Elisabeth Darrouzet, Thierry Vernet, and Norbert Rolland. 2011. "Heterologous Expression of Membrane Proteins: Choosing the Appropriate Host." *PLoS ONE* 6(12):10. doi: 10.1371/JOURNAL.PONE.0029191.

Bertani, Blake, and Natividad Ruiz. 2018. "Function and Biogenesis of Lipopolysaccharides." *EcoSal Plus* 8(1). doi: 10.1128/ECOSALPLUS.ESP-0001-2018.

Bertram, Ralph, Bernd Neumann, and Christopher F. Schuster. 2022. "Status Quo of Tet Regulation in Bacteria." *Microbial Biotechnology* 15(4):1101–19. doi: 10.1111/1751-7915.13926.

Bestawy, Walid El (University of Strathclyde). 2017a. "A P. Aeruginosa PA14 Transposon Mutant Library Screen Determines Tolerance Conferring Systems to n-Butyl Methacrylate."

Bestawy, Walid El (University of Strathclyde). 2017b. “Growth of P. Aeruginosa Transposon Insertion Mutants in n-Butyl Methacrylate.”

Bethany Halford. 2021. “Greener Route to Styrene.” *C&EN Global Enterprise* 99(8):7–7. doi: 10.1021/CEN-09908-SCICON4.

Blumer, C., and D. Haas. 2000. “Iron Regulation of the HcnABC Genes Encoding Hydrogen Cyanide Synthase Depends on the Anaerobic Regulator ANR Rather than on the Global Activator GacA in Pseudomonas Fluorescens CHA0.” *Microbiology* 146(10):2417–24. doi: 10.1099/00221287-146-10-2417/CITE/REFWORKS.

Bodey, G. P., R. Bolivar, V. Fainstein, and L. Jadeja. 1983. “Infections Caused by Pseudomonas Aeruginosa.” *Reviews of Infectious Diseases*.

Bodilis, Josselin, Sandrine Nsigue-Meilo, Ludovic Besaury, and Laurent Quillet. 2012. “Variable Copy Number, Intra-Genomic Heterogeneities and Lateral Transfers of the 16S RRNA Gene in Pseudomonas.” *PLoS ONE* 7(4):35647. doi: 10.1371/JOURNAL.PONE.0035647.

Boehm, Christian R., and Ralph Bock. 2019. “Recent Advances and Current Challenges in Synthetic Biology of the Plastid Genetic System and Metabolism.” *Plant Physiology* 179(3):794–802. doi: 10.1104/pp.18.00767.

Borden, Jacob R., and Eleftherios Terry Papoutsakis. 2007. “Dynamics of Genomic-Library Enrichment and Identification of Solvent Tolerance Genes for Clostridium

Acetobutylicum." *Applied and Environmental Microbiology* 73(9):3061–68. doi: 10.1128/AEM.02296-06/SUPPL_FILE/SUPP_FIG_TABLE_POST_REVIEW.PDF.

Britigan, B. E., G. T. Rasmussen, and C. D. Cox. 1994. "Pseudomonas Siderophore Pyochelin Enhances Neutrophil-Mediated Endothelial Cell Injury." *The American Journal of Physiology* 266(2 Pt 1). doi: 10.1152/AJPLUNG.1994.266.2.L192.

Bud, Robert. 2011. "Innovators, Deep Fermentation and Antibiotics: Promoting Applied Science before and after the Second World War." *Dynamis*.

Buschmann, Sabine, Eberhard Warkentin, Hao Xie, Julian D. Langer, Ulrich Ermler, and Hartmut Michel. 2010. "The Structure of Cbb3 Cytochrome Oxidase Provides Insights into Proton Pumping." *Science*. doi: 10.1126/science.1187303.

Cabot, Gabriel, Laura Zamorano, Bartolomé Moyà, Carlos Juan, Alfonso Navas, Jesús Blázquez, and Antonio Oliver. 2016. "Evolution of Pseudomonas Aeruginosa Antimicrobial Resistance and Fitness under Low and High Mutation Rates." *Antimicrobial Agents and Chemotherapy*. doi: 10.1128/AAC.02676-15.

Calero, Patricia, Sheila I. Jensen, Klara Bojanovič, Rebecca M. Lennen, Anna Koza, and Alex T. Nielsen. 2018. "Genome-Wide Identification of Tolerance Mechanisms toward p-Coumaric Acid in Pseudomonas Putida." *Biotechnology and Bioengineering*. doi: 10.1002/bit.26495.

Calos, Michéle P., and Jeffrey H. Miller. 1980. "Transposable Elements." *Cell* 20(3):579–95. doi: 10.1016/0092-8674(80)90305-0.

Carrara, J. B. ;. A. ;., C. D. N. ;. Barroso, F. F. ;. Tuon, H Faoro, Andre Bittencourt Lorusso, João Antônio Carrara, Carolina Deuttner, Neumann Barroso, Felipe Francisco Tuon, and Helisson Faoro. 2022. “Role of Efflux Pumps on Antimicrobial Resistance in Pseudomonas Aeruginosa.” *International Journal of Molecular Sciences 2022, Vol. 23, Page 15779* 23(24):15779. doi: 10.3390/IJMS232415779.

Castellani, C., H. Cuppens, M. Macek, J. J. Cassiman, E. Kerem, P. Durie, E. Tullis, B. M. Assael, C. Bombieri, A. Brown, T. Casals, M. Claustres, G. R. Cutting, E. Dequeker, J. Dodge, I. Doull, P. Farrell, C. Ferec, E. Girodon, M. Johannesson, B. Kerem, M. Knowles, A. Munck, P. F. Pignatti, D. Radojkovic, P. Rizzotti, M. Schwarz, M. Stuhrmann, M. Tzetis, J. Zielenski, and J. S. Elborn. 2008. “Consensus on the Use and Interpretation of Cystic Fibrosis Mutation Analysis in Clinical Practice.” *Journal of Cystic Fibrosis* 7(3):179–96. doi: 10.1016/J.JCF.2008.03.009.

Chesnay, Adélaïde, Éric Bailly, Laure Cosson, Thomas Flament, and Guillaume Desoubeaux. 2022. “Advent of Elexacaftor/Tezacaftor/Ivacaftor for Cystic Fibrosis Treatment: What Consequences on Aspergillus-Related Diseases? Preliminary Insights.” *Journal of Cystic Fibrosis* 21(6):1084–85. doi: 10.1016/J.JCF.2022.09.007.

Chevalier, Sylvie, Emeline Bouffartigues, Josselin Bodilis, Olivier Maillot, Olivier Lesouhaitier, Marc G. J. Feuilloley, Nicole Orange, Alain Dufour, and Pierre Cornelis. 2017. “Structure, Function and Regulation of Pseudomonas Aeruginosa

Porins." *FEMS Microbiology Reviews* 41(5):698–722. doi: 10.1093/FEMSRE/FUX020.

Ciofu, Oana, and Tim Tolker-Nielsen. 2019. "Tolerance and Resistance of Pseudomonas Aeruginosa Biofilms to Antimicrobial Agents—How P. Aeruginosa Can Escape Antibiotics." *Frontiers in Microbiology* 10(MAY):913. doi: 10.3389/FMICB.2019.00913.

Comolli, James C., and Timothy J. Donohue. 2004. "Differences in Two Pseudomonas Aeruginosa Cbb3 Cytochrome Oxidases." *Molecular Microbiology*. doi: 10.1046/j.1365-2958.2003.03904.x.

Condon, C., D. Liveris, C. Squires, I. Schwartz, and C. L. Squires. 1995. "RRNA Operon Multiplicity in Escherichia Coli and the Physiological Implications of Rrn Inactivation." *Journal of Bacteriology* 177(14):4152–56. doi: 10.1128/JB.177.14.4152-4156.1995.

Cornelis, Pierre, and Jozef Dingemans. 2013a. "Pseudomonas Aeruginosa Adapts Its Iron Uptake Strategies in Function of the Type of Infections." *Frontiers in Cellular and Infection Microbiology* 4(NOV):71138. doi: 10.3389/FCIMB.2013.00075/BIBTEX.

Cornelis, Pierre, and Jozef Dingemans. 2013b. "Pseudomonas Aeruginosa Adapts Its Iron Uptake Strategies in Function of the Type of Infections." *Frontiers in Cellular and Infection Microbiology* 3(NOV). doi: 10.3389/FCIMB.2013.00075.

Cox, S. D., and J. L. Markham. 2007. “Susceptibility and Intrinsic Tolerance of Pseudomonas Aeruginosa to Selected Plant Volatile Compounds.” *Journal of Applied Microbiology* 103(4):930–36. doi: 10.1111/J.1365-2672.2007.03353.X.

Dahl, Ola E., Liv J. Garvik, and Torstein Lyberg. 1994. “Toxic Effects of Methylmethacrylate Monomer on Leukocytes and Endothelial Cells in Vitro.” *Acta Orthopaedica*. doi: 10.3109/17453679408995423.

Dai, Zongjie, and Jens Nielsen. 2015. “Advancing Metabolic Engineering through Systems Biology of Industrial Microorganisms.” *Current Opinion in Biotechnology* 36:8–15. doi: 10.1016/J.COPBIO.2015.08.006.

Darling, P., M. Chan, A. D. Cox, and P. A. Sokol. 1998. “Siderophore Production by Cystic Fibrosis Isolates of Burkholderia Cepacia.” *Infection and Immunity* 66(2):874. doi: 10.1128/IAI.66.2.874-877.1998.

Dean, Charles R., Melissa A. Visalli, Steven J. Projan, Phaik Eng Sum, and Patricia A. Bradford. 2003. “Efflux-Mediated Resistance to Tigecycline (GAR-936) in Pseudomonas Aeruginosa PAO1.” *Antimicrobial Agents and Chemotherapy*. doi: 10.1128/AAC.47.3.972-978.2003.

Van Delden, Christian, Malcolm G. P. Page, and Thilo Köhler. 2013. “Involvement of Fe Uptake Systems and AmpC β-Lactamase in Susceptibility to the Siderophore Monosulfactam BAL30072 in Pseudomonas Aeruginosa.” *Antimicrobial Agents and Chemotherapy* 57(5):2095. doi: 10.1128/AAC.02474-12.

Denoeud, France, Jean Marc Aury, Corinne da Silva, Benjamin Noel, Odile Rogier, Massimo Delledonne, Michele Morgante, Giorgio Valle, Patrick Wincker, Claude Scarpelli, Olivier Jaillon, and François Artiguenave. 2008. "Annotating Genomes with Massive-Scale RNA Sequencing." *Genome Biology* 9(12):1–12. doi: 10.1186/GB-2008-9-12-R175/TABLES/5.

Donaldson, Scott H., Joseph M. Pilewski, Matthias Griese, Jon Cooke, Lakshmi Viswanathan, Elizabeth Tullis, Jane C. Davies, Julie A. Lekstrom-Himes, and Linda T. Wang. 2018. "Tezacaftor/Ivacaftor in Subjects with Cystic Fibrosis and F508del/F508del-CFTR or F508del/G551D-CFTR." *American Journal of Respiratory and Critical Care Medicine* 197(2):214–24. doi: 10.1164/RCCM.201704-0717OC/SUPPL_FILE/DISCLOSURES.PDF.

Du, Dijun, Xuan Wang-Kan, Arthur Neuberger, Hendrik W. van Veen, Klaas M. Pos, Laura J. V. Piddock, and Ben F. Luisi. 2018. "Multidrug Efflux Pumps: Structure, Function and Regulation." *Nature Reviews Microbiology*.

Du, Fei, Yun Qi Liu, Ying Shuang Xu, Zi Jia Li, Yu Zhou Wang, Zi Xu Zhang, and Xiao Man Sun. 2021. "Regulating the T7 RNA Polymerase Expression in E. Coli BL21 (DE3) to Provide More Host Options for Recombinant Protein Production." *Microbial Cell Factories* 20(1). doi: 10.1186/S12934-021-01680-6.

Dumon-Seignovert, Laurence, Guillaume Cariot, and Laurent Vuillard. 2004. "The Toxicity of Recombinant Proteins in Escherichia Coli: A Comparison of Overexpression in BL21(DE3), C41(DE3), and C43(DE3)." *Protein Expression and Purification* 37(1):203–6. doi: 10.1016/J.PEP.2004.04.025.

Dunlop, Mary J., Zain Y. Dossani, Heather L. Szmidt, Hou Cheng Chu, Taek Soon Lee, Jay D. Keasling, Masood Z. Hadi, and Aindrila Mukhopadhyay. 2011. "Engineering Microbial Biofuel Tolerance and Export Using Efflux Pumps." *Molecular Systems Biology* 7:487. doi: 10.1038/MSB.2011.21.

Edmondson, Claire, and Jane C. Davies. 2016. "Current and Future Treatment Options for Cystic Fibrosis Lung Disease: Latest Evidence and Clinical Implications." *Therapeutic Advances in Chronic Disease* 7(3):170. doi: 10.1177/2040622316641352.

Elborn, J. Stuart. 2016. "Cystic Fibrosis." *The Lancet* 388(10059):2519–31. doi: 10.1016/S0140-6736(16)00576-6.

Elmerich, C., A. Kondorosi, and W. E. Newton. 1994. *Biological Nitrogen Fixation for the 21st Century*. Springer-Science+ Business Media, B.V.

Emerson, Julia, Margaret Rosenfeld, Sharon McNamara, Bonnie Ramsey, and Ronald L. Gibson. 2002. "Pseudomonas Aeruginosa and Other Predictors of Mortality and Morbidity in Young Children with Cystic Fibrosis." *Pediatric Pulmonology* 34(2):91–100. doi: 10.1002/PPUL.10127.

Errasti-Murugarren, Ekaitz, Paola Bartoccioni, and Manuel Palacín. 2021. "Membrane Protein Stabilization Strategies for Structural and Functional Studies." *Membranes* 11(2):1–17. doi: 10.3390/MEMBRANES11020155.

Fabre, Lucien, Abigail T. Ntreh, Amira Yazidi, Inga v. Leus, Jon W. Weeks, Sudipta Bhattacharyya, Jakob Ruickoldt, Isabelle Rouiller, Helen I. Zgurskaya, and Jurgen

Sygusch. 2021. “A ‘Drug Sweeping’ State of the TriABC Triclosan Efflux Pump from Pseudomonas Aeruginosa.” *Structure (London, England : 1993)* 29(3):261. doi: 10.1016/J.STR.2020.09.001.

Fernandes, Pedro, Bruno Sommer Ferreira, and Joaquim Manuel Sampaio Cabral. 2003. “Solvent Tolerance in Bacteria: Role of Efflux Pumps and Cross-Resistance with Antibiotics.” *International Journal of Antimicrobial Agents* 22(3):211–16. doi: 10.1016/S0924-8579(03)00209-7.

Fernandez-Escamilla, Ana Maria, Gregorio Fernandez-Ballester, Bertrand Morel, Salvador Casares-Atienza, and Juan Luis Ramos. 2015. “Molecular Binding Mechanism of TtgR Repressor to Antibiotics and Antimicrobials.” *PLoS ONE* 10(9). doi: 10.1371/JOURNAL.PONE.0138469.

Fernando, Dinesh M., and Ayush Kumar. 2013. “Resistance-Nodulation-Division Multidrug Efflux Pumps in Gram-Negative Bacteria: Role in Virulence.” *Antibiotics*.

Fibrosis Foundation, Cystic. n.d. “2020 Patient Registry Annual Data Report.”

Firoved, Aaron M., and Vojo Deretic. 2003. “Microarray Analysis of Global Gene Expression in Mucoid Pseudomonas Aeruginosa.” *Journal of Bacteriology* 185(3):1071–81. doi: 10.1128/JB.185.3.1071-1081.2003/ASSET/5B8EB09C-6800-4AB0-9059-42AB6B3BF341/ASSETS/GRAPHIC/JB0330891002.JPEG.

Firoved, Aaron M., Wojciech Ornatowski, and Vojo Deretic. 2004. “Microarray Analysis Reveals Induction of Lipoprotein Genes in Mucoid Pseudomonas

Aeruginosa: Implications for Inflammation in Cystic Fibrosis." *Infection and Immunity* 72(9):5012. doi: 10.1128/IAI.72.9.5012-5018.2004.

Fisher, Michael A., Sergey Boyarskiy, Masaki R. Yamada, Niwen Kong, Stefan Bauer, and Danielle Tullman-Ercek. 2014. "Enhancing Tolerance to Short-Chain Alcohols by Engineering the Escherichia Coli AcrB Efflux Pump to Secrete the Non-Native Substrate n-Butanol." *ACS Synthetic Biology* 3(1):30–40. doi: 10.1021/SB400065Q.

Fox, Brian G., and Paul G. Blommel. 2009. "Autoinduction of Protein Expression." *Current Protocols in Protein Science* CHAPTER 5(SUPPL. 56):Unit. doi: 10.1002/0471140864.PS0523S56.

Francis, Vanessa I., Emma C. Stevenson, and Steven L. Porter. 2017. "Two-Component Systems Required for Virulence in Pseudomonas Aeruginosa." *FEMS Microbiology Letters* 364(11):104. doi: 10.1093/FEMSLE/FNX104.

Frossard, Stephen M., Aftab A. Khan, Eric C. Warrick, Jonathan M. Gately, Andrew D. Hanson, Michael L. Oldham, David Avram Sanders, and Laszlo N. Csonka. 2012. "Identification of a Third Osmoprotectant Transport System, the OsmU System, in Salmonella Enterica." *Journal of Bacteriology* 194(15):3861. doi: 10.1128/JB.00495-12.

Fujisawa, S., T. Atsumi, and Y. Kadoma. 2008. "Cytotoxicity of Methyl Methacrylate (MMA) and Related Compounds and Their Interaction with

Dipalmitoylphosphatidylcholine (DPPC) Liposomes as a Model for Biomembranes." *Oral Diseases*. doi: 10.1111/j.1601-0825.2000.tb00116.x.

Gabillard-Lefort, Claudie, Michelle Casey, Arlene M. A. Glasgow, Fiona Boland, Orla Kerr, Elaine Marron, Anne Marie Lyons, Cedric Gunaratnam, Noel G. McElvaney, and Emer P. Reeves. 2022. "Trikafta Rescues CFTR and Lowers Monocyte P2X7R-Induced Inflammasome Activation in Cystic Fibrosis." *American Journal of Respiratory and Critical Care Medicine* 205(7):783–94. doi: 10.1164/RCCM.202106-1426OC/SUPPL_FILE/DISCLOSURES.PDF.

Gavrilescu, Maria, and Yusuf Chisti. 2005. "Biotechnology-a Sustainable Alternative for Chemical Industry." *Biotechnology Advances* 23(7–8):471–99. doi: 10.1016/J.BIOTECHADV.2005.03.004.

Ghanei, Hamed, Priyanka D. Abeyrathne, and Joseph S. Lam. 2007. "Biochemical Characterization of MsbA from Pseudomonas Aeruginosa." *Journal of Biological Chemistry* 282(37):26939–47. doi: 10.1074/JBC.M702952200.

Ghoul, Melanie, Stuart A. West, Helle Krogh Johansen, Søren Molin, Odile B. Harrison, Martin C. J. Maiden, John B. Bruce, and Ashleigh S. Griffin. 2015. "Bacteriocin-Mediated Competition in Cystic Fibrosis Lung Infections." *Proceedings. Biological Sciences* 282(1814). doi: 10.1098/RSPB.2015.0972.

Gibson, Ronald L., Jane L. Burns, and Bonnie W. Ramsey. 2012. "Pathophysiology and Management of Pulmonary Infections in Cystic Fibrosis."

Https://Doi.Org/10.1164/Rccm.200304-505SO 168(8):918–51. doi: 10.1164/RCCM.200304-505SO.

Goldstein, D. Yitzchak, and Michael Prystowsky. 2017. "Autosomal Recessive Inheritance: Cystic Fibrosis." *Academic Pathology* 4. doi: 10.1177/2374289517691769.

Goli, Hamid R., Mohammad R. Nahaei, Mohammad A. Rezaee, Alka Hasani, Hossein S. Kafil, Mohammad Aghazadeh, Mojtaba Nikbakht, and Younes Khalili. 2018. "Role of MexAB-OprM and MexXY-OprM Efflux Pumps and Class 1 Integrons in Resistance to Antibiotics in Burn and Intensive Care Unit Isolates of Pseudomonas Aeruginosa." *Journal of Infection and Public Health*. doi: 10.1016/j.jiph.2017.09.016.

González-Guerrero, Manuel, Daniel Raimunda, Xin Cheng, and José M. Argüello. 2010. "Distinct Functional Roles of Homologous Cu+ Efflux ATPases in Pseudomonas Aeruginosa." *Molecular Microbiology* 78(5):1246–58. doi: 10.1111/J.1365-2958.2010.07402.X.

Goossens, Sander N., Samantha L. Sampson, and Annelies Van Rie. 2021. "Mechanisms of Drug-Induced Tolerance in Mycobacterium Tuberculosis." *Clinical Microbiology Reviews* 34(1):1–21. doi: 10.1128/CMR.00141-20.

Gotoh, Naomasa, Nobuko Itoh, Hideto Tsujimoto, Jun ichi Yamagishi, Yoshihiro Oyamada, and Takeshi Nishino. 1994. "Isolation of OprM-Deficient Mutants of Pseudomonas Aeruginosa by Transposon Insertion Mutagenesis: Evidence of

Involvement in Multiple Antibiotic Resistance." *FEMS Microbiology Letters*. doi: 10.1111/j.1574-6968.1994.tb07179.x.

Graeber, Simon Y., Sébastien Boutin, Mark O. Wielpütz, Cornelia Joachim, Dario L. Frey, Sabine Wege, Olaf Sommerburg, Hans Ulrich Kauczor, Mirjam Stahl, Alexander H. Dalpke, and Marcus A. Mall. 2021. "Effects of Lumacaftor-Ivacaftor on Lung Clearance Index, Magnetic Resonance Imaging, and Airway Microbiome in Phe508del Homozygous Patients with Cystic Fibrosis." *Annals of the American Thoracic Society* 18(6):971–80. doi: 10.1513/ANNALSATS.202008-1054OC/SUPPL_FILE/DISCLOSURES.PDF.

Grand View Research. 2019. *Polymethyl Methacrylate Market Size, Share & Trends Analysis Report By Product Type*.

Grosso-Becerra, María Victoria, Christian Santos-Medellín, Abigail González-Valdez, José Luis Méndez, Gabriela Delgado, Rosario Morales-Espinosa, Luis Servín-González, Luis David Alcaraz, and Gloria Soberón-Chávez. 2014. "Pseudomonas Aeruginosa Clinical and Environmental Isolates Constitute a Single Population with High Phenotypic Diversity." *BMC Genomics*. doi: 10.1186/1471-2164-15-318.

Guan, L., and T. Nakae. 2001. "Identification of Essential Charged Residues in Transmembrane Segments of the Multidrug Transporter MexB of Pseudomonas Aeruginosa." *Journal of Bacteriology*. doi: 10.1128/JB.183.5.1734-1739.2001.

Gunasekera, Thusitha S., Loryn L. Bowen, Carol E. Zhou, Susan C. Howard-Byerly, William S. Foley, Richard C. Striebich, Larry C. Dugan, and Oscar N. Ruiz. 2017. "Transcriptomic Analyses Elucidate Adaptive Differences of Closely Related Strains of Pseudomonas Aeruginosa in Fuel." *Applied and Environmental Microbiology* 83(10). doi: 10.1128/AEM.03249-16.

Gupta, Jaya A., Sagar Thapa, Madhulika Verma, Ritu Som, and Krishna Jyoti Mukherjee. 2020. "Genomics and Transcriptomics Analysis Reveals the Mechanism of Isobutanol Tolerance of a Laboratory Evolved Lactococcus Lactis Strain." *Scientific Reports* 10(1):10850. doi: 10.1038/S41598-020-67635-W.

Gyorfy, Zsuzsanna, Gabor Draskovits, Viktor Vernyik, Frederick F. Blattner, Tamas Gaal, and Gyorgy Posfai. 2015. "Engineered Ribosomal RNA Operon Copy-Number Variants of E. Coli Reveal the Evolutionary Trade-Offs Shaping RRNA Operon Number." *Nucleic Acids Research* 43(3):1783–94. doi: 10.1093/NAR/GKV040.

Hamada, Masakaze, Masanori Toyofuku, Tomoki Miyano, and Nobuhiko Nomura. 2014. "Cbb3-Type Cytochrome c Oxidases, Aerobic Respiratory Enzymes, Impact the Anaerobic Life of Pseudomonas Aeruginosa PAO1." *Journal of Bacteriology* 196(22):3881–89. doi: 10.1128/JB.01978-14/SUPPL_FILE/ZJB999093361SO1.PDF.

Hancock, Robert E. W., and David P. Speert. 2000. "Antibiotic Resistance in Pseudomonas Aeruginosa: Mechanisms and Impact on Treatment." *Drug Resistance Updates*. doi: 10.1054/drup.2000.0152.

Hasan, Chowdhury M., Sian Pottenger, Angharad E. Green, Adrienne A. Cox, Jack S. White, Trevor Jones, Craig Winstanley, Aras Kadioglu, Megan H. Wright, Daniel R. Neill, and Joanne L. Fothergill. 2022. “Pseudomonas Aeruginosa Utilizes the Host-Derived Polyamine Spermidine to Facilitate Antimicrobial Tolerance.” *JCI Insight* 7(22). doi: 10.1172/JCI.INSIGHT.158879.

Hassani, Bahia Khalfaoui, Chantal Astier, Wolfgang Nitschke, and Soufian Ouchane. 2010. “CtpA, a Copper-Translocating P-Type ATPase Involved in the Biogenesis of Multiple Copper-Requiring Enzymes.” *The Journal of Biological Chemistry* 285(25):19330. doi: 10.1074/JBC.M110.116020.

Hill, B. C. 1991. “The Reaction of the Electrostatic Cytochrome C-Cytochrome Oxidase Complex with Oxygen.” *Journal of Biological Chemistry*.

Hirakata, Yoichi, Ramakrishnan Srikumar, Keith Poole, Naomasa Gotoh, Takashi Suematsu, Shigeru Kohno, Shimeru Kamihira, Robert E. W. Hancock, and David P. Speert. 2002. “Multidrug Efflux Systems Play an Important Role in the Invasiveness of Pseudomonas Aeruginosa.” *The Journal of Experimental Medicine* 196(1):109. doi: 10.1084/JEM.20020005.

Hoffland, Ellis, Johanna Hakulinen, and Johan A. Van Pelt. 1996. “Comparison of Systemic Resistance Induced by Avirulent and Nonpathogenic Pseudomonas Species.” *Phytopathology*. doi: 10.1094/Phyto-86-757.

Hofmann, Lukas, Melanie Hirsch, and Sharon Ruthstein. 2021. “Advances in Understanding of the Copper Homeostasis in Pseudomonas Aeruginosa.”

International Journal of Molecular Sciences 22(4):1–23. doi: 10.3390/IJMS22042050.

Holt, Robert A., and Steven J. M. Jones. 2008. "The New Paradigm of Flow Cell Sequencing." *Genome Res* 18(6):839–46. doi: 10.1101/gr.073262.107.

Hughes, D. 2013. "Elongation Factors: Translation." *Brenner's Encyclopedia of Genetics: Second Edition* 466–68. doi: 10.1016/B978-0-12-374984-0.00468-X.

Hussey, J., C. Evans, R. Davies, N. Gilday, F. King, J. L. Whitehouse, N. Patel, and L. Jones. 2023. "P354 West Midlands Adult Cystic Fibrosis Centre Experience of the Effects of Kaftrio® on Patients within the Lung Transplant Programme." *Journal of Cystic Fibrosis* 22:S173. doi: 10.1016/s1569-1993(23)00724-5.

Huszczynski, Steven M., Joseph S. Lam, and Cezar M. Khursigara. 2020. "The Role of Pseudomonas Aeruginosa Lipopolysaccharide in Bacterial Pathogenesis and Physiology." *Pathogens* 9(1). doi: 10.3390/PATHOGENS9010006.

Hutchison, Clyde A., Ray Yuan Chuang, Vladimir N. Noskov, Nacyra Assad-Garcia, Thomas J. Deerinck, Mark H. Ellisman, John Gill, Krishna Kannan, Bogumil J. Karas, Li Ma, James F. Pelletier, Zhi Qing Qi, R. Alexander Richter, Elizabeth A. Strychalski, Lijie Sun, Yo Suzuki, Billyana Tsvetanova, Kim S. Wise, Hamilton O. Smith, John I. Glass, Chuck Merryman, Daniel G. Gibson, and J. Craig Venter. 2016. "Design and Synthesis of a Minimal Bacterial Genome." *Science* 351(6280). doi: 10.1126/SCIENCE.AAD6253/SUPPL_FILE/AAD6253-HUTCHISON-SM.PDF.

Ikehata, Yuuki, and Noriyuki Doukyu. 2022. “Improving the Organic Solvent Tolerance of Escherichia Coli with Vanillin, and the Involvement of an AcrAB-TolC Efflux Pump in Vanillin Tolerance.” *Journal of Bioscience and Bioengineering* 133(4):347–52. doi: 10.1016/J.JBIOSC.2021.12.015.

Ingenza Ltd. n.d. “Fermentation Trials for BMA Bioproduction Using P. Putida .”

International, Lucite. 2020. “Our Heritage.” Retrieved March 27, 2020 (https://www.luciteinternational.com/about-us-our-heritage-22/).

Irie, Yasuhiko, Melissa Starkey, Adrianne N. Edwards, Daniel J. Wozniak, Tony Romeo, and Matthew R. Parsek. 2010. “Pseudomonas Aeruginosa Biofilm Matrix Polysaccharide Psl Is Regulated Transcriptionally by RpoS and Post-Transcriptionally by RsmA.” *Molecular Microbiology* 78(1):158. doi: 10.1111/J.1365-2958.2010.07320.X.

Isken, Sonja, and Jan A. M. De Bont. 1996. “Active Efflux of Toluene in a Solvent-Resistant Bacterium.” *Journal of Bacteriology*. doi: 10.1128/jb.178.20.6056-6058.1996.

Jeannot, Katy, Sylvie Elsen, Thilo Köhler, Ina Attree, Christian van Delden, and Patrick Plésiat. 2008. “Resistance and Virulence of Pseudomonas Aeruginosa Clinical Strains Overproducing the MexCD-OprJ Efflux Pump.” *Antimicrobial Agents and Chemotherapy* 52(7):2455–62. doi: 10.1128/AAC.01107-07.

Jiang, Qian, Jiashun Chen, Chengbo Yang, Yulong Yin, Kang Yao, and Deguang Song. 2019. “Quorum Sensing: A Prospective Therapeutic Target for Bacterial Diseases.” *BioMed Research International* 2019. doi: 10.1155/2019/2015978.

Jones, Christopher M., Néstor J. Hernández Lozada, and Brian F. Pfleger. 2015. “Efflux Systems in Bacteria and Their Metabolic Engineering Applications.” *Applied Microbiology and Biotechnology* 99(22):9381. doi: 10.1007/S00253-015-6963-9.

Jones, Jane T., Kaesi A. Morelli, Elisa M. Vesely, Charles T. S. Puerner, Chetan K. Pavuluri, Brandon S. Ross, Norman van Rhijn, Michael J. Bromley, and Robert A. Cramer. 2023. “The Cystic Fibrosis Treatment, Trikafta, Affects Growth, Viability, and Cell Wall of Aspergillus Fumigatus Biofilms.” *BioRxiv* 2023.06.20.545692. doi: 10.1101/2023.06.20.545692.

Kaihami, Gilberto Hideo, Leandro Carvalho Dantas Breda, José Roberto Fogaça de Almeida, Thays de Oliveira Pereira, Gianlucca Gonçalves Nicastro, Ana Laura Boechat, Sandro Rogério de Almeida, and Regina Lúcia Baldini. 2017. “The Atypical Response Regulator AtvR Is a New Player in Pseudomonas Aeruginosa Response to Hypoxia and Virulence.” *Infection and Immunity* 85(8). doi: 10.1128/IAI.00207-17.

Kang, Donghoon, Daniel R. Kirienkoa, Phillip Webster, Alfred L. Fisher, and Natalia V. Kirienko. 2018. “Pyoverdine, a Siderophore from Pseudomonas Aeruginosa, Translocates into C. Elegans, Removes Iron, and Activates a Distinct Host Response.” *Virulence* 9(1):804. doi: 10.1080/21505594.2018.1449508.

Kang, Donghoon, Alexey V. Revtovich, Qingquan Chen, Kush N. Shah, Carolyn L. Cannon, and Natalia V. Kirienko. 2019. “Pyoverdine-Dependent Virulence of Pseudomonas Aeruginosa Isolates From Cystic Fibrosis Patients.” *Frontiers in Microbiology* 10. doi: 10.3389/FMICB.2019.02048/FULL.

Katz, Leonard, Yvonne Y. Chen, Ramon Gonzalez, Todd C. Peterson, Huimin Zhao, and Richard H. Baltz. 2018. “Synthetic Biology Advances and Applications in the Biotechnology Industry: A Perspective.” *Journal of Industrial Microbiology and Biotechnology*. doi: 10.1007/s10295-018-2056-y.

Keyte, Rebecca, Sophia Kauser, Michail Mantzios, and Helen Egan. 2022. “The Psychological Implications and Health Risks of Cystic Fibrosis Pre- and Post- CFTR Modulator Therapy.” *Chronic Illness*. doi: 10.1177/17423953221099042.

Kieboom, Jasper, Jonathan J. Dennis, Gerben J. Zylstra, and Jan A. M. De Bont. 1998. “Active Efflux of Organic Solvents by Pseudomonas Putida S12 Is Induced by Solvents.” *Journal of Bacteriology* 180(24):6769. doi: 10.1128/JB.180.24.6769-6772.1998.

De Kievit, T. R. 2009. “Quorum Sensing in Pseudomonas Aeruginosa Biofilms.” *Environmental Microbiology* 11(2):279–88. doi: 10.1111/J.1462-2920.2008.01792.X.

Kim, Daehwan, Ben Langmead, and Steven L. Salzberg. 2015. “HISAT: A Fast Spliced Aligner with Low Memory Requirements.” *Nature Methods 2015 12:4* 12(4):357–60. doi: 10.1038/nmeth.3317.

Kim, Hyun Soo, Na Rae Kim, Jungwoo Yang, and Wonja Choi. 2011. “Identification of Novel Genes Responsible for Ethanol and/or Thermotolerance by Transposon Mutagenesis in Saccharomyces Cerevisiae.” *Applied Microbiology and Biotechnology* 91(4):1159–72. doi: 10.1007/S00253-011-3298-Z.

Kim, Jee Hyun, Kathryn M. O’Brien, Ritu Sharma, Helena I. M. Boshoff, German Rehren, Sumit Chakraborty, Joshua B. Wallach, Mercedes Monteleone, Daniel J. Wilson, Courtney C. Aldrich, Clifton E. Barry, Kyu Y. Rhee, Sabine Ehrt, and Dirk Schnappinger. 2013. “A Genetic Strategy to Identify Targets for the Development of Drugs That Prevent Bacterial Persistence.” *Proceedings of the National Academy of Sciences of the United States of America* 110(47):19095–100. doi: 10.1073/PNAS.1315860110/SUPPL_FILE/PNAS.201315860SI.PDF.

Köhler, Thilo, Mehri Michéa-Hamzehpour, Uta Henze, Naomasa Gotoh, Lasta Kocjancic Curty, and Jean Claude Pechère. 1997. “Characterization of MexE–MexF–OprN, a Positively Regulated Multidrug Efflux System of Pseudomonas Aeruginosa.” *Molecular Microbiology* 23(2):345–54. doi: 10.1046/J.1365-2958.1997.2281594.X.

Konings, Anna F., Lois W. Martin, Katrina J. Sharples, Louise F. Roddam, Roger Latham, David W. Reid, and Iain L. Lamont. 2013. “Pseudomonas Aeruginosa Uses Multiple Pathways to Acquire Iron during Chronic Infection in Cystic Fibrosis Lungs.” *Infection and Immunity* 81(8):2697–2704. doi: 10.1128/IAI.00418-13/SUPPL_FILE/ZII999090219SO1.PDF.

Kotov, Vadim, Kim Bartels, Katharina Veith, Inokentijs Josts, Udaya K. Tiruttani Subhramanyam, Christian Günther, Jörg Labahn, Thomas C. Marlovits, Isabel Moraes, Henning Tidow, Christian Löw, and Maria M. Garcia-Alai. 2019. "High-Throughput Stability Screening for Detergent-Solubilized Membrane Proteins." *Scientific Reports 2019 9:1* 9(1):1–19. doi: 10.1038/s41598-019-46686-8.

Kwon, Soon Kyeong, Seong Keun Kim, Dae Hee Lee, and Jihyun F. Kim. 2015. "Comparative Genomics and Experimental Evolution of Escherichia Coli BL21(DE3) Strains Reveal the Landscape of Toxicity Escape from Membrane Protein Overproduction." *Scientific Reports 2015 5:1* 5(1):1–13. doi: 10.1038/srep16076.

Lamont, Iain L., Paul A. Beare, Urs Ochsner, Adriana I. Vasil, and Michael L. Vasil. 2002. "Siderophore-Mediated Signaling Regulates Virulence Factor Production in Pseudomonas Aeruginosa." *Proceedings of the National Academy of Sciences of the United States of America* 99(10):7072. doi: 10.1073/PNAS.092016999.

Larsen, P. I., L. K. Sydnes, B. Landfald, and A. R. Strøm. 1987. "Osmoregulation in Escherichia Coli by Accumulation of Organic Osmolytes: Betaines, Glutamic Acid, and Trehalose." *Archives of Microbiology* 147(1):1–7. doi: 10.1007/BF00492896.

Lee, Angela, Weimin Mao, Mark S. Warren, Anita Mistry, Kazuki Hoshino, Ryo Okumura, Hiroko Ishida, and Olga Lomovskaya. 2000. "Interplay between Efflux Pumps May Provide Either Additive or Multiplicative Effects on Drug Resistance." *Journal of Bacteriology* 182(11):3142. doi: 10.1128/JB.182.11.3142-3150.2000.

Lemonds, Andrew. n.d. “WO2014051971A1 - Process for Producing Mma and/or Maa from Acetone Cyanohydrin and Sulfuric Acid - Google Patents.” Retrieved August 2, 2022 (https://patents.google.com/patent/WO2014051971A1/en).

Lepissier, Agathe, Anne Sophie Bonnel, Nathalie Wizla, Laurence Weiss, Marie Mittaine, Katia Bessaci, Eitan Kerem, Véronique Houdouin, Philippe Reix, Christophe Marguet, and Isabelle Sermet-Gaudelu. 2023. “Moving the Dial on Airway Inflammation in Response to Trikafta in Adolescents with Cystic Fibrosis.” *American Journal of Respiratory and Critical Care Medicine* 207(6):792–95. doi: 10.1164/RCCM.202210-1938LE/SUPPL_FILE/DISCLOSURES.PDF.

Létoffé, Sylvie, Yongzheng Wu, Sophie E. Darch, Christophe Beloin, Marvin Whiteley, Lhousseine Touqui, and Jean Marc Ghigo. 2022. “Pseudomonas Aeruginosa Production of Hydrogen Cyanide Leads to Airborne Control of Staphylococcus Aureus Growth in Biofilm and in Vivo Lung Environments.” *MBio* 13(5). doi: 10.1128/MBIO.02154-22/SUPPL_FILE/MBIO.02154-22-S0007.PDF.

Li, X. Z., D. M. Livermore, and H. Nikaido. 1994. “Role of Efflux Pump(s) in Intrinsic Resistance of Pseudomonas Aeruginosa: Resistance to Tetracycline, Chloramphenicol, and Norfloxacin.” *Antimicrobial Agents and Chemotherapy*. doi: 10.1128/AAC.38.8.1732.

Li, Xian Zhi, Patrick Plésiat, and Hiroshi Nikaido. 2015. “The Challenge of Efflux-Mediated Antibiotic Resistance in Gram-Negative Bacteria.” *Clinical Microbiology Reviews*. doi: 10.1128/CMR.00117-14.

Li, Xian Zhi, Keith Poole, and Hiroshi Nikaido. 2003. “Contributions of MexAB-OprM and an EmrE Homolog to Intrinsic Resistance of Pseudomonas Aeruginosa to Aminoglycosides and Dyes.” *Antimicrobial Agents and Chemotherapy* 47(1):27–33. doi: 10.1128/AAC.47.1.27-33.2003/ASSET/90431A1E-1EB9-4EA3-9A23-7DCDCED86FA8/ASSETS/GRAPHIC/AC0130651004.JPEG.

Li, Xian Zhi, Li Zhang, and Keith Poole. 1998a. “Role of the Multidrug Efflux Systems of Pseudomonas Aeruginosa in Organic Solvent Tolerance.” *Journal of Bacteriology* 180(11):2987–91. doi: 10.1128/JB.180.11.2987-2991.1998/ASSET/B4A90E4C-4B03-4028-A9A3-CDA6F8FDA5EF/ASSETS/GRAPHIC/JB1181579003.JPEG.

Li, Xian Zhi, Li Zhang, and Keith Poole. 1998b. “Role of the Multidrug Efflux Systems of Pseudomonas Aeruginosa in Organic Solvent Tolerance.” *Journal of Bacteriology* 180(11):2987–91. doi: 10.1128/JB.180.11.2987-2991.1998.

Li, Xian Zhi, Li Zhang, and Keith Poole. 1998c. “Role of the Multidrug Efflux Systems of Pseudomonas Aeruginosa in Organic Solvent Tolerance.” *Journal of Bacteriology* 180(11):2987–91. doi: 10.1128/JB.180.11.2987-2991.1998.

Liberati, Nicole T., Jonathan M. Urbach, Sachiko Miyata, Daniel G. Lee, Eliana Drenkard, Gang Wu, Jacinto Villanueva, Tao Wei, and Frederick M. Ausubel. 2006. “An Ordered, Nonredundant Library of Pseudomonas Aeruginosa Strain PA14 Transposon Insertion Mutants.” *Proceedings of the National Academy of Sciences of the United States of America* 103(8):2833–38. doi: 10.1073/pnas.0511100103.

Lineback, Caitlinn B., Carine A. Nkemngong, Sophie Tongyu Wu, Xiaobao Li, Peter J. Teska, and Haley F. Oliver. 2018. “Hydrogen Peroxide and Sodium Hypochlorite Disinfectants Are More Effective against Staphylococcus Aureus and Pseudomonas Aeruginosa Biofilms than Quaternary Ammonium Compounds.” *Antimicrobial Resistance and Infection Control*. doi: 10.1186/s13756-018-0447-5.

Livermore, D. M. 2002. “Multiple Mechanisms of Antimicrobial Resistance in Pseudomonas Aeruginosa: Our Worst Nightmare?” *Clinical Infectious Diseases*. doi: 10.1086/338782.

Llanes, Catherine, Didier Hocquet, Christelle Vogne, Dounia Benali-Baitich, Catherine Neuwirth, and Patrick Plésiat. 2004. “Clinical Strains of Pseudomonas Aeruginosa Overproducing MexAB-OprM and MexXY Efflux Pumps Simultaneously.” *Antimicrobial Agents and Chemotherapy* 48(5):1797. doi: 10.1128/AAC.48.5.1797-1802.2004.

Loeschcke, Anita, and Stephan Thies. 2015. “Pseudomonas Putida—a Versatile Host for the Production of Natural Products.” *Applied Microbiology and Biotechnology*.

López, Cesar A., Timothy Travers, Klaas M. Pos, Helen I. Zgurskaya, and S. Gnanakaran. 2017. “Dynamics of Intact MexAB-OprM Efflux Pump: Focusing on the MexA-OprM Interface.” *Scientific Reports*. doi: 10.1038/s41598-017-16497-w.

López-Causapé, Carla, Gabriel Cabot, Ester del Barrio-Tofiño, and Antonio Oliver. 2018. “The Versatile Mutational Resistome of Pseudomonas Aeruginosa.” *Frontiers in Microbiology* 9(APR). doi: 10.3389/FMICB.2018.00685.

Lorusso, Andre Bittencourt, João Antônio Carrara, Carolina Deuttner Neumann Barroso, Felipe Francisco Tuon, and Helisson Faoro. 2022. “Role of Efflux Pumps on Antimicrobial Resistance in Pseudomonas Aeruginosa.” *International Journal of Molecular Sciences* 23(24). doi: 10.3390/IJMS232415779.

Losada, Patricia Moran, Philippe Chouvarine, Marie Dorda, Silke Hedtfeld, Samira Mielke, Angela Schulz, Lutz Wiehlmann, and Burkhard Tümmler. 2016. “The Cystic Fibrosis Lower Airways Microbial Metagenome.” *ERJ Open Research* 2(2). doi: 10.1183/23120541.00096-2015.

Love, Michael I., Wolfgang Huber, and Simon Anders. 2014. “Moderated Estimation of Fold Change and Dispersion for RNA-Seq Data with DESeq2.” *Genome Biology* 15(12):1–21. doi: 10.1186/S13059-014-0550-8/FIGURES/9.

Lutz, Jonathan K., and Jiyoung Lee. 2011. “Prevalence and Antimicrobial-Resistance of Pseudomonas Aeruginosa in Swimming Pools and Hot Tubs.” *International Journal of Environmental Research and Public Health*. doi: 10.3390/ijerph8020554.

Lyczak, Jeffrey B., Carolyn L. Cannon, and Gerald B. Pier. 2002. “Lung Infections Associated with Cystic Fibrosis.” *Clinical Microbiology Reviews* 15(2):194. doi: 10.1128/CMR.15.2.194-222.2002.

Machas, Michael, Gavin Kurgan, Omar A. Abed, Alyssa Shapiro, Xuan Wang, and David Nielsen. 2021. “Characterizing Escherichia Coli’s Transcriptional Response to Different Styrene Exposure Modes Reveals Novel Toxicity and Tolerance Insights.” *Journal of Industrial Microbiology & Biotechnology* 48(1–2):19. doi: 10.1093/JIMB/KUAB019.

Majiduddin, Fahd K., Isabel C. Materon, and Timothy G. Palzkill. 2002. “Molecular Analysis of Beta-Lactamase Structure and Function.” *International Journal of Medical Microbiology*. doi: 10.1078/1438-4221-00198.

Maldonado, Rita F., Isabel Sá-Correia, and Miguel A. Valvano. 2016. “Lipopolysaccharide Modification in Gram-Negative Bacteria during Chronic Infection” edited by C. Whitfield. *FEMS Microbiology Reviews* 40(4):480–93. doi: 10.1093/FEMSRE/FUW007.

Malhotra, Sankalp, Don Hayes, and Daniel J. Wozniak. 2019. “Cystic Fibrosis and Pseudomonas Aeruginosa: The Host-Microbe Interface.” *Clinical Microbiology Reviews* 32(3). doi: 10.1128/CMR.00138-18/ASSET/75EE1046-213B-4513-8CA1-46ED66543D23/ASSETS/GRAPHIC/CMR.00138-18-F0007.JPEG.

Manoj, Kelath Murali, Surjith Ramasamy, Abhinav Parashar, Daniel Andrew Gideon, Vidhu Soman, Vivian David Jacob, and Kannan Pakshirajan. 2020. “Acute Toxicity of Cyanide in Aerobic Respiration: Theoretical and Experimental Support for Murburn Explanation.” *Biomolecular Concepts* 11(1):32–56. doi: 10.1515/BMC-2020-0004.

Mao, Weimin, Mark S. Warren, Deborah S. Black, Takahumi Satou, Takeshi Murata, Takeshi Nishino, Naomasa Gotoh, and Olga Lomovskaya. 2002. “On the Mechanism of Substrate Specificity by Resistance Nodulation Division (RND)-Type Multidrug Resistance Pumps: The Large Periplasmic Loops of MexD from Pseudomonas Aeruginosa Are Involved in Substrate Recognition.” *Molecular Microbiology* 46(3):889–901. doi: 10.1046/J.1365-2958.2002.03223.X.

Marcos, Veronica, Zhe Zhou-Suckow, Ali Önder Yildirim, Alexander Bohla, Andreas Hector, Ljubomir Vitkov, Wolf Dietrich Krautgartner, Walter Stoiber, Matthias Griese, Oliver Eickelberg, Marcus A. Mall, and Dominik Hartl. 2015. “Free DNA in Cystic Fibrosis Airway Fluids Correlates with Airflow Obstruction.” *Mediators of Inflammation* 2015. doi: 10.1155/2015/408935.

Marisch, Karoline, Karl Bayer, Monika Cserjan-Puschmann, Markus Luchner, and Gerald Striedner. 2013. “Evaluation of Three Industrial Escherichia Coli Strains in Fed-Batch Cultivations during High-Level SOD Protein Production.” *Microbial Cell Factories*. doi: 10.1186/1475-2859-12-58.

Martin, Lois W., David W. Reid, Katrina J. Sharples, and Iain L. Lamont. 2011. “Pseudomonas Siderophores in the Sputum of Patients with Cystic Fibrosis.” *BioMetals* 24(6):1059–67. doi: 10.1007/S10534-011-9464-Z/METRICS.

Martins, Valdo R., Carlos J. B. Freitas, A. Rita Castro, Rita M. Silva, Eduardo J. Gudiña, João C. Sequeira, Andreia F. Salvador, M. Alcina Pereira, and Ana J. Cavaleiro. 2021. “Corksorb Enhances Alkane Degradation by Hydrocarbonoclastic Bacteria.” *Frontiers in Microbiology* 12. doi: 10.3389/FMICB.2021.618270/FULL.

Masuda, N., E. Sakagawa, S. Ohya, N. Gotoh, H. Tsujimoto, and T. Nishino. 2000. "Substrate Specificities of MexAB-OprM, MexCD-OprJ, and MexXY-OprM Efflux Pumps in Pseudomonas Aeruginosa." *Antimicrobial Agents and Chemotherapy* 44(12):3322. doi: 10.1128/AAC.44.12.3322-3327.2000.

Mathews, C., and S. Kirby. 2022. "The Experiences of Taking Kaftrio® for Cystic Fibrosis (CF)." *Journal of Cystic Fibrosis* 21:S135–S135. doi: 10.1016/S1569-1993(22)00573-2.

Maurice, Nicholas M., Brahmchetna Bedi, and Ruxana T. Sadikot. 2018. "Pseudomonas Aeruginosa Biofilms: Host Response and Clinical Implications in Lung Infections." *American Journal of Respiratory Cell and Molecular Biology*.

McColley, Susanna A., Stacey L. Martiniano, Clement L. Ren, Marci K. Sontag, Karen Rychlik, Lauren Balmert, Alexander Elbert, Runyu Wu, and Philip M. Farrell. 2022. "Disparities in First Evaluation of Infants with Cystic Fibrosis since Implementation of Newborn Screening." *Journal of Cystic Fibrosis*. doi: 10.1016/J.JCF.2022.07.010.

Mcdougald, Diane, Janosch Klebensberger, Tim Tolker-Nielsen, Jeremy S. Webb, Tim Conibear, Scott A. Rice, Sylvia M. Kirov, Carsten Matz, and Staffan Kjelleberg. 2008. "Pseudomonas Aeruginosa: A Model for Biofilm Formation." *Pseudomonas: Model Organism, Pathogen, Cell Factory* 215–53. doi: 10.1002/9783527622009.CH9.

Michel-Briand, Yvon, and Christine Baysse. 2002. “The Pyocins of Pseudomonas Aeruginosa.” *Biochimie* 84(5–6):499–510. doi: 10.1016/S0300-9084(02)01422-0.

Mima, Takehiko, Swati Joshi, Margarita Gomez-Escalada, and Herbert P. Schweizer. 2007. “Identification and Characterization of TriABC-OpmH, a Triclosan Efflux Pump of Pseudomonas Aeruginosa Requiring Two Membrane Fusion Proteins.” *Journal of Bacteriology* 189(21):7600. doi: 10.1128/JB.00850-07.

Minagawa, Shu, Hiroyuki Inami, Tomohisa Kato, Shinji Sawada, Tatsuya Yasuki, Shinichi Miyairi, Manabu Horikawa, Jun Okuda, and Naomasa Gotoh. 2012. “RND Type Efflux Pump System MexAB-OprM of Pseudomonas Aeruginosa Selects Bacterial Languages, 3-Oxo-Acyl-Homoserine Lactones, for Cell-to-Cell Communication.” *BMC Microbiology*. doi: 10.1186/1471-2180-12-70.

Miroux, Bruno, and John E. Walker. 1996. “Over-Production of Proteins in Escherichia Coli: Mutant Hosts That Allow Synthesis of Some Membrane Proteins and Globular Proteins at High Levels.” *Journal of Molecular Biology* 260(3):289–98. doi: 10.1006/JMBI.1996.0399.

Mitsubishi Chemcial Corporation UK. 2020. “PMMA Key Benefits.”

Mohedano, Marta Tous, Oliver Konzock, and Yun Chen. 2022. “Strategies to Increase Tolerance and Robustness of Industrial Microorganisms.” *Synthetic and Systems Biotechnology* 7(1):533. doi: 10.1016/J.SYNBIO.2021.12.009.

Mokhonov, Vladislav, Ekaterina Mokhonova, Eisaku Yoshihara, Ryoji Masui, Miyo Sakai, Hiroyuki Akama, and Taiji Nakae. 2005. “Multidrug Transporter MexB of Pseudomonas Aeruginosa: Overexpression, Purification, and Initial Structural Characterization.” *Protein Expression and Purification* 40(1):91–100. doi: 10.1016/J.PEP.2004.10.002.

Molina-Santiago, Carlos, Zulema Udaondo, María Gómez-Lozano, Soren Molin, and Juan Luis Ramos. 2017. “Global Transcriptional Response of Solvent-Sensitive and Solvent-Tolerant Pseudomonas Putida Strains Exposed to Toluene.” *Environmental Microbiology* 19(2):645–58. doi: 10.1111/1462-2920.13585.

Molloy, Mark P. 2008. “Isolation of Bacterial Cell Membranes Proteins Using Carbonate Extraction.” *Methods in Molecular Biology (Clifton, N.J.)* 424:397–401. doi: 10.1007/978-1-60327-064-9_30/FIGURES/30_1_978-1-60327-064-9.

Montemari, Anna Lisa, Valeria Marzano, Nour Essa, Stefano Levi Mortera, Martina Rossitto, Simone Gardini, Laura Selan, Gianluca Vrenna, Andrea Onetti Muda, Lorenza Putignani, and Ersilia Vita Fiscarelli. 2022. “A Shaving Proteomic Approach to Unveil Surface Proteins Modulation of Multi-Drug Resistant Pseudomonas Aeruginosa Strains Isolated From Cystic Fibrosis Patients.” *Frontiers in Medicine* 9:818669. doi: 10.3389/FMED.2022.818669.

Moore, Joseph D., Joseph P. Gerdt, Nora R. Eibergen, and Helen E. Blackwell. 2014. “Active Efflux Influences the Potency of Quorum Sensing Inhibitors in Pseudomonas Aeruginosa.” *ChemBioChem*. doi: 10.1002/cbic.201300701.

Moore, Stephanie M., Stephanie M. Hess, and James W. Jorgenson. 2016. “Extraction, Enrichment, Solubilization, and Digestion Techniques for Membrane Proteomics.” *Journal of Proteome Research* 15(4):1243. doi: 10.1021/ACS.JPROTEOME.5B01122.

Morgan, Sarah J., Soyeon I. Lippman, Gilbert E. Bautista, Joe J. Harrison, Christopher L. Harding, Larry A. Gallagher, Ann Chee Cheng, Richard Siehnel, Sumedha Ravishankar, Marcia L. Usui, John E. Olerud, Philip Fleckman, Randall D. Wolcott, Colin Manoil, and Pradeep K. Singh. 2019. “Bacterial Fitness in Chronic Wounds Appears to Be Mediated by the Capacity for High-Density Growth, Not Virulence or Biofilm Functions.” *PLoS Pathogens* 15(3). doi: 10.1371/JOURNAL.PPAT.1007511.

Moskowitz, Samuel M., and Robert K. Ernst. 2010. “The Role of Pseudomonas Lipopolysaccharide in Cystic Fibrosis Airway Infection.” *Sub-Cellular Biochemistry* 53:241. doi: 10.1007/978-90-481-9078-2_11.

Mosqueda, Gilberto, María Isabel Ramos-González, and Juan L. Ramos. 1999. “Toluene Metabolism by the Solvent-Tolerant Pseudomonas Putida DOT-T1 Strain, and Its Role in Solvent Impermeabilization.” *Gene* 232(1):69–76. doi: 10.1016/S0378-1119(99)00113-4.

Mossialos, Dimitris, and Grigoris D. Amoutzias. 2009. “Role of Siderophores in Cystic Fibrosis Pathogenesis: Foes or Friends?” *International Journal of Medical Microbiology : IJMM* 299(2):87–98. doi: 10.1016/J.IJMM.2008.06.008.

Murata, Takeshi, Misato Kuwagaki, Tomoko Shin, Naomasa Gotoh, and Takeshi Nishino. 2002. “The Substrate Specificity of Tripartite Efflux Systems of Pseudomonas Aeruginosa Is Determined by the RND Component.” *Biochemical and Biophysical Research Communications* 299(2):247–51. doi: 10.1016/S0006-291X(02)02626-8.

Murphy, Annabel C. 2011. “Metabolic Engineering Is Key to a Sustainable Chemical Industry.” *Natural Product Reports* 28(8):1406–25. doi: 10.1039/C1NP00029B.

Mutz, Kai Oliver, Alexandra Heilkenbrinker, Maren Lönne, Johanna Gabriela Walter, and Frank Stahl. 2013. “Transcriptome Analysis Using Next-Generation Sequencing.” *Current Opinion in Biotechnology* 24(1):22–30. doi: 10.1016/J.COPBIO.2012.09.004.

Nakae, Taiji, Akira Nakajima, Toshihisa Ono, Kohjiro Saito, and Hiroshi Yoneyama. 1999. “Resistance to β-Lactam Antibiotics InPseudomonas Aeruginosa Due to Interplay between the MexAB-OprM Efflux Pump and β-Lactamase.” *Antimicrobial Agents and Chemotherapy* 43(5):1301–3. doi: 10.1128/AAC.43.5.1301.

Nanda, Manisha, Vinod Kumar, and D. K. Sharma. 2019. “Multimetal Tolerance Mechanisms in Bacteria: The Resistance Strategies Acquired by Bacteria That Can Be Exploited to ‘Clean-up’ Heavy Metal Contaminants from Water.” *Aquatic Toxicology* 212:1–10. doi: 10.1016/J.AQUATOX.2019.04.011.

Nicolaou, Sergios A., Stefan M. Gaida, and Eleftherios T. Papoutsakis. 2010. “A Comparative View of Metabolite and Substrate Stress and Tolerance in Microbial Bioprocessing: From Biofuels and Chemicals, to Biocatalysis and Bioremediation.” *Metabolic Engineering* 12(4):307–31. doi: 10.1016/J.YMBEN.2010.03.004.

Niepa, Tagbo H. R., Liana Vaccari, Robert L. Leheny, Mark Goulian, Daeyeon Lee, and Kathleen J. Stebe. 2017. “Films of Bacteria at Interfaces (FBI): Remodeling of Fluid Interfaces by Pseudomonas Aeruginosa.” *Scientific Reports* 7(1):17864. doi: 10.1038/S41598-017-17721-3.

Nikaido, Hiroshi. 1996. “Multidrug Efflux Pumps of Gram-Negative Bacteria.” *Journal of Bacteriology*.

Nikaido, Hiroshi. 2010. “Structure and Mechanism of RND-Type Multidrug Efflux Pumps.” *Advances in Enzymology and Related Areas of Molecular Biology*. doi: 10.1002/9780470920541.ch1.

Nikaido, Hiroshi, and Jean Marie Pagès. 2012a. “Broad Specificity Efflux Pumps and Their Role in Multidrug Resistance of Gram Negative Bacteria.” *FEMS Microbiology Reviews* 36(2):340. doi: 10.1111/J.1574-6976.2011.00290.X.

Nikaido, Hiroshi, and Jean Marie Pagès. 2012b. “Broad-Specificity Efflux Pumps and Their Role in Multidrug Resistance of Gram-Negative Bacteria.” *FEMS Microbiology Reviews*.

Ochs, Martina, Sabine Veitinger, In Sook Kim, Dietrich Weiz, Annemarie Angerer, and Volkmar Braun. 1995. “Regulation of Citrate-dependent Iron Transport of Escherichia Coli: FecR Is Required for Transcription Activation by FeeI.” *Molecular Microbiology* 15(1):119–32. doi: 10.1111/J.1365-2958.1995.TB02226.X.

Oliver, Antonio, Rafael Cantón, Pilar Campo, Fernando Baquero, and Jesús Blázquez. 2000. “High Frequency of Hypermutable Pseudomonas Aeruginosa in Cystic Fibrosis Lung Infection.” *Science*. doi: 10.1126/science.288.5469.1251.

Oluyombo, Olubukola, Christopher N. Penfold, and Stephen P. Diggle. 2019. “Competition in Biofilms between Cystic Fibrosis Isolates of Pseudomonas Aeruginosa Is Shaped by R-Pyocins.” *MBio* 10(1). doi: 10.1128/MBIO.01828-18/ASSET/9D49AAD8-5AC3-42CB-A186-CCE3E8C2F809/ASSETS/GRAPHIC/MBIO.01828-18-F0006.JPEG.

van Opijnen, Tim, Kip L. Bodi, and Andrew Camilli. 2009. “Tn-Seq; High-Throughput Parallel Sequencing for Fitness and Genetic Interaction Studies in Microorganisms.” *Nature Methods* 6(10):767. doi: 10.1038/NMETH.1377.

Oswald, Christine, Heng Keat Tam, and Klaas M. Pos. 2016. “Transport of Lipophilic Carboxylates Is Mediated by Transmembrane Helix 2 in Multidrug Transporter AcrB.” *Nature Communications*. doi: 10.1038/ncomms13819.

Paradkar, Ashish. 2013. “Clavulanic Acid Production by Streptomyces Clavuligerus: Biogenesis, Regulation and Strain Improvement.” *The Journal of Antibiotics 2013 66:7* 66(7):411–20. doi: 10.1038/ja.2013.26.

Patnaik, Pradyot. 2010. “Hydrogen Cyanide.” in *Handbook of Environmental Analysis*.

Patnaik, Pratap R. 2000. “Penicillin Fermentation: Mechanisms and Models for Industrial-Scale Bioreactors.” *Critical Reviews in Biotechnology* 20(1):1–15. doi: 10.1080/07388550091144168.

Pierson, Leland S., and Elizabeth A. Pierson. 2010. “Metabolism and Function of Phenazines in Bacteria: Impacts on the Behavior of Bacteria in the Environment and Biotechnological Processes.” *Applied Microbiology and Biotechnology* 86(6):1659. doi: 10.1007/S00253-010-2509-3.

Pinkart, Holly C., James W. Wolfram, Robert Rogers, and David C. White. 1996. “Cell Envelope Changes in Solvent-Tolerant and Solvent-Sensitive Pseudomonas Putida Strains Following Exposure to o-Xylene.” *Applied and Environmental Microbiology*. doi: 10.1128/aem.62.3.1129-1132.1996.

Pitcher, Robert S., and Nicholas J. Watmough. 2004. “The Bacterial Cytochrome Cbb3 Oxidases.” *Biochimica et Biophysica Acta - Bioenergetics*.

Poole, Keith, Naomasa Gotoh, Hideto Tsujimoto, Qixun Zhao, Akihisa Wada, Tetsuo Yamasaki, Shadi Neshat, Jun Ichi Yamagishi, Xian Zhi Li, and Takeshl Nishino. 1996. “Overexpression of the MexC-MexD-OprJ Efflux Operon in NfxB-Type

Multidrug-Resistant Strains of Pseudomonas Aeruginosa." *Molecular Microbiology* 21(4):713–25. doi: 10.1046/J.1365-2958.1996.281397.X.

Poole, Keith, and Ramakrishnan Srikumar. 2005. "Multidrug Efflux in Pseudomonas Aeruginosa Components, Mechanisms and Clinical Significance." *Current Topics in Medicinal Chemistry* 1(1):59–71. doi: 10.2174/1568026013395605.

Privé, Gilbert G. 2007. "Detergents for the Stabilization and Crystallization of Membrane Proteins." *Methods* 41(4):388–97. doi: 10.1016/J.YMETH.2007.01.007.

Purkayastha, Debanjali, Kyla Agtarap, Kristy Wong, Onella Pereira, Jannie Co, Smita Pakhale, and Salmaan Kanji. 2023. "Drug-Drug Interactions with CFTR Modulator Therapy in Cystic Fibrosis: Focus on Trikafta®/Kaftrio®." *Journal of Cystic Fibrosis* 22(3):478–83. doi: 10.1016/J.JCF.2023.01.005.

Purssell, Andrew, Michael Fruci, Alaya Mikalauskas, Christie Gilmour, and Keith Poole. 2015. "EsrC, an Envelope Stress-Regulated Repressor of the MexCD-OprJ Multidrug Efflux Operon in Pseudomonas Aeruginosa." *Environmental Microbiology* 17(1):186–98. doi: 10.1111/1462-2920.12602.

Pust, Marie Madlen, Colin Francis Davenport, Lutz Wiehlmann, and Burkhard Tümmler. 2022. "Direct RNA Nanopore Sequencing of Pseudomonas Aeruginosa Clone C Transcriptomes." *Journal of Bacteriology* 204(1). doi: 10.1128/JB.00418-21/SUPPL_FILE/JB.00418-21-S0001.PDF.

Puzari, Minakshi, and Pankaj Chetia. 2017. “RND Efflux Pump Mediated Antibiotic Resistance in Gram-Negative Bacteria Escherichia Coli and Pseudomonas Aeruginosa: A Major Issue Worldwide.” *World Journal of Microbiology and Biotechnology* 33(2):1–8. doi: 10.1007/S11274-016-2190-5/FIGURES/3.

Quadroni, Manfredo, Peter James, Paola Dainese-Hatt, and Michael A. Kertesz. 1999. “Proteome Mapping, Mass Spectrometric Sequencing and Reverse Transcription-PCR for Characterization of the Sulfate Starvation-Induced Response in Pseudomonas Aeruginosa PAO1.” *European Journal of Biochemistry* 266(3):986–96. doi: 10.1046/J.1432-1327.1999.00941.X.

RABER, LINDA R. 2008. “PFIZER’S PENICILLIN LANDMARK.” *Chemical & Engineering News*. doi: 10.1021/cen-v086n028.p046.

Rademacher, Corinna, and Bernd Masepohl. 2012. “Copper-Responsive Gene Regulation in Bacteria.” *Microbiology (United Kingdom)*.

Ramos, Juan L., Estrella Duque, María Trinidad Gallegos, Patricia Godoy, María Isabel Ramos-González, Antonia Rojas, Wilson Terán, and Ana Segura. 2003. “Mechanisms of Solvent Tolerance in Gram-Negative Bacteria.” *Https://Doi.Org/10.1146/Annurev.Micro.56.012302.161038* 56:743–68. doi: 10.1146/ANNUREV.MICRO.56.012302.161038.

Ratjen, Felix A. 2009. “Cystic Fibrosis: Pathogenesis and Future Treatment Strategies.” *Respiratory Care* 54(5).

Reina-Bueno, Mercedes, Montserrat Argandoña, Manuel Salvador, Javier Rodríguez-Moya, Fernando Iglesias-Guerra, Laszlo N. Csonka, Joaquín J. Nieto, and Carmen Vargas. 2012. “Role of Trehalose in Salinity and Temperature Tolerance in the Model Halophilic Bacterium Chromohalobacter Salexigens.” *PLoS ONE* 7(3):33587. doi: 10.1371/JOURNAL.PONE.0033587.

Reinhart, Alexandria A., and Amanda G. Oglesby-Sherrouse. 2016. “Regulation of Pseudomonas Aeruginosa Virulence by Distinct Iron Sources.” *Genes 2016, Vol. 7, Page 126* 7(12):126. doi: 10.3390/GENES7120126.

Rhodes, Christopher J. 2018. “Plastic Pollution and Potential Solutions.” *Science Progress*.

Ridley, Kaden, and Michelle Condren. 2020. “Elexacaftor-Tezacaftor-Ivacaftor: The First Triple-Combination Cystic Fibrosis Transmembrane Conductance Regulator Modulating Therapy.” *The Journal of Pediatric Pharmacology and Therapeutics* 25(3):192–97. doi: 10.5863/1551-6776-25.3.192.

Rio, Donald C., Manuel Ares, Gregory J. Hannon, and Timothy W. Nilsen. 2010. “Purification of RNA Using TRIzol (TRI Reagent).” *Cold Spring Harbor Protocols* 2010(6). doi: 10.1101/PDB.PROT5439.

Rodríguez-Rojas, Alexandro, and Jesús Blázquez. 2009. “The Pseudomonas Aeruginosa PfpI Gene Plays an Antimutator Role and Provides General Stress Protection.” *Journal of Bacteriology* 191(3):844. doi: 10.1128/JB.01081-08.

Rojas, A., E. Duque, G. Mosqueda, G. Golden, A. Hurtado, J. L. Ramos, and A. Segura. 2001. “Three Efflux Pumps Are Required to Provide Efficient Tolerance to Toluene in Pseudomonas Putida DOT-T1E.” *Journal of Bacteriology* 183(13):3967–73. doi: 10.1128/JB.183.13.3967-3973.2001/ASSET/C66514EF-8CB5-46BD-8578-2B8ABCC2C533/ASSETS/GRAPHIC/JB1311616001.JPEG.

Romero, Manuel, Hazel Silistre, Laura Lovelock, Victoria J. Wright, Kok Gan Chan, Kar Wai Hong, Paul Williams, Miguel Cámara, and Stephan Heeb. 2018. “Genome-Wide Mapping of the RNA Targets of the Pseudomonas Aeruginosa Riboregulatory Protein RsmN.” *Nucleic Acids Research* 46(13):6823. doi: 10.1093/NAR/GKY324.

Rosenfeld, Nitzan, Michael B. Elowitz, and Uri Alon. 2002. “Negative Autoregulation Speeds the Response Times of Transcription Networks.” *Journal of Molecular Biology* 323(5):785–93. doi: 10.1016/S0022-2836(02)00994-4.

Ruhluel, Dilem, Joanne L. Fothergill, Daniel R. Neill, and Siobhan O’Brien. 2022. “Development of Liquid Culture Media Mimicking the Conditions of Sinuses and Lungs in Cystic Fibrosis and Health.” *F1000Research* 11. doi: 10.12688/F1000RESEARCH.125074.2.

Rumpf, Christine, Jonas Lange, Bianca Schwartbeck, and Barbara C. Kahl. 2021. “Staphylococcus Aureus and Cystic Fibrosis—A Close Relationship. What Can We Learn from Sequencing Studies?” *Pathogens* 10(9). doi: 10.3390/PATHOGENS10091177.

Rutherford, Steven T., and Bonnie L. Bassler. 2012. “Bacterial Quorum Sensing: Its Role in Virulence and Possibilities for Its Control.” *Cold Spring Harbor Perspectives in Medicine* 2(11). doi: 10.1101/CSHPERSPECT.A012427.

Ryall, B., J. C. Davies, R. Wilson, A. Shoemark, and H. D. Williams. n.d. “Pseudomonas Aeruginosa, Cyanide Accumulation and Lung Function in CF and Non-CF Bronchiectasis Patients.” doi: 10.1183/09031936.00159607.

Sakurai, Keisuke, Seiji Yamasaki, Kaori Nakao, Kunihiko Nishino, Akihito Yamaguchi, and Ryosuke Nakashima. 2019. “Crystal Structures of Multidrug Efflux Pump MexB Bound with High-Molecular-Mass Compounds.” *Scientific Reports*. doi: 10.1038/s41598-019-40232-2.

Santajit, Sirijan, and Nitaya Indrawattana. 2016. “Mechanisms of Antimicrobial Resistance in ESKAPE Pathogens.” *BioMed Research International*.

Sanya, Daniel Ruben Akiola, Djamila Onésime, Grazia Vizzarro, and Nicolas Jacquier. 2023. “Recent Advances in Therapeutic Targets Identification and Development of Treatment Strategies towards Pseudomonas Aeruginosa Infections.” *BMC Microbiology 2023 23:1* 23(1):1–18. doi: 10.1186/S12866-023-02832-X.

Schuster, Martin, C. Phoebe Lostroh, Tomoo Ogi, and E. P. Greenberg. 2003. “Identification, Timing, and Signal Specificity of Pseudomonas Aeruginosa Quorum-Controlled Genes: A Transcriptome Analysis.” *Journal of Bacteriology* 185(7):2066–79. doi: 10.1128/JB.185.7.2066-2079.2003/ASSET/EDDEE75F-FE73-44CC-81D3-5BC187DB29AE/ASSETS/GRAPHIC/JB0731131007.JPEG.

Sciuto, Alessandra Lo, Alessandra M. Martorana, Regina Fernández-Piñar, Carmine Mancone, Alessandra Polissi, and Francesco Imperi. 2018. “Pseudomonas Aeruginosa LptE Is Crucial for LptD Assembly, Cell Envelope Integrity, Antibiotic Resistance and Virulence.” *Https://Doi.Org/10.1080/21505594.2018.1537730* 9(1):1718–33. doi: 10.1080/21505594.2018.1537730.

Seddon, Annela M., Paul Curnow, and Paula J. Booth. 2004. “Membrane Proteins, Lipids and Detergents: Not Just a Soap Opera.” *Biochimica et Biophysica Acta (BBA) - Biomembranes* 1666(1–2):105–17. doi: 10.1016/J.BBAMEM.2004.04.011.

Seeger, Markus A., André Schiefner, Thomas Eicher, François Verrey, Kay Diederichs, and Klaas M. Pos. 2006. “Structural Asymmetry of AcrB Trimer Suggests a Peristaltic Pump Mechanism.” *Science*. doi: 10.1126/science.1131542.

Sennhauser, Gaby, Magdalena A. Bukowska, Christophe Briand, and Markus G. Grütter. 2009. “Crystal Structure of the Multidrug Exporter MexB from Pseudomonas Aeruginosa.” *Journal of Molecular Biology*. doi: 10.1016/j.jmb.2009.04.001.

Sette, Marco, Paul Van Tilborg, Roberto Spurio, Robert Kaptein, Maurizio Paci, Claudio O. Gualerzi, and Rolf Boelens. 1997. “The Structure of the Translational Initiation Factor IF1 from E.Coli Contains an Oligomer-Binding Motif.” *The EMBO Journal* 16(6):1436–43. doi: 10.1093/EMBOJ/16.6.1436.

Sosinski, Lo M., Christian Martin H, Kerri A. Neugebauer, Lydia Ann J. Ghuneim, Douglas V. Guzior, Alicia Castillo-Bahena, Jenna Mielke, Ryan Thomas, Marc McClelland, Doug Conrad, and Robert A. Quinn. 2022. “A Restructuring of Microbiome Niche Space Is Associated with Elexacaftor-Tezacaftor-Ivacaftor Therapy in the Cystic Fibrosis Lung.” *Journal of Cystic Fibrosis : Official Journal of the European Cystic Fibrosis Society* 21(6):996. doi: 10.1016/J.JCF.2021.11.003.

Spivey, James J., Makarand R. Gogate, Joseph R. Zoeller, and Richard D. Colberg. 1997. “Novel Catalysts for the Environmentally Friendly Synthesis of Methyl Methacrylate.” *Industrial and Engineering Chemistry Research* 36(11):4600–4608. doi: 10.1021/IE970139R.

Stancu, Mihaela Marilena. 2018. “Production of Some Extracellular Metabolites by a Solvent-Tolerant Pseudomonas Aeruginosa Strain.” *Waste and Biomass Valorization* 9(10):1747–55. doi: 10.1007/S12649-017-9967-0/FIGURES/6.

Starosta, Agata L., Jürgen Lassak, Kirsten Jung, and Daniel N. Wilson. 2014. “The Bacterial Translation Stress Response.” *FEMS Microbiology Reviews* 38(6):1172. doi: 10.1111/1574-6976.12083.

Stickland, Hannah G., Peter W. Davenport, Kathryn S. Lilley, Julian L. Griffin, and Martin Welch. 2010. “Mutation of NfxB Causes Global Changes in the Physiology and Metabolism of Pseudomonas Aeruginosa.” *Journal of Proteome Research* 9(6):2957–67. doi: 10.1021/PR9011415.

Stover, C. K., X. Q. Pham, A. L. Erwin, S. D. Mizoguchi, P. Warrener, M. J. Hickey, F. S. L. Brinkman, W. O. Hufnagle, D. J. Kowallk, M. Lagrou, R. L. Garber, L. Goltry, E. Tolentino, S. Westbrock-Wadman, Y. Yuan, L. L. Brody, S. N. Coulter, K. R. Folger, A. Kas, K. Larbig, R. Lim, K. Smith, D. Spencer, G. K. S. Wong, Z. Wu, I. T. Paulsen, J. Relzer, M. H. Saler, R. E. W. Hancock, S. Lory, and M. V. Olson. 2000. "Complete Genome Sequence of Pseudomonas Aeruginosa PAO1, an Opportunistic Pathogen." *Nature*. doi: 10.1038/35023079.

Studemeister, A. E., and J. P. Quinn. 1988. "Selective Imipenem Resistance in Pseudomonas Aeruginosa Associated with Diminished Outer Membrane Permeability." *Antimicrobial Agents and Chemotherapy*. doi: 10.1128/AAC.32.8.1267.

Suzuki, Sakura, Ayako Tatsuguchi, Eiko Matsumoto, Masahito Kawazoe, Tatsuya Kaminishi, Mikako Shirouzu, Yutaka Muto, Chie Takemoto, and Shigeyuki Yokoyama. 2007. "Structural Characterization of the Ribosome Maturation Protein, RimM." *Journal of Bacteriology* 189(17):6397. doi: 10.1128/JB.00024-07.

Sykes, Michael T., and James R. Williamson. 2009. "A Complex Assembly Landscape for the 30S Ribosomal Subunit." *Annual Review of Biophysics* 38(1):197. doi: 10.1146/ANNUREV.BIOPHYS.050708.133615.

Symmons, Martyn F., Evert Bokma, Eva Koronakis, Colin Hughes, and Vassilis Koronakis. 2009. "The Assembled Structure of a Complete Tripartite Bacterial

Multidrug Efflux Pump." *Proceedings of the National Academy of Sciences of the United States of America*. doi: 10.1073/pnas.0900693106.

Tamburrino, Giulia. 2018. "Structural Characterization of Bacterial Membrane Proteins via Molecular Dynamics Simulations and Electrophysiology."

Tate, Steve, G. MacGregor, M. Davis, J. A. Innes, and A. P. Greening. 2002. "Airways in Cystic Fibrosis Are Acidified: Detection by Exhaled Breath Condensate." *Thorax* 57(11):926–29. doi: 10.1136/THORAX.57.11.926.

Teixeira, Miguel C., Luís R. Raposo, Nuno P. Mira, Artur B. Lourenço, and Isabel Sá-Correia. 2009. "Genome-Wide Identification of Saccharomyces Cerevisiae Genes Required for Maximal Tolerance to Ethanol." *Applied and Environmental Microbiology* 75(18):5761. doi: 10.1128/AEM.00845-09.

Thi, Minh Tam Tran, David Wibowo, and Bernd H. A. Rehm. 2020. "Pseudomonas Aeruginosa Biofilms." *International Journal of Molecular Sciences* 21(22):1–25. doi: 10.3390/IJMS21228671.

Tilloy, Valentin, Anne Ortiz-Julien, and Sylvie Dequin. 2014. "Reduction of Ethanol Yield and Improvement of Glycerol Formation by Adaptive Evolution of the Wine Yeast Saccharomyces Cerevisiae under Hyperosmotic Conditions." *Applied and Environmental Microbiology* 80(8):2623. doi: 10.1128/AEM.03710-13.

Tollerson, Rodney, and Michael Ibba. 2020a. "Translational Regulation of Environmental Adaptation in Bacteria." *Journal of Biological Chemistry* 295(30):10434–45. doi: 10.1074/JBC.REV120.012742.

Tollerson, Rodney, and Michael Ibba. 2020b. “Translational Regulation of Environmental Adaptation in Bacteria.” *The Journal of Biological Chemistry* 295(30):10434. doi: 10.1074/JBC.REV120.012742.

Tomati, Valeria, Stefano Costa, Valeria Capurro, Emanuela Pesce, Cristina Pastorino, Mariateresa Lena, Elvira Sondo, Marco Di Duca, Federico Cresta, Simona Cristadoro, Federico Zara, Luis J. V. Galietta, Renata Bocciardi, Carlo Castellani, Maria Cristina Lucanto, and Nicoletta Pedemonte. 2022. “Rescue by Elexacaftor-Tezacaftor-Ivacaftor of the G1244E Cystic Fibrosis Mutation’s Stability and Gating Defects Are Dependent on Cell Background.” *Journal of Cystic Fibrosis*. doi: 10.1016/J.JCF.2022.12.005.

Tralau, Tewes, Stéphane Vuilleumier, Christelle Thibault, Barry J. Campbell, C. Anthony Hart, and Michael A. Kertesz. 2007. “Transcriptomic Analysis of the Sulfate Starvation Response of Pseudomonas Aeruginosa.” *Journal of Bacteriology* 189(19):6743. doi: 10.1128/JB.00889-07.

Tsutsumi, Kenta, Ryo Yonehara, Etsuko Ishizaka-Ikeda, Naoyuki Miyazaki, Shintaro Maeda, Kenji Iwasaki, Atsushi Nakagawa, and Eiki Yamashita. 2019. “Structures of the Wild-Type MexAB–OprM Tripartite Pump Reveal Its Complex Formation and Drug Efflux Mechanism.” *Nature Communications*. doi: 10.1038/s41467-019-09463-9.

Tucker, Nicholas, and Charles Begley. 2021. “Genomic and Transcriptomic Characterisation of Pseudomonas Sp. for the Production and Degradation of Plastic Monomers.”

Tuon, Felipe Francisco, Leticia Ramos Dantas, Paula Hansen Suss, and Victoria Stadler Tasca Ribeiro. 2022. “Pathogenesis of the Pseudomonas Aeruginosa Biofilm: A Review.” *Pathogens 2022, Vol. 11, Page 300* 11(3):300. doi: 10.3390/PATHOGENS11030300.

Tyrrell, Jean, and Máire Callaghan. 2016. “Iron Acquisition in the Cystic Fibrosis Lung and Potential for Novel Therapeutic Strategies.” *Microbiology* 162(Pt 2):191. doi: 10.1099/MIC.0.000220.

Uygun, Sahra, Cheng Peng, Melissa D. Lehti-Shiu, Robert L. Last, and Shin Han Shiu. 2016. “Utility and Limitations of Using Gene Expression Data to Identify Functional Associations.” *PLoS Computational Biology* 12(12). doi: 10.1371/JOURNAL.PCBI.1005244.

Varela, Cristian A., Mauricio E. Baez, and Eduardo Agosin. 2004. “Osmotic Stress Response: Quantification of Cell Maintenance and Metabolic Fluxes in a Lysine-Overproducing Strain of Corynebacterium Glutamicum.” *Applied and Environmental Microbiology* 70(7):4222. doi: 10.1128/AEM.70.7.4222-4229.2004.

Vasylkivska, Maryna, and Petra Patakova. 2020. “Role of Efflux in Enhancing Butanol Tolerance of Bacteria.” *Journal of Biotechnology* 320:17–27. doi: 10.1016/J.JBIOTEC.2020.06.008.

Veit, Gudio, Radu G. Avramescu, Annette N. Chiang, Scott A. Houck, Zhiwei Cai, Kathryn W. Peters, Jeong S. Hong, Harvey B. Pollard, William B. Guggino, William

E. Balch, William R. Skach, Garry R. Cutting, Raymon A. Frizzell, David N. Sheppard, Douglas M. Cyr, Eric J. Sorscher, Jeffrey L. Brodsky, and Gergely L. Lukacs. 2016. “From CFTR Biology toward Combinatorial Pharmacotherapy: Expanded Classification of Cystic Fibrosis Mutations.” *Molecular Biology of the Cell* 27(3):424–33. doi: 10.1091/MBC.E14-04-0935/ASSET/IMAGES/LARGE/424FIG2.JPEG.

Veit, Guido, Ariel Roldan, Mark A. Hancock, Dillon F. da Fonte, Haijin Xu, Maytham Hussein, Saul Frenkiel, Elias Matouk, Tony Velkov, and Gergely L. Lukacs. 2020. “Allosteric Folding Correction of F508del and Rare CFTR Mutants by Elexacaftor-Tezacaftor-Ivacaftor (Trikafta) Combination.” *JCI Insight* 5(18). doi: 10.1172/JCI.INSIGHT.139983.

Verchére, Alice, Isabelle Broutin, and Martin Picard. 2012. “Photo-Induced Proton Gradients for the in Vitro Investigation of Bacterial Efflux Pumps.” *Scientific Reports*. doi: 10.1038/srep00306.

Verchère, Alice, Manuela Dezi, Vladimir Adrien, Isabelle Broutin, and Martin Picard. 2015. “In Vitro Transport Activity of the Fully Assembled MexAB-OprM Efflux Pump from Pseudomonas Aeruginosa.” *Nature Communications*. doi: 10.1038/ncomms7890.

Vollmer, Waldemar, Bernard Joris, Paulette Charlier, and Simon Foster. 2008. “Bacterial Peptidoglycan (Murein) Hydrolases.” *FEMS Microbiology Reviews* 32(2):259–86. doi: 10.1111/J.1574-6976.2007.00099.X.

De Vos, Daniel, Magali De Chial, Christel Cochez, Silke Jansen, Burkhard Tümmler, Jean Marie Meyer, and Pierre Cornelis. 2001. "Study of Pyoverdine Type and Production by Pseudomonas Aeruginosa Isolated from Cystic Fibrosis Patients: Prevalence of Type II Pyoverdine Isolates and Accumulation of Pyoverdine-Negative Mutations." *Archives of Microbiology* 175(5):384–88. doi: 10.1007/S002030100278.

Wacker, Tobias, Juan J. Garcia-Celma, Philipp Lewe, and Susana L. A. Andrade. 2014. "Direct Observation of Electrogenic NH4+ Transport in Ammonium Transport (Amt) Proteins." *Proceedings of the National Academy of Sciences of the United States of America* 111(27):9995–10000. doi: 10.1073/PNAS.1406409111/SUPPL_FILE/PNAS.1406409111.SAPP.PDF.

Wagner, Samuel, Mirjam M. Klepsch, Susan Schlegel, Ansgar Appel, Roger Draheim, Michael Tarry, Martin Högbom, Klaas J. van Wijk, Dirk J. Slotboom, Jan O. Persson, and Jan Willem de Gier. 2008. "Tuning Escherichia Coli for Membrane Protein Overexpression." *Proceedings of the National Academy of Sciences of the United States of America* 105(38):14371–76. doi: 10.1073/PNAS.0804090105/SUPPL_FILE/ST2.XLS.

Waite, Richard D., Anastasia Papakonstantinopoulou, Eddie Littler, and Michael A. Curtis. 2005. "Transcriptome Analysis of Pseudomonas Aeruginosa Growth: Comparison of Gene Expression in Planktonic Cultures and Developing and Mature Biofilms." *Journal of Bacteriology* 187(18):6571–76. doi:

10.1128/JB.187.18.6571-6576.2005/SUPPL_FILE/PA_BIOFILM_NOTE___SUPPLEMENTARY_TABLES.PDF.

Wang, Xiaodong R. obert, and Chenglong Li. 2014. “Decoding F508del Misfolding in Cystic Fibrosis.” *Biomolecules* 4(2):498. doi: 10.3390/BIOM4020498.

Whiteley, Marvin, M. Gita Bangera, Roger E. Bumgarner, Matthew R. Parsek, Gail M. Teitzel, Stephen Lory, and E. P. Greenberg. 2001. “Gene Expression in Pseudomonas Aeruginosa Biofilms.” *Nature 2001 413:6858* 413(6858):860–64. doi: 10.1038/35101627.

Williamson, Gordon, Giulia Tamburrino, Adriana Bizior, Mélanie Boeckstaens, Gaëtan Dias Mirandela, Marcus Bage, Andrei Pisliakov, Callum M. Ives, Eilidh Terras, Paul A. Hoskisson, Anna Maria Marini, Ulrich Zachariae, and Arnaud Javelle. 2020. “A Two-Lane Mechanism for Selective Biological Ammonium Transport.” *ELife* 9:1–41. doi: 10.7554/ELIFE.57183.

Willim Bauer, JR., and Rohm and Haas Co. 2012. “Methacrylic Acid and Derivatives.” in *Ullman’s Encyclopedia of Industrial Chemistry*. JNC Academic Books.

Willke, Th, and K. D. Vorlop. 2004. “Industrial Bioconversion of Renewable Resources as an Alternative to Conventional Chemistry.” *Applied Microbiology and Biotechnology* 66(2):131–42. doi: 10.1007/S00253-004-1733-0.

Wingett, Steven W., and Simon Andrews. 2018. “FastQ Screen: A Tool for Multi-Genome Mapping and Quality Control.” *F1000Research* 7:1338. doi: 10.12688/F1000RESEARCH.15931.2.

Winstanley, Craig, and Joanne L. Fothergill. 2009. “The Role of Quorum Sensing in Chronic Cystic Fibrosis Pseudomonas Aeruginosa Infections.” *FEMS Microbiology Letters* 290(1):1–9. doi: 10.1111/J.1574-6968.2008.01394.X.

Wofford, Joshua D., Naimah Bolaji, Nathaniel Dziuba, F. Wayne Outten, and Paul A. Lindahl. 2019. “Evidence That a Respiratory Shield in Escherichia Coli Protects a Low-Molecular-Mass FeII Pool from O2-Dependent Oxidation.” *Journal of Biological Chemistry* 294(1):50–62. doi: 10.1074/JBC.RA118.005233/ATTACHMENT/1FFF7539-1026-4AB0-AF61-224813C651B6/MMC2.PDF.

Woodcock, Stuart D., Karl Syson, Richard H. Little, Danny Ward, Despoina Sifouna, James K. M. Brown, Stephen Bornemann, and Jacob G. Malone. 2021. “Trehalose and α-Glucan Mediate Distinct Abiotic Stress Responses in Pseudomonas Aeruginosa.” *PLoS Genetics* 17(4). doi: 10.1371/JOURNAL.PGEN.1009524.

Wüllner, Dominik, Maren Gesper, Annika Haupt, Xiaofei Liang, Pei Zhou, Pascal Dietze, Franz Narberhaus, and Julia E. Bandow. 2022. “Adaptive Responses of Pseudomonas Aeruginosa to Treatment with Antibiotics.” *Antimicrobial Agents and Chemotherapy* 66(1). doi: 10.1128/AAC.00878-21.

Xiong, Lifeng, Jade L. L. Teng, Michael G. Botelho, Regina C. Lo, Susanna K. P. Lau, and Patrick C. Y. Woo. 2016. “Arginine Metabolism in Bacterial Pathogenesis and Cancer Therapy.” *International Journal of Molecular Sciences* 17(3). doi: 10.3390/IJMS17030363.

Xiong, Yan Qiong, Michael L. Vasil, Zaiga Johnson, Urs A. Ochsner, and Arnold S. Bayer. 2000. “The Oxygen- and Iron-Dependent Sigma Factor PvdS of Pseudomonas Aeruginosa Is an Important Virulence Factor in Experimental Infective Endocarditis.” *The Journal of Infectious Diseases* 181(3):1020–26. doi: 10.1086/315338.

Yazawa, Hisashi, Hitoshi Iwahashi, and Hiroshi Uemura. 2007. “Disruption of URA7 and GAL6 Improves the Ethanol Tolerance and Fermentation Capacity of Saccharomyces Cerevisiae.” *Yeast* 24(7):551–60. doi: 10.1002/YEA.1492.

Yoon, Sang Sun, Robert F. Hennigan, George M. Hilliard, Urs A. Ochsner, Kislay Parvatiyar, Moneesha C. Kamani, Holly L. Allen, Teresa R. DeKievit, Paul R. Gardner, Ute Schwab, John J. Rowe, Barbara H. Iglewski, Timothy R. McDermott, Ronald P. Mason, Daniel J. Wozniak, Robert E. W. Hancock, Matthew R. Parsek, Terry L. Noah, Richard C. Boucher, and Daniel J. Hassett. 2002. “Pseudomonas Aeruginosa Anaerobic Respiration in Biofilms: Relationships to Cystic Fibrosis Pathogenesis.” *Developmental Cell* 3(4):593–603. doi: 10.1016/S1534-5807(02)00295-2.

Zhang, Mengru, Kayleigh Brindle, Melanie Robinson, Debbie Ingram, Tanya Cavany, and Alyn Morice. 2022. “Chronic Cough in Cystic Fibrosis: The Effect of Modulator Therapy on Objective 24-h Cough Monitoring.” *ERJ Open Research* 8(2). doi: 10.1183/23120541.00031-2022.

Zufferey, Rachel, Oliver Preisig, Hauke Hennecke, and Linda Thöny-Meyer. 1996. “Assembly and Function of the Cytochrome Cbb3 Oxidase Subunits in

Bradyrhizobium Japonicum." *Journal of Biological Chemistry*. doi: 10.1074/jbc.271.15.9114.